

# **Microclimate design methods for energy-saving houses on various site conditions in Korea**

Technische Universität Berlin  
Fakultät VI. Planen Bauen Umwelt  
Zur Erlangung des Grade  
Doktorin der Ingenieurwissenschaftler

**Dr. –Ing**  
genehmigte Dissertation  
vorgelegt von  
**Min Kyeong Kim**  
aus Süd Korea

Promotionsausschuss:

Vorsitzender: Prof. Dr. –Ing. Peter Herrle

Berichter : Prof. Dipl.-Ing. Claus Steffan

Berichter: Prof. Dr. rer. nat. Dieter Scherer

Tag der wissenschaftlichen Aussprache : 9. 7. 2008

Berlin 2008

D 83

# Contents

List of Figures .....	IV
List of Tables.....	IX
Abstract .....	XI
Acknowledgement.....	XIII
1. Introduction.....	1
1.1. Importance of energy-saving .....	1
1.2. Need for energy simulation .....	5
1.3. Research objective.....	7
1.4. Constraints.....	9
1.5. Structure of thesis .....	1 1
Research flowchart.....	1 3
2. Energy-saving and climate in the Passive House.....	1 4
2.1. Energy in Passive House.....	1 4
2.2. Human comfort factor.....	1 6
2.2.1. Psychometric comfort scale .....	1 7
2.2.2. Comfort zone .....	1 9
2.3. Aerodynamic and energy contents .....	2 0
2.4. Design for energy gain.....	2 2
2.5. Design for heat loss.....	2 6
2.6. Thermal insulation.....	3 0
2.7. Thermal mass .....	3 4
3. Microclimate design for energy-saving.....	3 9
3.1. Microclimate and building.....	3 9
3.1.1. Definition of Macro- and Microclimate .....	3 9
3.1.2. Microclimate design.....	4 0
3.1.3. Climate design process.....	4 1
3.2. Arrangement.....	4 2
3.2.1. Microclimate effects adapting wind direction.....	4 2
3.2.2. Optimum building orientation.....	4 4
3.2.3 Topography.....	4 5

3.2.4. Building attachment and courtyard .....	5 0
3.3 Form.....	5 3
3.3.1. Windbreak.....	5 3
3.3.2. Building geometry and form .....	5 6
3.3.3. Internal partitioning.....	5 7
3.3.4. Courtyard roofing .....	5 8
3.3.5. Roof opening and stack effect.....	6 0
3.4. Façade elements.....	6 2
3.4.1. Microclimate in opening control.....	6 2
3.4.2. Opening locations and shapes .....	6 3
3.4.3. Projected building structure.....	6 6
3.4.4. Opening slits.....	6 8
3.5. Analysis of building microclimate .....	7 0
3.5.1. Problems for energy assessment .....	7 0
3.5.2. Previous methods.....	7 1
3.5.3. Hybrid model for microclimate analysis .....	7 5
3.5.4. Experimental expression of models .....	7 7
4. Microclimate energy simulation.....	8 1
4.1. Multi-zone energy simulation.....	8 1
4.1.1. Multi-zone simulation method using EP .....	8 1
4.1.2. Calculation of internal temperatures in multi-zones.....	8 3
4.2. Microclimate energy variation model.....	8 6
4.2.1. Outdoor model.....	8 7
4.2.2. Indoor model.....	9 1
4.3. Multi-scale EP-CFD analysis.....	9 3
4.4. Graph modeling for real house analysis .....	9 5
5. Microclimate design methods in S. Korea: Simulation results using unit EP-CFD .....	9 9
5.1. Arrangement .....	1 0 2
5.1.1. Microclimate of building orientation: the highest heating gain and small indoor airflow ....	1 0 2
5.1.2. Microclimate on topography: large microclimate cooling effect with high air pressure.....	1 0 3
5.1.3. Microclimate of courtyard cooling: thermodynamic air circulation through the house .....	1 0 4
5.1.4. Microclimate of courtyard roof: atrium passive heating using courtyard.....	1 0 6
5.2. Form.....	1 0 8
5.2.1. Microclimate in roof shapes: strong shading and control of wind stream direction .....	1 0 8
5.2.2. Microclimate of curved roof: minimum wind resistance and small eddy current.....	1 1 0
5.2.3. Microclimate in fence design: deriving small wind and airflow on the site .....	1 1 1
5.2.4. Microclimate of windbreaks: cold wind protection in winter .....	1 1 2
5.2.5. Microclimate in building over pilotis: cooling efficiency of airflow under the floor.....	1 1 4
5.2.6. Microclimate of heat diffusion: Indoor airflow for heat recovery .....	1 1 6
5.3. Façade elements.....	1 1 8
5.3.1. Microclimate of window shape: Fast and well-distributed cross-ventilation .....	1 1 8

5.3.2. Microclimate of window shape: optimal inlet design for ventilation and passive solar design.....	1 2 0
5.3.3. Microclimate of building projection: enhancing microclimate pressure and protecting direct solar gain.....	1 2 2
6. Application of microclimate simulation to a real-house design.....	1 2 5
6.1. A real-house in a suburb of Seoul, S. Korea.....	1 2 5
6.2. Converting Model from CAD to IFC.....	1 2 7
6.3. Climate data and features.....	1 2 9
6.4. Microclimate design elements .....	1 3 2
6.5. Energy efficiency .....	1 3 6
7. Conclusions .....	1 4 5
Appendix .....	1 5 7
Bibliography .....	1 6 9



# List of Figures

## 1. Introduction

Figure 1.1. Annual changes in average surface temperature and changes of CO <sub>2</sub> .....	1
Figure 1.2. Classification of 10 elements using the solar energy from passive to active level .....	4
Figure 1.3. Climate of local regions in S. Korea.....	6
Figure 1.4. Climate scales, (a) time and distance scales, (b) macro- and microclimate.....	8
Figure 1.5. An example of S. Korean site set-up including slope areas.....	10

## 2. Energy-saving and climate in the Passive House

Figure 2.1. CO <sub>2</sub> emissions for the buildings sector including electricity .....	14
Figure 2.2. Energy consumption in residential sectors of some cities .....	16
Figure 2.3. Psychometric chart of Seoul .....	18
Figure 2.4. Actual temperature as perceived by a person and MRT .....	19
Figure 2.5. Relationship between body temperature and the energy balance, (a) the components over a range of environmental temperatures, (b) the four modes ....	21
Figure 2.6. Typical design approach when considering solar access by G. Watrous in Kentucky .....	22
Figure 2.7. Angles of visible sky for the average DF calculation .....	23
Figure 2.8. Outdoor heat balance of longwave radiation, (a) the diagram, (b) an example in Berlin, <i>Stglitz</i> .....	24
Figure 2.9. Indoor heat balance diagram and an example of longwave radiation from internal exchange.....	25
Figure 2.10. Solar shading, (a) devices by C. Scarpa, (b) overhang.....	27
Figure 2.11. Very large roof overhangs of Robie house by F.L. Wright .....	28
Figure 2.12. Areas of opening required in winter and summer, volume to area ratio for stack-driven ventilation .....	29
Figure 2.13. Temperature gradient of a composite wall .....	30
Figure 2.14. Calculating heat transfer .....	31
Figure 2.15. U-value of a ground floor, (a) for solid floor and suspended floor, (b) solid floors with all over insulation .....	32
Figure 2.16. Thermal bridge .....	33
Figure 2.17. Effect of position of thermal mass on the inside temperature.....	34
Figure 2.18. The relationship between density and thermal conductivity .....	34

Figure 2.19. Thermal mass in solar-air-collector by E.S. Morse in Salem, Massachusetts .....	3 5
Figure 2.20. Thermal mass for passive cooling of Tono Inax pavilion 1998.....	3 6
3. Microclimate design for energy-saving	
Figure 3.1. Wind streamlines around a building, (a) schematic distribution of wind pressure and wind shadow, (b) the pattern for the building forms and layouts.....	4 3
Figure 3.2. Wind streamlines and wind shadow by building arrangement .....	4 3
Figure 3.3. House orientation considering the sun path .....	4 4
Figure 3.4. <i>Schöneiche</i> (nearby Berlin) ecological house complex by Gölling and Schmidt.....	4 5
Figure 3.5. Aluminum city terrace in Pennsylvania by W. Gropius and M. Breuer .....	4 6
Figure 3.6. Solar radiation on slope, (a) total daily direct-beam radiations, (b) shadow range for distance between buildings .....	4 6
Figure 3.7. Slope wind systems, (a) interplay of slope and valley winds for a day, (b) streamlines in slopes and building arrangement .....	4 8
Figure 3.8. Airflow patterns over moderate topography.....	4 9
Figure 3.9. Utilization of topography and site condition, (a) house by Körner and Stotz in <i>Murrhardt</i> , (b) Korean traditional architectural scheme .....	4 9
Figure 3.10. Several types of court for wind protection .....	5 0
Figure 3.11. Building attachment, (a) annex building against regional wind, (b) layered structures of <i>Dokrak-Dang</i> .....	5 1
Figure 3.12. Airflow patterns corresponding to the function of $H/W$ and $L/W$ .....	5 1
Figure 3.13. The thermal system of a courtyard house .....	5 2
Figure 3.14. Barrier usage and the influence, (a) layered walls of Korean architecture, (b) the wind speed in the vicinity in the open, (c) wind streamline zones .....	5 3
Figure 3.15. Shading of backyard .....	5 5
Figure 3.16. The effects of building geometry .....	5 6
Figure 3.17. Energy-saving house at <i>Fläming Str.</i> in Berlin by A. Salomon & Scheidt .....	5 6
Figure 3.18. Internal airflow patterns using several partitions, (a) the diagrams, (b) airflow patterns of in complex partitions.....	5 7
Figure 3.19. Ventilation parametric models for the courtyard roofing .....	5 8
Figure 3.20. Public housing at <i>Köpeniker Str.</i> in Berlin by O. Steidle .....	5 9
Figure 3.21. Exposed roof-ventilation holes of the gable roof of Mr. Eu's house .....	6 0
Figure 3.22. Stack effect of an IHK's office in <i>Karlsruhe</i> by C. Steffan .....	6 1
Figure 3.23. Performance of different wind direction with shape and angles of opening .....	6 4
Figure 3.24. Opening sizes control of <i>Janggyeong Panjeon</i> , (a) the structure, (b) mean airflow speed ..	6 6
Figure 3.25. Horizontal projections and airflow patterns .....	6 7
Figure 3.26. Out-standing structures, in the Korean traditional residence .....	6 8
Figure 3.27. Opening slits of <i>Janggyeong Panjeon</i> on the elevation of a module .....	6 9
Figure 3.28. Debis tower in Berlin designed by R. Piano .....	6 9
Figure 3.29. Airflow patterns of ventilation for several slit types .....	7 0

Figure 3.30. The geometric representation of building zones and the structural component graph.....	7 2
Figure 3.31. The analyzed variable parameters as the flow in the grid network .....	7 4
Figure 3.32. Validity for with and without CFD in a building model.....	7 4
Figure 3.33. 3D CFD.....	7 5
Figure 3.34. Experimental expression, (a) predicted and observed pressure coefficients ( $C_Q$ ), (b) energy balance between wall and room air .....	7 8
 4. Microclimate energy simulation	
Figure 4.1. Input interface of EP.....	8 2
Figure 4.2. EP schematic and modules.....	8 3
Figure 4.3. Multi-zone analytical energy simulation of EP.....	8 3
Figure 4.4. Two layer examples for deriving the Laplace transform extension to include sources and sinks .....	8 4
Figure 4.5. Controlling temperature scheme for heating and cooling. ....	8 6
Figure 4.6. Simulation model and three modules .....	8 6
Figure 4.7. Sloping topographical design process.....	8 9
Figure 4.8. Outdoor model .....	9 0
Figure 4.9. Thermo- and aerodynamic processes, (a) thermodynamic, (b) airflow by aerodynamic microclimate.....	9 1
Figure 4.10. Numerical solution in the Fluent .....	9 3
Figure 4.11. Multi-scale scheme using macroclimate and microclimate scales.....	9 4
Figure 4.12. Graph modeling, (a) graph model of EP method for the 3 zones, (b) relationship between AirflowNetwork and regular EP objects.....	9 6
Figure 4.13. Allocating EP's volume average value to CFD nodes of the volume .....	9 6
 5. Microclimate design methods in S. Korea: Simulation results using unit EP-CFD	
Figure 5.1. Result of orientation of the CFD, (a) 2D plot, (b) 3D plot .....	1 0 2
Figure 5.2. Result of building in topography .....	1 0 3
Figure 5.3. Comparison of thermal condition with cooling gain .....	1 0 4
Figure 5.4. A cooling scheme of a Korean traditional house on topography .....	1 0 4
Figure 5.5. Result of courtyard cooling between house and courtyard, (a) air velocity and the microclimate air circulation, (b) thermodynamic air circulation ....	1 0 5
Figure 5.6. Air temperature of courtyard, (a) indoor and outdoor by day and night, (b) with and without roof .....	1 0 6
Figure 5.7. Result of courtyard roof, (a) thermal condition of courtyard in winter, (b) comparison of airflows between courtyard with roof and without roof.....	1 0 7
Figure 5.8. Result of gable roof with shading overhang and roof ventilation .....	1 0 8
Figure 5.9. Result of curved roof, (a) air-streamline comparison between gable roof and curved roof, (b) pressure and thermal condition of curved roof .....	1 0 9

Figure 5.10. Comparison of thermal condition (a) cooling gain between flat and gable roof, (b) indoor and exterior wall temperatures between gable and curved roofs .....	1 0 9
Figure 5.11. Result of fence design in Korean house, (a) 3D streamline plot of airflow, (b) the present state of Mr. Jung's house .....	1 1 1
Figure 5.12. Cold wind protection, (a) using wall and projection, (b) using trees.....	1 1 2
Figure 5.13. Average indoor temperatures of no wind shelter, shelters using wall and projection and using tree .....	1 1 3
Figure 5.14. Building over pilotis, (a) result of flow field and a Korean pavilion, (b) comparison of wind pressure distribution for different porosities (%) .....	1 1 4
Figure 5.15. Comparison of thermal condition with cooling gain between ventilation using pilotis and cross-ventilation of low-set building .....	1 1 5
Figure 5.16. Thermodynamic heat diffusion process using isothermal particle tracking.....	1 1 6
Figure 5.17. Difficulty in visualizing thermo- and aerodynamic simultaneously, (a) simple zone, (b) two different heating zones .....	1 1 7
Figure 5.18. Temperature of the zone-to-zone natural ventilation.....	1 1 8
Figure 5.19. Airflow pattern in cross-ventilation, (a) uniform window shape, (b) non-uniform window shape, (C) 3D streamline plot of airflow .....	1 1 9
Figure 5.20. Comparison between uniform window and non-uniform window, (a) pressure and air velocity, (b) average outdoor and indoor temperatures .....	1 2 0
Figure 5.21. Airflow plots of horizontal inlet with temperature .....	1 2 1
Figure 5.22. Cooling performance for window shape and air velocities.....	1 2 1
Figure 5.23. Microclimate of building projection, (a) pressure difference between of horizontal and vertical projection, (b) horizontal projection, (c) vertical projection .....	1 2 3
Figure 5.24. Comparison of thermal condition of cross-ventilation with horizontal and vertical projections and without projection .....	1 2 4
6. Application of microclimate simulation to a real-house design	
Figure 6.1. Pine Tree House by S.Y. Choi, (a) drawings, (b) views .....	1 2 6
Figure 6.2. CAD model of Pine Tree House .....	1 2 7
Figure 6.3. Difference between CAD and IFC .....	1 2 8
Figure 6.4. Adaptable mesh for better analysis resolution near model edges .....	1 2 8
Figure 6.5. Heating and cooling loads by the difference of solar radiation between Seoul and Berlin .....	1 2 9
Figure 6.6. Korean climate analysis using EP over 1 year .....	1 3 2
Figure 6.7. Microclimate design elements of Pine Tree House .....	1 3 3
Figure 6.8. Heating and cooling loads, (a) by change of slope angle, (b) by change of window ratios, (c) by change of insulation thickness .....	1 3 8
Figure 6.9. Comparison of heating and cooling loads EP-CFD method using microclimate design models	

.....	1 3 9
Figure 6.10. EP-CFD simulation results of Pine Tree House .....	1 4 1
Figure 6.11. Zone temperature comparison between passive method and HVAC model .....	1 4 2
Figure 6.12. 1 year temperature comparison between a passive method and a combination of passive method and flow net of microclimate design .....	1 4 3
7. Conclusions	
Figure 7. 1 Classification by heating and cooling effects of elements in Table 7.3.....	1 4 9
Figure 7.2. Energy simulation method using EP-CFD coupling. ....	1 5 0

# List of Tables

1. Introduction	
2. Energy-saving and climate in the Passive House	
Table 2.1. Thermal sensation scale for the PMV, .....	1 8
Table 2.2. Solar heat gain through single thickness of common window glass through an unshaded window.....	2 6
Table 2.3. Comparison of global radiation of four countries .....	2 7
Table 2.4. Climate data in summer and winter in S. Korea .....	2 7
3. Microclimate design for energy-saving	
Table 3.1. The factors and related issues .....	4 0
Table 3.2. Planning issues and the effects.....	4 1
Table 3.3. The amount of wind reduction measured against varying heights and object shapes .....	5 4
Table 3.4. The effects of planting in Chicago .....	5 5
Table 3.5. Effects of clerestory on average internal airflow rates .....	6 0
Table 3.6. Airflow related to the opening location or wind direction .....	6 5
Table 3.7. Effects of wing-walls on cross-ventilation and the wind direction .....	6 7
Table 3.8. Strategies for the coupling of the CFD and multi-zone model .....	7 7
Table 3.9. Analytic method for cross-ventilation of single buildings.....	7 8
4. Microclimate energy simulation	
Table 4.1. The physical properties that can be analyzed using CFD.....	8 7
Table 4.2. The advantages of CFD.....	8 9
Table 4.3. Outdoor model and indoor model concerned to chapter, (a) outdoor model, (b) indoor model.....	9 0
Table 4.4. The utilization of microclimate modification .....	9 2
Table 4.5. Sub-tools of Fluent software .....	9 2
Table 4.6. Procedure of Fluent solver.....	9 3
Table 4.7. Process of EP-CFD coupling .....	9 5
Table 4.8. Graph models of EP and CFD .....	9 6



## **Abstract**

# **Mikroklimatische Designmethoden für energiesparende Häuser an verschiedenen Standorten in Korea**

Min Kyeong Kim

Eingereicht zum Fachgebiet Architektur, Institut für Gebäudetechnik und Entwerfen im Juni 2008 für den Grad des Doktor Ingenieur im Fachgebiet Architektur

### **Thesen zur Dissertation:**

Ein kleines territoriales Gebiet in Korea weist verschiedene mikroklimatische Bedingungen auf, je nachdem, wie viel Sonne, Schatten, Feuchtigkeit und Winden es ausgesetzt ist. Diese mikroklimatischen Bedingungen können durch zielgerichtete Betrachtung aller Elemente bei der Entwicklung und beim Bauen beeinflusst werden, so durch die Nutzung geneigter Geländeflächen, die Anwendung einer 3-dimensionalen Geometrie, wie die Kombination von architektonischen Elementen des Neubaues und der Einbeziehung bereits auf der Geländefläche existierenden Gebäuden. Diese Studie untersucht die Nutzung mikroklimatischer Veränderungen für ein effektives Niedrigenergiegedesign unter Einbeziehung der von Elementen der traditionellen koreanischen Bauweise und des Passivhauses.

Die untersuchte Methode der mikroklimatischen Analyse kann zu zeitlichen und räumlichen Vorhersage bezüglich der Gebäudegeometrie genutzt werden. Eine Kombination u.a. von passiver solarer Gewinne, gezielten Schutzmassnahmen vor kalten Winden, Sicherung der Zirkulation der Raumluft und natürlicher Belüftung sowie der Berücksichtigung der Sonnenscheindauer und der Ausbreitung des Schattens ist eine wichtige Voraussetzung für behagliches Wohnen und Arbeiten zu jeder Jahreszeit. Zugleich kann so eine wirkungsvolle Einflussnahme auf die Senkung des Energieverbrauches genommen werden. Für die passive Gewinne und Kühlung ist unbedingt eine ständige Betrachtung der Veränderungen in den mikroklimatischen Bedingungen erforderlich, um die



höchstmögliche Energieeffizienz in den Gebäuden zu sichern. Die vorliegende Arbeit enthält die Untersuchung der mikroklimatischen Veränderungen zur Nutzung der räumlichen Planung eines Gebäudes, des effektiven Einsatzes von Niedrigenergiemethoden, des Passivhaus-Standards und allgemeine physikalische Grundlagen in den Energiesimulationsmethoden.

Die heißen und feuchten Sommer in Korea, erfordern immer zu beachten, dass eine ausreichende Luftzirkulation in den Gebäuden gewährleistet wird. So ist die Be- und Entlüftung eine wichtige Voraussetzung für die konvektive Kühlung oder Verdunstungskühlung in den Gebäuden. Der erforderliche Luftfluss in einem Gebäude wird durch die Geometrie und der Betrachtung des Unterschieds von Lufttemperatur und des Luftdrucks erreicht. Die Betrachtung der Positionen bereits bestehender Gebäude ist für die Führung des Luftflusses von großer Wichtigkeit. Die Gebäudegeometrie und die Gebäudeorientierung hat eine größere Wirkung auf die Tendenz des Luftflusses als die Luftgeschwindigkeit.

Diesen Effekt richtig genutzt, wird er zu einer wichtigen Quelle der Energieeinsparung. Eine neuartige Simulationsmethode in der Kombination der Simulation von Multi-Zonen und CFD kann zu einer wirkungsvollen Analyse effektiver Energiespareffekte im Bereich der passiven und mikroklimatischen Elemente der Gestaltung von Gebäuden und Einrichtungen genutzt werden. Der Multi-Zone Energiesimulationstools „Energie Plus“ kann für die Erlangung von Parametern zur Vereinfachung der Energiesparprobleme für die verschiedensten Gebäudezonen (Räume, Flure usw.) genutzt werden. Diese Methode ist aber nicht geeignet, um Variationen in der Geometrie von Gebäuden zu behandeln, da sie in ihrer Gesamtheit nur auf Schätzungen von durchschnittlichen Werten bezogen auf Energieverbrauch, Temperatur, Feuchtigkeit usw. beruht. Besser geeignet für Variationen in der Gebäudegestaltung ist die CFD Methode mit unterteilender „Grid-Unit“. Sie ermöglicht genauere Ergebnisse zu den Schätzungen des Luftflusses und der zielgerichteten Veränderung des thermischen Zustands. Für die Gestaltung eines Hausmodells in Südkorea, sind Fallstudien und Methoden der Energieeinsparung, immer einer gründlichen Bewertung und Analyse, bezogen auf die vorherrschenden mikroklimatischen Bedingungen zu unterziehen.

## Acknowledgement

# Danksagung

Ich möchte mich bedanken

bei Prof. Claus Steffan für die Betreuung meiner Arbeit;

bei Prof. Dieter Scherer, mit dem ich lange ein Büro teilen durfte und der mir bei allen computertechnischen Problemen eine unendliche Hilfe war;

bei Prof. Paul Uwe Thamsen des Fluidsystemdynamik Institutes, für die CFD Arbeit;

bei Anke Sippel und bei Klaus Sippel, die mir speziell in den letzten 3 Jahren in Berlin eine große Hilfe waren;

bei Heon, Farshad und Kollen in dem Institut für Ökologie, für ihre Freundschaften und ihre aufrichtige Kritik;

bei Gwyneth Edwards, Petra Pham und Robert Crouch, für ihre kurze aber wichtige Freundschaft und für die Korrektur in Englisch;

Am allermeisten bedanke ich mich allerdings bei meinen Eltern, für ihre Liebe und ihre jahrelange Unterstützung;

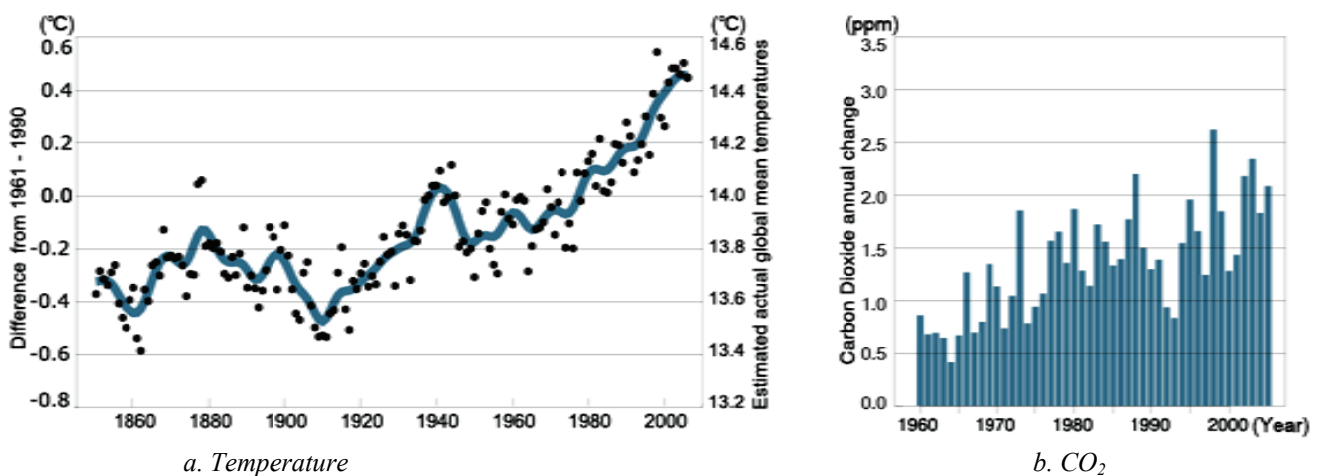
Vielen Dank!

Kim, Min Kyeong  
Berlin, den 11. July 2008

# 1. Introduction

## 1.1. Importance of energy-saving

Climate has constantly formed the global features of the Earth since the beginning of time. The history of climate is bound up with the origin and adaptation of life on the Earth. Recently, the ecosystem of the Earth has been disrupted due to human activities which have dramatically altered the chemical composition of the global atmosphere, with substantial implications for the climate. Energy sources needed for human activities are obtained by the combustion of fossil fuels. By-products of fossil fuels such as primarily carbon dioxide ( $\text{CO}_2$ ), methane ( $\text{CH}_4$ ) and nitrous oxide ( $\text{N}_2\text{O}$ ) etc., which are called “Greenhouse Gases (GHGs)”, are generated and act as a partial blanket for the longwave radiation reflected from the surface into the atmosphere. Rising concentrations of GHGs warm the Earth’s climate. A popular phrase “Global Warming” is nowadays being used to define the phenomena. Increasing global temperature will cause sea levels to rise, increase the intensity of extreme weather events and change the amounts and patterns of precipitation. Other effects of global warming include changes in agricultural yields, trade routes, glacier retreat, species extinctions and the spread of the ranges of disease vectors.



**Figure 1.1.** Annual changes in average surface temperature and changes of  $\text{CO}_2$  [The Intergovernmental Panel on Climate Change (IPCC) 2007].

For the evaluation of the risk of climate change caused by human activity, the Intergovernmental Panel on Climate Change (IPCC) was established in 1988 by the World Meteorological Organization (WMO) and the United Nations Environment Programme (UNEP),<sup>1</sup> and has published several reports on topics relevant to the implementation of the UN Framework Convention on Climate Change (UNFCCC).<sup>2</sup> The IPCC Fourth Assessment Report (AR4)<sup>3</sup> provides a comparison between projections of climate change in past reports and current observations. Fig.1.1-*a* indicates that the global average air temperature near the Earth's surface rose  $0.76 \pm 0.19^\circ\text{C}$  during the 100 year period ending in 2005 and will rise a further  $1.1^\circ\text{C}$  to  $6.4^\circ\text{C}$  during the 21st century. The rate of warming averaged over the last 50 years is  $0.13 \pm 0.03^\circ\text{C}$  per decade, which is nearly twice that for the last 100 years. The global average surface temperature has increased, especially since about 1950. The bars and line shown in Fig.1.1-*b* represent annual changes in global mean CO<sub>2</sub> concentration and the annual increases that would occur if all fossil fuel emissions stayed in the atmosphere. Global GHG emissions have grown with an increase of 70% between 1970 and 2004, and the total amount of GHGs in the atmosphere has increased by about 35%.

It is clear that the problem of GHGs is related to buildings since buildings involve consumption of energy, and thereby cause GHG emissions. The WG-III<sup>4</sup> report of IPCC AR4 identifies that building is one of the main contributors to global warming. Between 1970 and 1990, direct emissions from buildings grew by 26%, and remained at approximately at 1990 levels thereafter. However, the buildings sector has a high level of electricity use and hence the total of direct and indirect emissions in this sector is 75% higher than direct emissions alone. The UN Economic Commission for Europe (UNECE) also published similar statistical results,<sup>5</sup> showing that 50% to 60% of total energy in the world is used for building operation and maintenance.

In Asia, few low-energy houses have been developed although the international dimensions of Asian energy insecurity have grown more difficult. The regional increases in CO<sub>2</sub> emissions by commercial buildings is 30% from developing Asia, 29% from North America and 18% from the OECD Pacific region. For the regional increases in CO<sub>2</sub> emissions in residential buildings, developing Asia accounts for 42% and Middle East/North Africa for 19%.<sup>6</sup> South Korea is also responsible for the large CO<sub>2</sub> emissions due to its rapid and large-scale industrialization and automotive revolution. Although S. Korea is the world's 26th-largest country in population and 11th in Gross Domestic Product (GDP), S. Korea was 10th globally in primary energy consumption in 2002, 7th in oil usage, and 5th in crude oil

---

<sup>1</sup> The WMO and the UNEP are two organizations of the UN.

<sup>2</sup> The UNFCCC is an international environmental treaty that acknowledges the possibility of harmful climate change.

<sup>3</sup> The IPCC published the first assessment report in 1990, a supplementary report in 1992, a second assessment report in 1995, and a third assessment report in 2001. AR4 was released in 2007. The IPCC AR4 consists of four reports, WG-I: The Scientific Basis, WG-II: Impacts, Adaptation and Vulnerability, WG-III: Mitigation and The AR4 Synthesis Report. WG: Working Groups.

<sup>4</sup> See footnote 3.

<sup>5</sup> Economic Commission for Europe 1996.

<sup>6</sup> The Intergovernmental Panel on Climate Change (IPCC) 2007.

imports. S. Korea confronts some of the most severe energy security issues in the world. S. Korea lacks domestic sources of energy to fuel its remarkable, rapidly growing, and energy intensive economy. Of the total energy supply, 84% comes from abroad and it is one of the highest levels<sup>7</sup> in the world. To make matters worse, it is unusually dependent on oil as a fuel source i.e. 50% of the primary energy from oil compared with a global average of 38%. The amount of discharged CO<sub>2</sub> person<sup>-1</sup> is close to 3.5 tons, and it is equivalent to the average of the OECD's level. Household heating makes up 67.7% of CO<sub>2</sub> sources. The scale is increasing and will be in the top 5 in 2010 and over the OECD's level in 2020.<sup>8</sup>

Governmental awareness of energy security problems furthers low-energy housing and development. For example, the US Green Building Council (USGBC) has led to a green building rating system called "Leadership in Energy and Environmental Design (LEED)" which provides a list of standards. The LEED rating system 4 levels<sup>9</sup> according to the energy performance of a building using an evaluation checklist which addresses six major categories: Sustainable sites, Water efficiency, Energy and atmosphere, Materials and resources, Indoor environmental quality and Innovation and design process. Buildings can qualify for 4 levels of certification. Only 35 of all residences, public and complex buildings in S. Korea could get the 1st or the 2nd grade by the LEED rating system until December 2005 due to the lack of S. Korean governmental policy.<sup>10</sup> Recently, low-energy housing has started to play a more important role in the establishment of Korea's future energy policy.

Awareness of sustainability has shifted the concerns of engineers, architects, inventors and decision makers towards a sustainable architectural design approach. Energy efficiency over the entire life cycle of a building can be achieved by the concept of sustainable architecture. Architects use many different techniques to reduce the energy needs of buildings and increase their ability to capture or generate their own energy. For example, a passive solar design allows buildings to harness sunlight for energy efficiently without active mechanical systems such as photovoltaic cells and solar hot water panels. It converts sunlight into usable heat, causes air movement for ventilating, or stores heat for future use, without the assistance of other energy sources. A passive building design generally has a very low surface area with high thermal mass to minimize heat loss.

Fig.1.2 represents a classification between active and passive design elements. A passive design utilizes building design elements e.g. windows, sunspace and thermal mass etc. to improve the building's energy performance while an active design employs some mechanics e.g. water/air collector, heat exchanger, photovoltaic, heat pumps.

---

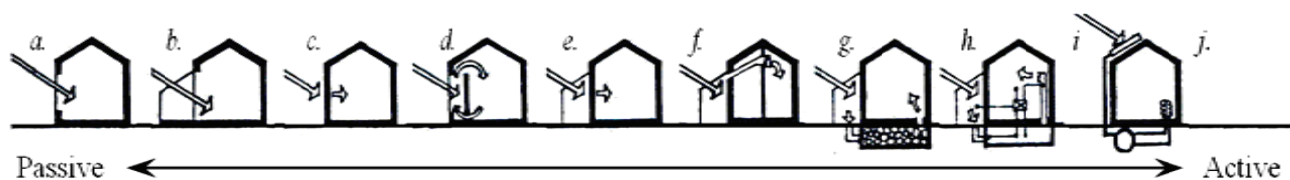
<sup>7</sup> By comparison, Japan imports 82% of its energy, Germany 60%, and the United States only 27%.

<sup>8</sup> Calder 2005.

<sup>9</sup> Platinum (52-69 points), Gold (39-51 points), Silver (33-38 points), Certified (26-32 points) and non-innovation points.

<sup>10</sup> The Korea Institute of Construction Technology (KICT) 2005.

In colder climates, heating system design is a primary focus for sustainable architecture because they are typically one of the largest single energy drains in buildings. In warmer climates, passive cooling<sup>11</sup> is also important to avoid overheating. However, in climates with four seasons such as S. Korea, a proper mixture of heating and cooling control is difficult to plan directly without using computer simulation.



**Figure 1.2.** Classification of 10 elements using the solar energy from passive to active level, a. south window, b. sunspace, c. thermal mass, d. Trombe wall, e. fore-building of glass, f. mechanics in a ~ e, g. additional storage in a ~ e, h. automatic control in a ~ g, i. water/air collectors with heat exchanger, j. high-efficient collectors (e.g. vacuum collector), photovoltaic, heat pumps etc. in a ~ i [Gonzalo 1994].

Reducing energy consumption with low energy control or switching to low carbon fuels and renewable energy are called active methods to reduce GHG emissions from buildings. With advances in architectural technology, low-energy houses, Passive House<sup>12</sup> and sustainable architecture<sup>13</sup> concepts enable improvements in the energy efficiency of new and existing buildings, to achieve the most diverse, greatest and most cost effective environmental solution. Since the 1970s, when solar architecture was first proposed, several passive methods for designs had been developed e.g. environmental architecture in the 1980s and ecological/green design and sustainable architecture in the 1990s. Low-energy house<sup>14</sup> has become a new paradigm for the 21st century by high technologies. Passive House has demonstrated energy consumption reductions of 70% to 90% in many locations of the world, without using any active power generation systems.

<sup>11</sup> Passive cooling refers to technologies or design features used to cool buildings naturally.

<sup>12</sup> The term “passive” implies that mechanical components like pumps and fans are not used. Passive house refers to the rigorous, voluntary, *Passivhaus* standard for energy-use in buildings. It results in low-energy houses that require little energy for space heating. The designs include passive solar design, high efficiency lighting and appliances, highly efficient ventilation and cooling systems, solar water heaters, insulation materials and techniques.

<sup>13</sup> From the root words “*sustenerere*” i.e. *sus* (under) + *tenere* (to hold); to keep in existence; to maintain or prolong, it is related to the concept of “green building” (or “green architecture”, “eco-design”, or “design for environment”). The two terms, however, are often used interchangeably to relate to any building designed with environmental goals in mind, often regardless of how they actually function in regard to such goals. Sustainable architecture applies techniques of sustainable design to architecture and attempts to reduce the collective environmental impacts during the production of building components, during the construction process, as well as during the lifecycle of the building. This design practice emphasizes efficiency of heating and cooling systems, alternative energy sources such as passive solar, appropriate building siting, reused or recycled building materials, on-site power generation (solar technology, ground source heat pumps, wind power), rainwater harvesting for gardening and washing, and on-site waste management such as green roofs that filter and control storm water run-off.

<sup>14</sup> In general, the meaning of the term “low-energy house (*Niedrigenergiehaus*)” has changed over time, and will certainly change in the future. Right now, it is generally considered to be one that uses around half of the German & Swiss low-energy standards mentioned below for space heating, typically in the range 30~20 kWh m<sup>-2</sup>year<sup>-1</sup>.

## 1.2. Need for energy simulation

Increased living standards in the developed world have increased energy consumption in the building sector. According to reports of Santamouris and Asimakopoulos (1996), the total number of world cooling units is more than 240 million. The reports also represent that the cooling units consume 15% of world electricity. In S. Korea, the number of houses which have an electric air conditioner or fans has rapidly increased and the electric consumption per person has greatly jumped from 4006 kWh person<sup>-1</sup> in 1996 to 7191 kWh person<sup>-1</sup> in 2006.<sup>15</sup> The balance between energy conservation and the distributed point-of-use generation of renewable energy e.g. solar energy and wind energy etc. is a key factor to achieve energy-saving in the building sector. The design significantly departs from conventional construction practice and the energy consumption can be reduced by an appropriate passive design. For example, in hot and dry climates, e.g. Mediterranean, solar protection can reduce 20% of the cooling loads and air conditioning can be completely avoided since the internal heat gains are not important. However, energy-saving in a largely varying climate is often seen for architects to be too complex or too time consuming. A largely varying climate in S. Korea (i.e. cold and dry in winter, hot and humid in summer) requires consideration of both heat gain and heat loss. For example, passive solar design gives some heating gain in cold winter, but the heating gain makes the condition uncomfortable in hot summer.

Korean climate<sup>16</sup> is cold and dry during winter and extremely hot and humid in summer. The southern regions are classified as subtropical zone affected by warm ocean waters including the East Korea Warm Current. Fig.1.3-*a* shows the climate zones in S. Korea. The entire Korean peninsula is influenced by the East Asian monsoon in midsummer and the frequent incidence of typhoons in autumn. The majority of rainfall takes place during the summer months, with nearly half during the monsoon alone. During the spring and fall seasons, the movement of high atmospheric pressures brings clear and dry weather to the peninsula. The graphs shown in Fig.1.3-*b* are the local temperature and rainfall. The yearly average temperature ranges 6°C to 16°C with a relatively high temperature variance throughout the regions and the average temperature across the peninsula, with the exception of the mountainous areas, ranges 10°C to 16°C. In August, which is considered to be the hottest month of the year, the average temperature ranges 26°C to 32°C whereas in January, which is considered to be the coldest month of the year, it falls below freezing between -6°C to -7°C. In this climate, the thermal interactions between a building and its external environment are complex. To account for the complexities of the energy transfer processes occurring between inside and outside and among its various components and

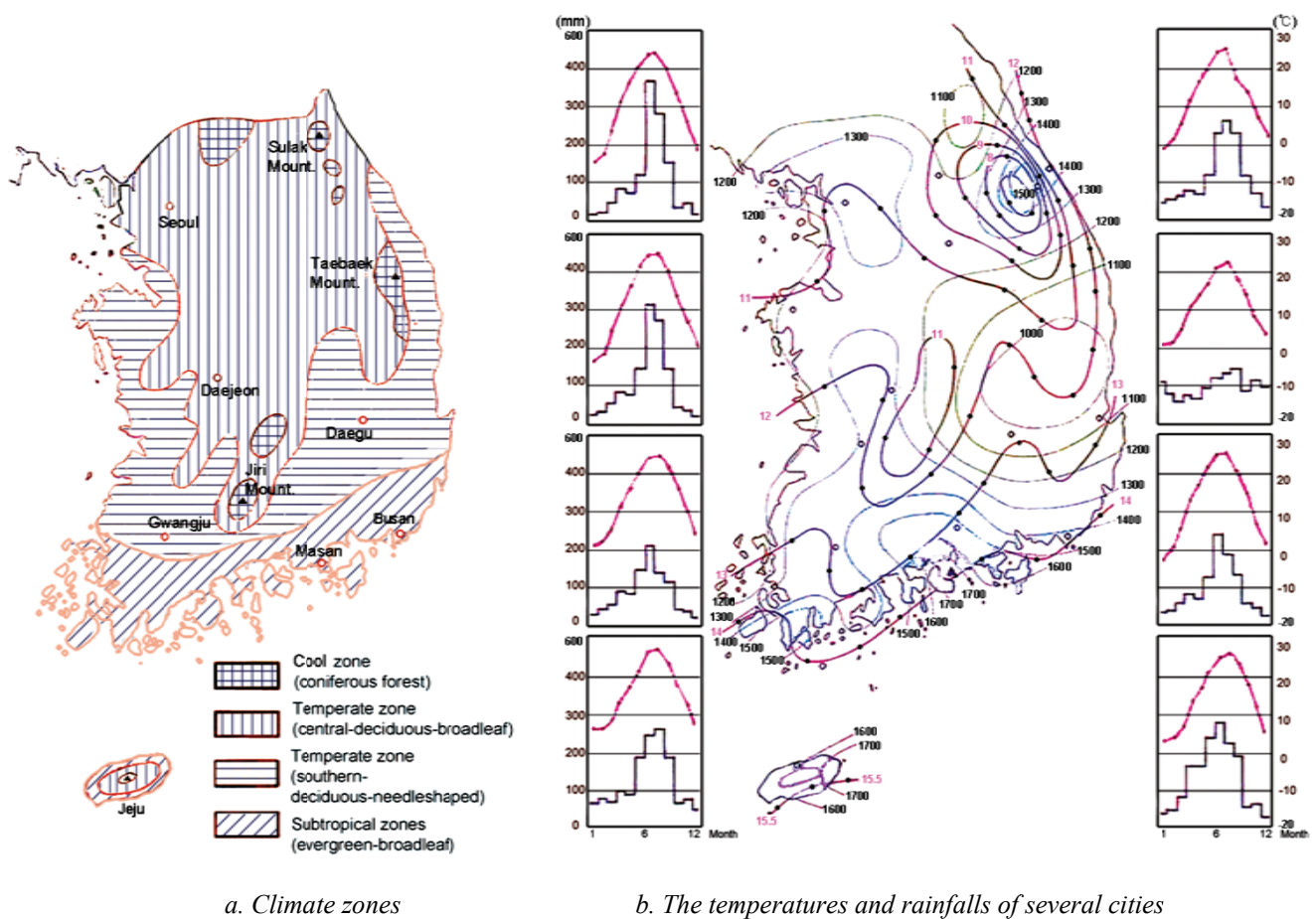
---

<sup>15</sup> Korea Electric Power Corporation 2007.

<sup>16</sup> See chapter 6.3.

systems, computer simulation software e.g. DOE-2, BLAST, TRNSYS and EnergyPlus (EP)<sup>17</sup> have developed.

For a long term considering environment, maintenance and energy costs etc., the total building cost will be much higher than building construction costs. Hence, building energy simulation is used as a tool in architecture, for determining compliance with building standards and for the long term economic optimization of building components. There are various economic consequences of the decisions made during the design process. Energy simulation attempts to account for a lot of factors in determining the heating, cooling and ventilation loads within a building, the equipment types and sizes, and the cost to operate this equipment.



**Figure 1.3.** Climate of local regions in S. Korea [S.H. Lee et al. 2005, Britannica Encyclopaedia 2004].

Climate is an environmental factor affecting architecture and its built environment.<sup>18</sup> Energy simulation analyzes climate data to provide complementary information about the energy performance and

<sup>17</sup> The US department of energy 2007a.

<sup>18</sup> The phrase “built environment” refers to the man-made surroundings that provide the setting for human activity, ranging from the large-scale civic surroundings to the personal places.



accurate comfort prediction. Energy simulation software can predict the energy performance of a building with both passive designs and active building envelopes. However, the programs are based on the zonal approach in an attempt to reduce computation time and complexity. The zonal approach breaks down the object into zones, where each zone is considered to be in a thermal state. However, this method is unable to give an accurate and detail prediction result since the real thermal state of a zone is not uniform. The Computational Fluid Dynamics (CFD) approach is the quantitative process of modeling fluid flows by the numerical solution of governing partial differential equations or other mathematical equations of motion mass, and enthalpy conservation. The CFD approach uses realistically representative of the true 3D environment with non-uniform energy distributions. 3D space is divided into grids, where each node on the grid is given an initial value for different environmental parameters. This approach represents thermo- and aerodynamic movements and more accurately than the zonal approach. For this reason, there is a need to spend a lot more time and effort in simulation preparation.

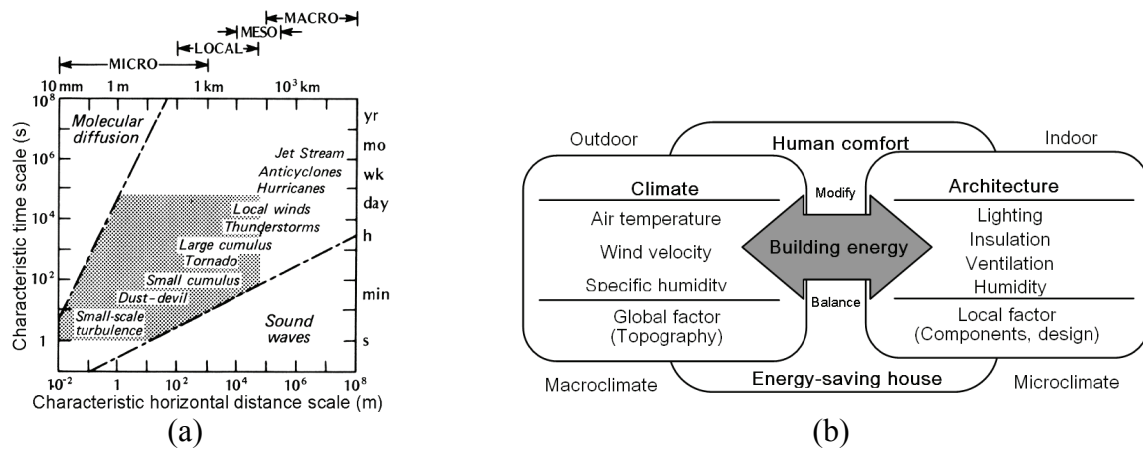
### 1.3. Research objective

A problem with energy simulation tools is that climate data is not on the scale of individual buildings. General climate data of a region are generated by a weather station which is located across several hundred kilometers. The simulation tools generally assume isothermal condition<sup>19</sup> in a building zone and set up the zones to utilize such large-scale climate data for the building energy analysis and comfort prediction. However, a building can be placed in a local atmospheric zone where the climate differs from the surrounding area. Such a local climate with small-scale atmospheric phenomena is called “microclimate”. Fig.1.4 (a) shows four different climate scales i.e. micro-, local-, meso- and macroclimate. A small area such as a garden or courtyard can have several different microclimates depending on how much sunlight, shade, or exposure to the wind there is at a particular spot. Microclimate within a given area is usually influenced by hills, hollows, geometric structures or proximity to bodies of water.

Microclimate is strongly related to energy balance which is a systematic presentation of energy flows and transformations. When energy source is concentrated at a particular spot, the energy is continuously moved from an area of high concentration to an area of low concentration in a given volume. Similarly, microclimate around the building can be modified by the environment and even by architect’s designs. Microclimate is important because it can alter the building’s energy efficiency. The building thermal condition can be modified by energy gains, leakages and distributions related to energy balance. In this

---

<sup>19</sup> Zonal energy simulation methods use Finite Volume Method (FVM) which has a single node with an average temperature value for each zone. A zone is considered as an iso-thermal condition with the average temperature.



**Figure 1.4.** Climate scales, (a) time and distance scales, (b) macro- and microclimate [Oke 1987, author].

study, a novel design method which considers microclimate for the energy-saving is studied. A combination of zonal and CFD methods is employed for energy simulation of the building.

Air temperature is the most important to predict for human comfort and to determine the building energy since it is a measure of thermal content in the air. Air temperature is made by a joint effect with precipitation, humidity and wind speed and air pressure which significantly influences heat transport through the air. Temperature can be used as a tracer to detect the spatial and temporal variations of microclimate in the structures and spaces e.g. walls, roofs, windows, doors, courtyard and rooms etc. However, it is very difficult to predict accurate air temperature in the complex morphological structure with aggregated walls and volumes of a building. A zonal method which divided the structure into small zones is used to predict initial thermal state. The average air temperature of each zone is estimated using general and large-scale climate data and different temperatures between adjacent zones derives thermo- and aerodynamic flows related to energy balance. CFD analysis predicts variances from the zone's average temperature, which are the microclimate effects. Thermal variation between the building in- and outside is inter-space ventilation which is affected by different height-to-width room ratios. The surface elements of each room have different physical properties as well as different exposure to thermal content. Energy balance between adjacent rooms generates thermodynamic flow. This combination of zonal and CFD methods acts a hierarchical and multi-scale prediction from macroclimate to microclimate. Microclimate analysis in this study enables to predict temporal and spatial variances in the planning. Fig.1.4 (b) illustrates the relationship between macro- and microclimate in a building simulation and macroclimate means general large-scale climate data for the large area, which are distinguished from the microclimate.

Research objective is summarized as

- Investigation for novel and advanced energy-saving methods in a house design
- Extension of the existing energy simulations, which considers microclimate around a house
- Establishment of microclimate factors influencing the low-energy house.

- Quantitative analysis and evaluation of the factors

To achieve the microclimate energy-saving, design elements are considered by following questions:

- What is the building microclimate?
- Which microclimate phenomena will be considerable for energy-saving in buildings?
- Why does a complex Passive House need energy simulation?
- What is missing in previous energy simulation for complex Passive House designs?
- What is the method of energy simulation?
- How can microclimate effects be analyzed?
- Is architectural design considering microclimate efficient?

This study evaluates the indoor comfort problem in a real house model and tries to improve the human comfort condition without large energy requirements. A certain number of hypotheses are set out using common knowledge for Passive House designs:

- West orientation of the building façade is not sufficient for assuring good thermal insulation for whole houses in slope topography.
- Elimination of shading devices from the façade dramatically affects increasing heat entering through the windows into the house.
- Bad insulation is partly responsible for the lack of convenient thermal comfort in the house.
- Microclimate effects can be often observed with the lack of thermal comfort.
- A suitable microclimate design improves the energy efficiency of the house in some special climate.

## 1.4. Constraints

(1) In this study, influences of neighboring buildings are not considered since analysis of microclimate in and around a building increases complexity. However, this consideration enables concentration on the accuracy of the building analysis.

(2) This study assumes that the building site is a simple slope model without deformation. A simple slope model is useful for architects to define several site conditions with topography and makes the geometric analysis easy. Fig.1.5 shows a normal site condition with topography in S. Korea. In Seoul, the percentage of slope areas for building reconstruction is amounted to 66.5%.<sup>20</sup>

---

<sup>20</sup> Kang 1996.



**Figure 1.5.** An example of S. Korean site set-up including slope areas.

(3) Only  $0^\circ$  to  $19^\circ$  slopes are considered. According to data of Ministry of Construction and Transportation (MOCT) of S. Korea, only 32.5% of the land is flat with  $0^\circ$  to  $9^\circ$  slopes which a normal or flatland design can be applied.  $10^\circ$  to  $29^\circ$  slopes are possible to be developed by slope design. However, slopes above  $30^\circ$  are impossible to be used for building sites. In S. Korea,  $10^\circ$  to  $29^\circ$  slopes make up 53.2% of the total land. Within these angles, a lot of slope and flatland designs are mixed. Above  $20^\circ$ , totally different forms from flatland designs should be considered.<sup>21</sup>

(4) This study targets high density housing in S. Korea. It is strongly related to a ratio between the population and the total habitable land. The population of S. Korea is 48 million people, which are about 60% of 82.43 million in Germany. The habitable land in Seoul is  $606\text{km}^2$  and the population is 10.35 million people. The population density (people  $\text{m}^{-2}$ ) of S. Korea is 17.994, which is lower than 20.246 of Paris but higher than 13.657 of Tokyo, 9.475 of New York City and 2.093 of Hong Kong.<sup>22</sup>

(5) The study target is a detached dwelling. About 80% of residences in Seoul were detached dwellings before the 1970s;<sup>23</sup> developments from the detached dwellings to high rise apartments have decreased living quality and made several environmental problems. Recently, the percentage of high rise apartments in Seoul is 55.2% and detached dwellings and apartment units are respectively 22.8% and 17.3%. It was caused by development policy during the 1970s and the 1990s to solve the population explosion of Seoul after the rapid industrialization. However, it is clear that an innovative design to improve the living quality and the economic attraction for the choice of a future detached dwelling or to propagate the low storey and high density houses widely is a continuing solution to reform the problems of prevailing high rise apartments progressively.

In the last 15 years, an apartment is seen as an investment, with large profit margins. In recent years, the S. Korean government policy which bans the large profits is in operation. 64% of old age people in S.

<sup>21</sup> H.J. Kim 2001.

<sup>22</sup> Seoul Statistical Yearbook 2007.

<sup>23</sup> Seoul Statistical Yearbook 2007.

Korea are living in detached dwellings and only 17.3% in apartments. The fact suggests that the fashion of apartments was not for living but for profit. If no profit will be expected in the future real estate market by efforts by the S. Korean government, actual demands will pursue the living quality or to prepare for old age. A form of detached dwelling or the low storey and high density house in S. Korea which are built by environmentally friendly and “well-being” concepts may be expected to be popular. The goal of this study is to expand them and for this reason, a residence model in one suburb of Seoul has been chosen.

## **1.5. Structure of thesis**

Chapter 2 introduces heating and cooling in Passive House designs in various climates and the importance of energy-saving in the designs. Advanced Passive House design methods use energy simulation which predicts energy gain, loss and distribution of building sectors in the design procedure. This chapter describes common physical bases in energy simulation methods.

Many aspects for an energy-saving house which can be considered for the climate response, but not all of them can be useful for the climate. Heating and cooling in a passive design are not always efficient for human comfort, and additional energy should be input to try to correct the climate, actively. Therefore, it is important to establish at the early stage which elements in passive design cause the problems. Hence, the next chapter describes the energy-saving issues and the ill-posed problems of the existing passive designs. Energy-saving which is developed in this study is obtained by advanced design with computer simulation which can measure thermo- and aerodynamic variations by microclimate in the design.

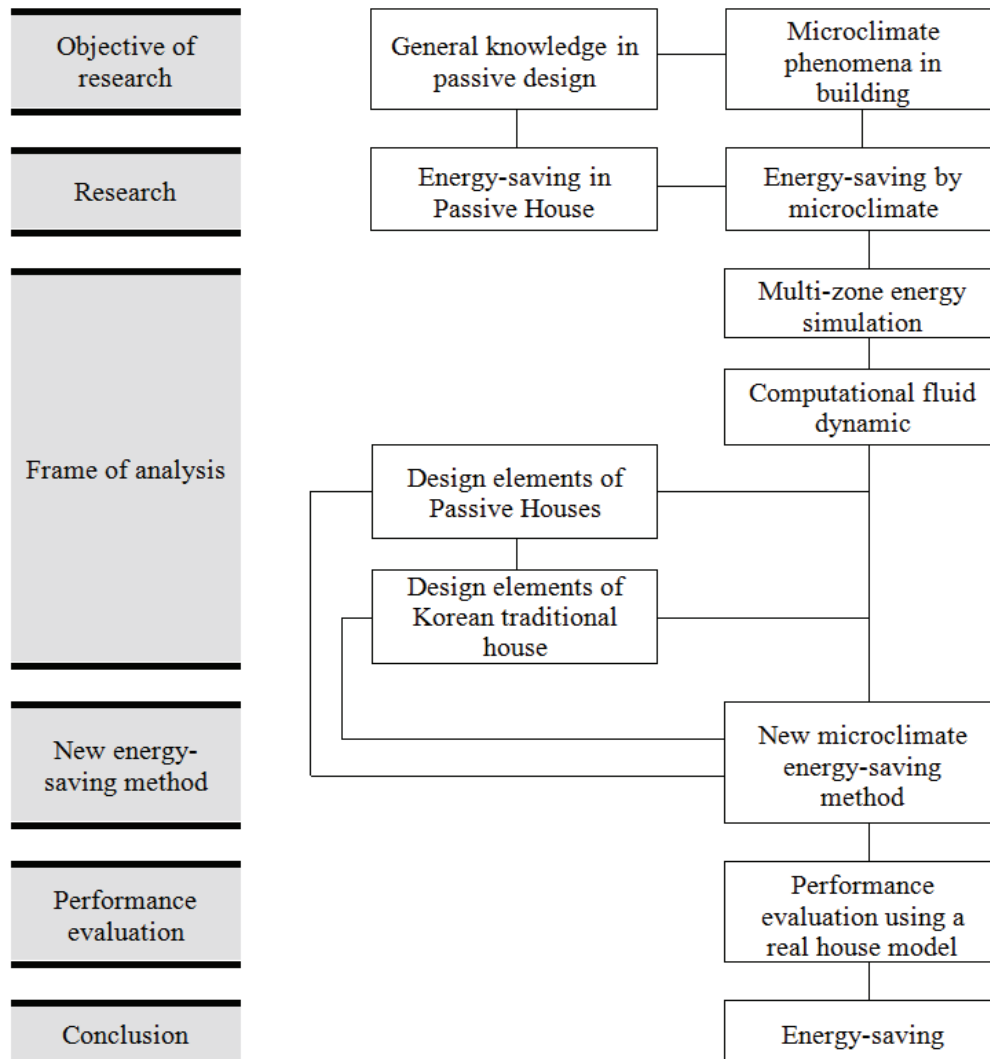
Passive and dynamic control of microclimate is helpful to accomplish the energy efficiency in the building. Chapter 3 gives the details of the high-performance novel design with microclimate energy-saving methods including dynamic flow controls. It includes issues of site planning and general concepts for building forms and the elements to modify the flow as well. The method can predict energy details, distributions, gains and losses in the thermo- and aerodynamic phenomena in building sectors. The simulation result enables to provide detail information about the energy usage and leakage in the zones. The method plays an important role in determining the overall efficiency of a complex architectural design with an early consideration that can be a great benefit. For example, when the methods are applied in a difficult mixed climate i.e. seasonally hot-humid and cold-dry, it makes the appropriate decision of an architectural design easier and economical. The numerical simulation is used to analyze microclimate effects by several design elements.

In chapter 4, a novel simulation model combining multi-zone and CFD energy simulations is introduced for the analysis of energy-saving aspects in passive and microclimate design elements. The multi-zone model generally uses a parameterization method to simplify the energy-saving problem for each space in a building. However, the model is not appropriate to handle the dynamic energy variations since it calculates the averages for each zone volume. On the contrary, the CFD method using subdivided grid units is more suitable for the microclimate analysis. However, the main difficulty of CFD is the convergence of the problem with the solution. These problems can be solved by a multi-scale hybrid method combining the multi-zone and the CFD models. The several climate scales can be a volume and the subdivision, which are adapted in units of the multi-scales.

A case study using a real Passive House model in the mixed climate of S. Korea is represented in chapter 5 and 6. Energy-saving houses using general passive features are tested and evaluated in the house model. The multi-zones are simulated to evaluate the energy performance of the passive designs. If the microclimate method is tested, the difference of the energy usages can be compared by a quantitative analysis. The comparison between one of the most famous multi-zone energy simulation tools EnergyPlus (EP) and the simulation of microclimate energy-saving model in this study are evaluated to prove the efficiency of the novel method.

The Conclusions and the future study are represented in chapter 7. This method can be utilized to bring about valuation items in microclimate phenomena to accomplish the energy-saving and the prediction possibility.

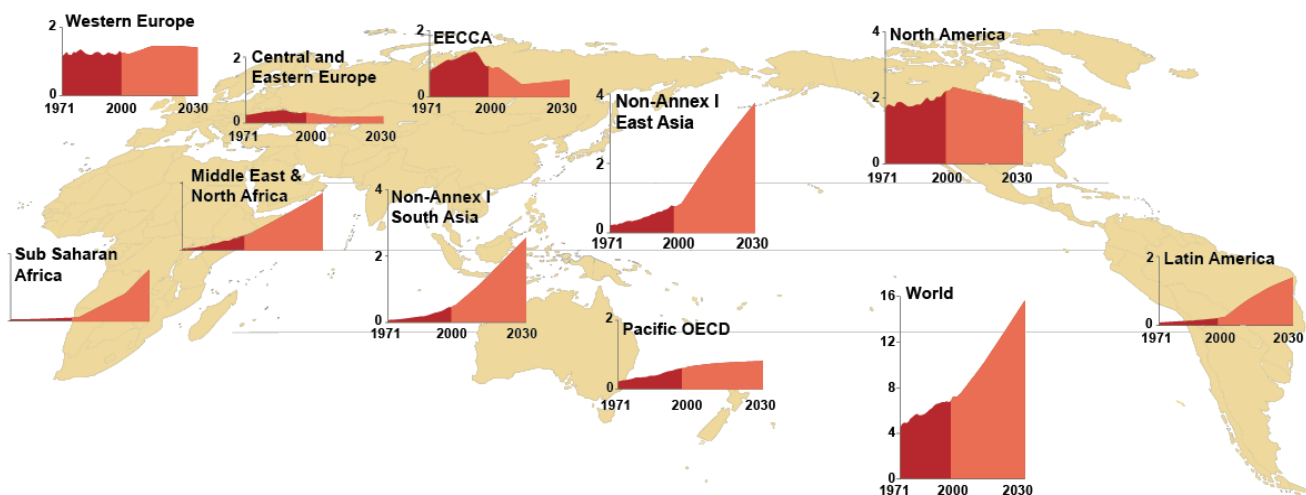
## Research flowchart



## 2. Energy-saving and climate in the Passive House

### 2.1. Energy in Passive House

In the field of architecture, a lot of endeavors for energy-saving, prevention against pollution and recycling resources were made, since 50% to 60% of the total energy in the world is used for building and maintenance of architecture.<sup>24</sup> Fig.2.1 shows the CO<sub>2</sub> emissions scenario for the buildings sectors of 10 world regions produced by IPCC (2007). There will be approximately 81% increase of total CO<sub>2</sub> emissions from 8.6 GtCO<sub>2</sub> emissions in 2004 to 15.6 GtCO<sub>2</sub> emissions in 2030. This scenario shows a range of increasing buildings related CO<sub>2</sub> emissions. Especially most increases of CO<sub>2</sub> emissions are produced in the developing world: Developing Asia, Middle East and North Africa, Latin America and sub-Saharan Africa, in that order. East Asia shows increase of more than 150%.



**Figure 2.1.** CO<sub>2</sub> emissions for the buildings sector including electricity [The Intergovernmental Panel on Climate Change (IPCC) 2007].

Realizing the low-energy houses require an integrated design process which involves architects, engineers, contractors and clients, with full consideration of opportunities in reducing building energy

<sup>24</sup> Economic Commission for Europe 1996.



demands. A lot of European countries are promoting the construction and distribution of low-energy buildings since the largest savings in energy-use can be obtained in new buildings through building design and operating plan. An EU project called CEPHEUS (the Cost Efficient Passive Houses as European Standards) is an example of the largest Passive House project which has built 221 houses<sup>25</sup> using Passive House standards.

Passive house method focuses to accomplish energy-saving by architectural planning and modeling with minimum or without a mechanical assistance. However, it needs a lot of expertise and solutions because a Passive House design is composed of several thousand building components. Conservation of energy in innovations of architectural design should be checked for correspondence the Passive House Standard and the world's premier test of energy efficiency. The following specifications have proven to achieve the Passive House Standard:<sup>26</sup>

- Insulation value of the envelope must be under  $0.15 \text{ W m}^{-2}\text{K}^{-1}$ .
- The external envelope must be constructed without thermal bridges.
- An air leakage test must be performed, and the air exchange result must not exceed 0.6 times  $\text{h}^{-1}$  by over and under-pressurization tests with a pressure of 50Pa.
- Windows, i.e. frame and glazing, must have total U-values under  $0.8 \text{ W m}^{-2}\text{K}^{-1}$ , and glazing must have total solar energy transmittance of at least 50% to achieve heat gains in winter.
- Ventilation systems must be designed with the highest efficiency of heat recovery and have minimal electricity consumption.
- A domestic hot water generation and distribution system with minimal heat losses should be used.
- It is essential to use highly efficient electrical appliances and lighting and total primary energy consumption has to be below  $120 \text{ kWh m}^{-2}\text{year}^{-1}$ .

Since the 1970s as solar architecture was first proposed, more advanced ideas were developed for Passive House: environmental architecture in the 1980s, ecological/green design and sustainable architecture in the 1990s. Nowadays they are integrated in new paradigms for the 21st century including high technologies, e.g. “Zero Energy Building” and “Green Building”. The methods additionally utilize natural energy, life-cycle-cost and comfortability modeling etc. to improve the energy efficiency of building and to suppress an increment in entropy leading to a disordered state of energy. Green space or Biotope can be also considered to recover the ecological balance. However, one of the most important factors is the improvement in the heating and cooling consumption for the economic feasibility of these technologies.

Ulseth et al. (1999) estimated the expected development of the heating and the cooling consumption in

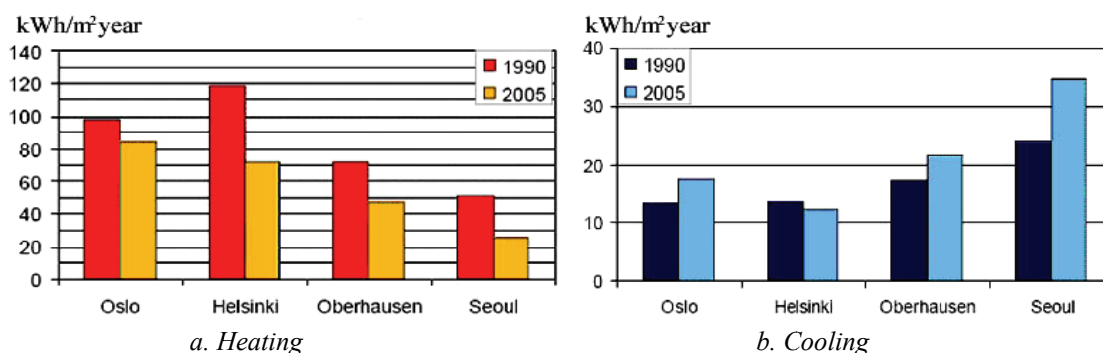
---

<sup>25</sup> Feist et al. 2001.

i.e. 84 houses were in Austria, 72 in Germany, 40 in France, 20 in Sweden and 5 in Switzerland.

<sup>26</sup> Feist et al. 2001.

a future building stock by comparing to today. For the purpose, a simulation tool calculated the heating and cooling loads and the energy consumption of a “typical” office building and a “typical” residential building in 1990, and compared the loads and energy consumption to an expected “typical” building in 2005. The simulation assumed typical climate situations of 4 countries; Norway, Finland, Germany and S. Korea, and the local climate data are based on a standardized “reference year”. Buildings are based on the national building codes in respective countries. Fig.2.2 represents the comparison of heating and cooling energy consumptions in residential sectors of the countries. In the case of S. Korea, the heating energy consumption was  $50 \text{ kWh m}^{-2}\text{year}^{-1}$  in 1990 and 44% lower than  $28 \text{ kWh m}^{-2}\text{year}^{-1}$  in 2005. 40% cooling energy consumption was increased from  $25 \text{ kWh m}^{-2}$  to  $35 \text{ kWh m}^{-2}\text{year}^{-1}$ . Designing a building to be energy efficient is difficult without understanding the relative importance of factors which contribute to achieving energy-saving. Hence, the following chapters focus on setting out effective energy-saving factors. Each of the following chapters introduces some elements and their features in helping to produce low energy buildings.



**Figure 2.2.** Energy consumption in residential sectors of some cities [Ulseth et al. 1999].

## 2.2. Human comfort factor

Human comfort may be the most important aspect of energy consumption. If the occupiers are not satisfied with the comfort condition of the building, they consume more energy to make better conditions for themselves. The human body has a complex thermodynamic mechanism susceptible to slight temperature change in the environment. Human skin is always exchanging heat with the surroundings through thermodynamic mechanisms such as radiation, conduction and convection. It can be determined by steady-state heat transfer and the energy balance between the body and the environment. The human comfort level can be also affected by air motion in building where the room temperature is varying with inflows and outflows. In energy simulation studies, building comfort is generally controlled by four major factors: air temperature, Mean Radiant Temperature (MRT), humidity and airflow. However, it is clear that human comfort is a very complex issue for decisions on

building design policy since there is always a likelihood of some mismatch between the design intention and the real human perception. The relationship between the factors and comfort is not necessarily additive and practically never linear. Temperature and humidity largely affect human comfort more than other factors, and thereby understanding these factors is very important. Psychometric measures such as Givoni chart, Mahoney table and PMV (Predicted Mean Vote) etc. are studied for this purpose.

### 2.2.1. Psychometric comfort scale

Climate is a key factor for building design and it influences on the effectiveness of social activity, human comfort, health, physical resource and energy-use etc. Psychometric comfort scale is used to indicate measures of effectiveness, and the psychometric chart provides a graphic representation of the comfort state and the climate at a location. The most famous psychometric measures are the Givoni chart,<sup>27</sup> Mahoney diagram<sup>28</sup> and PMV. Psychometric comfort measures can be used to make building design policy. For example, if temperature and humidity are outside of the comfort zone, ventilation and dehumidification should be considered in building design.

Fig.2.3 shows the Givoni chart for the climate of S. Korea. The horizontal and vertical axes of the chart respectively indicate temperature scale and moisture scale. The air temperature represented by the horizontal axis of the chart is known as the dry bulb temperature. The vertical axis is known by a number of names, such as specific humidity, absolute humidity and humidity ratio. They all represent the same measure: the amount of water by weight in the air.<sup>29</sup> If the temperature of the air is decreased to the point at which it can hold no more moisture, the air becomes saturated. The corresponding temperature is called “dew point”. When the air is cooled to the dew point, it is at 100% relative humidity (RH). This saturation point is represented by the outer, curved boundary of the chart. The brightness in the graph represents the frequency of days corresponding to the value. In Fig.2.3, the seasonal climate of Korea can be estimated, and a lot of hot and humid days in summer and cold and dry days in winter make uncomfortable conditions. The square area in the chart represents the psychometric comfort condition. The Mahoney diagram<sup>30</sup> offers a lot of design recommendations, e.g. layout, spacing, air movement, openings, walls, roofs, protection from rain, size of opening, position of openings, protection of openings, walls, floors, roofs and external features etc., for human comfort by analyzing the Givoni chart. However, the Givoni chart and the Mahoney diagram are often not exact in

---

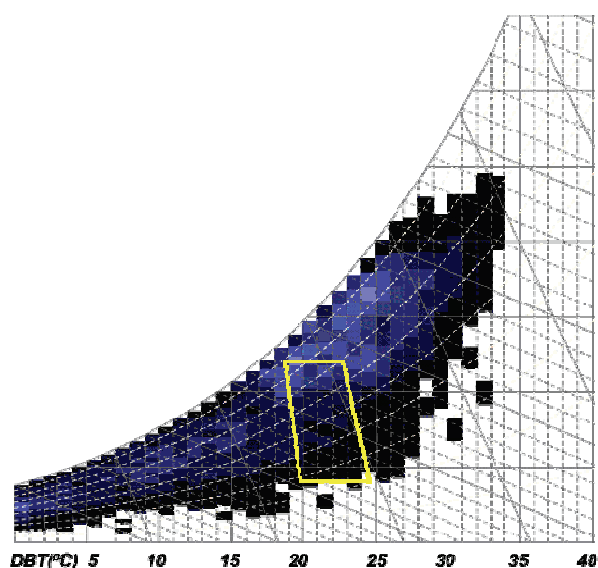
<sup>27</sup> Givoni chart is also called psychometric chart.

<sup>28</sup> Daoudi 2002.

<sup>29</sup> The units often can be given by the moisture scale, which is represented by two other names: vapor pressure, which is the partial pressure exerted by the moisture in the air, and dew point temperature which is an exponential temperature scale representing the temperature at which moisture will begin to condense from a given unit of air.

<sup>30</sup> Casey 2002.

measuring the real condition of how humans feel because they do not consider the narrower range of temperatures arising from detailed environments. For example, the felt temperature of a window façade with solar radiant gain in a cold winter may not be cold but be warmer than in reality.



Scale	Sensation
+3.5	Very hot
+2.5	Hot
+1.5	Warm
+0.5	Slightly warm
0.5	Neutral comfort
-1.5	Slightly cool
-2.5	Cool
-3.5	Cold
	Very cold

**Figure 2.3.** Psychrometric chart of Seoul [author]. **Table 2.1.** Thermal sensation scale for the PMV, *metabolite rate 80W, 0.9 clo* [Mayer and Matzarakis 1999].

To solve the problem, physiologically relevant indices which are derived from the human energy balance to detailed environments were established.<sup>31</sup> A model for the thermal complex of human energy balance is Munich Energy Balance for Individuals (MEMI), which uses the assessment index Physiologically Equivalent Temperature (PET). A final output of the model is the calculated Mean Radiant Temperature (MRT) which is required in the energy balance model for humans and thermal indices such as PET, Standard Effective Temperature (SET) and Predicted Mean Vote (PMV, ISO 3787).<sup>32</sup> Recently, PMV is used for the physiologically relevant evaluation of thermal components of urban and regional climate which are based on the human energy balance. The PMV index quantifies the degree of discomfort according to the psychological scales which are listed in Table 2.1. Negative values indicate uncomfortable feelings due to a hot sensation. Zero is the neutral point, representing comfort. In a case study<sup>33</sup> for different designs of the planning called “Stuttgart 21”, PMV and PET are derived from the parameters of wind, temperature, humidity and radiation for 2 different meteorological situations. These parameters determine the thermal comfort in the community. In densely built up regions or poorly ventilated city centers, effects of the air temperature and humidity are also studied.

<sup>31</sup> Höppe 1993.

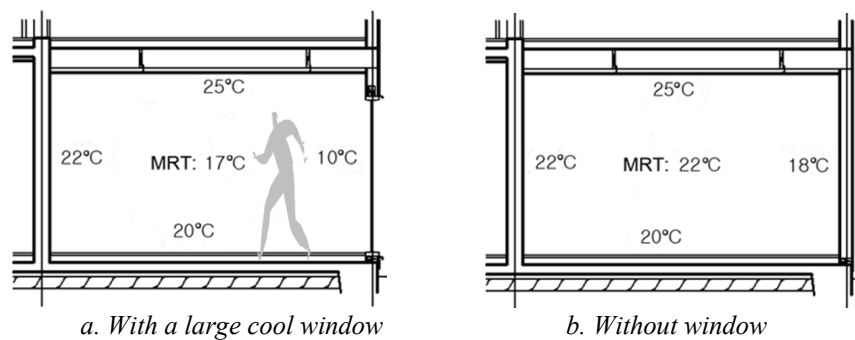
<sup>32</sup> Mayer and Matzarakis 1999.

The German VDI-Guideline 3787, VDI: *Verein Deutscher Ingenieure*/ German Engineering Society.

<sup>33</sup> [www.lohmeyer.de/air-eia/casestudies/](http://www.lohmeyer.de/air-eia/casestudies/)

### 2.2.2. Comfort zone

A lot of statistical studies, which arrive at a quantitative description of human comfort, have been performed on large numbers of subjects of all ages, sexes and nationalities. The results of these studies provide a comfort zone with a relatively wide band of acceptability in which 80% of the population experiences the sensation of thermal comfort. Psychometric charts can be used to show graphically the condition of the comfort zone. However, only a few studies have attempted to express the additional major comfort variables such as Mean Radiant Temperature (MRT) and air motion.



**Figure 2.4.** Actual temperature as perceived by a person and MRT [author].

The MRT of a space is really the measure of the combined effects of temperatures of surfaces within that space. The MRT is the measure of all these surface areas and temperatures acting on a person's location in the room. Even in an environment with some differences between the air temperature and the surface temperature of the walls, ceiling, windows and floor etc., a building zone which is well insulated and does not have extensive glazing as Fig.2.4-b shows have small temperature differences between the air and the surfaces. However, if there is a significant difference in the space as Fig.2.4-a represents, this difference will affect the perception of comfort. For the center of a zone, each surface plays an equal part in determining the average. However, if the person was sitting near a large window with a temperature of 10°C, the MRT would be in a region of 17°C. At the optimum level, the radiant exchange of the human body with the surroundings can account for about 50% of the body's ability to lose heat. Therefore, if MRT is increased, the net radiant exchange from the body to the surroundings will decrease. Inversely, if MRT is decreased, the net radiant exchange from the body to its surroundings will increase. This has proven to be a very powerful passive building technique for both heating and cooling.

A large air motion across the skin can greatly increase the tolerance for higher temperature and humidity levels. HVAC studies by Fanger (1870) showed that at least 28°C, a very large air velocity of 91.44m min<sup>-1</sup> across the skin can maintain the human comfort even in 100% relative humidity. Ceiling

fans were used to produce this air motion. At below 50% relative humidity (RH), much higher temperatures up to 32°C are also comfortable at this air velocity. Air motion across the skin accomplishes cooling through both convective and latent energy, i.e. evaporation of perspiration from the skin transfers. Since skin temperatures are relatively high, even 32°C air temperatures can carry off some excess heat. Additionally, at high RH, near or at 100%, if dry bulb air temperatures are lower than skin temperatures, evaporation from the skin will occur. By the use of materials capable of storing relatively large amounts of thermal energy, e.g. concrete and masonry products, water, and Phase Change Materials (PCMs) etc. heat collection and rejection techniques can be effectively applied to Passive Houses. The studies of the comfort zone in effective design were provided by Givoni (1994). By architectural design with thermal mass and ventilation, various building zones based on exterior climate can have additional comfort producing potentials. A research of Loxsom and Clarke (1980) indicated that radiative night cooling in conjunction with thermal mass and air motion can extend the results of Givoni.

### 2.3. Aerodynamic and energy contents

The psychometric measures are important since the total energy in temperature and vapor content (i.e. energy content) of building air can be calculated.<sup>34</sup> The total air energy is achieved by the sum of both the temperature content and vaporized moisture content. The temperature content is physically called “sensible heat”.<sup>35</sup> The moisture content is called “latent energy” since the vapor in the air represents approximately 334 kJ kg<sup>-1</sup> of latent heat energy. Normally, the humidity of the air is not generally regarded as being important since the humidity percentage usually ranges from about the mid 30s to the upper 60s and occupants are quite able to tolerate this range.<sup>36</sup> However, if the humidity is in the upper 60s along with high air temperatures and very little air movement this may give rise to a larger proportion of the occupants feeling uncomfortable.

The sum of the latent energy and the sensible heat is called the air enthalpy (kJ kg<sup>-1</sup>). Air at 0°C and 0% RH is assumed, by convection, to have an enthalpy of 0 and is used as the base for the enthalpy scale. In

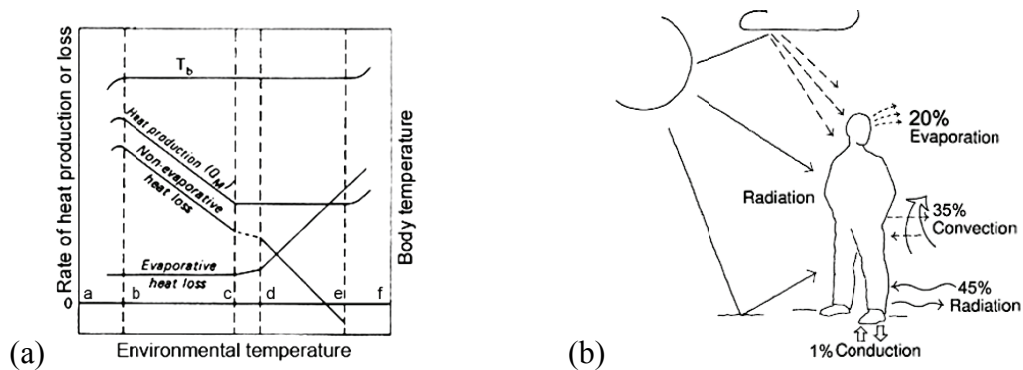
---

<sup>34</sup> Fairey 1994.

<sup>35</sup> Sensible heat is potential energy in the form of thermal energy or heat. The thermal body must have a temperature higher than its surroundings. The thermal energy can be transported via conduction, convection, radiation or by a combination thereof. The quantity or magnitude of the sensible heat is the product of the body's mass, its specific heat capacity and its temperature above a reference temperature. A transport of heat from a warm area to a cold area is affected by the sensible heat in the form of warm air moving toward the cold air, and by latent heat as cold air moving toward the warm area.

<sup>36</sup> Ward 2004.

Fig.2.5 (a), the lines of constant air enthalpy<sup>37</sup> follow almost exactly the line of constant wet bulb temperature that can be simply measured by a relatively accurate measurement of the heat content of the air. The higher the wet bulb temperature, the greater the energy content of the air. Hence, enthalpy can be used for numerical calculations of the energy required to change the conditions of the air e.g. heating, refrigeration and air conditioning. Through understanding this process, it will be easier to evaluate and modify designs to maintain thermal comfort.



**Figure 2.5.** Relationship between body temperature and the energy balance, (a) the components over a range of environmental temperatures, deep-body temperature  $T_b$ , (b) the four modes [Oke 1987, modified from Rosenlund 2000].

The wet bulb temperature can be rather easily measured by a standard thermometer which has its sensing bulb encased in a wetted wick that is subjected to air motion across its surface. Air motion across the surface of the wick and wet bulb causes moisture to evaporate from the wick. This evaporation process cools the wick and the sensing bulb by an amount which is directly proportional to the additional amount of moisture which the air-stream is capable of absorbing. In other words, saturated air would, theoretically, not cool the wetted bulb by a substantial amount. Therefore, for the greater difference in temperature between the wet and dry bulb thermometers, the lower moisture and energy content of that air-stream.

This is also the method by which evaporative cooling of the skin occurs and is the major reason that relative humidity levels have such great import on the body's ability to maintain comfort. In arid climates, the evaporative principle can be used to advantage to cool the air. The swamp cooler exchanges the sensible heat of the air (i.e. temperature content in the air) with latent heat (i.e. moisture content in the air), and the air is thereby cooled along a line of constant wet bulb temperatures.

The other mechanism is by convective cooling using air velocity. As the humidity of the air increases, evaporative cooling of the skin is reduced and eventually ceases when very high humidity is reached. At such a discomfort humidity level, one way to help the evaporation of sweat from the body is to increase

<sup>37</sup> a~b zone: hypothermia, b~e zone: thermoregulation, c~d zone: least thermoregulatory effect, c~e zone: minimal metabolism, e~f zone: hyperthermia, b: temperature of summit metabolism and incipient hypothermia, c: critical temperature, d: temperature of marked increase in evaporative loss, e: temperature of incipient hyperthermia.

the airflow rate over the body. This is convective cooling which is efficient in the subtropical region. The faster the air passes over the body, the more its ability to remove heat by convection is increased. The cross-ventilation of a building is advantageous to get the higher air velocity. However, if the air speed is too high then we feel a draught and if too low, we feel stuffy. Fig.2.5 (b) illustrates the four modes of energy balance in the human body.

## 2.4. Design for energy gain

Energy-saving in buildings is closely related to the climate since the designs should be adapted to the seasonal demand for energy. The demand for energy in a Passive House is dependent upon the energy gain from the climate. The most important source of energy gain in passive design method is solar access. A typical solar access situation where the southeast to the southwest aspects of the building are open to the sun is represented in Fig.2.6. Leaving open the south façade allows maximization of its effect when considering solar heating. The east or west façade is more susceptible to receiving low altitudes of sun in the morning and evening. Low altitudes of sun contributes to likely overheating and is always more difficult to handle the problem than the higher altitude sun during the midday. If glazing on the east and west façade is avoided or the south façade is shaded, the overheating effects can be eliminated.



**Figure 2.6.** Typical design approach when considering solar access by G. Watrous in Kentucky [The Kentucky Division of Energy 2003].

Since windows allow the sun to penetrate or lose the heat to the outside, the larger window allows the greater gain but also has the greater heat loss. To balance between these energy flows, glazing ratios are optimized by considering the orientation, location, obstructions and user requirements. The glazing ratios of 30% to 50% in the region are generally accepted for buildings which do not use mechanical cooling. The orientation of the glazing should be carefully considered. East-facing windows let in solar radiation early in the morning and warm the space. West-facing windows may overheat the space in the afternoon. A closely related term to glazing is the Daylight Factor ( $DF$ ), which is a direct function of the window size and shape. This is a simple ratio between the amounts of light available outside and the amount of light falling on a particular surface. The range of the  $DF$  is 0~1. The  $DF$  is made up of three

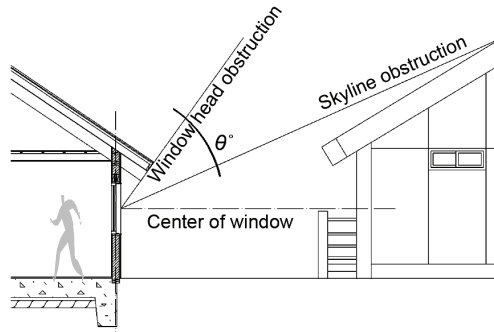


components such as direct light from the sky, reflected light from external surfaces of other buildings or internally reflected light. The average<sup>38</sup> for a room is estimated as

$$DF_{avg} = \frac{A_g \theta \gamma}{A(1-R^2)} \quad \text{Eq.1}$$

where  $\theta$  is the angle of visible sky measured from the center of the window shown in Fig.2.7 and  $\gamma$  is the transmittance of glazing, e.g. 0.85 for clear glass and 0.5 for tinted glass.  $A$  is the total area of room surfaces such as floor, walls and ceiling, and  $A_g$  is the glazed area.  $R$  is the mean reflectance of the surfaces, e.g. 0.7 for light finishes. The initial size of glazing area can be estimated by the ratio  $A_g/A$ .

The  $DF$  for a sun-space is estimated using a combination of transmittance  $T \approx T_g T_m T_f$  in the area of roof aperture ( $\text{m}^2$ ).  $T_g$  is the transmittance of the glass e.g. 0.8 for single glazing and 0.65 for double glazing.  $T_m$  is the maintenance factor, 0.7 for horizontal glazing, 0.8 for tilted glazing and 0.9 for vertical glazing.  $T_f$  is a correction factor for light that is trapped in the room since the angle of view is 0.5 at the edge of the space and 0.7 in the center.



**Figure 2.7.** Angles of visible sky for the average  $DF$  calculation [author].

In winter, the glazing has a lower air temperature than the surrounding air which causes the air near the surface of the glass to cool due to heat losses. In the summer, direct solar radiation by glazing causes overheating. The direct solar gain on a surface is a combination of the absorption of direct and diffuse solar radiation given by

$$G_{solar} = \alpha \left( I_{direct} \cos \phi \frac{A_{sunlight}}{A} + I_{diffuse} F_{sky} + I_{gnd} F_{gnd} \right) \quad \text{Eq.2}$$

where  $\alpha$  is solar absorptance of the surface,  $\phi$  is angle of incidence of the sun's rays and  $A_{sunlight}$  is sunlight area.  $I_{direct}$ ,  $I_{diffuse}$  and  $I_{gnd}$  are respectively the intensities of direct radiation, sky diffuse radiation and ground reflected diffuse radiation. The view factors to ground and sky are calculated using the tilt angle  $\phi$  of the surface as,<sup>39</sup>

<sup>38</sup> Ward 2004.

<sup>39</sup> Walton 1983.

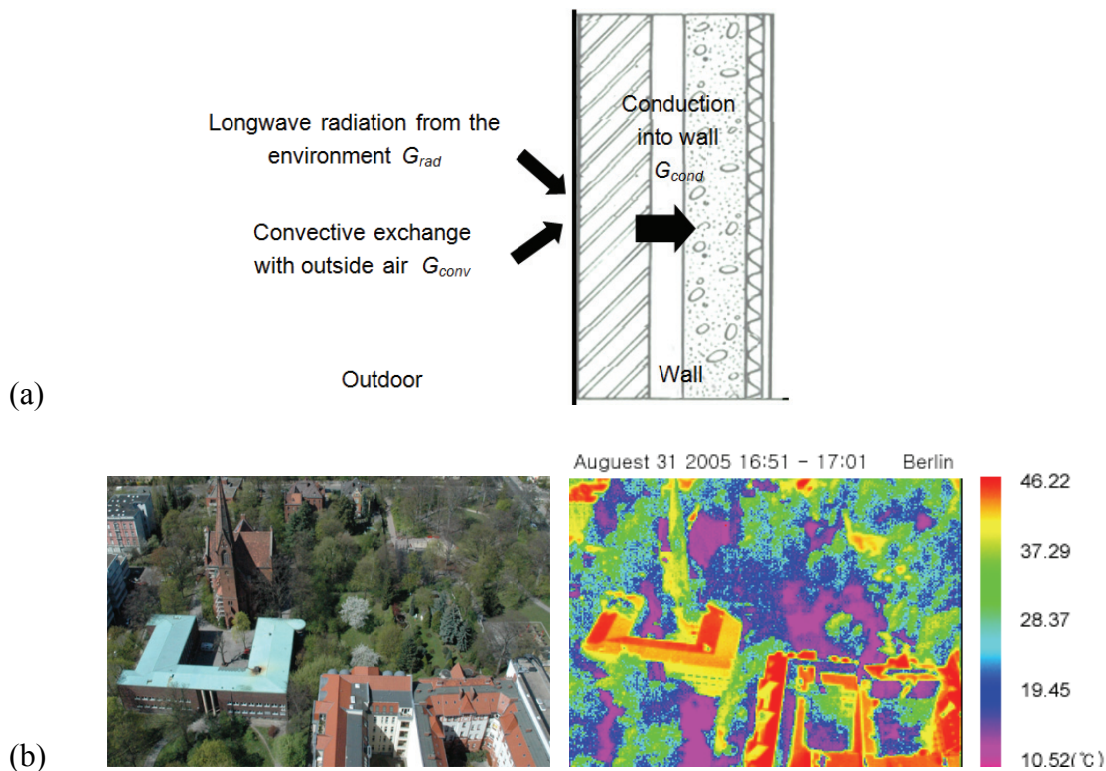
$$F_{gnd} = 0.5(1 + \cos \phi) \text{ and } F_{sky} = 0.5(1 + \cos \phi) \quad \text{Eq.3}$$

The thermal efficiency of a cave style glazing is better than jut style. Tilted glazing is better than horizontal glazing.

The sunlight warms up the walls of a house which absorb solar energy as well. Through absorption by surfaces, the air temperature increases. Some passive heating system may include heating water in a container using solar radiation, or using natural daylight to read or perform various tasks. The energy gain in solar designs or systems is represented by the heat balance of conduction, radiation and convection (usually natural). Fig.2.8 illustrates the diagram of the outside heat balance. Simplified procedures generally combine the radiation and convection terms by using the energy-balance concept.

$$G_{rad} + G_{conv} - G_{cond} = 0 \quad \text{Eq.4}$$

The radiative heat gain  $G_{rad}$  is net long wavelength (thermal) radiation flux exchange with the air and surroundings.  $G_{conv}$  and  $G_{cond}$  are respectively convective flux exchange with outside air and conduction heat flux into the wall.<sup>40</sup>



**Figure 2.8.** Outdoor heat balance of longwave radiation, (a) the diagram, (b) an example in Berlin, Stglitz [author, Scherer 2006].

If we let the boundary condition as an enclosure consisting of building exterior surface, surrounding ground surface, and sky, the radiative gain ( $G_{rad}$ ) can be calculated as the sum of components due to

<sup>40</sup> Walton 1983.

radiation exchange with the ground, sky and air. The radiation heat flux is calculated from the surface absorptive, surface temperature, sky and ground temperatures, and sky and ground view factors.

$$G_{rad} = G_{gnd} + G_{sky} + G_{air} \quad \text{Eq.5}$$

Applying the Stefan-Boltzmann Law to each component yields

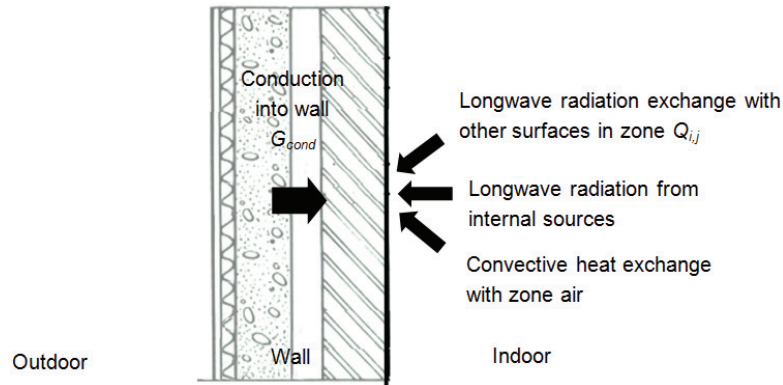
$$G_{rad} = \sigma F_{gnd} (T_{surf}^4 - T_{gnd}^4) + \sigma F_{sky} (T_{surf}^4 - T_{sky}^4) + \sigma F_{air} (T_{surf}^4 - T_{air}^4) \quad \text{Eq.6}$$

where  $\sigma = 5.67 \cdot 10^{-8} \text{ W m}^{-2} \text{ K}^{-4}$  is Stefan-Boltzmann constant.  $T_{surf}$ ,  $T_{gnd}$ ,  $T_{sky}$  and  $T_{air}$  are temperatures of outside surface, ground surface, sky and air.  $F_{gnd}$ ,  $F_{sky}$  and  $F_{air}$  are the longwave view factors of surface to ground surface, sky and air temperature.

Heat transfer rate due to exterior convection  $G_{conv}$  is calculated as

$$Q_{conv} = hA(T_{surf} - T_{air}) \quad \text{Eq.7}$$

where  $Q_{conv}$  is rate of exterior convective heat transfer,  $h$  is the convection coefficient related to material roughness and local surface wind speed and  $A$  is the surface area.<sup>41</sup>



**Figure 2.9.** Indoor heat balance diagram and an example of longwave radiation from internal exchange [author].

The longwave-radiation heat exchange between surfaces depends on surface temperatures, spatial relationships between surfaces and surroundings, and material properties of the surfaces. Fig.2.9 exemplifies the indoor heat balance with longwave radiation from internal exchange. The relevant material properties of the surface e.g. emissive and absorptive are complex functions which are related with temperature, angle, and wavelength for each participating surface. A grey interchange model based on the *ScriptF* concept<sup>42</sup> simplifies the complexity. The method relies on a matrix of exchange coefficients between pairs of surfaces that include all exchange paths between the surfaces. If we assume that all surface radiation properties are grey and all radiation is diffuse, all reflections,

<sup>41</sup> Walton 1983

<sup>42</sup> Hottel and Sarofim 1967.

absorptions and re-emissions from other surfaces in the enclosure are included in the exchange coefficient, which is called *ScriptF*. The long wave radiant exchange between surfaces *i* and *j* are,

$$Q_{i,j} = A_i F_{i,j} (T_i^4 - T_j^4) \quad \text{Eq.8}$$

where  $F_{i,j}$  is the *ScriptF* between surfaces *i* and *j*.

## 2.5. Design for heat loss

If the heat gains cannot be balanced by the loss, a space will be overheated by internal heat gains. In order to determine the possibility of overheating occurring, a rough approximation of overheating in a space is estimated in two divided areas of passive and non-passive zones. If the glazing area of passive and non-passive zones is estimated, the overheating by the solar load can be estimated.

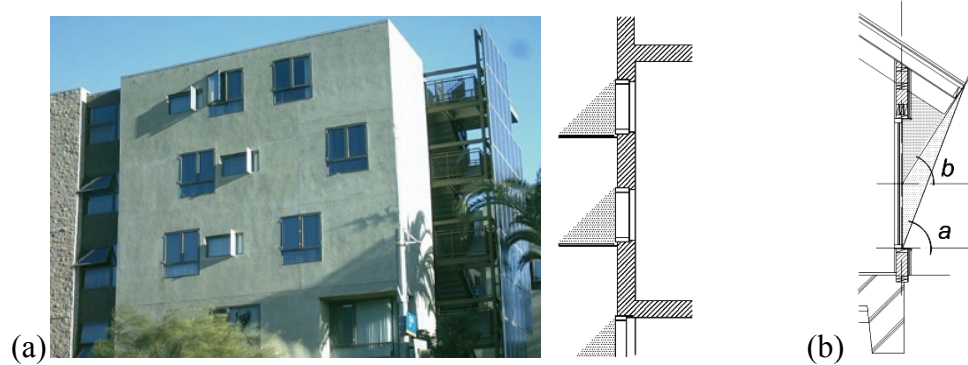
**Table 2.2.** Solar heat gain through single thickness of common window glass through an unshaded window [Saini 1970].

Type of shade, finish on side exposed to the sun	Heat gain (%)
Outside slatted shade, slats set to prevent direct sun falling on glass, white, cream.	15
Outside commercial bronze shading screen, consisting of narrow metal slats, solar altitude above 40° so that no direct sun falls on glass, dark	15
Outside canvas awning, sides open, dark or medium color.	25
Inside Venetian blinds, slats set to prevent direct sunshine passing though, diffuse reflecting aluminum.	45
Ditto, white, cream	55
Inside roller shutter fully drawn, dark	80

To prevent overheating, the windows of the overheating area should be protected from direct solar gains. Internal and external shading efficiently removes the gains. Since internal shading only serves to direct the gains which are already in the space having passed through the window, external shading is more efficient for the overheating. While solar shading must give good protection in summer, in winter when the sun is not so strong and lower in the sky, the solar protection must be able to allow sufficient daylight and natural ventilation to enter the building. Horizontal shading devices are appropriate to blind south-facing windows but not appropriate with east or west facing windows. Different types of solar shading devices have the different percentage of the external radiation protection. Table 2.2 clearly shows the effect of various types of shading devices for instantaneous solar heat gain through a single thickness of a common window glass.

Fig.2.10 represents the external shading devices with horizontal overhang. The angle *a* and *b* respectively determines the angle from a line perpendicular to the bottom of the window to the edge of the overhang and from the middle of the window to the edge of the overhang. These angles represent

100% and 50% shading of the window. The inside effective equivalent temperature with shading overcomes the upper limitation of heat comfortable part i.e. when  $t_{ef} > 26^\circ\text{C}$ .<sup>43</sup> Simultaneously, solar radiation itself to the window is  $325.5\text{ W m}^{-2}$ . Table 2.3 and 2.4 respectively represent the global radiation of Korea and the comparison with four countries and the climate data of Korean summer and winter.<sup>44</sup>



**Figure 2.10.** Solar shading, (a) devices by C. Scarpa, (b) overhang [author].

**Table 2.3.** Comparison of global radiation of four countries [E.J. Lee et al. 2004].

	Spring	Summer	Autumn	Winter	Mean	
S. Korea (A)	4.48	4.41	3.14	2.35	3.60	A=100%
	124%	123%	87%	65%	100%	
Central-Japan (B)	4.49	4.67	3.00	2.23	3.55	B/A=99%
	121%	132%	84%	63%	100%	
Germany (C)	3.69	4.88	1.68	0.94	2.88	C/A=80%
	128%	169%	58%	33%	100%	
Swiss (D)	4.09	5.46	2.3	1.15	3.25	D/A=90%
	126%	168%	71%	35%	100%	

**Table 2.4.** Climate data in summer and winter in S. Korea [E.J. Lee et al. 2004].

	Summer (Jun. ~Aug.)	Winter (Dec. ~Feb.)
Mean Temperature	23 ~ 26°C	-5 ~ 5°C
Relative Humidity	75 ~ 85%	50 ~ 75%
Characteristics	Subtropical Climate	Continental Climate

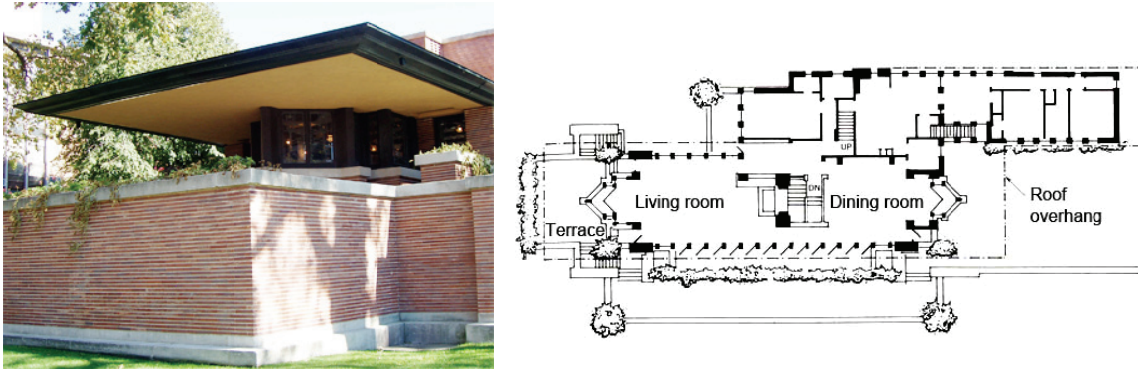
Korea is located on the center of Northeast Asia between  $33^\circ\text{N}$  to  $43^\circ\text{N}$  and  $124^\circ\text{E}$  to  $132^\circ\text{E}$  which is the middle latitude. The climate is featured by the mid-latitudinal location and peninsular configuration. Korea has four distinct seasons with similar lengths. It has a humid, East Asian monsoonal climate in summer and a dry cold and continental climate in winter. The mean temperature during winter is generally below freezing and widely different from summer. In summer it is very hot, rainy, and humid. The monsoon season begins with the heaviest rain in late June and continues until July. The end of

<sup>43</sup> B.S. Kim and K.H. Kim 2004.

<sup>44</sup> E.J. Lee et al. 2004.

September to November is the autumn season which is dry due to dry air from the continent to the north. The winter weather is cold and dry.

Since solar radiation is the most important factor in heating, solar shading at midday should maximize heat resistance. The Robie house has very large roof overhangs to shade walls made entirely of glass doors and windows that could be opened for ventilation as Fig.2.11 shows. Since Chicago has very hot and humid summers, plentiful ventilation and full shade were the major cooling strategies before air conditioning became available.<sup>45</sup>



**Figure 2.11.** Very large roof overhangs of Robie house by F.L. Wright [author, Lechner 1991].

Windows are the main ways for solar heat to enter but also for natural ventilation. When the air is supplied and extracted by wind, the difference in air density makes buoyancy. The larger the windows, the more effective the ventilation will occur. However, to make natural ventilation work effectively, openings at both low and high levels within the building are also necessary to promote the buoyancy or stack effect. A solar chimney creates a column of air at a higher temperature. This generates higher pressure differences and so further enhances the stack effect. The internal plan form of the building should be as simplified as possible e.g. open plan spaces effectively offer little resistance to airflows but highly partitioned spaces raise the resistance across or up the building. A stack can also be generated through an atrium, which will additionally act as a buffer to reduce infiltration heat loss.

The factors which affect the natural ventilation are set out as

- The shape orientation and depth of the building.
- The window design to make efficiency of air distribution
- The provision of flow paths for the air – sun spaces, stacks or windows.
- The internal layout should permit easy access to the windows.
- The resistance of flow through partitioned spaces
- Exhaust paths such as a stack or windows.
- The existence of open windows not to interfere with the operation of blinds

---

<sup>45</sup> Lechner 1991.

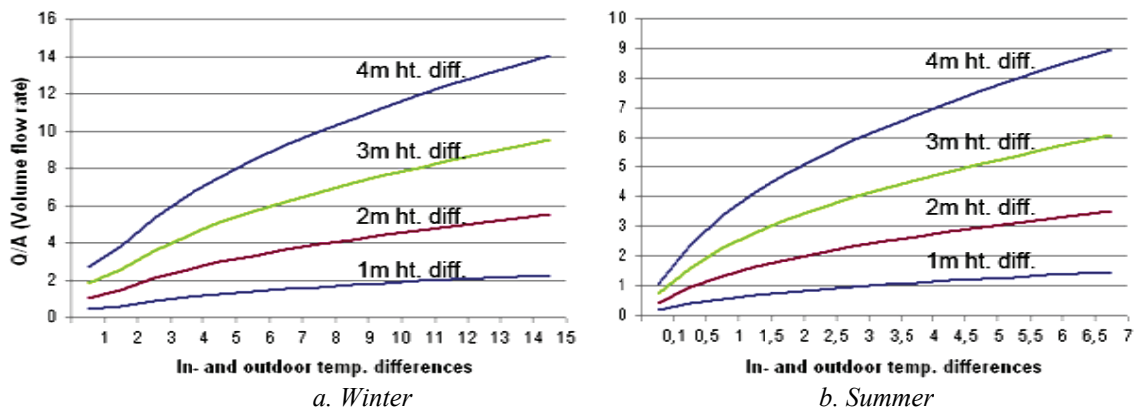


In the types of windows, tilting windows generally are regarded as being the best type to use. When cooling is required, some form of trickle ventilation provided either by devices or small clearstory openings can be also considered. Trickle ventilators are designed to provide the minimum fresh air requirements to a space, to promote natural cooling and to minimize moisture build-up. There are a number of ways in which a window can open and, depending on type, the air distributes to the space in slightly different ways.

The opening size for natural ventilation is the most frequently asked issue. The solution is related to the microclimate of the site.<sup>46</sup> A simplified estimation of the size of windows for a naturally ventilated building can be represented by volume flow rate to area of opening  $Q \text{ (m}^3 \text{ s}^{-1}) / A \text{ (m}^2)$ ,<sup>47</sup>

$$\frac{Q}{A} = C_d [2 \times g(h_{npl} - h) \frac{T_{ins} - T_{out}}{T_{ins}}]^{\frac{1}{2}} \quad \text{Eq.9}$$

$C_d$  is the discharge coefficient i.e. normally 0.61 and  $g=9.81 \text{ m s}^{-2}$  is the acceleration due to gravity. The relationship between the opening size and the temperature is given by the height of opening  $h$  (m) and of neutral pressure  $h_{npl}$  (m) and the inside temperature  $T_{ins}$  (K) and the outside temperature  $T_{out}$  (K). The volume flow rate is dependent upon the pressure passing an opening and is related to the stack effect. A smaller opening size, large difference of in/out temperatures and opening heights result in a larger volume flow rate since they bring large pressure i.e. stack-driven ventilation.



**Figure 2.12.** Areas of opening required in winter and summer, volume to area ratio for stack-driven ventilation [author].

Using this relationship, Fig.2.12 gives the results for S. Korean winter and summer indoor temperature, 19.5°C and 24°C. Although the stack-driven ventilation is an especially efficient cooling concept in summer, flow-driven effects, e.g. temperature and moisture balancing can be considered in winter because in/out temperature difference is generally larger in winter. For example, in vernacular architecture, the temperature and moisture balancing is very important to maintain the building climate

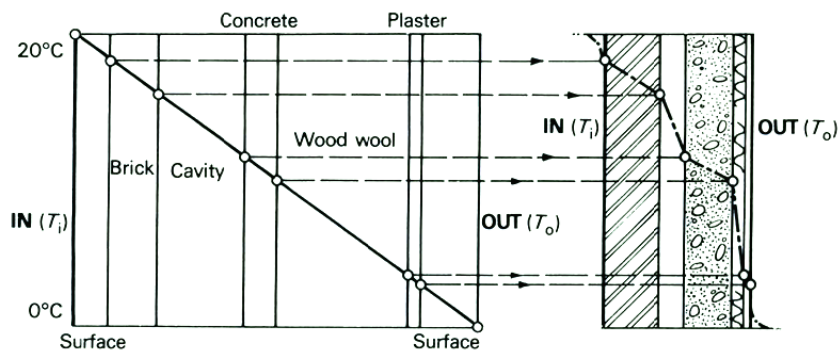
<sup>46</sup> The Chartered Institute of Building Service Engineers (CIBSE) 1997.

<sup>47</sup> Ward 2004.

control. Natural ventilation occurs, however, the neutral pressure line is not exactly defined for every building. The neutral pressure line should be about 0.25m above the highest ceiling since the height difference generates very large variation in the volume flow rate both in winter and summer. In practical use, the height difference is a more important issue than temperature difference due to the large effects.

## 2.6. Thermal insulation

Energy tends to move from a warm indoor area to a cool outdoor area, and thereby a building loses heating in winter or cooling in summer through walls, roofs, floors and windows. Fig.2.13 represents the phenomena through the cross-section of a composite wall with the thermal properties of several materials i.e. brick, cavity, concrete, wood wool and plaster, where the line shows the temperature gradient. Dense materials such as brick and wood wool can act as thermal insulation since dense materials have a high resistance of heat transfers. Thermal insulation is a mechanism which helps to reduce heat losses, and the rate of the energy movement is determined by the thermal insulation properties of the materials.



**Figure 2.13.** Temperature gradient of a composite wall [Koenigsberger et al. 1974].

The term of U-value is used to determine the resistance of heat transfers in a combination of materials. U-value is calculated by a steady-state heat transfer equation across the structure with known certain properties of the materials<sup>48</sup>

$$U = \frac{1}{\sum \text{Thermal resistances of each element in the structure}(R)} \quad \text{Eq.10}$$

The thermal resistance of each material is given by

$$R = \frac{\text{Thickness } (L)}{\text{Thermal conductivity } (K)} \quad \text{Eq.11}$$

<sup>48</sup> Ward 2004.



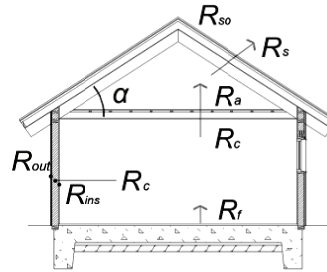
A rough estimation of energy transfers across a structure with  $n$  materials can be established by the sum of thermal resistances of  $n$  numbers.

$$U = \sum_{k=1}^n \frac{1}{R_k} = \sum_{k=1}^n \frac{K_k}{L_k} \quad \text{Eq.12}$$

Thermal resistance is related to the heat transfers at the surfaces of the materials and takes place by convection heat transfer. In a house shown in Fig.2.14, the resistance of the inside surface  $R_{ins}$ , the resistance of outside surfaces  $R_{out}$  and the thermal resistance of floor  $R_f$  are dependent upon the exposure of the surface where  $R_k$  is resistance of  $n$  numbers. The U-value is calculated as

$$U = \sum_{k=1}^n \frac{1}{R_k + R_{ins} + R_{out} + R_f} = \sum_{k=1}^n \frac{K_k}{L_k} + \frac{K_{ins}}{L_{ins}} + \frac{K_{out}}{L_{out}} + \frac{K_f}{L_f} \quad \text{Eq.13}$$

where each thermal resistance  $R$  can be rewritten by the thickness  $L$  and the thermal conductivity  $K$  as Eq. 11.



**Figure 2.14.** Calculating heat transfer [author].

For the slope roof structures with the angle  $\alpha$  as shown in Fig.2.14, the following equation determines the heat transfer from a room through a loft and then through the roof structure as

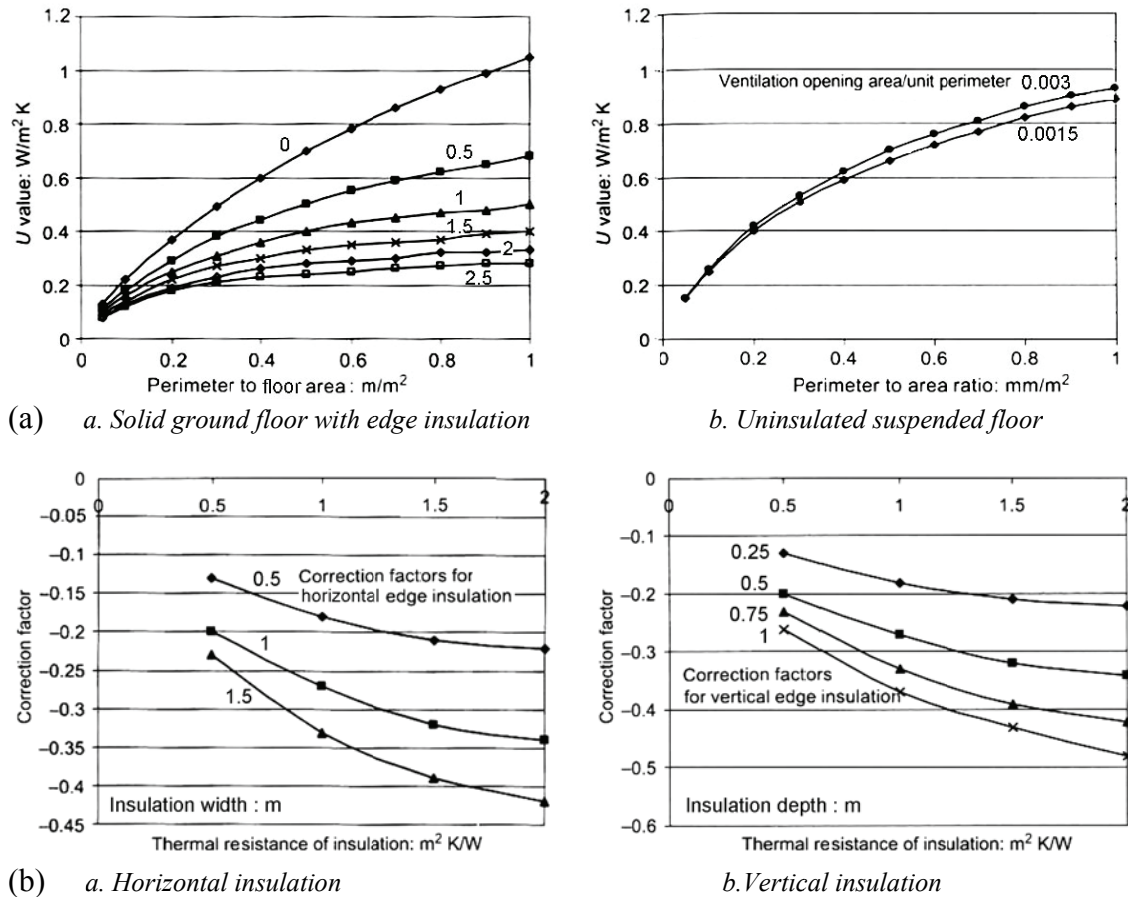
$$U_{roof} = \frac{1}{R_s \cos \alpha + R_a + R_c + R_{si}} \quad \text{Eq.14}$$

where  $R_s$  is the sum of the thermal resistances of the roof materials and the outside surface resistance  $R_{si}$ ,  $R_a$  is the thermal resistance of the attic space and  $R_c$  is the thermal resistance of the ceiling.

For a structure footing, both losses through the ground below the building and the edges should be minimized since heat losses to the ground can be significant. Fig.2.15 (a)-a compares U-values of partially insulated solid ground floors for the percentages of ground covered by insulation. Higher percentage of insulation makes lower U-values for the large perimeters to floor area ratios. The Fig.2.15 (a)-b gives U-values of uninsulated suspended floors for various perimeters to area ratios and for two levels of ventilation openings. Uninsulated suspended floors under ventilation reduce the value of thermal insulation. Hence, when the floor is insulated, a correction factor is necessary. This correction factor is based on the U-value of the floor construction and set out as

$$U_{insulated\ floor} = \frac{1}{(1/U_o) - 0.2 + R_f} \quad \text{Eq.15}$$

where  $U_{insulated\ floor}$  is the U-value of the insulated suspended floor,<sup>49</sup>  $U_o$  is the U-value of floor construction and  $R_f$  is the thermal resistance of the floor construction.  $1/U_o$  is the surface resistance on the upper and underside of the floor i.e. normally 0.17. The correction factors for the insulation positioned either vertically or horizontally around the edge of the building are represented in Fig.2.15 (b).



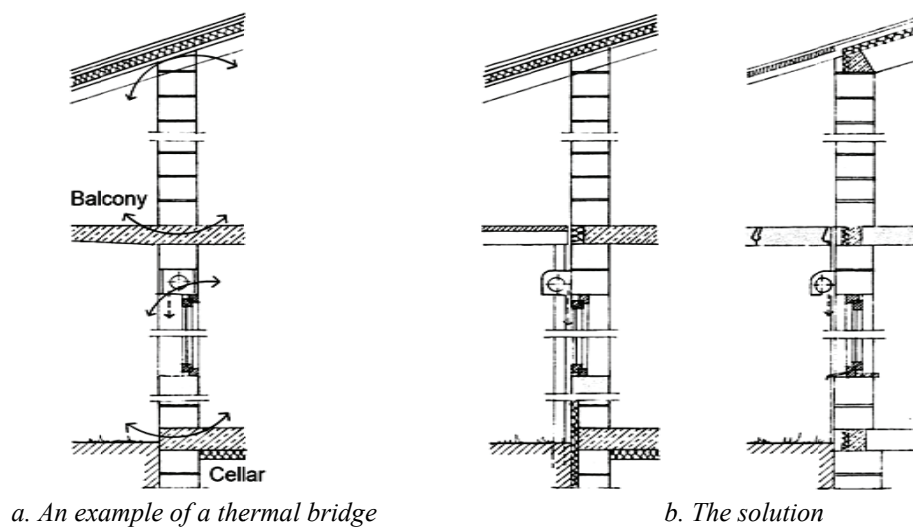
**Figure 2.15.** U-value of a ground floor, (a) for solid floor and suspended floor, (b) solid floors with all over insulation [Ward 2004].

Most building materials are able to absorb moisture in the form of vapor and this can pass through the surface. The mechanisms at play in heat and moisture transfer across a surface are:

- Conduction through the solid parts of the material
- Convection at the surfaces – both inside and outside surfaces including any cavities
- Radiation to or from the surfaces
- Moisture transmission through the surface

<sup>49</sup> Ward 2004.

In winter, moisture holding ability of the air decrease. If the air is saturated at a surface which has a lower temperature than the room, moisture forms either on the surface or within the structure i.e. condensation. The temperature which moisture occurs is known as the dew point temperature. If the temperature of the material is below the dew point temperature, moisture in the air is condensed, and it results in interstitial condensation in the materials. If a material takes up more moisture, the thermal conductivity is affected. The overall result is that the material becomes less efficient to act as an insulator, and other more detrimental effects may occur. When the air temperature increases in summer, the ability of the air to hold moisture also increases at a faster rate. If air enables to hold more moisture, it feels drier since the relative humidity decreases. The moisture in the material is evaporated and moves into the air. These situations should be taken into account when calculating the overall U-value of a wall.



**Figure 2.16.** Thermal bridge [Gonzalo 1994].

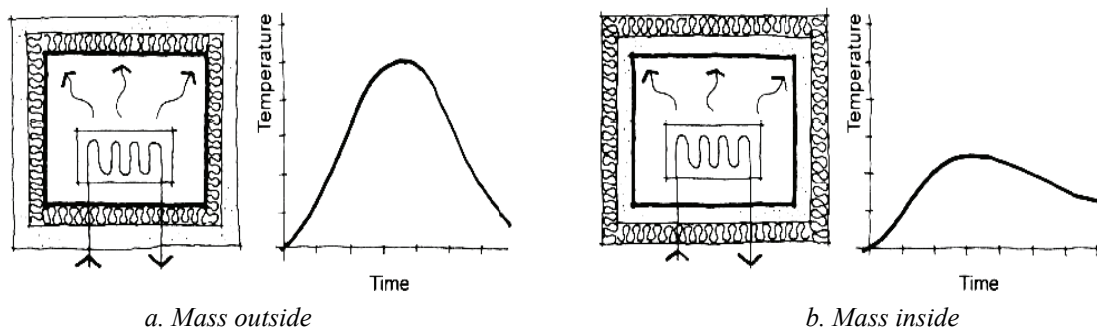
A thermal bridge is created when materials that are poor insulators come in contact, allowing heat to flow through the path created. Insulation around a bridge is of little help in preventing heat loss or gain due to thermal bridging; the bridging has to be eliminated, rebuilt with a reduced cross-section or with materials that have better insulating properties, or with an additional insulating component. Thermal bridges occur where materials of different thermal properties are used, the result is shown in differential heat flow rates. It results in parts of the structure being significantly cooler than another part. Fig.2.16 shows a thermal bridge at the lintel of a window and the solution using a wind shield proposed by Gonzalo (1994).

## 2.7. Thermal mass

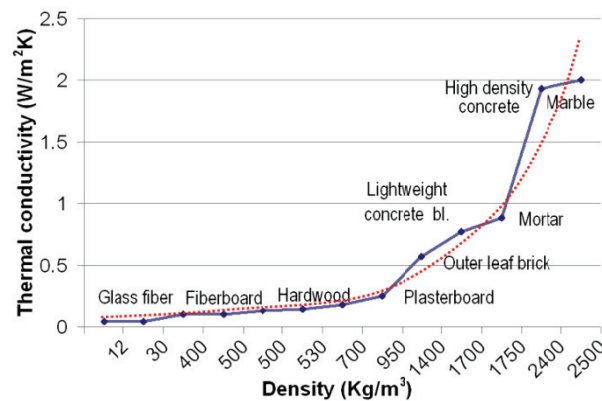
Since a thermal insulation reduces the heat loss in winter and avoids excessive heat gain in summer, insulation is necessary to most passive house design. However, a building is operated for the complete year with high, medium and low outside temperatures, and insulation material which cannot store thermal energy is referred to as a material with low thermal mass. In a building with large amount of insulation, the internal temperature will easily rise or drop with the heat gain or loss. Hence, thermal mass is cooperatively used to avoid the problem of insulation.

An installation of thermal mass constructed of identical materials of brick and polystyrene is shown in Fig.2.17. *a* and *b* respectively have the polystyrene to the inside and the outside. If both are heated simultaneously with the same source, and the inside temperatures are differently varied over a period. The space with the thermal mass outside the building is more balanced than inside the building.

Thermal mass has an ability to store thermal energy for heating or cooling and high thermal mass



**Figure 2.17.** Effect of position of thermal mass on the inside temperature [Ward 2004].

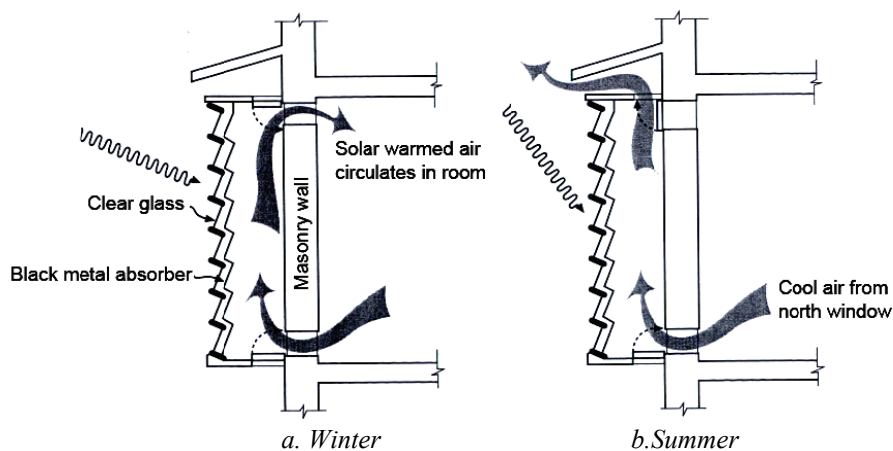


**Figure 2.18.** The relationship between density and thermal conductivity [author].

materials are dense and heavy. As the quantity of mass increases, the potential to store heat is significantly increased and is usually able to cope with the heat inputs over long periods. Fig.2.18 represents the relationship between the density and thermal conductivity of several materials. This relationship is general and can readily be applied to most building materials. The higher thermal conductivity a material has, the more heat can be readily transferred through the material.

In a cold season, a thermal mass absorbs and stores heat during sunny periods. When the heat is not desirable in the living space of a building, the mass releases the heat during overcast periods or during the night. In the hot season, the internal mass remains at a lower temperature than outside keeping the occupants at a more comfortable temperature. Then cooling the internal mass can be achieved by ventilation during cooler periods, typically at night.

Thermal mass is generally used in solar design with some typical heating systems such as a Trombe wall.<sup>50</sup> When a building faces the sun, uninsulated walls of brick, stone, or concrete directly absorbs sunlight. If these walls are on the interior, and glass installed in front of the walls, convective heat loss will be reduced. During the night, the heat will be emitted into interior, and the air temperature will be raised. Fig.2.19-*a* shows the usage of a thermal mass in solar-air-collector for winter. This is a similar characteristic with the Trombe wall. Fig.2.19-*b* illustrates in summer how a room with thermal mass removes the heated air using natural ventilation with selective openings for airflows.



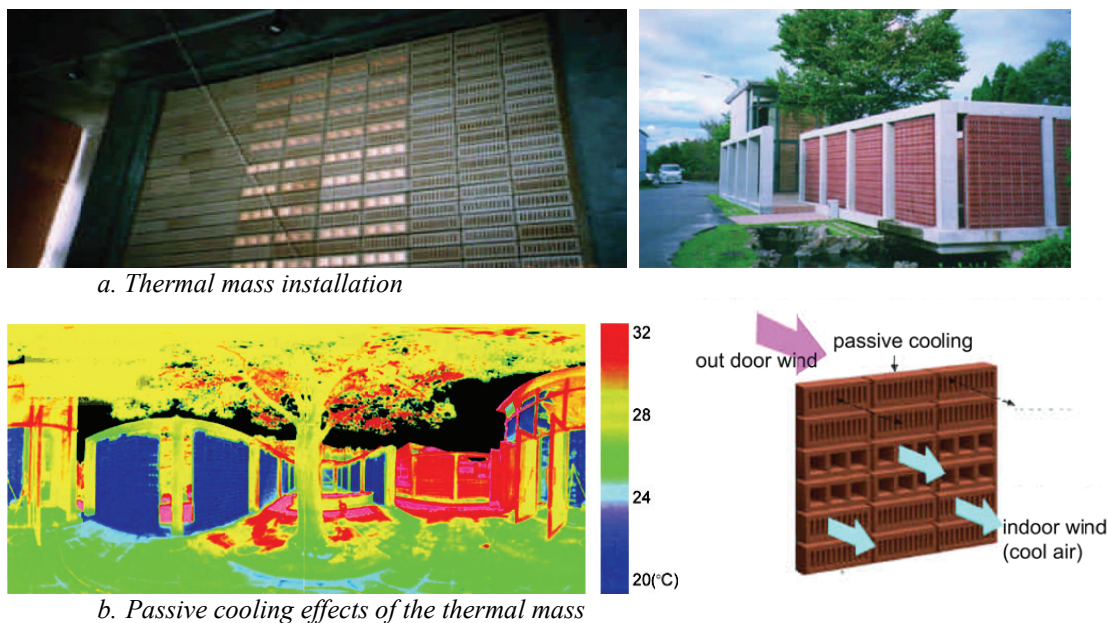
**Figure 2.19.** Thermal mass in solar-air-collector by E.S. Morse in Salem, Massachusetts [Porteous 2001].

The thermal storage function is an important aspect of passive design, when the specification requires that the amount of mechanical cooling is minimized. In practical cooling designs, thermal masses are located in the floor or ceiling where it is relatively easy to pass air over surface or water through the material. The location of thermal mass makes it possible to supply cool air to the floor in the evening or to pass cool outside air over the ceiling slab in the evening and night. Both methods have the effect of

<sup>50</sup> Trombe wall was first developed by architect J. Michel as a simplified version of the solar-air-collector in the last 1960s.

cooling the slab and thereby allowing the slab to absorb heat during the occupied period. The design is accepted when 2°C to 4°C drops in the inside peak room temperature during the day can be achieved by the thermal mass in a building. Very high thermal mass can be used for passive cooling. The Tono Inax pavilion which was built by architect T. Ashihara in 1998 exemplifies the cooling effect using very high thermal blocks. Temperature drop is achieved in holes of the block, and the air passed through the holes is cooled. Fig.2.20 shows how thermal blocks provide passive cooling with natural ventilation. In the blocks, about 8°C to 10°C drop can be observed.

The passive heating and cooling concept can be utilized even in active solar architecture. The building transfers heat between the collectors, the thermal mass, and the living space using water or air, often with a complex pump system. Some buildings use thermal mass to absorb internal heat rather than sunlight. For example, concrete on the interior of a building can hold excess heat generated from lights and equipments for living during the day, and release the heat during the night.



**Figure 2.20.** Thermal mass for passive cooling of Tono Inax pavilion 1998 [WSBC 2005].

High thermal mass buildings are often regarded as buildings that have reasonably stable internal temperatures. These buildings never seem hot in summer or cold in winter. However, the most important aspect of thermal mass such as heavy materials is the cost penalty, and the estimation of the optimal usage of thermal mass is needed to save the construction costs. The designs using thermal mass are able to cope with fluctuations in room temperature which occur during the day due to solar gain, occupant and equipment gains. A rough calculation of the heating time of the construction  $T$  (h) and  $r_c$  ( $\text{m}^2\text{K W}^{-1}$ ) is the thermal resistance of the material,<sup>51</sup>

<sup>51</sup> Ward 2004.

$$T = \frac{0.5(m \times c \times r_c)}{3600}, \quad r_c = \frac{d}{\lambda} \quad \text{Eq.16}$$

where  $m$  is the mass per square meter of material ( $\text{kg m}^{-2}$ ),  $c$  is the specific heat of the material ( $\text{J kg}^{-1} \text{K}^{-1}$ ),  $d$  is the thickness (m) and  $\lambda$  is the thermal conductivity ( $\text{W m}^{-1} \text{K}^{-1}$ ).

# 3. Microclimate design for energy-saving

## 3.1. Microclimate and building

### 3.1.1. Definition of Macro- and Microclimate

Microclimate is situated in a local atmospheric zone where it is related with the energy distribution. The definition of “macro-” and “micro-” depends on the spatial distance, and “-climate” is the environmental variation. Climatologists have concerned with the causality of these climates, while architects have interested in the effects of climate to the buildings.

The macroclimate can be analyzed statistically in the annual climate data that can indicate the climate characteristic of a particular region. For example, the urban climatology concentrated on the heat island and progressively focused to the microclimate related to the building geometry.<sup>52</sup> The aim is a study of energy exchanges between the urban canopy and the overlaying boundary layer or the surface, air and mass.<sup>53</sup>

Meanwhile, architects want to know a kind of microclimate called indoor climate to improve the building performance. They calculate energy loads of a building to maintain internal comfort. Interest for these issues started at the oil crisis of 1973.<sup>54</sup> The passive solar and energy efficiency by the mutual obstructions between buildings attracted attention. The passive solar design targets in managing the potential of the sun, and a solar envelope was proposed to maximize solar availability into the buildings by the amount of absorption versus reflectance of radiation.<sup>55</sup> Next, there were several studies to link the indoor climates and to remove the mutual obstruction between buildings in the high density. The heating and cooling gains highly relate to mutuality between outdoor and indoor environments. For example, the air permeability gives the potential for airflow and ventilation cooling through a building. The

---

<sup>52</sup> Landsberg 1981, Barry and Chorley 1987, Oke 1987, Oke et al. 1991, Escourrou 1991, Kuttler 2004.

<sup>53</sup> Mills 1997.

<sup>54</sup> Olgyay 1973, Markus and Morris 1980.

<sup>55</sup> Knowles 1981.



relationship between macro- and microclimate allows accurate analysis for building energy performance and adaptations for a comfortable condition.

Extensive studies on microclimatology were done by Geiger et al. (1995) and by Landsberg (1981). The influence of different slopes, ridges, valleys, and even glaciers on the microclimate is carefully studied. The climatic factors are wind speed, access to solar radiation, humidity and temperature of the air, and associated building factors are topography, orientation and building geometry. Table 3.1 shows the climate factors of a building and related issues to analysis of microclimate effect.

**Table 3.1.** The factors and related issues [author].

Factors	Related issues
Wind exposure	Infiltration, ventilation level and energy distribution, thermo- and aerodynamic pressure
Sunlight exposure	Local heating and pressure in the area
Precipitation	Building materials, insulation performance
Moisture	Wet materials degrade quickly and wet insulation conducts the heat.
Local temperature	Energy balance, heating and cooling requirements
Building topography	Access and the streamline of airflow to distribute the energy
Building orientation	The amount of contact and access between outdoor and indoor climates
Indoor condition	Heat gains and the absorption versus reflectance of radiation, air permeability for cooling

### 3.1.2. Microclimate design

The building microclimate can be achieved by building geometry, e.g. building surface, density, barrier, terrain, 3D objects and huge plant etc., which introduces a pathway of airflow, a windbreak and a non-uniform solar access etc. For example, a protected courtyard design against cold air can easily make warmer than exposed situations. The deviation in climate plays an important role in architectural planning. Most studies for microclimate have focused on the aspect proportion or height-to-width ratio, the orientations and the form of buildings, and the mixture of materials, the density or the rate of mixture.

Table 3.2 shows the planning issues by the factors of microclimate around building and the positive effects. In site selection, favorable locations should be considered with every elevation difference, character of land cover, which induce variations in a local climate. A less favorable site can be improved by windbreaks and surrounding surfaces that induce an advantageous reaction to temperature and radiation impacts. A good passive design which gives some shade in summer and allows the sun to penetrate as much as possible in winter consider the positioning, orientation and height of buildings. Deciduous trees aid to achieve the windbreak and seasonal irradiation impacts related to the albedo<sup>56</sup> of walls and other structures facing the sun. These make a substantial effect on the microclimate of intervening spaces as well as the heating of the buildings themselves. The energy balance in form and the

<sup>56</sup> The ratio of the amount of solar radiation is reflected by a body to the amount incident upon it.

mixture of material is also related with the irradiation of floor and walls.<sup>57</sup> Exposure versus shadow patterns affects the surface temperatures and consequently the amount of heat transferred to air as the sensible heat flux and consecutively the air temperature.<sup>58</sup> The potential of airflow at low level also depends on these factors.<sup>59</sup> The building materials of the surfaces were also found to be decisive in the heat storage rate<sup>60</sup> as well as in the nocturnal cooling rate.<sup>61</sup>

**Table 3.2.** Planning issues and the effects [author].

Planning issues	Effects
- Improved solar radiation for heating and lighting - The use of insulation and draught proofing presents excessive energy consumption.	Lower winter heating costs
- Wind, temperature and vapor variation for ventilation and cooling - The provision of external shading, thermal mass and the use of night cooling make comfortable indoor air condition.	Reduce overheating in summer and exceedingly dry in winter
- High contact with the surrounding - Well-balanced temperature and vapor on the site - Pleasant outdoor air can be exchanged with indoor air.	Create more pleasant outdoor conditions
- Low impact of environment - Pleasant outdoor condition	Improve growth of external plants and trees

However, all of these studies have focused at only one side of the indoor or outdoor. Few researches have performed for the microclimate of a building across outdoor and indoor to balance temperature and humidity for human comfort. A spatial modeling of microclimate effects, which can affect the human adaptive behavior to thermal stress,<sup>62</sup> can be helpful to plan optimal energy loads in a house.

### 3.1.3. Climate design process

If a building has a control that reacts to climates, the results are presented in terms of the operative cost for thermal comfort and the time when comfort is reached. Although the architecture design is fundamentally correct in all aspects, thermal condition is uncertain. Hence, climate should be taken into account at the early design stages deciding on the overall concept of a project, on the layout and orientation of buildings, on the shape and the geometry on the spaces between buildings. Koenigsberger et al. (1974) distinguished between three stages in climate design:

1. Forward analysis, which includes data collection and ends with a sketch design
2. Plan developments, which include the design of solar controls, overall insulation properties, ventilation principles and activity adaptation

<sup>57</sup> Mills 1997, Bourbia and Awbi 2004.

<sup>58</sup> Nakamura and Oke 1988, Yoshida et al. 1990/91, Santamouris et al. 1999.

<sup>59</sup> Hussein and Lee 1980, de Paul and Shieh 1986, Nakamura and Oke 1988, Santmouris et al. 1999.

<sup>60</sup> Oke 1976.

<sup>61</sup> Arnfield 1990, Mills 1997.

<sup>62</sup> Thermal stress is defined as the physical and physiological reactions of the occupant to temperatures that fall outside of the occupant's normal comfort zone.

3. Element design comprises closer examination and optimization of all individual design elements within the frames of the agreed overall design concept.

This consecutive approach uses rather simple tools in the forward analysis which gives some overall principles. Since in the last stage, it was practically impossible to go back and correct systematic errors, only minor changes in thermal performance could be obtained by a different element design. To remedy this, it is necessary to give the architect a set of methods and powerful tools which integrates data, knowledge and case studies for climate adaptation in the planning process. Developing appropriate and powerful tools and inclusion of evaluation and feedback in the system is therefore crucial to better integrate climate issues in a design process. Since the climate fluctuation is highly unpredictable in a short-term, a climate adaptation in a predictable way needs climate data over the long term. Information of climate variables is collected and made available in a number of forms e.g. maximum and minimum values, average values, probabilities and frequencies and time series.<sup>63</sup>

## **3.2. Arrangement**

### **3.2.1. Microclimate effects adapting wind direction**

Microclimate effects include spatially influenced phenomena, e.g. heat transfer, thermal balance, humidification and insulation etc., which can be observed by partial differences in a local area. Since partial differences form gradients, microclimate can be analyzed and visualized as a kind of flow with the gradient. For example, if you are in a cold valley, your minimum winter temperatures may be lower than what the other area indicates, because cold air is heavier than warm air and cold air is accumulated in the valley. The main driving force causes the difference of air pressure and temperature, and the air moves on the gradients with differences of air pressures and temperature. The difference of temperature which derives air pressure and thereby airflow is called aerodynamic pressure and thermodynamic pressure. The aerodynamic pressure often causes horizontal ventilation i.e. draught, and the thermodynamic pressure causes vertical airflow from the bottom upwards.

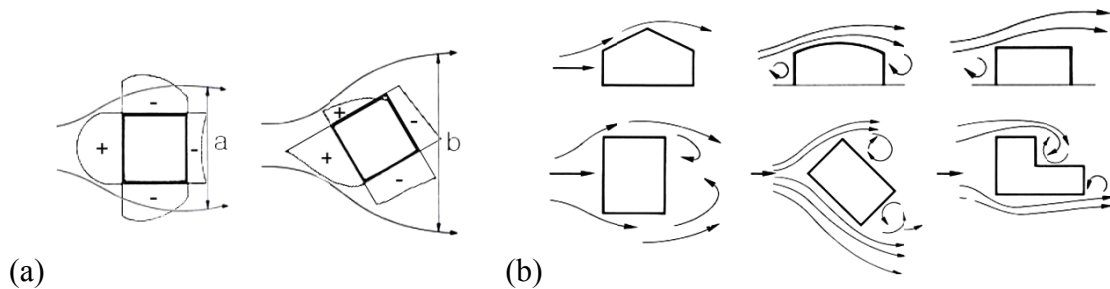
Airflow through buildings occurs with the difference of the pressure across the building, and the thermal balance may result in more comfort conditions for the same energy input. The airflow derives a small movement of air and thermal buoyancy, e.g. stack effects. These effects change proportionally according to strengths of the prevailing wind and the temperature. In principle, movement of air across the building occurs between areas of negative (-) and positive (+) pressure. Microclimate effects are observed between these polarities of pressure. Fig.3.1 (a) illustrates the polarities. When the building is

---

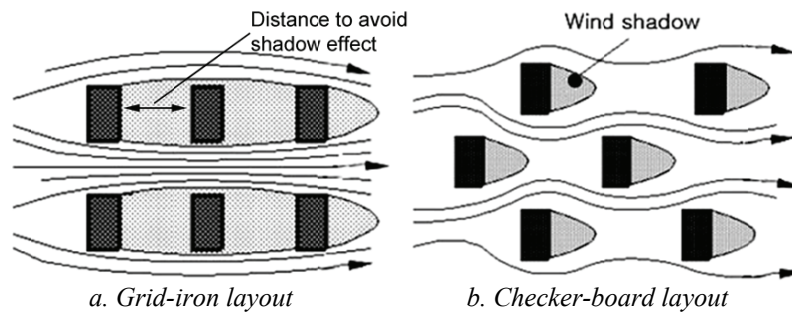
<sup>63</sup> Dingman 2002.

oriented as Fig.3.1 (a) shows, a greater velocity is created on windward faces, and the wind shadow will be much broader and the negative pressures which generate suction effects will be increased. However, the erroneous analysis of these effects causes inefficient window designs. For cooling, the wind should be well entered by windows and distributed through the whole building.

If openings are widely distributed over different façades of the building, the subsequent airflows will be well distributed over the whole building.<sup>64</sup> The resistance of airflow through the building determines the actual airflow rate. Natural ventilation, suction and infiltration occurs through different pressure across the building. The shape and orientation of the building are directly related to the wind streamline around volumes as Fig.3.1 (b) shows.



**Figure 3.1.** Wind streamlines around a building, (a) schematic distribution of wind pressure and wind shadow, (b) the pattern for the building forms and layouts [Givoni 1969, Koenigsberger et al. 1974, Markus and Morris 1980].



**Figure 3.2.** Wind streamlines and wind shadow by building arrangement [Koenigsberger et al. 1974].

Other obvious factors affecting airflow around the building are the physical relationship to surrounding volumes and obstacles e.g. other buildings, fences and trees etc. The arrangement between high and low rise buildings and obstacles often increases the wind pressures and the air velocity. The position of buildings in the leeward shadow or the suction zone of other structures has influence on the amount of air passing through the inlets of naturally ventilated buildings. Fig.3.2-a shows wind shadow effects.<sup>65</sup> In order to avoid a shadow effect caused by the second row of buildings, the distance between the buildings should be over at least 6 times of the height of the first row of buildings obstructing the second

<sup>64</sup> Baker and Steemers 1999.

<sup>65</sup> Koenigsberger et al. 1974.

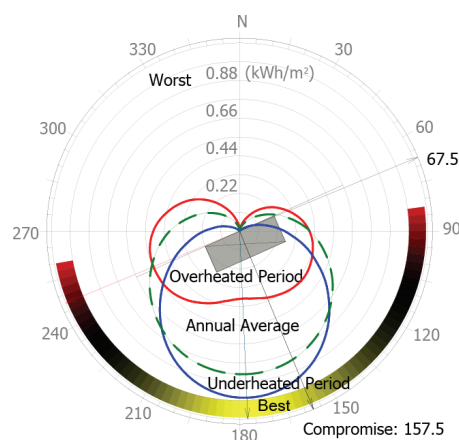
row of buildings. Alternatively, using a staggered in a checker-board pattern shown in Fig.3.2-*b*, shadow and stagnant air zones are almost eliminated.

For the microclimate design, another important factor to choose building orientation is the wind direction. The windward in the hot season and in the cold season in the place of construction should be considered to decide the proper house direction which uses cool wind in summer and prevents the cold wind from blowing into the house in winter. In Korean climate, the best orientation for the house is the southeast because in summer the cool wind blows into the frontal windows and in winter the Siberian cold wind blows from northwest.

### 3.2.2. Optimum building orientation

In the Passive House design, the building orientation is strongly related to the solar radiation. The orientation of the building and its position on the site also have a strong influence on how and when sunlight and air currents can enter, thus affecting daylight, air conditioning, ventilation and many other aspects. The efficacy of passive methods included at later design stages depends largely on the initial decision on how to situate the building within its immediate habitat. For example, east and west are bad directions since all the year-round the solar radiation is more deeply into the room and the related air temperature is the highest. The house facing southward is the best, because the solar radiation is little in summer and is the highest in winter. The optimum building orientation of Seoul, Korea is simulated by using average daily incident radiation on a vertical surface and the best orientation is South-Southeast i.e. clockwise  $157.5^\circ$  from North. Fig.3.3 represents the simulation results using the sun path for energy performance.

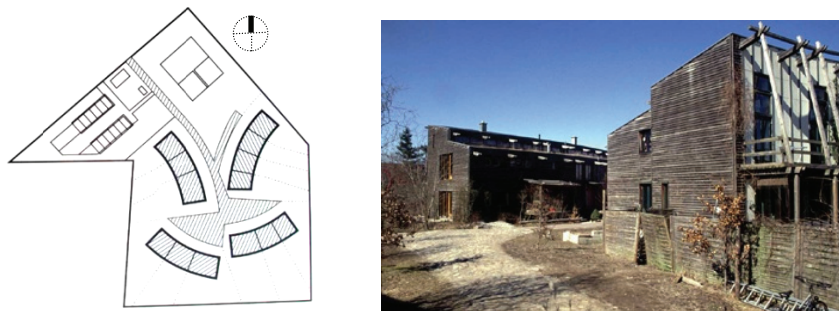
For summer cooling, the aerodynamic pressure using wind is much more important since room



**Figure 3.3.** House orientation considering the sun path [author].

temperatures inside and outside differ little in summer and the thermodynamic pressure is often very small. It is necessary to organize well horizontal ventilation by considering the direction of the house. The choice of the building orientation depends on the following four factors: the wind direction in hot and cold seasons in the place of construction, the distribution of solar radiation on the different surfaces of the building, the topological features and the requirements of architectural composition. The best house orientation of the local climate should be chosen by statistically analyzing the factors of the solar gain, ventilation and shadow effects.

Fig.3.4 shows the arrangement of houses in *Schöneiche*, an ecological house complex which considers the direction of the sun and natural form for the building arrangement. The south façades of south buildings have solar water heating panels which are used for hot water and space heating. The building shapes minimize wind shadows when the main wind flows from the north direction. Otherwise, building orientation in Korean climate, i.e. hot-humid in summer and cold-dry in winter, is difficult because the best summer ventilation and solar shading equipment to avoid excessive solar radiation should be maximized for cooling.



**Figure 3.4.** *Schöneiche* (nearby Berlin) ecological house complex by Gölling and Schmidt [author].

### 3.2.3 Topography

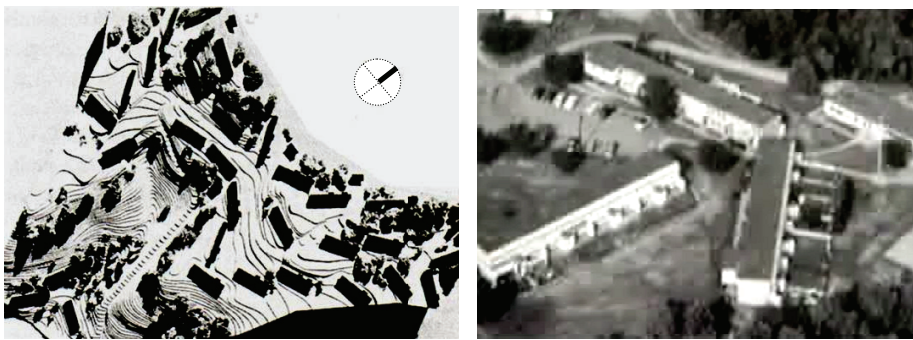
Korea has a large amount of topography in the land. The terrain of Korea forms the gently lowering western sea, rises progressively in the east side and forms mountain ranges with a steep slope on the eastern sea side. The total size of the land is 99,284km<sup>2</sup>. Most of the land consists of low mountain districts and the average altitude is 482m. The plain area with the gradient below 5° is only about 23%. 70% of the whole land is slopes of 20° and more.

W. Gropius noted that the southern exposure is superior from the living point of view because of the steep angle of the sun during the hot season of the year. However, if the buildings have to be put on rolling ground e.g. Fig.3.5; the orientation of the buildings should be adjusted from the southern

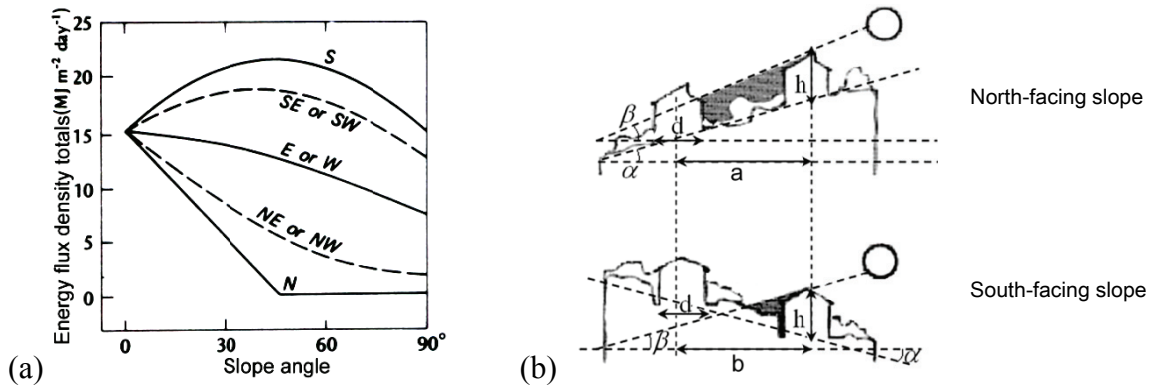


exposure. Furthermore, the views from the house and the wind direction of the region have to be considered as well. When all these factors are balanced, an optimal plan with the location on the contour is reached. W. Gropius and M. Breuer created simple, modern houses, grouped in thirty-five multi-unit structures situated on a sloping hillside, taking advantage of southern exposure, sharing grassy lawns, and maintaining a bit of privacy with walled-in porches in the Aluminum city terrace housing.

The consideration of terrain in cities has an importance for the hillside development. The topography has profound effects on the microclimate. Small differences in slope may create remarkably large modifications in the microclimate since the hilly area brings about the difference of energy supplies. Imbalanced energy movement such as anabatic and katabatic winds forms on the hill due to the difference of air pressure caused by the difference of local heat distribution



**Figure 3.5.** Aluminum city terrace in Pennsylvania by W. Gropius and M. Breuer [Aronin 1953].



**Figure 3.6.** Solar radiation on slope, (a) total daily direct-beam radiations, (b) shadow range for distance between buildings,  $a > b$  [Oke 1987, author].

Spatial energy distributions of this type form an excellent base or the understanding of microclimatic variations in regions of complex topography. Slope climate (sometimes called terrain climate or exposure climate) is determined by the different amounts of longwave radiation received by an inclined surface as compared with a horizontal surface. The solar radiation and wind velocity in slope areas are larger than in flat areas as Fig.3.6 (a) represents. They are incident upon slopes of differing angles and aspects at latitude of  $45^{\circ}\text{N}$  at the times of the equinoxes. The building orientation results for the morning

are warmer and drain earlier in hillside areas by the sun especially toward the south. The maximum load would be on a south 45° slope; whereas no direct-beam would reach north-facing slopes of greater than 45° angle. To avoid shading of building, the development of the slope site needs a distance considering solar and topography angles between the buildings as

$$a = \frac{h - d \tan \alpha}{\tan d\alpha + \tan \beta} \quad \text{Eq.17}$$

where  $a, b$  and  $d$  are respectively the distance between buildings and the size of a building.  $\alpha$  and  $\beta$  are respectively solar angle and topography angle. Fig.3.6 (b) represents the shadow range related to the distance between buildings. South-facing slopes allow tighter spacing  $b$  without loss of sunshine. The north façade has low energy flux density for large slope angle while the density is increasing for the south façade. North-facing slopes need a wider range of  $a$ , or otherwise it causes severe overshadowing. Developing slope area has higher building density than flat area since the building on the slope is more suitable to get sunshine. When the slope angle is larger, smaller pitch of building considering sunshine and higher land using rate are available. However, the careful design to maintain the scenic view is needed.

By day, the air above the slopes can be more easily heated than the center of the lower land. Fig.3.7 (a) illustrates the interplay of slope and valley winds during a clear summer day with light winds. As the day progresses, the down-valley wind dies out with further heating. In the evening, the down-slope wind sets in. The slope winds are anabatic, and the valley wind fills the valley and moves upstream with the anti-valley wind coming downstream. Unstable upslope (i.e. the anabatic) flow arises with a closed circulation across the land involving air sinking in the center. It is at speeds of  $2\text{m s}^{-1}$  to  $4\text{m s}^{-1}$  with a maximum at about 20m to 40m from the surface.<sup>66</sup> In hot and humid condition, it leads to the greater precipitation along the ridges. Since the cross-valley circulation effectively transports the sensible heat from the surrounding surfaces to warm the whole valley atmosphere, the valley air is much warmer and a plain-to-mountain flow develops. Since the maximum pressure gradient is near the surface, the maximum wind speed is as close to the ground. Above the ridges, an anti-valley air flowing down the valley occurs through day.

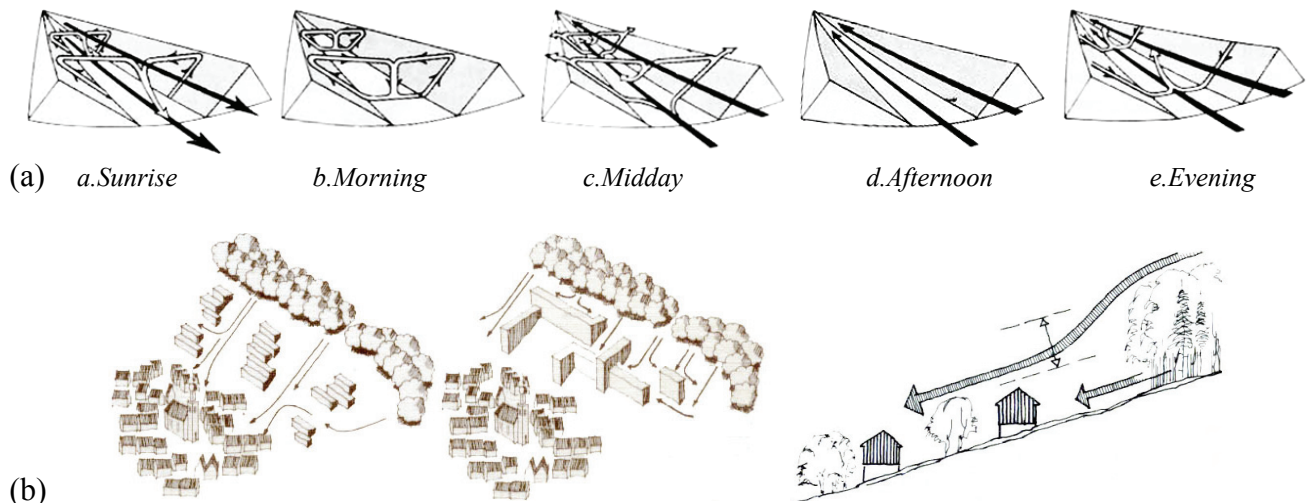
At night, the slope winds are katabatic and reinforce the mountain wind that flows downstream, with the anti-mountain air flowing in the opposite direction above. Since the valley surfaces are cool by the emission of longwave radiation and cool air is heavier than warm, the outgoing radiation at night causes a cold air layer to form near the ground surface and the air slides down. These katabatic winds usually flow at about  $2\text{m s}^{-1}$  to  $3\text{m s}^{-1}$ , but greater speeds are observed where the cold layer is thicker and where the slope is steeper. Cold air behaves somewhat like water flowing towards the lowest points. The

---

<sup>66</sup> Geiger et al. 1995.



convergence of these slope winds at the valley center result in a weak lifting motion. All of these katabatic flows combine into a down-valley flow known as the mountain wind that seeps out of the mountain valleys onto the adjacent lowlands. The anti-mountain winds flow up valley aloft. The drainage of cold air down-slope or down-valley intermittently surges rather than a continuous flow. On winter nights, some valleys would be colder than neighboring slopes about 10° and more. Airflow occurs towards the valley floor. According to Geiger et al. (1995), valley walls affect the distribution of the nocturnal temperatures by dam action, and the concave terrain forms cold air lakes or cold air puddles.



**Figure 3.7.** Slope wind systems, (a) interplay of slope and valley winds for a day, (b) streamlines in slopes and building arrangement [Geiger et al. 1995, Franke 1977].

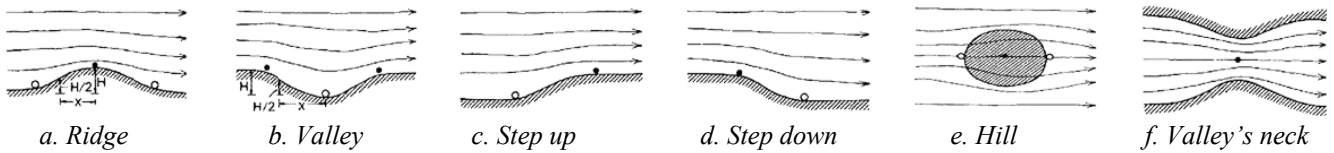
Fig.3.7 (b) shows an example of the building arrangement for streamlines in slopes. A wind is blocked by the setbacks of buildings and plantation of trees along the streets. The arrangement of buildings takes the shape of the natural streamline, wind effectively produces the induced air movement through the wind paths. Natural ventilation of a building is affected by the streamlines resulting from the prevailing wind path over the natural terrain and existing obstructions of the site. The exposure to airflow will affect the air infiltration through the building shell.

Oke (1987) introduced the flow over moderate topography. The varying elevation of the surface over moderate topography i.e. slope up to about 17°, usually brings about the adjusting flow. Essentially an increase in the ground elevation which vertically constricts the flow results in acceleration. Conversely, a drop of elevation results in a deceleration. Fig.3.8 represents some topographic forms in comparison of the flows. The increasing elevation results in speeding up to the maximum at the hilltop. On the hill, a wind speeds up over it like a ridge, but also around it with a maximum at the summit and on the valley's neck forms a jetting through the gap with a maximum at its narrowest point. The decreasing elevation results in slowing down with a minimum speed near the base of the slope for flow downwards. On a valley, the wind speed decreases and forms the maximum shelter near its floor. Talyor and Lee

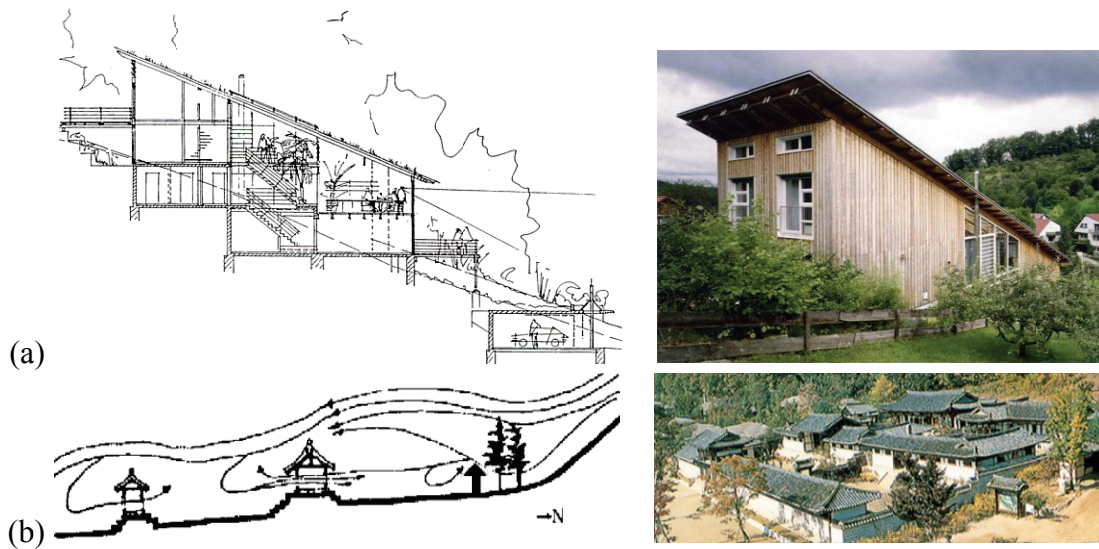
(1984) observed these wind speeds and they suggested the maximum amplification factor as,

$$\bar{u}_{\max} / \bar{u}_{\text{up}} = 1 + C(H / X) \quad \text{Eq.18}$$

where  $\bar{u}_{\text{up}}$  is the upstream mean wind speed at the same height above its local surface and  $\bar{u}_{\max}$  is the speed above the hilltop.  $H$  is the height of the topographic feature and  $X$  is the distance from the crest of the hill or top of the upstream point where the height equals  $H/2$ .  $C$  is recommended 2.0 for  $a$ , 1.6 for  $e$  and 0.8 for  $c$ .



**Figure 3.8.** Airflow patterns over moderate topography, maximum point (●), minimum point (○) [Oke 1987].



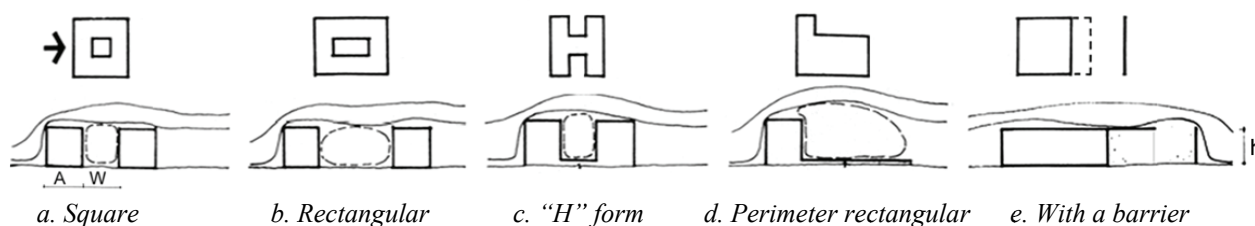
**Figure 3.9.** Utilization of topography and site condition, (a) house by Körner and Stotz in *Murrhardt*, (b) Korean traditional architectural scheme [Gunßer 2001, K.H. Lee 1986, author].

The drawing of Fig.3.9 (a) shows a house design with a suitable idea on an extreme slope. This house has been built adaptable on a northwest slope, where is on 13m slim wide and 45m depth site. Under the slope roof, four staggered levels were designed that are divided by the two storey winter garden in the middle part. The depth of the house is not visible from the hill side. The roof is tilted  $22^\circ$  follows the slope angle. Fig.3.9 (b) represents a hillside house of Korea. The Korean traditional architecture is located generally on the south slope that has a site condition with obstacles of trees and walls. This placement has an advantage to block the Siberian continental airflow (i.e. the northwest airflow in winter). The backside (i.e. north) hill and trees play a role as valley walls to avoid the strong cold wind from the northwest. The hill with trees produces a relatively large wake size acting as a windbreak that reduces 30% to 50% of the flow rate depending on the distance between the individual trees. The backside wall is the secondary block to avoid the slow wind with a relatively small wind wake area. The

wall is not only visual but also the wind control element. The gradational blocking in Korean traditional architecture is an efficient open space zoning considering the Korean seasonal airflow and the mentioned microclimate effects. Fig.3.9 (b) represents the Korean seasonal airflow pattern and traditional architecture scheme.

### 3.2.4. Building attachment and courtyard

The investigation on real geometric arrangement rather than scattered building is important since it brings about microclimate effects as much as building geometry. When a building links to the others, a courtyard is formed as Fig.3.10 shows. The wind passing over the linked buildings has a circulation feature driven by the above-roof wind.<sup>67</sup> The central courtyard perfectly protects the direct wind even if the building may be orientated in any direction. If the depth of the courtyard  $W$  is changed, the protection is maintained within the depth not exceeding 3 times of building size  $A$ . For a courtyard exceeding the size of  $3A$ , the long axis should be perpendicular to the wind direction.<sup>68</sup> A perimeter square court, i.e. “H” shape, has the same efficiency with the central square courtyard. Eddy whirls occur through wind sideslip around building limits the depth of the court to  $3A$ .



**Figure 3.10.** Several types of court for wind protection [Saini 1970].

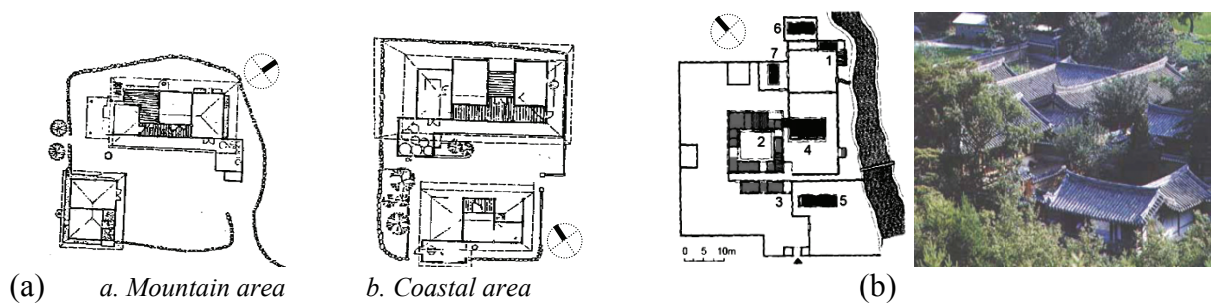
For the fully exposed space, the erection of a barrier is essential and the protection should be to the leeward side of the building. The efficiency of a barrier is related to the height  $h$  and distance from building face  $W$ . The amount of wind entering the courtyard increases with unit distance from the building face. By a combination of side barriers and roof overhangs, the enclosure is extended to a greater depth with a wind protection, since these elements protect both overhead and side. For a barrier of height  $h$ , no effects by airflow are evident up to a distance of 6.10m from the building face.

Korean traditional house constructions also have building attachments of walls and annex buildings as Fig.3.11 shows. For the arrangement, architects considered the main wind direction. In order to be profitable with the southeasterly wind, this is the main wind in summer, annex buildings and outer wall composite layers need to avoid large winds and be able to give a comfortable breeze on the floored

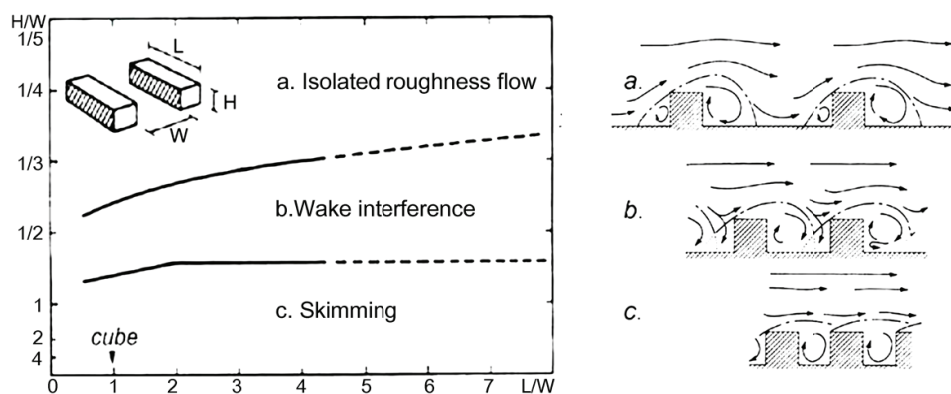
<sup>67</sup> Nakamura and Oke 1988, Santamouris et al. 1999.

<sup>68</sup> Saini 1970.

room of the main building. Small internal depth makes the interpenetration of solar radiation and the flow of small wind easy. In mountain area, a form using Korean alphabet “ㄱ” is used to avoid the north and northwest wind i.e. continental cold winds in winter as Fig.3.11 (a)-a shows. In the coastal areas, the annex building is located in front of the main building to break the sea breeze of the frontage. A courtyard between the main building and annex buildings shown in Fig.3.11 (a)-b does not have large wind. The Korean building forms organic spaces with a layered structure by the walls, the main building and its annexes. Fig.3.11 (b) represents the layered open spaces in a Korean traditional house *Dokrak-Dang* which is a model of *Seouler Garten* in Berlin. The buildings in Korea were built in 1463 and have expanded until 1835. Each building has an independent space which is divided by the walls like cells.



**Figure 3.11.** Building attachment, (a) annex building against regional wind, (b) layered structures of *Dokrak-Dang* [S.J. Lee 1988, M.K. Kim 2001].



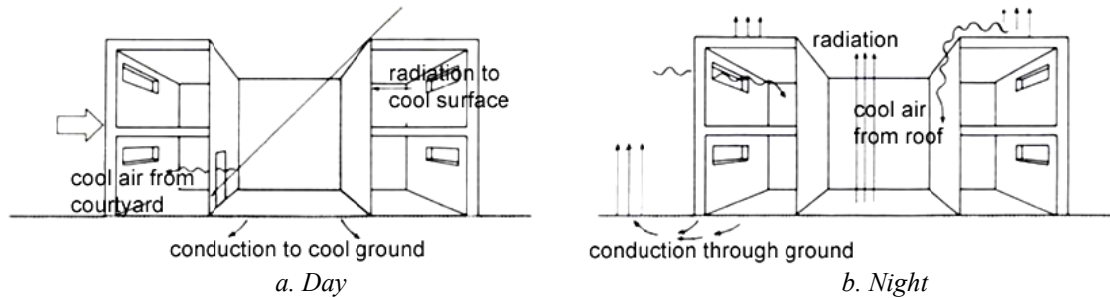
**Figure 3.12.** Airflow patterns corresponding to the function of  $H/W$  and  $L/W$  [Toudert 2005].

If air flows over building arrays, the microclimate is more complex. Three patterns are different due to the aspect ratio<sup>69</sup> ( $H/W$ ) and building ratio<sup>70</sup> ( $L/W$ ) as shown in Fig.3.12. When no interaction between the windward and leeward exists, the isolated roughness flow occurs in a courtyard between well spaced buildings as *a*. When the  $H/W$  increases, i.e. a narrow courtyard, the wakes are disturbed leading to a wake interference flow as *b*. With further increase of  $H/W$ , the courtyard becomes isolated and roof level wind leads a skimming flow shown in *c*.

<sup>69</sup> Hussein and Lee 1980.

<sup>70</sup> Hosker 1985.

In the courtyard dwelling, a stable circulatory vortex is established by the correlation of wind speed between in-courtyard and above roof-level. Even with light winds, the circulatory vortex in the courtyard can be formed by thermal imbalances due to the geometry of courtyard and the irradiation. Fig.3.13 explains the thermal system of courtyard dwellings. Since adjacent buildings, pavements and dry ground heat up quickly and the reflected heat radiation influences towards the building during the day, and at night, they will reradiate the heat stored during the day.



**Figure 3.13.** The thermal system of a courtyard house [Koenigsberger et al. 1974].

Impermeable surfaces such as solid roofs and streets influence the microclimate by impacting on the radiation or energy respectively. As a result, ambient temperatures surrounding buildings rise and lead to discomfort conditions or increased energy use for cooling. However, the deepest courtyard has the northern façades which are slightly 1~2°C cooler due to the self-shading properties of the courtyard configurations.<sup>71</sup> The vortex transports the heat and exchanges warming air in the courtyard for cool air above the roof. If the irradiated surfaces are shifted, the flow regime is also altered to others.<sup>72</sup>

The speed of the vortex is related to three mechanisms,<sup>73</sup>

- The ambient airflow above the roofs
- The vertical layer of air in the courtyard
- Advection from the corners of buildings

If the wind speed above a roof is larger, the vortex enlarges since the higher ambient winds contribute to transmit more energy from the upper to the lower vortex. The wind direction modifies the incidence of ambient air at the building corner. The parallel component of winds determines the stretching of the vortex, and the transversal component drives the vortex in the courtyard. A parallel wind to the building axis generates the uplifting flow along the walls due to the increased friction near the wall. A wind above a roof with some angle to the building axis, a spiral-type vortex is induced.<sup>74</sup> This oblique incidence improves the indoor ventilation in comparison to a perpendicular incidence.<sup>75</sup> Non-uniform

<sup>71</sup> Bensalem 1995.

<sup>72</sup> Sini et al. 1996, Kim and Baik 1999.

<sup>73</sup> Santamouris et al. 1999, Baik et al., 2000.

<sup>74</sup> Wedding et al. 1977, Dabberdt et al. 1973, Nakamura and Oke 1988, Santamouris et al. 1999.

<sup>75</sup> Wiren 1985/87, Bensalem 1991.

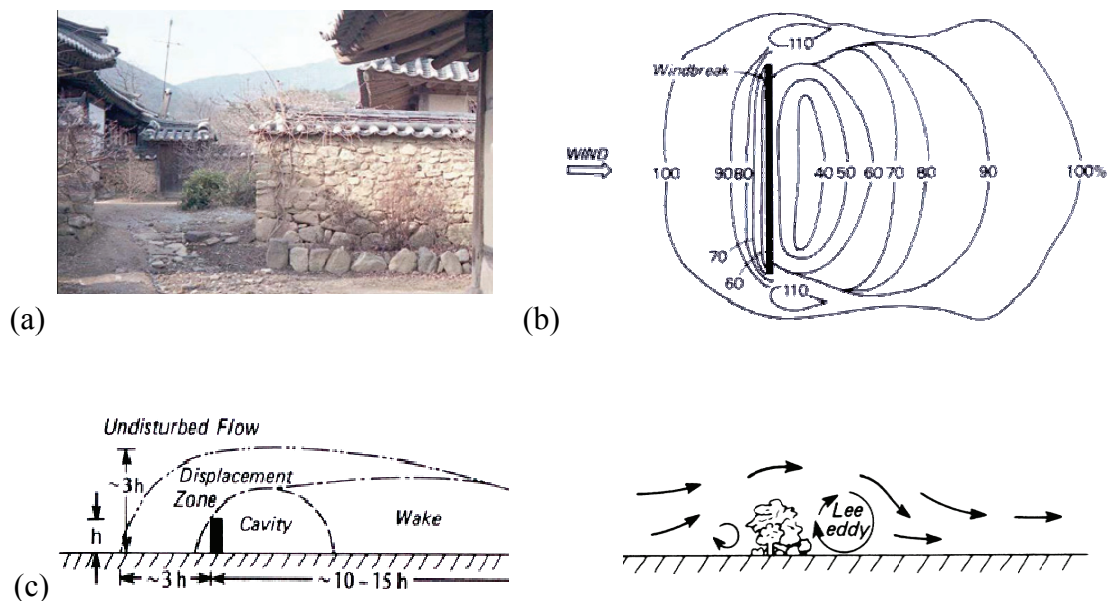


building heights and a wider courtyard also promote the ventilation and the mixing of air.<sup>76</sup>

### 3.3 Form

#### 3.3.1. Windbreak

3D objects such as wall and huge plants can protect wind and radiate heat. Sometimes they block energy flow and localize climate. The influence is measured by the percentage of reduction of horizontal wind speed in comparison to the upwind. Layered structures of Korean traditional houses uses low walls, interrupting a visual range and the large door in the walls as Fig.3.14 (a) represents. The barrier is comprehended as a closing device from the outside but, seen the point-of-view from *Maru*,<sup>77</sup> provides a sense of continuity to the court spaces. The layered wall structure offers not only a visual opening and shutting but also microclimate modifications.



**Figure 3.14.** Barrier usage and the influence, (a) layered walls of Korean architecture, (b) the wind speed in the vicinity in the open, (c) wind streamline zones [author, Oke 1987].

Oke (1987) introduced that wind speed can be modified by a barrier with different densities. If the barrier is very dense, wind speed is considerable immediately reduced to the “lee eddy” due to little or no penetration. However, the wind speed relatively quickly regains its former value when the distance from the barrier increases. The relationship between the height of barrier  $h$  and the distance related to wind speed is shown in Fig.3.14 (c). If the barrier width is significantly larger than  $h$ , the flow can

<sup>76</sup> Chan et al. 2001.

<sup>77</sup> The *Maru* is a wood-floored verandah in front of a room shown in Korean traditional architecture.

eliminate. Therefore, the pattern of wind speed in the lee conforms more to that of a high density barrier, so no advantage is gained. The lines are parallel to the direction of flows. Airflow encounters a solid barrier placed normal to its original direction. The horizontal and vertical dimensions in terms of the barrier height are efficient to compare the effects of different-sized barriers. The barrier affects flow to at least  $3h$  above the surface. If a 10% speed reduction is assumed, the air passing by a solid barrier provides its influence to about  $10h$  to  $15h$  downwind.

A barrier with low density provides a “cushion” in the cavity zone. The point with 90% recovery of the wind speed occurs at  $15h$  to  $20h$ . The reduced wind speeds can be observed as far as at the  $40h$ . A drawing in Fig.3.14 (b) represents a distribution of wind speed and a medium density windbreak. The finite length of the barrier generates the spatial pattern which areas near the ends of the barrier experience increased wind speeds and probably greater turbulence. Behind a barrier, decreased turbulence reduces the fluxes of heat and the microclimate vertical profiles are steeper than in the open. The barrier being perpendicular to the wind is more effective. In a day, the sensible heat gives higher air temperatures than in the open. At night, radiative heat loss on the surface is not efficiently replenished from the atmosphere, and thus the air temperatures are lower.

Woodruff and Zingg (1952) found the windward reduction in velocity through the analysis of airflows around four types of barriers, i.e., vertical plate, triangular and cylindrical shapes and model trees, using  $11.176 \text{ m s}^{-1}$  input velocity as Table 3.3 represents. There is no 75% reduction for trees since there is a jet movement in the air through them. Trees cause a more extended area of protection than other shapes. This is marked by the  $27h$  distance to a 25% reduction and the relatively great distance between a 25% and a 50% reduction in velocity. The vertical plate ranks the second best protection reducing about 44% more than the cylindrical shape. The plate also reduces the velocity about 10% more than the triangular shape at both near and far distances.

**Table 3.3.** The amount of wind reduction measured against varying heights and object shapes [Woodruff and Zingg 1952].

Object	75% reduction	50% reduction	25% reduction
Vertical plate	13.0 h	15.5 h	21.5 h
Triangular shape	10.5 h	15.0 h	20.5 h
Cylindrical shape	7.0 h	9.0 h	14.0 h
Model trees	-	13.5 h	27.0 h

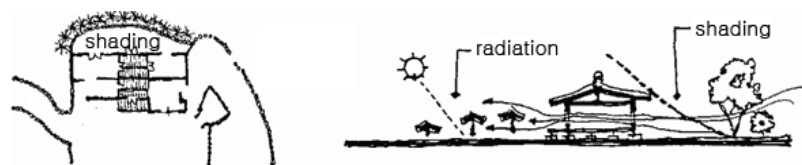
The surrounding plants are a modifying factor to improve the microclimate.<sup>78</sup> They are advantageous to the neighboring building due to the effects on the meteorological factors, e.g.  $T_a$ ,  $RH$  or  $v$ , or to the induced energy savings in the buildings such as a result of less heating and/or cooling loads. The three main properties to improve the microclimate for the site comfort are shading, humidification i.e.

<sup>78</sup> Escourrou 1991, Akbari et al. 1995, Avissar 1996, Taha et al. 1997.

evapotranspiration and windbreak.<sup>79</sup> A numerical modeling or a comparison of various scenarios have been performed in a number of related issues such as the seasonal growth of plants and changes of density and size etc.

Fig.3.15 shows that the composition of a Korean traditional house is a large front yard and a small backyard. Thermodynamic ventilation occurs due to the radiation difference between the front yard and the backyard. The front yard should not have large plants that can disrupt the breeze in summer, the dense and large plants in the backyard enables to block the reflection of solar radiation and the cold and strong wind in winter. The residential area has 50% less wind speed by the dense and large plants.<sup>80</sup> The thermodynamic ventilation acts even in the absence of wind since it occurs with the difference in air density between indoor and outdoor.

Trees in the backyard increase shadow in summer, and the kind of tree and a proper position is chosen to increase the amount of shadow for the hottest time. The leaves absorb most of the solar radiation, transform a part of the radiant energy to the chemical energy by photosynthesis, and thereby reduce the heating rate of the yards. The air temperature decreases about 3°C to 5°C on a fine day. Dense plants produce a relatively small wind wake area and the recirculation region with low velocity eddies behind the obstruction. A short and high line of trees, on the other hand, can produce a relatively large wake size acting as a windbreak.<sup>81</sup> The density of plants generates distinct flow patterns. For a line of plants starting at about 1.5m from the ground, 30% to 50% of the airflow rates can be according to the distance between the individual trees. Since the wind can flow underneath and between large plants such as tree, the distance with the building is not significant for the ventilation purpose.



**Figure 3.15.** Shading of backyard [K.H. Lee 1986].

**Table 3.4.** The effects of planting in Chicago [McPherson and Nowak 1993].

	Effect	Reducing energy efficiency (%)
Summer	Shading	37
	Evapotranspirative cooling	42
Winter	Lower wind speeds	21

<sup>79</sup> Moffat and Schiler 1981.

<sup>80</sup> McPherson et al. 1994.

<sup>81</sup> Honjo and Takakura 1990, McPherson et al. 1994

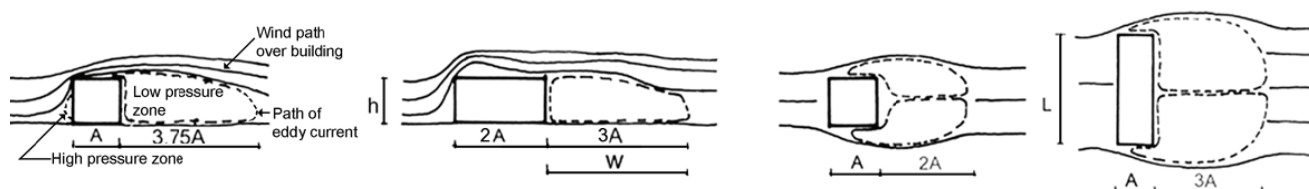


McPherson and Simpson (1995) assessed various trees' properties on energy-savings. Chicago<sup>82</sup> gained 50% to 65% energy-savings from green cover in residential areas where the energy needs are high. Annual savings created per tree are as shown in Table 3.4. The efficiency also depends on the orientation. A tree located for shading the west wall is as efficient as two identical trees on the east. On the south, the benefits are slightly lower by the negative effects of obstruction in winter.

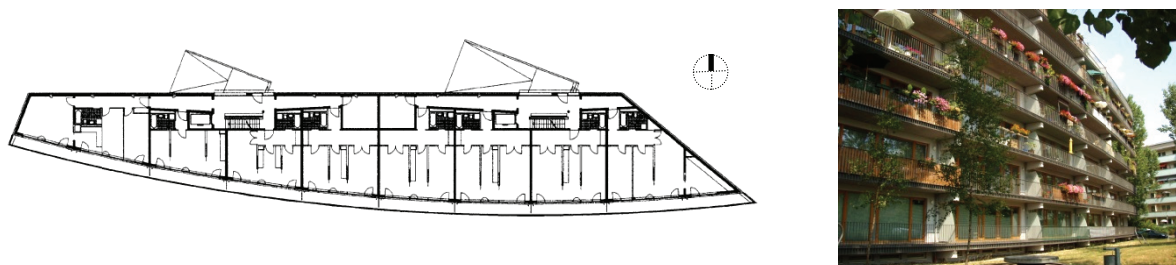
### 3.3.2. Building geometry and form

Since a building performs as a very dense solid barrier, the building geometry also affects the downwind eddy. The shape of wind depends on the changes in the proportion of the buildings and the direction and speed of wind. If the main air stream becomes turbulent during flow, the wind has a tendency to disappear. Fig.3.16 represents the relationship between building scales and wind shapes. The building shape with the building's height  $h$  and the length  $L$  modifies the amount of winds in a building façade. The increase in the unit building length  $L$  increases the size of downwind eddy current  $W$  due to the sideslip of air. Increasing the building size  $A$  enlarges the length of downwind eddy.

The optimal geometric form has been modeled for energy-saving of a prefabricated apartment block. An energy-saving house shown in Fig.3.17 has an untypical shape of volume and position setting to maximize the energy-saving. The disc-like building geometry, that stands facing to the south, has a convex curvature on the south side consisting of coated heat-insulating glass. The convex curvature



**Figure 3.16.** The effects of building geometry [Saini 1970].



**Figure 3.17.** Energy-saving house at *Fläming Str.* in Berlin by A. Salomon & Scheidt [www.stadtent-wicklung-berlin.de, author].

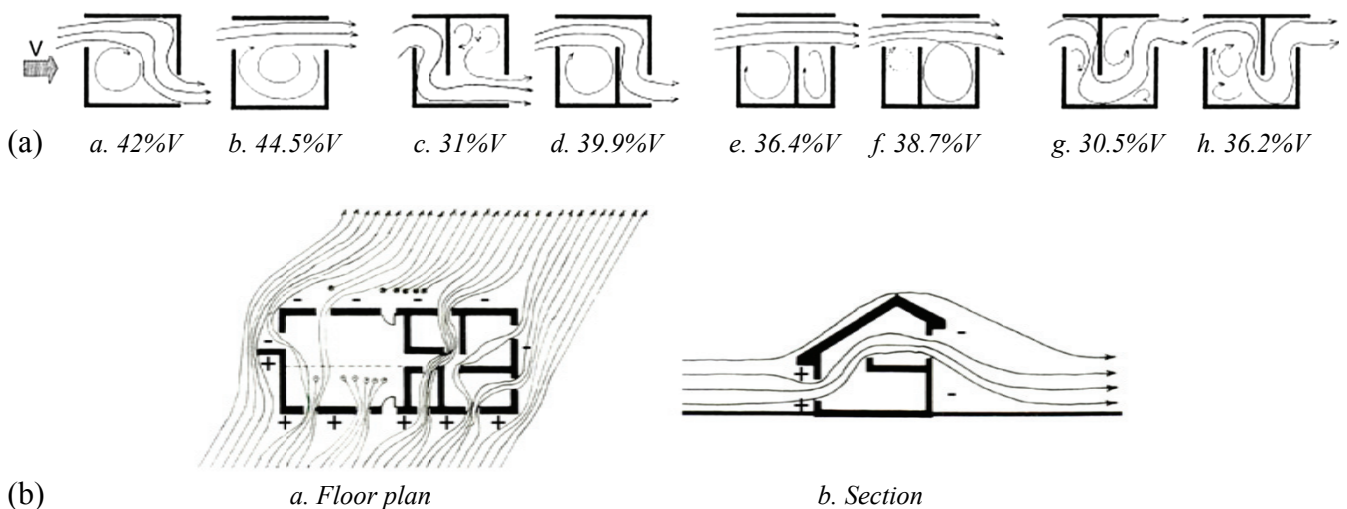
<sup>82</sup> The Chicago Urban Forest Climate Project (CUFCP) was established to increase the understanding of how afforestation within urban areas influences local climate, energy-use and air quality.

increases the solar access, and a continuous row of balconies with transparent balustrades façade layer allows the sunlight entering the room even in winter. The horizontal structuring elements such as balconies and balustrade railings and the transparent façade layer of horizontal glass elements with narrow profiles create a lightweight appearance for the building. The north façade with two access zone with staircases is an almost closed and highly insulated with vertical narrow slits. A zone with the bathrooms forms a heat buffer for the rooms facing south and locates behind the architecturally ambivalent and unsatisfying high perforated wall. The energy consumption of the building geometry does not exceed over  $40\text{kWh m}^{-2}$ .

### 3.3.3. Internal partitioning

The indoor building geometry forms with internal partitioning. An apartment consists of a number of interconnected rooms with the internal partitions. The internal partitions are installed to create a zone with still air since they drop the air velocity and make the distribution of air velocities more uniform. It is the reason why the multi-zoned buildings usually have very low ventilation rates due to the partitioning. If the width of a building is greater than the depth of its rooms, a room must be ventilated in conjunction with other rooms. However, partitioning with a proper opening makes higher airflow velocity even in a large volume.

Subdivisions with inner walls reduce the internal velocities of the whole, with the greatest reduction in average speed being from 44.5% to 30.5%. The arrangement of the partition's openings makes a number of airflow patterns as Fig.3.18 (a) shows. The window location allows the air to flow directly from inlet to outlet openings or forces it to change direction a number of times before leaving the room,



**Figure 3.18.** Internal airflow patterns using several partitions, (a) the diagrams, (b) airflow patterns of in complex partitions [Givoni 1969, Lechner 1991].

and these changes impose a higher resistance on airflow. The size of the internal opening should be designed to avoid appreciable additional resistance to airflow. The velocities are lowest when the partition is in front and nearer to the inlet window and the air has 30.5% to 31% of inlet air velocity. It is better to install partitions near the outlet and the air velocity is 36.2% to 39.9%.<sup>83</sup> Since a greater total area of the apartment may be ventilated by the main stream, satisfactory ventilation can be obtained where air has to pass from one room to another as Fig.3.18(b)-a, as long as the connections between the rooms remain open when the ventilation is required. It is preferable for the upwind room to be the larger. A high degree of porosity in the partition should be considered to enable the natural ventilation in the multi-zone building. Gandemer et al. (1992) suggested a minimum porosity of 50%.

Vertical movements of airflow exist in the building partitions. The arrows Fig.3.18 (b)-b shows vertical airflow patterns in a section of the building. If there is only one window at the first floor in the house, there is no airflow in the second floor. However, with a small outlet in the second floor, the natural ventilation in the second floor is possible since the positive (+) and negative (-) pressure areas around the building form. Airflow through the building should go from positive to negative pressure areas. Trace each windward arrow through or around the building to meet its downwind counterpart. When the airflow is forced to flow vertically to another floor plan, the airflow pattern should be smoothly connected, not cross, end or make sharp turns, since spaces that are not crossed by airflow may not receive enough ventilation. Even in complex partitions, all airflows are naturally connected and relocation of windows and additional fins change the airflow pattern.

### 3.3.4. Courtyard roofing

During wintertime, the fully glazed atrium building has a benefit which is warmer than the open courtyard dwelling. The roof atrium building has 1 °C to 2 °C higher temperature during daytime due to the solar heat gains. Although less insulation is gained from the roof transparent surfaces, the better isolation of the courtyard yields warmer the environment. Another benefit is that the atrium may be more pleasant since it is less windy. However, these features have a disadvantage of cooling in the case of overheating in the summer.



**Figure 3.19.** Ventilation parametric models for the courtyard roofing [Bensalem 1991].

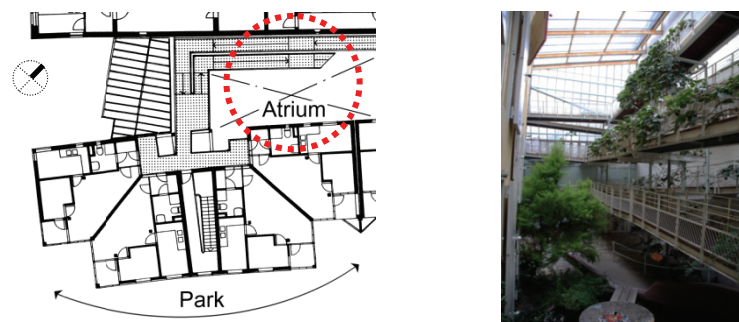
<sup>83</sup> Givoni 1969.

Bensalem (1991) studied the indoor thermal condition using the parametric model with several ventilation strategies and observed the several ventilation rates and patterns. Fig.3.19 shows the experimental ventilation models for the wind tunnel test with an open courtyard and glazed roofing, cross ventilated room and the combination of both. The indoor conditions of a glazed atrium with fully closed windows are unbearable, since the operative temperatures on daytime are above 33 °C. Whenever a single glass roof of a courtyard is used, cross-ventilation through the room windows which allow different ventilation rates improves the indoor climate.

When only the roof windows are opened, the airflow pattern is similar to the open courtyard. If the room windows are opened, while the roof vents are closed, the indoor conditions are slightly warmer by 0.5 °C in average than that of the courtyard dwelling. A combination of the roof window opening and the cross-ventilation through the room windows induces greater air movements and the indoor air temperatures are decreased. The wind tunnel test with the atrium configurations shows 0.5m s<sup>-1</sup>, whereas in the two previous cases it is 0.25m s<sup>-1</sup>. The improvement of air movement enlarges the thermal comfort zone<sup>84</sup> of 26 °C to 28 °C or 30 °C for PMV 0 with 1.0 *clo* and 1 *met*, air velocity of 0.1 m s<sup>-1</sup>. It means that the comfort time can be increased to up to 3 hours of the day time.

The use of a partly opaque monitor roof provides better shading in summer than the fully glazed ones. By shading the court, the coolest conditions for the surrounding room can be obtained. The comfort time is then increased up to 5 hours to 6 hours in most of the rooms except in the northern ones facing the wind, in which, comfort is reached in the whole occupancy period. Shading the façade windows and improving the insulation of the building also leads to greater improvement.

Fig.3.20 shows a public housing with a glasshouse covering a large inner court designed by O. Steidle. The structure is a conversion of the existing transverse wing of two-housing modules that are divided by diagonal walls. The four-storey row is set off from the firewall roughly by the depth of the building. The



**Figure 3.20.** Public housing at *Köpeniker Str.* in Berlin by O. Steidle [modified from Heckmann 1994, author].

<sup>84</sup> Markus and Morris 1980.

1 *clo*: A measure of thermal resistance and includes the insulation provided by any layer of trapped air between skin and clothing and insulation value of clothing itself. 21 °C, 50% RH, 5m/s air movement.

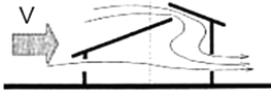
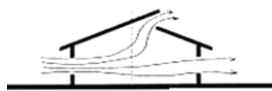
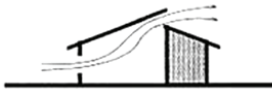


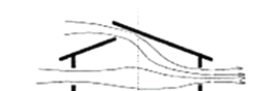

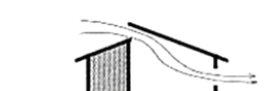
1 *met*: Estimation of Metabolic rate, typical metabolic rate for a sedentary person, 58.2 W m<sup>-2</sup>h<sup>-1</sup>.

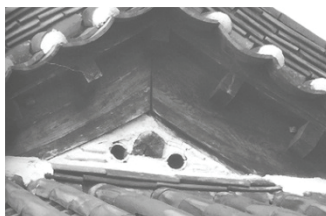
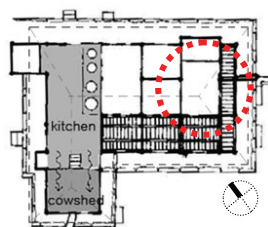
intermediate space was transformed into a glassed-in access hall with ramps the length of the building. The housings are accessed through a short entry hallway. In the housings along the access hall, the kitchens and baths are lit and ventilated via the hall: the outside-oriented housings have inside baths, but kitchens with large windows to the park. The glass surfaces in front of the sleeping and living areas developed around the façade recesses and the kitchen and the small bedroom can be entered from the living room. The hall is covered by roofs of glass and a passive energy concept enables for efficient planting under the glass roof.

### 3.3.5. Roof opening and stack effect

Ventilation is concerned with the supply of fresh air and especially in hot climates the promotion of convective cooling with the air movement at a relatively slow rate. The two main ways in which natural ventilation occurs are through the stack effect in calm conditions, through combined stack effect and wind and through wind only at air speed in excess of  $3\text{ m sec}^{-1}$ . Since the velocities above the roof level are much greater than at wall level, roof openings with clerestory windows, ridge projections or wind-catchers<sup>85</sup> can derive more airflow. They are particularly advantageous in densely built areas which have significantly smaller projections than the building volumes. Gandemer et al. (1992) tested the effectiveness of clerestory openings in roofs by wind tunnels and showed that the clerestory area

**Table 3.5.** Effects of clerestory on average internal airflow rates [Busato 2003].

			
	84%V	78%V	54%V
			
	69%V	66%V	48%V
Not good	Good		



**Figure 3.21.** Exposed roof-ventilation holes of the gable roof of Mr. Eu's house [M.K. Kim 2001].

<sup>85</sup> They potentially act either as air inlets or as extractors depending on the wind direction.



needs to be at least 20% of the cross-sectional area of the building perpendicular to the window direction.

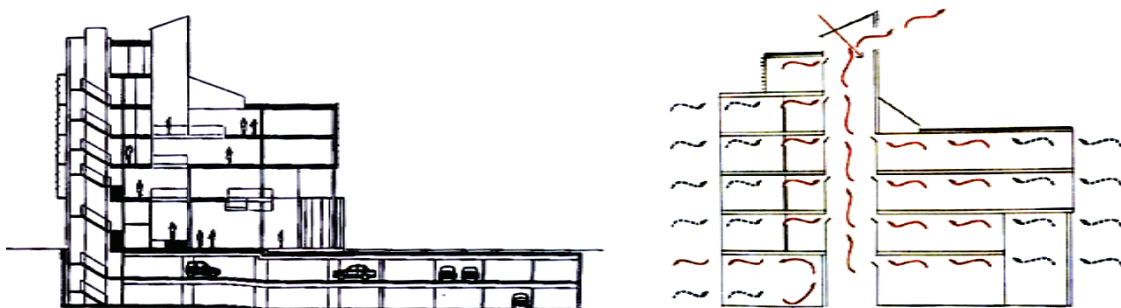
A properly designed clerestory opening increases the average indoor air speed in cross-ventilated rooms as much as 40% by openings and 15% by inlets.<sup>86</sup> Table 3.5 illustrates the incorrect positioning of clerestory openings relative to the building's central axis. The best position for inlets is in the upwind part of the roof and in the downwind part for exhausts. The introduction of roof ventilation may be a particularly useful strategy for a deep-planed space or kitchen where flow rates cannot sufficiently be provided by a single window opening.

In Korean traditional house designs, exposed roof-ventilation holes are often installed. Fig.3.21 shows an exposed roof-ventilation hole of the gable roof of Mr. Eu's house. The house has a shape of the Korean alphabet “ㅓ” and is composed of 3 layered spaces with several annex buildings on a sloped hill. Since the layered spaces need ventilation, the roof opening is effectively designed to discharge the warm air in the kitchen. Since warmer airflow vent out of the top part of the opening through loft of rooms, cool air is drawn at the bottom of the rooms.

Thermal type ventilation utilizes the stack effect which is a thermal force caused by temperature difference and air density. Ventilating shafts are installed to exploit the stack effect in a building. If many shafts are installed in a great cross-sectional area, there may be a large temperature difference and a large motive force, and therefore the more air will be moved. The motive force is the “stack” pressure as

$$P_s = 0.042 \times h \times T \quad \text{Eq.19}$$

where  $P_s$  is the stack pressure (Pa) in the height of stack  $h$  (m) for the temperature difference  $T$  (°C). Since a stack pressure promotes the vertical air movement, shafts are effective for internal ventilation in climate conditions where the temperature difference in winter is large. The air passing through the central space moves from the bottom corner of the wall of each room facing the wall to the openings at



**Figure 3.22.** Stack effect of an IHK's office in *Karlsruhe* by C. Steffan [Lefèvre 2002].

<sup>86</sup> Bittencourt 1993.

the top of the same wall. It works well with buildings of three or more stories as Fig.3.22 represents.

Warm and light air rise in an internal multi-storey solar chimney with venting at roof level. While the sun heats a solar chimney at the top of the building, the air moves in a duct. The temperature differences significantly increases airflow. The ventilation can provide a comfortable temperature without air conditioning. Since the shaft is large enough and located high, the inlets and outlets maximize the effect of prevailing winds.

## **3.4. Façade elements**

### **3.4.1. Microclimate in opening control**

If the difference between the indoor and outdoor temperatures is not large, the vertical pressure gradients do not differ between inside and outside since the difference between the air densities is not large. In this situation, an aerodynamic pressure with ventilation is higher than a thermodynamic pressure. If the air pressure on either side is equal by a single opening at a certain level in the building, there is no thermodynamic airflow and stack effect through this opening. Therefore, effective horizontal aerodynamic ventilation with wind is more important to modify the microclimate than stack effect ventilation. If the indoor air is warmer and thereby less dense than the outdoor air, a vertical pressure gradient in the building is smaller than one of the outside, and the indoor air does not flow well. If the air pressure between inside and outside, and above and below is different, the ventilation rate is proportional to the density of the air. For two openings at different heights, if the indoor temperature is higher than outside, a pressure difference forms. While a depression inducing an inward flow occurs at the lower level, high indoor pressure occurs near the upper opening and the air flows outwards. Thus, the indoor air can circulate. For the lower indoor temperature, the positions are interchanged and the flow direction reversed.

Olgyay (1973), first proposed to systemize the incorporation of climate into architectural design. However, the method just considers the outdoor climate data only and it is not suitable to the largely varied indoor environment by outdoor climate. It is thus suitable for application only in humid regions where ventilation is essential during a day and there is little difference between the indoor and outdoor conditions. The application particularly in the subtropics, leads to erroneous results in Korean climate since the indoor climate does not always needs ventilation.

### 3.4.2. Opening locations and shapes

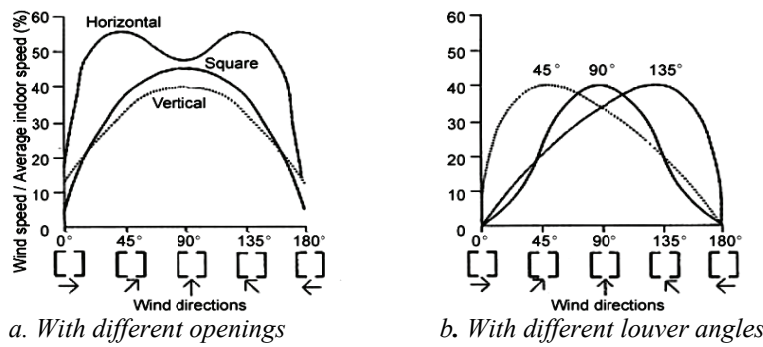
For the design of an individual space, air distributions or concentrated jets should be determined to plan the most preferred ventilation. The main factors affecting airflow patterns are the sizes and shapes of inlet apertures. The location, type and configuration of the inlets and the configuration of other adjacent elements such as internal partitions and projections etc. affect the ventilation performance.

The opening sizes and shapes are important factors that determine airflow inside a building. If air flows straight through the room, ventilations occur only in a limited part that has high air velocity. The cost of windows is expensive, i.e. a square meter of window is normally 2.5 times more expensive than a square meter of wall. A large window is more difficult to shield a direct solar penetration or a cold wind. In a district in high latitude, the main function of windows is to obtain natural lights, and the window shape is often vertically rectangular. In a tropical region, the window mainly performs ventilation, thus the window shape is frequently horizontally rectangular.

Dăng (1985) analyzed the efficiency of different window heights for a hot and humid climate. If the height of a window is greater, the air can move quicker above the upper half of the room. On the contrary, the air velocity decreases for the lower half. When the height of a window is small, the air velocity is large, and the shape of the streamline is narrow. A large window performs better for the indoor ventilation. However, the width of the window should not be smaller than 0.5 times of the width of the room to generate air streams covering at least 70% of the floor area. The window form with a medium height and a large width stretches the air streams, and thereby has the best efficiency for natural ventilation. Moreover, it is the easiest to shield direct solar penetrations or a cold wind.

The shape and configuration of opening modifies the internal airflow. For a fixed opening size, a horizontally square and vertically shaped inlet yields different air motions in the room. Horizontal inlets provide larger internal airflows than squared or vertical inlets. A wind incidence angle of  $90^\circ$  i.e. perpendicular to the window surface offers the optimal performance for horizontal inlets. Fig.3.23-*a* shows the percentage of indoor air speeds for different locations of openings. Hence, the introduction of vertical louvers increases the performance of ventilation in horizontally shaped inlets since they can catch more winds. Fig.3.23-*b* represents the percentage of indoor air speeds for different angles of louvers. Although a rectangular opening also provides well-distributed internal airflows, the performance is not enough to cover the room.





**Figure 3.23.** Performance of different wind direction with shape and angles of opening [Busato 2003].

Two openings in opposite walls improves ventilation rates, and the natural ventilation using two openings is referred to as “cross-ventilation”. If there is one opening, the air velocity is almost independent of the wind direction and the indoor velocity is approximately 10% to 15% of the external wind. With two openings for both the windward and the leeward sides, the average velocity is much higher, ranging from 30% to 50% of the external wind speed for the different inlet and outlet sizes, the wind direction and the axis between inlet and outlet.<sup>87</sup> In a study of indoor air motion,<sup>88</sup> a simulation using two windows with 1/4 size of the wall performed at the center of the opposite wall showed some features as follows;

1. The relationship between the outer wind speed and the average indoor air speed generally is in the linear proportion.
2. A room normally has wind shadow with vortex after inflows. Therefore, a part of inflows has worse distribution of air speed and direction.
3. If the model’s length is long, the distribution of indoor air velocity is slowly decreased.

The performance of ventilation using adjacent windows extremely depends on the wind direction since the ventilation performance of windows on adjacent walls depends on the pressure distributions closely related to the wind direction. Table 3.6-*a* classifies the wind direction into good or bad cases. Some ventilation is possible in an asymmetric placement of windows since the pressure at the center is relatively higher than the pressures at the sides of the windward wall. Table 3.6-*b* illustrates the ventilation performance of windows at a side of a building. The pressure is greater at the center of the windward wall than at the edges and some pressure difference in the asymmetric placement of windows exists even though there is no pressure difference in the symmetric scheme.

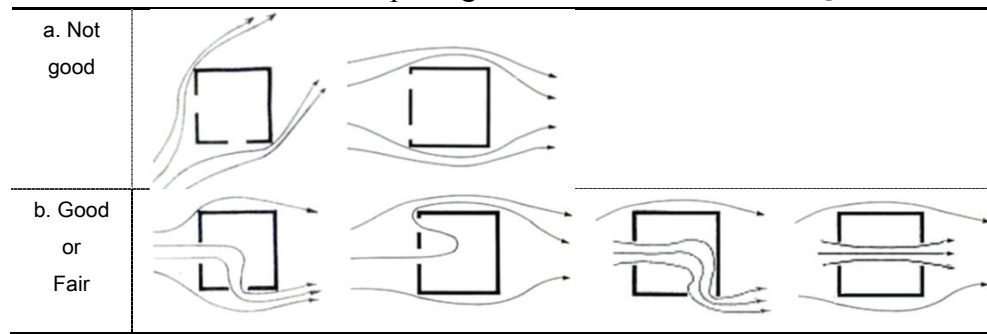
The outlet size affects the indoor airflow rates. If the outlet is larger than the inlet opening, a large airflow rate occurs. A smaller outlet than the inlet, the air velocity cannot be distributed over the room.<sup>89</sup> In this case, part of the kinetic energy converts to static pressure near the leeward opening. For the same

<sup>87</sup> Givoni 1969.

<sup>88</sup> H.T. Kim et al. 1988.

<sup>89</sup> Givoni 1969.

**Table 3.6.** Airflow related to the opening location or wind direction [modified from Lechner 1991].



size of inlet and outlets, the internal air speed is related to the building envelope irrespective of the angle of incidence of the wind.

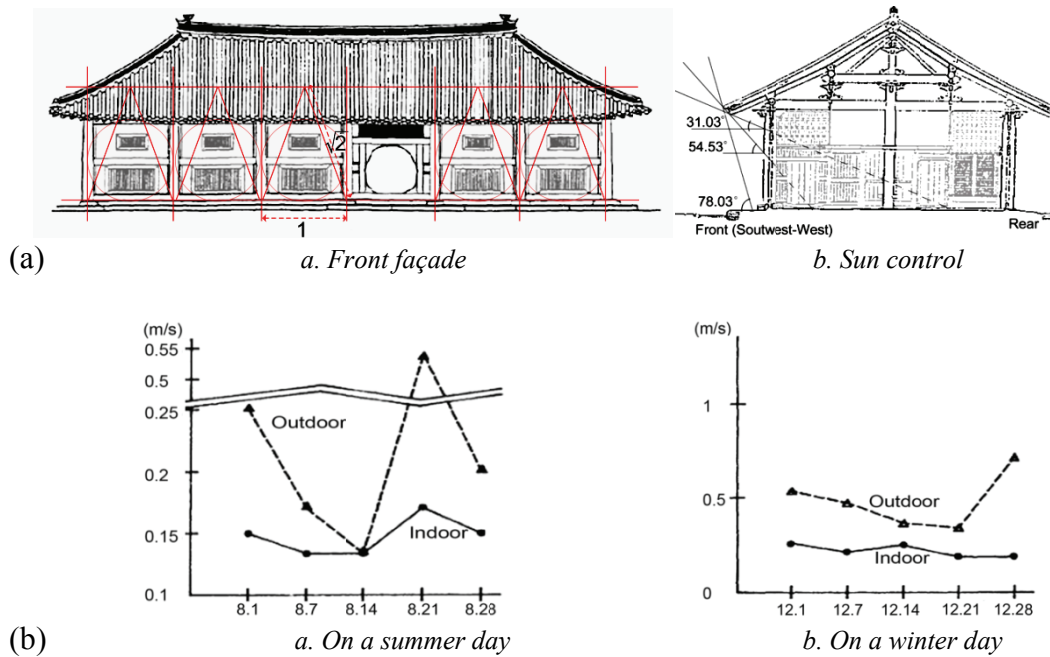
Although the cross-ventilation using windows of two opposite walls are optimum in rooms with openings, such configuration is not common.<sup>90</sup> If the angle of wind is perpendicular to the inlet for most configurations, opposed to inclined wind incidences, the high average air speeds can be achieved by openings in two adjacent walls. The total size of the openings in the walls with the smallest area of openings almost determines the internal air distributions with intermediate openings. It is also an important point in planning a multi-zone space.

The different opening sizes between inlet and outlet modifies the airflow shape and solar penetration. In Korea, the *Janggyeong Panjeon*<sup>91</sup> in *Haeinsa* Temple uses different sizes of the upper and lower parts for the front windows arrangement. The front windows form an iso-scales triangle with base size 1, height  $\sqrt{2}$  as Figure 3.24 (a) shows, and the rear windows are reversely arranged. In the front elevation, the lower part opening size is 4 times larger than the upper part one. In the rear elevation, the upper part opening size is 1.5 times greater than the lower part one. The opening size comes up to around 18% to 29% of the front-backside wall area and this result gives the constant air circulation. The design intended to be effective cross-ventilation for preservation of woodblocks of scriptures against deterioration.

The building is quite famous in Korea due to the efficient ventilation, effective moisture prevention, proper balance of temperatures and well-designed arrangements. The building features different size and shape, of the windows at each wall of the building, different height of each side wall, arrangement of shelves in the hall, and the location of the building. Recently, computer simulations found out the airflow characteristic in *Janggyeong Panjeon* shows very well distributed airflows in the room even though the building is 60.5 m wide and 35 m deep. Fig.3.24 (b) shows that the indoor air velocity is very stable and low with about 0.15m/s while the outdoor air velocity is varying. On a winter day a breeze

<sup>90</sup> Bittencourt 1993.

<sup>91</sup> It was added in the UNESCO world heritage lists in 1995.



**Figure 3.24.** Opening sizes control of *Janggyeong Panjeon*, (a) the structure, (b) mean airflow speed [modified from Y.W. Lee 1986, S.M. Lee 1999].

with a velocity of 0.5m/s, the indoor air velocity is 50% lower. In summer, the building inside is cooler than outside, and the room has uniform temperature distribution through the four seasons. The horizontal and vertical gradients have uniformity of less than 2 °C.

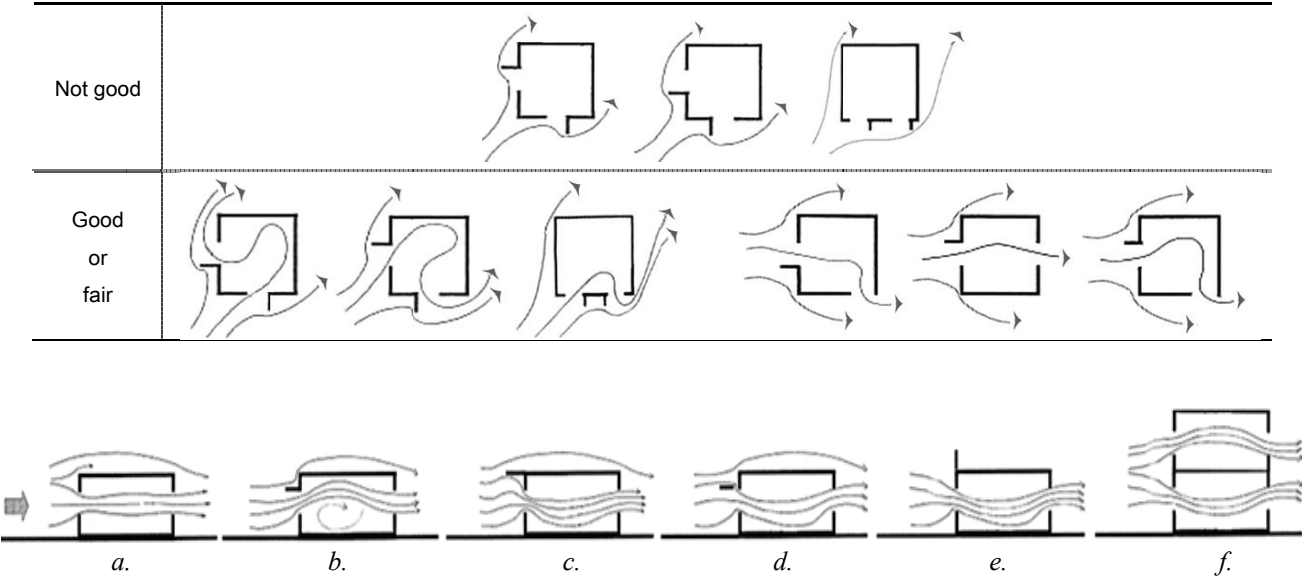
Although it doesn't have any heating and cooling equipment, the dehumidification performance of the building enables sunlight control or ventilation performance for the preservation of the wood printing blocks in the hot and humid summer and the dry and cold winter over 600 years. *Janggyeong Panjeon* is a good example of control temperature and humidity by only microclimate.

### 3.4.3. Projected building structure

The vertical projections such as external wing-walls or internal partitions can modify the internal airflow shape and rates since they derive the pressure difference. If the wind blows obliquely up to 60°, a wall with a vertical projection can induce cross-ventilation in rooms with only a single exterior wall.<sup>92</sup> The position and size of external projections are related to the prevailing wind. External projections act as a vertical wind-catcher. The internal ventilation rates are enhanced especially for skewed and perpendicular winds. The vertical projections are efficient to modify the pattern and direction of internal flow by altering the pressure around the inlet. For example, fin walls can significantly increase

<sup>92</sup> Givoni 1969.

**Table 3.7.** Effects of wing-walls on cross-ventilation and the wind direction [Busato 2003, Lechner 1991].



**Figure 3.25.** Horizontal projections and airflow patterns [modified from Busato 2003].

ventilation through windows on the same wall and side of a building by changing the pressure distribution. However, an incorrect usage, e.g. several fins placed on the same side of each window or blocking a streamline, makes the opposite effect such as blocking of the natural flows, and thereby poor ventilation. Table 3.7 shows the several flow patterns by vertical projections.

For the shading properties, horizontal projections such as overhangs, canopies and verandas are frequently used in a house design. They can modify internal air patterns from Fig.3.25-*a* to Fig.3.25-*b* or Fig.3.25-*c*, due to increasing the amount of the entering airflow. Fig.3.25-*a* is the room without horizontal projection, and Fig.3.25-*b* and Fig.3.25-*c* respectively shows rooms with different locations of horizontal projections. As Fig.3.25-*b* represents, the horizontal projection placed above the opening eliminates the downward airflow at the inlet and pushes the air-stream towards the ceiling. The air circulation passing above the occupant's head, i.e. upward flow, is of little use for direct cooling in a living space. However, this may be efficient for spaces such as kitchens where air extraction at high levels is desirable. The introduction of a distance between the projection and window, as Fig.3.25-*c* shows, will tend to reinstate the upward flows into the original course of flow shown in Fig.3.25-*a*. A gap between projection and building, shown in Fig.3.25-*d*, similarly recovers the downward flow by modifying the downward pressure at the top of the inlet opening. Meanwhile, a large solid surface with the elevation builds the relatively large magnitude of pressures, and increases the air-stream in an opposite direction. The airflow pattern is very similar to the case of Fig.3.25-*c*. Fig.3.25-*e* illustrates a large solid surface with the elevation and another possible remedy is a large roof parapet wall. In a two-storey building shown in Fig.3.25-*f*, airflows on the ground floor may be satisfactory with downward flow, but the airflow on the upper floor shapes upward flow due to the ceiling of the ground floor.

In Korean traditional houses, a peculiar floor structure for summer called *Maru* is often attached to the main building. Fig.3.26-*a* shows the structure of the *Maru*. The *Maru* is used as a main floored room to enjoy the summer life as shown in Fig.3.26-*a*. The *Maru* allows lighting and ventilation and avoids the moisture from the ground in summer. The most important features of the structure are the orientation exposed to the south and the usage of a void bottom. In summer, the two walls of living space on the floor can be opened and a cross-ventilation occurs. The air underneath the floor is also cross-ventilated and additionally much cooler than the living space due to the double shading use of the large roof overhang and the deep floor structure. Since this process needs a good shading of over 35% under the roof in summer, Korean traditional architectures generally have out-standing roofs with eave supporters



**Figure 3.26.** Out-standing structures, in the Korean traditional residence [author, K.H. Lee 1986].

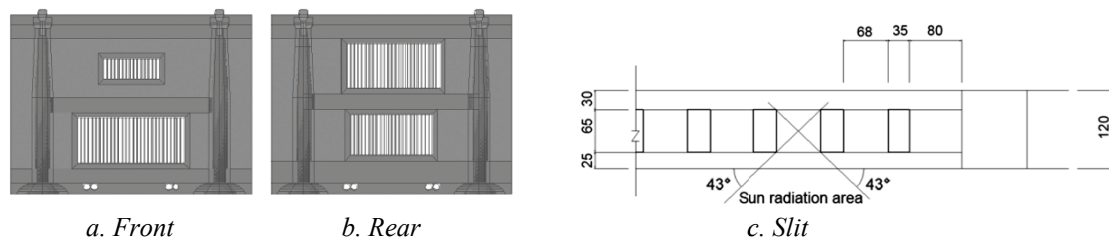
as Fig.3.26-*b* shows. The deep eaves keep direct sunlight out of the rooms in summer, which has 60% size of column, is favorable to avoid the overheating and the heavy rain. The difference of radiation on the floor induces a microclimate effect with a small charcoal brazier. If air flows through the opened space on the floor, the cool air of the bottom can be exuded onto the floor due to the difference of air density. In winter, a door closes the north wall on the floor, cross-ventilation does not occur anymore, and thereby the microclimate effect is stopped. The well-designed roof considering the solar altitude allows a high radiation heating with a deep solar penetration into the *Maru*. The length of the eaves is 1m to 1.2m fitted to the altitude of the sun promotes the radiation in winter. Fig.3.26-*c* respectively represents the cross section of the roof structure with eave supporters and the seasonal solar angles allowing for summer shading and winter heating.

#### 3.4.4. Opening slits

For adjusting direct penetration of several outdoor factors such as solar radiation and wind, opening slits such as louvers, жалousies and horizontally pivoted sashes are often attached in front of openings. Some opening slits such as fins also change the direction of the penetration. In Korean traditional architecture design, lattice window and rattan blinds are always used to provide soft sunlight.



Vertical mullions shown in Fig.3.27 generate horizontal shadows and the shape of shadows depends on the deepness and size of mullions. The advantage of vertical mullions is that they temporarily provide solar radiation. These slits perform as a fixed vertical louver that can block solar radiation after sunrise and before sunset. In the case of opening slits of *Janggyeong Panjeon*, the size of the interval is 65~70 mm, and Figure 3.27c shows the horizontal cut for the details. The drawing uses the average interval of window size with 20 bars since the size of interval is not regular. The slanted lines mark the possible range of solar radiation area.



**Figure 3.27.** Opening slits of *Janggyeong Panjeon* on the elevation of a module [author].

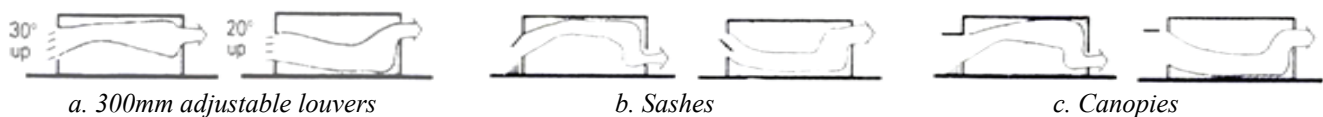


**Figure 3.28.** Debris tower in Berlin designed by R. Piano [author, [www.buildingenvelopes.org](http://www.buildingenvelopes.org)].

Louvered openings can increase the amount of airflow by coupling with other elements with high-level shading projections and perforated blocks since they act as a wind-catcher. R. Piano is developing a technologically sophisticated and highly effective curtain wall operating system. The curtain wall offers considerable advantages in terms of the conservation of energy, lighting, user control and comfort. It combines traditional materials and natural ventilation with innovative technology (pivoting panels with sensor control). South, East and West façades, that have high solar exposure as well as the façades of the interior atrium are highly detailed and show environmentally advanced solutions in curtain wall design. Fig.3.28 shows a building with glass panels with louvers at east, south and west elevations and double skin façade designed by R. Piano. Operable glass louver supported by two axes that hold the glass blades and truss rods that activate their openings, are placed 27 inches outside an inner wall of operable glass windows. The outer glass panels open up to a 70° angle of rotation, they reflect light differently depending on the angle that they are pivoted at and allow for warm weather ventilation. Sensors, that are programmed to open during the night and ventilate the heat accumulated during the day, control them. The louvers allow cooling breezes to enter the building, making air-conditioning supplementary and not mandatory. The mechanical system operates only when the temperature drops

below 5 °C or exceeds 20 °C. The building achieves natural ventilation for around 60% of the year. The maintenance platforms between the two skins act as horizontal sunshades. The combination of the double skin wall and louvers is extremely effective in reducing the heat penetration during the summer and produces a greenhouse effect during the winter. The exposed concrete wall at the outer edges of the floors maximizes the heat gain in the winter, and it absorbs the excess heat with its thermal mass properties during the day and radiates it back at night.

Adjustable horizontal louvers are especially beneficial since they allow greater control of the direction of airflow. The up to 20° upwards position of blades shown in Fig.3.29-*a* can still channel the flow into the room. Sashes can divert the upward airflow as Fig.3.29-*b* represents. A casement or reversible pivot sash makes downwards airflow in the room. Canopies shown in Fig.3.29-*c* can eliminate the effect of pressure build-up above the window. The pressure below the windows enforces upward flow direction. When the canopy makes a downward pressure, a flow directs into the living zone.



**Figure 3.29.** Airflow patterns of ventilation for several slit types [Busato 2003, Koenigsberger et al. 1974].

## 3.5. Analysis of building microclimate

### 3.5.1. Problems for energy assessment

Climate design tools such as the comfort diagram, solar charts, and heat gain and loss estimations help architects at an early design stage to establish the guidelines, recommendations or design solutions for energy-saving. These tools are not efficient to investigate the quantitative assessment for single or multiple design elements.<sup>93</sup> However, computer simulation tools, e.g. EnergyPlus (EP), TRNSYS, CONTAM, and SPARK etc., are more precise and quantitative to estimate the energy consumption since they can quickly analyze complex influential effects of several designs. However, the parametric analysis is not sufficient to analyze the building microclimate since they just establish the rough designs.

The European Parliament has drawn up the directive on “Energy Performance of Buildings (EPBD)” to harmonize requirements within the European Community and to frame them in a mandatory and

<sup>93</sup> Bensalem 1995.

holistic way. The German Energy Conservation Regulation “*Energieeinsparverordnung*” (EnEV,2001), implemented in February 2002, refers to a calculation methodology for the energy performance of buildings which already covers most of the aspects mentioned in the general framework for a calculation procedure in the EPBD. The German DIN (German Standardization Institute) V 18599 is an Excel-based calculation tool. The DIN V 18599 series of preliminary standards provide a method of calculating the overall energy balance of buildings. DIN 18599 is dealing with the energetic assessment of buildings in a much more detailed way.

However, there are a few tools to deal with several climate modifications of building design in the energy assessment. Climate models are classified by several scales: from kilometers to few centimeters. The main problem with the parametric analysis always uses a large scale that is probably suitable for urban planning issues. However, the microclimate modification of the building design is substantially variable in the large scale. Thus, the computer simulation tools for parametric analysis cannot be used for building microclimate analysis. For example, natural ventilation is very difficult to analyze with the parametric model accurately although the tools can predict the performance of mechanical ventilation systems. There are four main complex factors for the analysis of natural ventilation.

- Geometric dimensions of building site
- Exterior and interior configurations of buildings
- Aerodynamic variation by airflow movement
- Thermodynamic pressure by the temperature variation

### **3.5.2. Previous methods**

Despite the difficulty to analyze the microclimate modification, a lot of research has been carried out to understand microclimate phenomena e.g. heat diffusion, natural ventilation, solar radiation heating and evaporative cooling etc. Most research has utilized three methods as follows<sup>94</sup>

#### **(1) Model/field experimental method**

Field experiments can provide the temporal average airflow rate passing through a naturally ventilated building. Katayama and Tsutsumi et al. (1996) performed a full-scale measurement of 4 indoor thermal factors, i.e. airflow speed, air temperature, wet bulb temperature and globe temperature, using a field experimental method. However, the problem is the complexity to obtain a good measurement. Model experiments are much suitable to be more controllable and reliable than the field experimental method.

---

<sup>94</sup> Tan 2005.

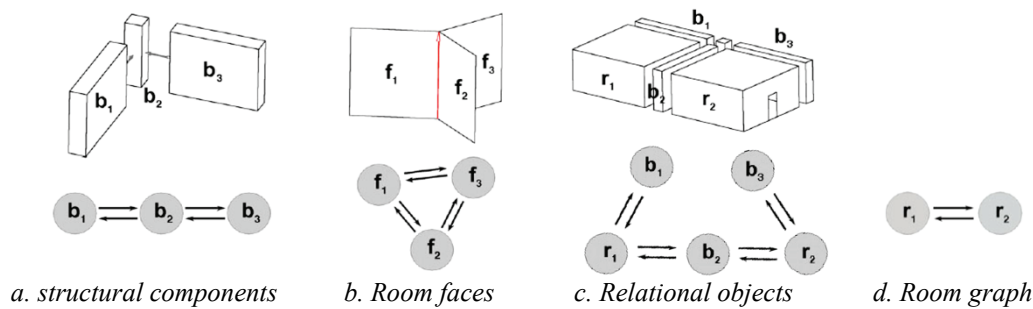


A model with several design parameters for wind tunnel test provides the wind pressure coefficients around buildings. For example, model experiments with several types of windows can provide several detailed information on the velocity coefficients, jet contraction coefficients and discharge coefficients.<sup>95</sup> A wind tunnel investigation virtually analyzes the aerodynamic effects on the pressure distribution on building adjacent.<sup>96</sup>

## (2) Analytical methods

When we investigate the complex physical phenomena, some assumptions are efficient to simplify the problem and derive simplified equations. For example, the design of natural ventilation systems for passive cooling is very difficult to predict the natural forces, buoyancy offsets, the prediction of ventilation rates, position and size of the openings. However, analytical methods can investigate the complex problem by a simplified geometry model, e.g. simple analytical formulas for a volume or a zone. A theoretical expression for the stratification interface compares to an ousting model, and a good agreement with the experiment measurements can be obtained.

For the multi-volume or –zone, the expression of each zone is combined to another to accomplish relatively networked-zone models. A multi-zone model assumes that a building zone has only one homogeneous condition with a uniform temperature and pressure. Several zones can be connected with other zones with different condition by openings between rooms and/or openings to the outside. The multi-zone analysis is the decomposition of the entire model into a so-called “connection model” or “graph model” as Fig.3.30 represents. A graph of the zones shows the physical structure with connections between zones.



**Figure 3.30.** The geometric representation of building zones and the structural component graph [van Treeck and Rank 2004].

Several sub-level units ( $r_{1,2}$ ,  $f_{1,2,3}$ ,  $b_{1,2,3}$ ), that define room, wall, roof and floor etc. shown in Fig.3.30 , visualize the analysis structures for computer simulation. The topological relations between all faces can be derived by the graph of room faces. For example, wall is a unit being outside, inter-zone or inside

<sup>95</sup> Flourentzou et al. 1998.

<sup>96</sup> Jozwiak et al. 1995.

walls. The room graph represents the geometric property between the indoor and outdoor or in the indoor air volumes. The graph model provides simplicity, straightforward solutions that allow the prediction of bulk flow through the whole building driven by wind buoyancy or mechanical systems. Most building analysis software is based on the multi-zone model.

TRNSYS<sup>97</sup> and EP<sup>98</sup> are the most famous programs to analyze a complex building energy by breaking the problem into a series of smaller components. Each small component is independently analyzed at first, gradually couples with other components and forms a large component system. Although the software tools solve a parametric equation of mass and energy balance for multi-zone buildings, they cannot represent detailed temperature and airflow distributions related to the thermal and aerodynamic effects in the complex geometric configuration.

### **(3) CFD methods**

Computational Fluid Dynamics (CFD) method numerically solves a set of partial differential equations for the conservation of mass, momentum (i.e. Navier-Stokes) equations, thermal energy, and concentrations. Navier and Stokes found the generic form of differential equations in the 19th century as a simple variation function derived by a small, or finite, volume of fluid. The variable represents predicted quantities such as pressure, velocities in three directions, temperature, concentration and turbulence quantities at any point in the 2- and 3 dimensional models. Small modifications, e.g. the amount advection into the volume or diffused out from it, can be represented by a variable in the space. The method can provide a detail of distributed air temperature, velocity and contaminant concentration within individual spaces and turbulence models throughout an entire building.

The main process includes the geometry definition, the grid generation and the numerical simulation. The geometric definition sets up the boundary conditions where the problems are located, and the grid generation entails the specification of the physical configuration by dividing the boundary conditions up into a grid containing of small volume units. The partial differentials between nodes on the grid are iteratively solved. Fig.3.31-*a* shows the grid generation with physical configuration and Fig.3.31-*b* represents a partial differential, i.e. flow, in the grid. For example, the mass flow rate  $m$  between two nodes  $i$  and  $j$  sets up in the grid, and a flow  $A_{ij}$  between  $i$  and  $j$  is derived by different pressures  $p$  at the nodes.  $K_{ij}$  is pressure loss coefficient of the flow between node  $i$  and  $j$ . The accuracy of result depends on the size of the grid. When the sums of total errors for all the variables reach a predetermined and acceptable level, the final solution can be obtained. The acceptable level is called “convergence into the solution”.

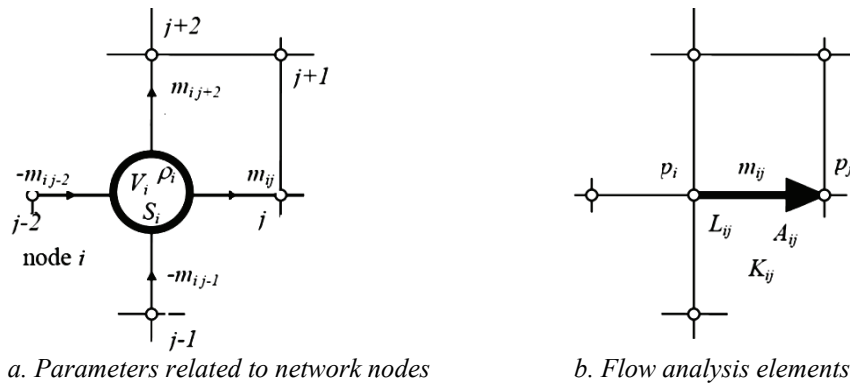
---

<sup>97</sup> <http://www.trnsys.com>.

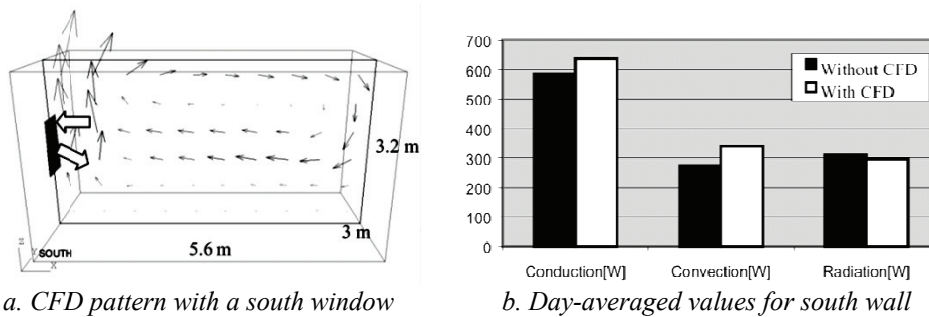
<sup>98</sup> The US department of energy 2007.

In recent years, CFD has attracted due to the reliability for the evaluation of indoor thermal comfort and air quality. Modern energy simulation tools using CFD are specifically designed to address the heating and ventilation problem in a building. However, it is still complex to apply CFD to the real architectural designs and the process requires a large system power.

The CFD method also provides detailed thermal environment and contaminant information. Fig.3.32 shows that CFD can analyze a higher resolution of the thermal conditions e.g. conduction, convection and radiation. The south wall shown in Fig.3.32-*a* gains heat from room air and other surfaces by convection and radiation, respectively, and then transfers the heat to the outside by conduction through the wall. In Fig.3.32-*b*, a comparison between the CFD method and another method without CFD shows great differences in the day-average thermal analysis of a room. The increase of convective heat transfer that can be analyzed in the coupled CFD calculation enlarges 9.4% of the total heating load requirement. Moreover, the increase of heating load can be greater for the case with windows on the south wall due to the effects of convection than another analysis method without CFD.



**Figure 3.31.** The analyzed variable parameters as the flow in the grid network [Tuomaala 2002].

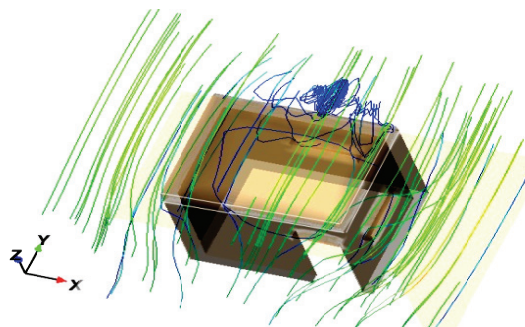


**Figure 3.32.** Validity for with and without CFD in a building model [Kendrick 1993].

### 3.5.3. Hybrid model for microclimate analysis

A naturally ventilated and thermally inhomogeneous building modifies the building microclimate due to the evolution of outside airflow and inside buoyancy, stack effects and thermal flows with a fluctuating direction and magnitude, turbulence, temperature, humidity, shortwave and longwave radiations fluxes. The microclimate modification can be defined by the fundamental laws of dynamics and thermodynamics of fluids, i.e. equations of conservation of mass, momentum, heat and moisture. Topological and geometric building designs also affect the microclimate changes. Terrains and surrounding buildings definitely have strong impacts on the natural ventilation performance, particularly on the wind-driven ventilation. The internal sources and sinks modify the distributions of temperature and specific humidity. An advection-diffusion equation that describes the loss of flow speed in internal source/sink terms can define the microclimate modification induced by the topological and geometric factors.

Typical multi-zone models cannot accurately predict the effects of microclimate modifications. For example, Pedestrian wind comfort depends on the types of activity, dressing, specific weather e.g. air temperature, relative humidity, solar radiation and mostly determined by the wind speed and air temperature. 3D CFD methods can estimate accurately local airflows and the condition distribution in details as Fig.3.33 shows. The variations in the airflow, being affected by site-specific design, building geometry and topography etc., easily show the interconnections of temperature, humidity and velocity in the space. Simulation results under different periods, e.g. round a year, season, week and day etc., can show different indoor conditions.



**Figure 3.33.** 3D CFD [author].

In a micro scale, a 3D flow model is thermal and energy analysis needs high complexity. Recently, hybrid models are studied to simplify the process by some assumptions and constraints in the parameterization. For example, the air flow analysis of CFD improves some constraint for multi-zone

ventilation simulation. A multi-zone simulation can offer the initial condition to the CFD simulation. A recent interest of the building simulation research is the integration between a CFD method and another simple energy simulation method. Zhai (2003) introduced several coupling strategies to integrate a CFD method with the EnergyPlus (EP) simulation. Negrao (1995) also studied a CFD simulation integrating the building thermal simulation in the EP in order to improve the building energy consumption and the indoor air equality. His work especially focused to solve the ambiguity problem of the boundary condition in the CFD method using EP. EP interactively gives a feedback of building thermal changes to the CFD solver. There are several reasons that EP is suitable for the integration:

1. The performance of EP has proven through the long history. The initial prototype was developed by Clarke (1977). After that, it has been under constant development until today.<sup>99</sup>
2. It was well validated through large scale exercises.<sup>100</sup>
3. It has its own coupling capability between the energy simulation and CFD for combined building and plant systems. External coupling admits the use of user-defined functions to set up a broad range of parameters. A comparison between internal and external coupling is available.<sup>101</sup>

Gao and Chen (2003) developed three strategies for the coupling of the CFD and multi-zone model as in Table 3.8. The virtual coupling does not mix a CFD simulation with a multi-zone simulation in the coupling procedure. This coupling calculates air pressures using the CFD method and then input the pressures into a multi-zone simulation tool. In the Quasi-dynamics coupling, CFD applies to the simulation of each single zone in a multi-zone network. A CFD analysis makes reliable information about the airflow field in a single zone. The accurate analysis of a zone can improve the calculation of another single zone. This means that transferring results of a CFD simulation once back to the multi-zone model, the multi-zone model simulation re-runs to update the results. This procedure is called “ping-pong”. The fully dynamic coupling is an extension of the quasi-dynamic coupling for the complete multi-zone. The CFD’s grid is laid on the multi-zone model’s network and substitutes a particular zone. The dynamic coupling method requires a mutual feedback called “onion” between the multi-zone and CFD simulations.

A combination of a CFD method and multi-zone energy simulation method can provide complementary information for energy movements in the building. For a turbulence scheme, a model combining 3D flow and 2D energy simulations significantly reduces the complexity and saves the processing time.<sup>102</sup> These works mainly are utilized to improve the result in mechanical ventilation simulation. A multi-zone model predicts the average temperature in all zones and overall airflow, while a CFD

---

<sup>99</sup> Djunaedy 2005.

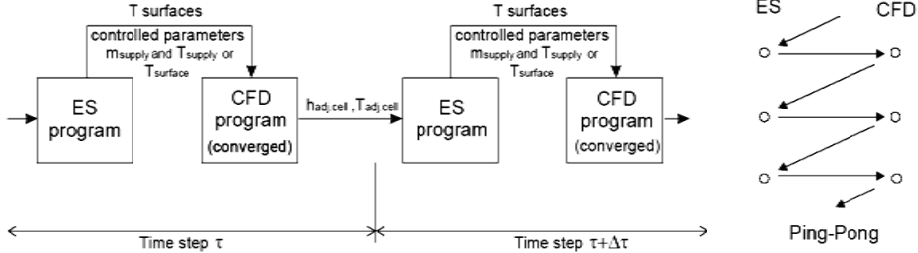
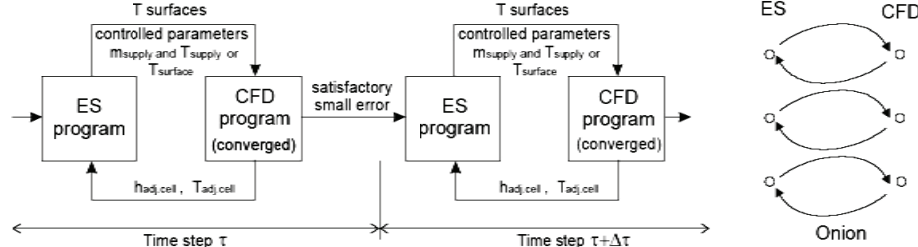
<sup>100</sup> Lomas et al. 1994, Vandaele and Wouters 1994.

<sup>101</sup> Negrao 1995, Beausoleil-Morrison 2000.

<sup>102</sup> Arnfield et al. 1998.

method can get the details of temperatures and airflows in some particular zones.

**Table 3.8.** Strategies for the coupling of the CFD and multi-zone model.

Virtual coupling	<ul style="list-style-type: none"> <li>- This method separately simulates a CFD method and a multi-zone method.</li> <li>- Flow pressures are calculated by CFD method</li> <li>-The flow pressures are used for a multi-zone simulation</li> </ul>
Quasi-dynamics coupling	<ul style="list-style-type: none"> <li>-CFD improves the result of each single zone in multi-zone simulation</li> <li>- Multi-zone network combines the state of each single zone</li> <li>-More reliable results for a single zone can be obtained by airflow analysis</li> <li>-The result transfers once back to the multi-zone model and re-run like "ping-pong"<sup>103</sup></li> </ul> 
Fully dynamic coupling	<ul style="list-style-type: none"> <li>-An extension of the quasi-dynamic coupling method to the whole multi-zone coupling</li> <li>-Substitution a particular zone of the multi-zone model's network</li> <li>-Mutual feedback called "onion"<sup>104</sup> between the multi-zone model and CFD simulations</li> </ul> 

### 3.5.4. Experimental expression of models

Since the prediction of airflow rates within buildings is difficult, the energy simulation uses simplifications and assumptions. Bittencourt (1993) introduced a simplified method using pressure coefficients obtained by wind tunnel tests with solid models. A problem of this simplification method is that the pressure coefficients are reliable only for buildings with porosities of up to 25%. With a large percentage of porosities, airflow rates tend to be over-estimated since airflows through the building modify the external pressures. Higher porosities over 50% are considerable for ventilation of a multi-zone building in warm and humid climate.

The cooling effect of ventilation can be defined by a function of air temperature, airflow rate and heat

<sup>103</sup> Hensen 1999.

<sup>104</sup> Novoselac 2005.

capacity.<sup>105</sup> We can estimate heat loss due to ventilation rates empirically as

$$Q = 1300N(T_i - T_o) \quad \text{Eq.20}$$

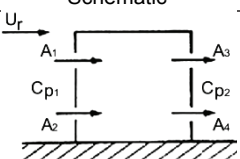
where  $N$  is the ventilation rate ( $\text{m}^3 \text{s}^{-1}$ ), and  $T_i$  and  $T_o$  are respectively indoor and outdoor temperature (K).  $Q$  is heat loss or gain rate (w), and 1300 is volumetric specific heat of air ( $\text{J m}^{-3}\text{K}^{-1}$ ). The number of Air Change rate per Hour (ACH) is defined by observing the volume of air entering (or leaves) into the space and the volume of space.

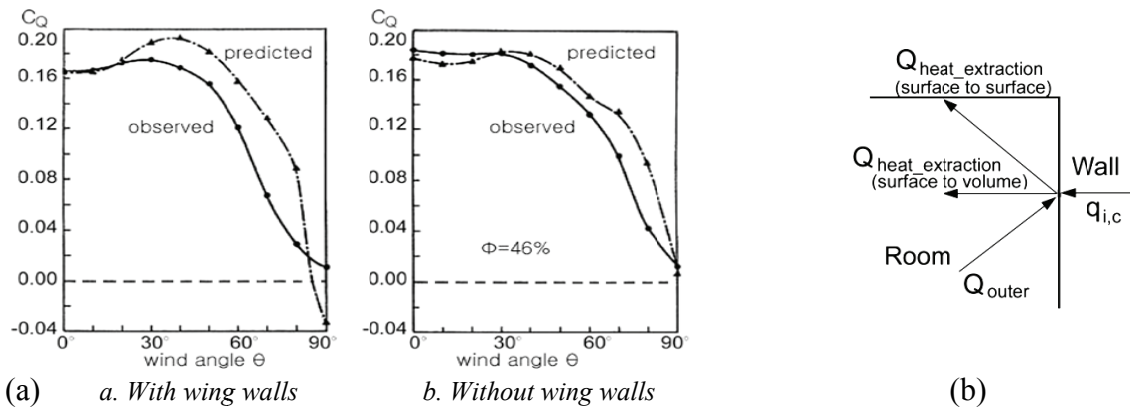
$$ACH = 3600R / V \quad \text{Eq.21}$$

where  $R$  and  $V$  are respectively infiltration rate ( $\text{m}^3 \text{s}^{-1}$ ) and volume of room ( $\text{m}^3$ ).<sup>106</sup>

The analytical method simplifies airflow movement as a function of pressure difference in a sealed building. Cross-ventilation in a single building is simplified by theoretical expression for the geometric connection of volumes, walls and openings as Table 3.9 shows.  $Q_w$  ( $\text{m}^3 \cdot \text{s}^{-1}$ ) is airflow rate,  $C_d$  is discharge coefficient<sup>107</sup> of openings and  $A_w$  ( $\text{m}^2$ ) is the area of equivalent openings.  $U_r$  ( $\text{m s}^{-1}$ ) is outdoor reference wind speed, and  $\Delta C_p$  is wind pressure-drop coefficient<sup>108</sup> as a function of the angle of incidence and distance from obstructions.

**Table 3.9.** Analytic method for cross-ventilation of single buildings [Vickery and Karakatsanis 1978].

Conditions	Schematic	Formula
Wind only		$Q_w = C_d A_w U_r (\Delta C_p)^{1/2}$ $1 / A_w^2 = 1 / (A_1 + A_2)^2 + 1 / (A_3 + A_4)^2$



**Figure 3.34.** Experimental expression, (a) predicted and observed pressure coefficients ( $C_Q$ ), (b) energy

<sup>105</sup> Koenigsberger et al. 1974.

<sup>106</sup> Liddament 1986.

<sup>107</sup> The discharge coefficient is often assumed 0.65.

<sup>108</sup> If the angle of incidence perpendicular to opening is  $0^\circ \leq \text{Ur angle} \leq 30^\circ$ , the coefficient is 1.2 for typical values for building in an open field and  $0.1 + 0.0183 (90^\circ - \text{Ur angle})$  for  $30^\circ \leq \text{Ur angle} \leq 90^\circ$ .

balance between wall and room air [Vickery and Karakatsanis 1978, Zhai and Chen 2001].

For higher porosities, further corrections are possible by the error of the flow coefficients. Fig.3.34 (a) compares the predicted and observed coefficients for buildings with 46% porosity with and without wing walls.<sup>109</sup> The predicted coefficients may include particular errors when the incident angle of the wind is skewed to the façade between 0°, i.e. parallel to opening, and 45°.

A multi-zone energy simulation utilizes the energy balance equations<sup>110</sup> derived from the analytic method of inter zone air and surface heat transfer. The energy balance equation for a room air is

$$\sum_{i=1}^N q_{i,c} A_i + Q_{other} - Q_{heat\_extraction} = \rho V_{room} C_p \Delta T / \Delta t \quad \text{Eq.22}$$

where  $\sum q_{i,c} A_i$  is convective heat transfer from enclosed  $N$  surfaces to the room air by the convective flux  $q_{i,c}$  from a surface  $i$ , and  $A_i$  is the area of total surface.  $Q_{heat\_extraction}$  and  $Q_{other}$  respectively denote the heat extraction rate of a room and heat gains from lights, people, appliances and infiltration etc.  $\rho V_{room} C_p \Delta T / \Delta t$  is the energy change of room volume  $V_{room}$  where  $\rho$  is the air density, and  $C_p$  is air specific heat. The temperature change of room air  $\Delta T$  can be observed by the sampling time interval  $\Delta t$ , i.e. normally one hour. Fig.3.34 (b) illustrates the energy balance on the interior surfaces of wall, ceiling, floors, roofs and slabs.

Assuming the uniform and known room air temperature, the interior surface temperature can be determined by simultaneously solving the surface heat-balance equation. Inversely, the convective heat transfer of the enclosure surfaces determines the cooling and heating loads. A multi-zone simulation uses these methods to solve the heat-balance equation or to calculate heating and cooling loads. However, the method cannot estimate partial variations caused by a microclimate modification. Computational dynamic principles can define partial variations e.g. airflows driven by the temperature gradients and/or by the external wind pressures. CFD is a numerical method to solve the equations of partial variations.

CFD consists of three main steps: building modeling, definition using 3D grids and numerical solution. The modeling of a building includes the arrangement of the various assemblies, geometries, enclosures, assignment of materials, the respective thermal properties, sources of radiant and convective heat, solar gains, occupancy and air resistances etc. The grid definition splits the building into a number of units for analysis. Thus, the size of grid is directly related to the complexity of solution and the size of errors. A more complex model requires a larger number of grid arrays and larger computer power.

A combination of the multi-zone energy simulation and the CFD method is used for the energy

---

<sup>109</sup> Vickery and Karakatsanis 1978.

<sup>110</sup> Zhai and Chen 2001.



simulation in this study. The multi-zone method predicts the average temperature using Finite Volume Method (FVM) that analyzes one node point per a zone. The CFD method refines the single node result of FVM at using multi-grids. EP and *Fluent*<sup>111</sup> respectively performs the multi-zone simulation and dynamic simulation. A new proposal in this study is the allocation of multi-scale grids for the CFD, a coarse scale grid is used for the analysis of large outdoor winds, and fine scale grids with a large number of nodes is used to update the result of the coarse scale results. The results of FVM can be easily updated by the CFD method with a fine grid since the FVM uses a coarse scale grid for multi-zone analysis.

---

<sup>111</sup> <http://fluent.com/>

*Fluent Inc.* is a company based in Lebanon, New Hampshire that develops software for CFD.

# 4. Microclimate energy simulation

## 4.1. Multi-zone energy simulation

### 4.1.1. Multi-zone simulation method using EP

Multi-zone energy analysis and Computational Fluid Dynamics (CFD) methods respectively provide the complementary information of mean and variance of energy in the building zones. The multi-zone analysis method such as EnergyPlus (EP) addresses to calculate the energy performance of building zones and building envelopes installed for HVAC.<sup>112</sup> The results are averaged indoor condition with cooling/heating loads, coil loads and energy consumption in a time interval, e.g. from a sub-hour or hour, day to a year. However, the EP cannot analyze the microclimate effects in the building. On the other hand, CFD tools, such as *Fluent* software, can analyze the partial differences in air velocity, temperature, a relative humidity and contaminant concentration, that may offer some detailed prediction of the thermal comfort in building zones. For example, some partial differences are observed as dynamics of thermal and energy flows. Hence, a combination of EP and CFD can evaluate the average energy consumption and energy gains with a microclimate modification.

EP has many innovative simulation capabilities such as time steps of less than one hour, heat valance-based zone simulation multi-zone airflow, thermal comfort and photovoltaic systems. Version 2.0 has extensive examples of HVAC input files, weather processor, heat/cool option on furnace, air loop, high temperature radiant heating/cooling, more operative controls for all radiant modeling, desiccant dehumidifier, system sizing, plenum (return and supply), example active Trombe wall input template, air cooled condenser, energy meters, low temp radiant heating/cooling, interior surface convection, evaporative cooler models, airflow sizing, improved sky model for daylight calculations, ability to read multiple interval per hour weather data files, return air heat gain (from lights) enhancement calculation, flat plate exhaust air heat recovery.

---

<sup>112</sup> Crawley et al. 2001.

```

SUBROUTINE ManageSimulation      ! Main driver routine for this module
BeginSimFlag = .TRUE.
EndSimFlag = .FALSE.
CALL OpenOutputFiles
CALL GetProjectData
CALL GetEnvironmentInfo         ! Get the number and type of Environments
DO Envirn = 1, NumOfEnvirn      ! Begin environment loop ...
  BeginEnvirnFlag = .TRUE.
  EndEnvirnFlag = .FALSE.
  WarmupFlag = .TRUE.
  DayOfSim = 0
  DO WHILE ((DayOfSim.LT.NumOfDayInEnvirn).OR.(WarmupFlag)) ! Begin day loop ...
    DayOfSim = DayOfSim + 1
    BeginDayFlag = .TRUE.
    EndDayFlag = .FALSE.
    DO HourOfDay = 1, 24      ! Begin hour loop ...
      BeginHourFlag = .TRUE.
      EndHourFlag = .FALSE.
      DO TimeStep = 1, NumOfTimeStepInHour ! Begin time step (TINC) loop ...
        BeginTimeStepFlag = .TRUE.
        EndTimeStepFlag = .FALSE.
        ! Set the End_Flag variables to true if necessary. Note that each flag builds on
        ! the previous level. EndDayFlag cannot be .true. unless EndHourFlag is also .true., etc.
        ! Note that the EndEnvirnFlag and the EndSimFlag cannot be set during warmup.
        ! Note also that BeginTimeStepFlag, EndTimeStepFlag, and the
        ! SubTimeStepFlags can/will be set/reset in the HVAC Manager.
        IF ((TimeStep.EQ.NumOfTimeStepInHour).THEN
          EndHourFlag = .TRUE.
          IF (HourOfDay.EQ.24) THEN
            EndDayFlag = .TRUE.
            IF ((.NOT.WarmupFlag).AND.(DayOfSim.EQ.NumOfDayInEnvirn)) THEN
              EndEnvirnFlag = .TRUE.
              IF (Envirn.EQ.NumOfEnvirn) THEN
                EndSimFlag = .TRUE.
              END IF
            END IF
          END IF
        END IF
        CALL ManageWeather
        CALL ManageHeatBalance
        BeginHourFlag = .FALSE.
        BeginDayFlag = .FALSE.
        BeginEnvirnFlag = .FALSE.
        BeginSimFlag = .FALSE.
      END DO
      ! ... End time step (TINC) loop.
    END DO
    ! ... End hour loop.
  END DO
  ! ... End day loop.
END DO
  ! ... End environment loop.
CALL CloseOutputFiles
RETURN
END SUBROUTINE ManageSimulation

```

**Figure 4.1.** Input interface of EP [The US department of energy 2007a].

The input is a text form with a number of entities as Fig.4.1 shows. The recent version of interface is improved to have IFC<sup>113</sup> to IDF generation capability,<sup>114</sup> HVAC input templates, example passive input template, moisture calculations, thermal comfort modeling and reporting.<sup>115</sup> It is possible to use shading of sky IR by obstructions, controls for natural ventilation through windows, 3D surface coordinates, inter zone airflow and natural ventilation (COMIS), reference data sets.<sup>116</sup> There are lots of HVAC equipments e.g. fan coil, unit heater, unit ventilator, window AC simulations, *EPMacro* i.e. macro capability for input files (auxiliary program), fenestration calculations, frame and dividers, window multiplier, spectral input for glass, and window U-value and solar heat gain coefficient report HVAC loop modeling, including branch-based input and flow resolver, simple launch program for EP, exhaust fan, fan control, fan motor placement, simple input and output preprocessor, reference data sets for materials and constructions etc. Fig.4.2 represents the modules of EP.<sup>117</sup>

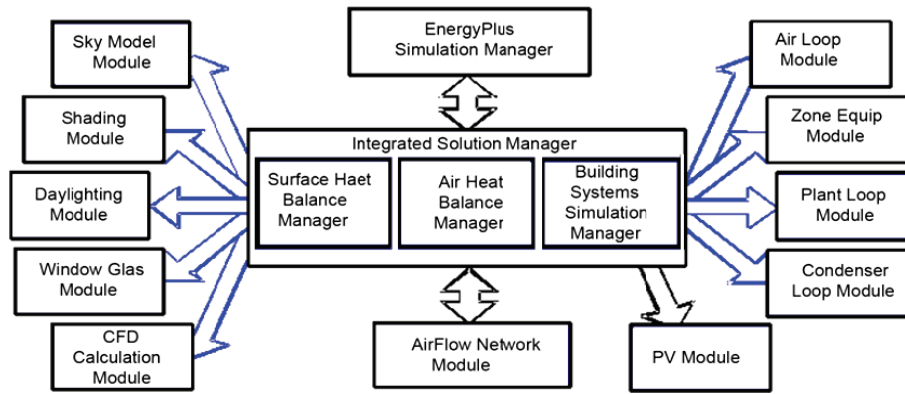
<sup>113</sup> IFC: Industry Foundation Classes, ISO/PRF PAS 16739.

<sup>114</sup> CAD interoperability.

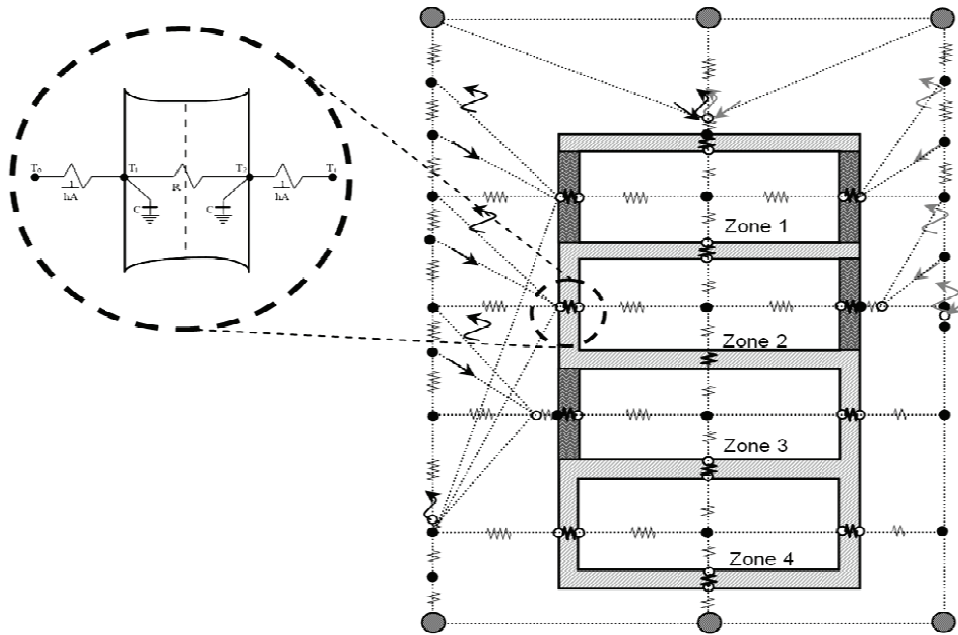
<sup>115</sup> Fanger 1970.

<sup>116</sup> IDF “libraries” for materials, constructions etc.

<sup>117</sup> Mendler and Odell 2006.



**Figure 4.2.** EP schematic and modules [The US department of energy 2007a].



**Figure 4.3.** Multi-zone analytical energy simulation of EP [The US department of energy 2007, author, modified from Tanimoto et al. 2004].

#### 4.1.2. Calculation of internal temperatures in multi-zones

EP uses an extension of time series solution in Finite Volume Method (FVM) to calculate the internal temperatures i.e. volume-to-volume connections from heat sources. Fig.4.3 illustrates the FVM method including physical parameters. The parameters can be optimized by the time series solution shown in Eq.23. A node network of space volumes including heat sources or sinks is shown in Fig 4.3. From the energy balance equation of a multi-zone in Eq.22, the equation with finite difference nodal temperatures  $T_1, T_2, \dots, T_{n-1}, T_n$  for  $n$  number nodes explains the variations of air temperature between space volumes. For a simple one layer slab with two interior nodes and convection at both sides, the

resulting finite difference equations are given by

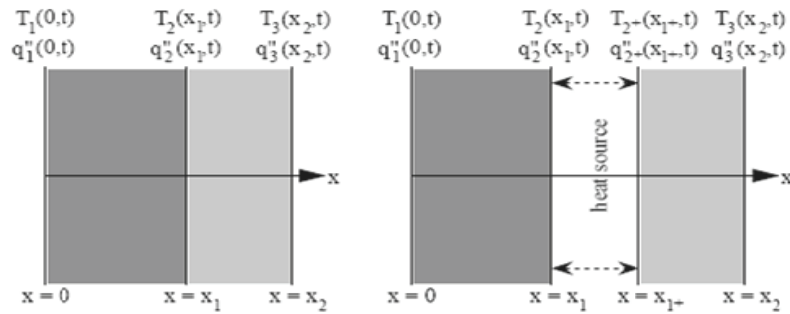
$$q_0'' = A(T_1 - T_0)C \frac{dT_1}{dt} = hA(T_0 - T_1) + \frac{T_2 - T_1}{R}, \quad C \frac{dT_2}{dt} = hA(T_i - T_2) + \frac{T_1 - T_2}{R}, \quad q_i'' = A(T_i - T_2) \quad \text{Eq.23}$$

where  $q_i''$  denotes the heat flux for the  $i$ -th node.  $C$  is air specific heat, and  $A$  is the area of the surface exposed to the environmental temperatures.

The analytic functions are formulated by Laplace transform including sources or sinks. Two methods with Laplace transform were introduced by Degiovanni (1988). The first method represents how a source which varies as a function of time and location can be incorporated. The equation involves some fairly complicated terms with spatial derivatives. The second method shows more details involving the addition of a source or sink between two layer elements as Fig.4.4 shows. The Laplace transform extension of two layers, e.g. a wall with two different materials, is,

$$\begin{bmatrix} T_2(s) \\ q_2(s) \end{bmatrix} = \begin{bmatrix} A_2(s) & B_2(s) \\ C_2(s) & D_2(s) \end{bmatrix} \begin{bmatrix} T_3(s) \\ q_3(s) \end{bmatrix} \quad \text{Eq.24}$$

where the parameters are also given in Fig.4.4.  $x$  is a vector of state variables,  $t$  is time, and  $A$ ,  $B$ ,  $C$  and  $D$  are coefficient matrices. The arrow means the direction of the heat sink.



**Figure 4.4.** Two layer examples for deriving the Laplace transform extension to include sources and sinks [The US department of energy 2007].

For the first layer, it was determined that in the Laplace domain

$$\begin{bmatrix} T_1(s) \\ q_1(s) \end{bmatrix} = \begin{bmatrix} A_1(s) & B_1(s) \\ C_1(s) & D_1(s) \end{bmatrix} \begin{bmatrix} T_2(s) \\ q_2(s) \end{bmatrix} \quad \text{Eq.25}$$

To link the two layers and include the heat source between them, the following substitutions are made:

$$\begin{bmatrix} T_2(s) \\ q_2(s) \end{bmatrix} = \begin{bmatrix} T_{2+}(s) \\ q_{2+}(s) \end{bmatrix} + \begin{bmatrix} 0 \\ q_{source}(s) \end{bmatrix}$$

$$\begin{bmatrix} T_1(s) \\ q_1(s) \end{bmatrix} = \begin{bmatrix} A_1(s) & B_1(s) \\ C_1(s) & D_1(s) \end{bmatrix} \left\{ \begin{bmatrix} T_{2+}(s) \\ q_{2+}(s) \end{bmatrix} + \begin{bmatrix} 0 \\ q_{source}(s) \end{bmatrix} \right\}$$

$$\begin{bmatrix} T_1(s) \\ q_1(s) \end{bmatrix} = \begin{bmatrix} A_1(s) & B_1(s) \\ C_1(s) & D_1(s) \end{bmatrix} \left\{ \begin{bmatrix} A_2(s) & B_2(s) \\ C_2(s) & D_2(s) \end{bmatrix} \begin{bmatrix} T_3(s) \\ q_3(s) \end{bmatrix} + \begin{bmatrix} 0 \\ q_{source}(s) \end{bmatrix} \right\}$$

$$\begin{bmatrix} T_1(s) \\ q_1(s) \end{bmatrix} = \begin{bmatrix} A_1(s) & B_1(s) \\ C_1(s) & D_1(s) \end{bmatrix} \begin{bmatrix} A_2(s) & B_2(s) \\ C_2(s) & D_2(s) \end{bmatrix} \begin{bmatrix} T_3(s) \\ q_3(s) \end{bmatrix} + \begin{bmatrix} A_1(s) & B_1(s) \\ C_1(s) & D_1(s) \end{bmatrix} \begin{bmatrix} 0 \\ q_{source}(s) \end{bmatrix} \quad \text{Eq.26}$$

If a layer is added to the left side of the first layer, the entire right side of the Eq.26 can be multiplied by the transmission matrix of the new layer. Conversely, if a layer is added to the right of the second layer, the vector containing the Laplace transform of the temperature variations can be replaced by the product of the transmission matrix of the new layer and the vector at the next state. The term dealing with the heat source is not affected. While Eq.27 is correct for any single or multi-layered elements, the first term in the heat source transmission matrix does not appear to match the compactness of the other terms in the matrix equation. Hence, for the  $n$ -th nodes, the extended series can be bundled by a generalized equation which is correct for any single or multi-layered elements as

$$\begin{bmatrix} q_1(s) \\ q_{n+1}(s) \end{bmatrix} = \begin{bmatrix} \frac{D(s)}{B(s)} & \frac{-1}{B(s)} \\ \frac{1}{B(s)} & \frac{-A(s)}{B(s)} \end{bmatrix} \begin{bmatrix} T_1(s) \\ T_{N+1}(s) \end{bmatrix} + \begin{bmatrix} d(s) - \frac{D(s)b(s)}{B(s)} \\ \frac{b(s)}{B(s)} \end{bmatrix} (q_{source}(s)) \quad \text{Eq.27}$$

The terms in the heat source transmission matrix may appear to be reversed. It is expected that only the layers to the left of the source will affect  $q_1(s)$ , but the presence of  $b(s)$  in the element multiplied by  $q_{source}(s)$  to obtain  $q_1(s)$  seems to be contradictory. In fact, the entire term,  $b(s)/B(s)$ , must be analyzed to determine the effect of  $q_{source}(s)$  on  $q_1(s)$ . In essence, the appearance of  $b(s)$  removes the effects of the layers to the right of the source from  $B(s)$  leaving only the influence of the layers to the left of the source.<sup>118</sup>

For a transient solution, the airflow rate between  $i$ -th and  $j$ -th node can be approximated by the conservation assumption of air mass as<sup>119</sup>

$$\frac{dm_i}{dt} = \sum_j F_{j,i} + F_i \quad \text{Eq.28}$$

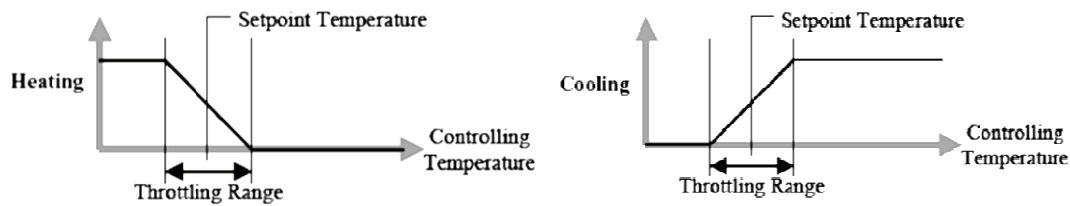
where  $m_i$  is the mass of air in the  $i$ -th node, and  $F_{j,i}$  and  $F_i$  respectively denote the airflow rate between  $i$ -th and  $j$ -th node and the non-flow process at the  $i$ -th node that is generally assumed as a quasi-steady initial condition  $dm_i/dt=0$ .

When multi-zones are set up with the FVM with a number of nodes, a control of the volume-to-volume heat transfer from a heat source to a sink is the next issue, since a control is a problematic issue for HVAC studies. A setpoint scheme is used to maintain the comfort temperature and the sum of energy consumption is calculated. Fig.4.5 illustrates the setpoint temperature scheme for heating and cooling.

<sup>118</sup> The US department of energy 2007.

<sup>119</sup> Tan 2005.

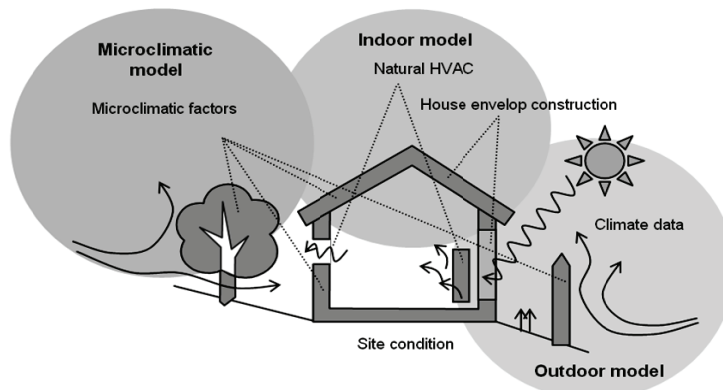
The total building energy consumption can be estimated by the sum of energy inputs for heating and cooling.



**Figure 4.5.** Controlling temperature scheme for heating and cooling [The US department of energy 2007].

## 4.2. Microclimate energy variation model

The multi-zone energy simulation described in chapter 4.1 is not efficient to simulate effects of microclimate modification since the model uses a combination of linear equations. For example, EP does not have any detail information between a source and a sink, although it can estimate the state and values, i.e. parameters, of a source and a sink. Microclimate modifies the state of building air with a continuous form e.g. air-flow, pressure difference, evapotranspiration, and temperature variation etc. and forms thermo- and aerodynamic flows. The flows are affected by an architectural design that modifies the geometry of space. This means that a design element can modify the microclimate in the building and thereby ventilation performance, heat balance and energy efficiency etc. For example, the amount of opening, affects the ventilation performance and the natural cooling possibility. The air flow analysis accompanies the topographical or geometrical considerations. The sloping topography determines the path of airflows and the building geometry modifies the path. Microclimate analysis needs a high resolution analysis with a large amount of grid. If the architect can get information of the microclimate modification, the building energy performance will be improved. Adequate microclimate architectural designs can result over 25% energy-saving compared to conventional house design for one



**Figure 4.6.** Simulation model and three modules [author].

year.<sup>120</sup>

Here, three models for a microclimate architectural design are proposed: outdoor model, indoor model and microclimate model. These models make it possible to analyze separately the climate condition of outdoor and indoor energy performance, and the mutual relationship between the indoor and outdoor conditions is estimated by microclimate model. Fig.4.6 illustrates the relationship between the three modules. For the simulation of models, each module has a capability that can be sophisticatedly modulated and functionally optimized by the CFD method. Additionally, the modules can be mutually cooperated between the functions with an energy-saving effect. The energy balance among the models is the mediator between thermal condition and microclimate modification. When an architect inputs a design, the influences for outdoor and indoor thermal condition are calculated and evaluated for the energy-saving. If the design is not adequate to save building energy, the simulation tool shows quantitative results such as energy gain or loss.

#### 4.2.1. Outdoor model

Outdoor model shows the direct relationship between the atmospheric process and indoor climate condition. Although some models of outdoor thermal comfort have studied to approximate the thermal condition of the street, field and urban etc. from several climate data, recent methods can simulate different scales of atmospheric processes. Outdoor climate models can be classified according to their scales that range from kilometers to a few centimeters. Although the general climate can be defined by macro scale, this is not suitable to use for architecture design since smaller scale modifications than building size occur. Microclimate should be considered to discriminate the microclimate effect in the partial architectural design.

**Table 4.1.** The physical properties that can be analyzed using CFD [Novoselac 2005].

Concept	Concerned equation
Continuity	$\frac{\partial \rho u_i}{\partial x_i} = 0$
Momentum	$\frac{\partial \rho u_i}{\partial x_i} + \frac{\partial \rho u_i u_j}{\partial x_j} = \frac{\partial p}{\partial x_i} + \frac{\partial}{\partial x_j} \left[ \mu \left( \frac{\partial u_i}{\partial x_j} + \frac{\partial u_j}{\partial x_i} \right) - \overline{\rho u_i' u_j'} \right] + \rho \beta (T_0 - T) g_i$
Energy	$\frac{\partial \rho T}{\partial \tau} + \frac{\partial \rho u_j T}{\partial x_j} = \frac{\partial}{\partial x_j} \left[ \frac{\mu}{Pr} \frac{\partial T}{\partial x_j} - \overline{\rho u_j' T'} \right] + S_i$
Concentration	$\frac{\partial \rho c}{\partial \tau} + \frac{\partial \rho u_j c}{\partial x_j} = \frac{\partial}{\partial x_j} \left[ \frac{\mu}{Sc} \frac{\partial c}{\partial x_j} - \overline{\rho u_j' c'} \right] + S$

<sup>120</sup> Hawkes and Forster 2002.



In a micro scale, 3D air flows should be analyzed and visualized to obtain information of thermal and energy processes. Typically, these processes employ a simplified turbulence scheme. A computer simulation with CFD tool numerically solves the thermo- and aerodynamic equations that can be represented by a set of partial differences of temperatures, pressures, density and velocity etc. It can provide the distribution, balance and concentration of thermal condition in an individual space or throughout the entire building. In a building space, air velocity generates an indoor airflow's Reynolds number that is in the transient of turbulent range.  $\bar{\phi} = \phi + \phi'$  is the flow property where  $\phi$  is the sum of a time average and  $\phi'$  is a fluctuation in the governing N-S equations. The form of the RANS (Reynolds-averaged Navier-Stokes) equations can be obtained by conservation of continuity, momentum, energy, concentration shown in Table 4.1. The continuity is the property of being continuous between topological spaces form. The mathematical property is obeyed by mathematical objects in which all elements are within a neighborhood of nearby points. The momentum equation defines the product of the mass and velocity of an object. Since energy is strictly conserved and is also locally conserved, the energy equation in the Table defines the energy transferring from the potential energy to kinetic energy and then back to potential energy constantly. The concentration is the measure of how much of a given substance there is mixed with another substance. The equation is very similar to the energy equation.

These concerned equations consist of values of pressure  $p$ , component velocity  $u_i$ , where  $i = 1, 2, 3$ , temperature  $T$ , and concentration  $c$  with air density  $\rho$ , air viscosity  $\mu$ , *Prandtl* number  $Pr$ , Schmidt number  $Sc$  and specific capacity  $c$ . The term  $\rho\beta(T_0 - T)g_i$  is the *Boussinesq* model for the thermal buoyancy effect on momentum where  $\beta$  is the thermal expansion coefficient of air,  $g$  is the gravitational acceleration, and  $T_0$  is the reference temperature. The source terms for energy and concentration are respectively denoted by  $S_t$  and  $S_c$ .<sup>121</sup>

The thermal comfort sensation in outdoor spaces is a factor that significantly influences the house shape and the pattern of heating and cooling. In a hot and humid area, an opened house is preferred to increase natural ventilation. Actually the heating and cooling designs depend on prevailing climatic conditions of the outdoor spaces. The outdoor model is the starting point for architecture designs based on climate data and site condition. The model is based on the fundamental laws of thermodynamics and prognoses the evolution of airflow, turbulence, temperature, humidity and short- and longwave radiation fluxes. A CFD method is suitable to analyze the model since it provides a well-founded numerical basis for the fundamental laws of fluid dynamics and thermodynamics. The advantages of CFD are shown in Table 4.2. CFD can obtain information of in-stationary, non-hydrostatic, prognoses all exchange processes including wind flow turbulence, radiation fluxes and temperature and humidity. It allows a process of several time periods from a day, week to year cycle. The high resolution of partial differences allows a

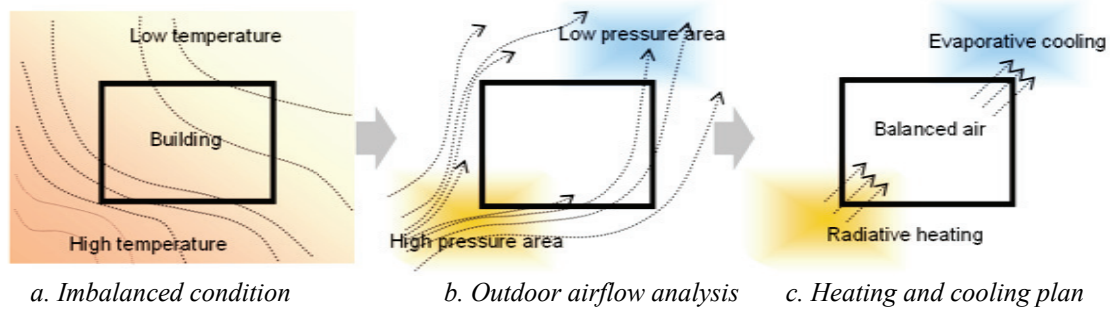
---

<sup>121</sup> Novoselac 2005.

detailed representation of complex structures, e.g. representation of buildings with various shapes, heights, design details and irregular geometrical forms etc. Analysis of various types of specific structure and properties composed of several layers is possible.

**Table 4.2.** The advantages of CFD [author].

Application ranges	<ul style="list-style-type: none"> <li>- Microclimate dynamics model</li> <li>- Analysis in a day, week and year cycles</li> <li>- In-stationary, non-hydrostatic, prognoses all exchange processes</li> <li>- Airflow turbulence, radiation fluxes, temperature and humidity</li> </ul>
Possible representations	<ul style="list-style-type: none"> <li>- Detailed representation of complex structures</li> <li>- Representation of buildings</li> <li>- Various shapes, heights, design details, irregular geometric forms</li> </ul>
Various input models	<ul style="list-style-type: none"> <li>- Various types of specific properties and structure</li> <li>- Porous obstacle to wind and solar radiation</li> <li>- Physiological processes of evapotranspiration</li> <li>- Complexes volume with several layers</li> <li>- Availability of various ground</li> <li>- Providing a large number of outputs with a limited number of inputs</li> </ul>
Resolutions	<ul style="list-style-type: none"> <li>- Allowing high spatial resolution</li> <li>- Allowing the high temporal resolution</li> <li>- Fine reading of the microclimate changes</li> <li>- Fine reading related to urban geometry</li> </ul>
Additionally possible ranges	<ul style="list-style-type: none"> <li>- Outdoor comfort</li> <li>- Calculation availability of Mean radiant temperature</li> </ul>



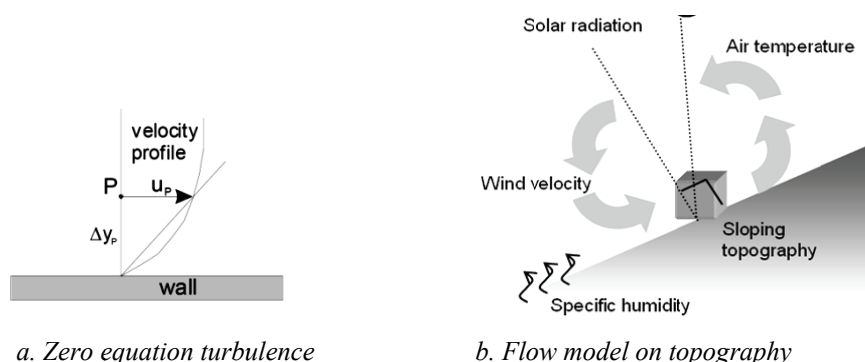
**Figure 4.7.** Sloping topographical design process [author].

Fig.4.7 shows an example of a heating and cooling plan derived by site and airflow analysis of a sloping topography. Such an inhomogeneous site condition modifies microclimate due to the differences of possible solar radiation and wind exposure. Topography, barrier and projection design affect air velocity and pressure. The outlet boundary condition is defined by outlet pressure and by zero gradients to the outlet surface for all other variables. The outlet boundary condition with the velocity in the vicinity of the surface can be defined by components parallel to the surfaces. Chen and Xu (1998) introduced a zero equation turbulence model for the boundary condition as Fig.4.8-a illustrates. The velocity  $U_p$  of flow is increased by a point  $P$  where is far from the surface of wall by a distance  $\Delta y_p$ .

On a sloping topography, e.g. a hilly area, the estimation of relative temperature is useful to plan a proper

façade and window designs for passive solar heating or ventilation cooling. The non-uniform thermal condition on topography should be concerned for energy-saving. Some modern buildings are often designed to utilize the imbalance thermal condition for heating and cooling by circulating heated air or water by a control system. The microclimate modification on the sloping topography yields the different results. When the site condition is analyzed by the outdoor simulation model, architects can choose proper building type, positioning, form, barriers, opening and courtyard etc. for energy-saving.

The outdoor model provides an optimization possibility for the modification of the topological site to improve the energy efficiency. It includes landscaping, thermal control of outer wall, façade and windows design. For example, a special type of ecological object is planned to protect the building from the harsh extremes of summer sun and chilling winter winds. It improves comfort both inside and outside the home, and reduces the need for supplementary heating and cooling. The outdoor model is associated to wide energy simulation ranges such as building orientation, topography, barrier, building geometry, microclimate ventilation described in the previous chapters. Table 4.3 (a) shows the number of previous chapters corresponding to the outdoor models.



**Figure 4.8.** Outdoor model [Chen and Xu 1998, author].

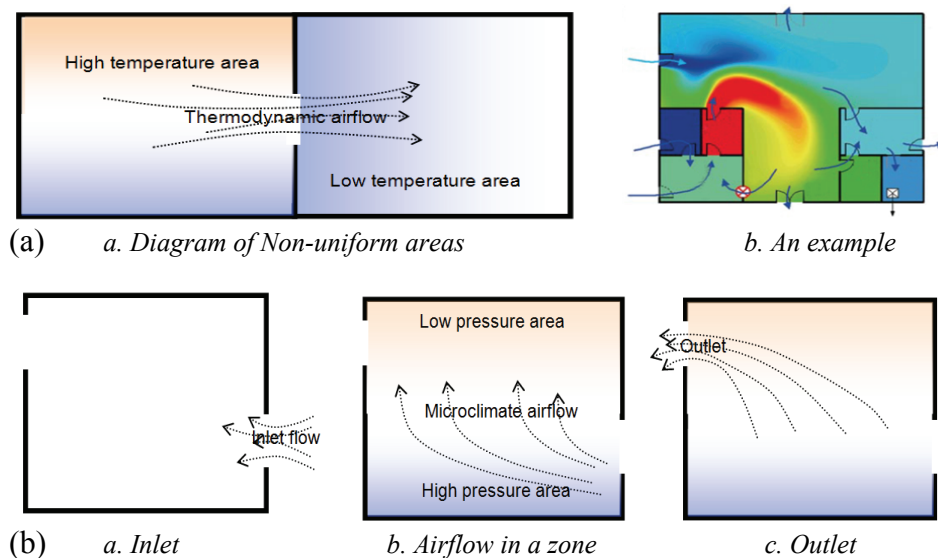
**Table 4.3.** Outdoor model and indoor model concerned to chapter, (a) outdoor model, (b) indoor model [author].

(a) Outdoor model	Applicable chapter	(b) Indoor model	Applicable chapter
Building orientation	Chapter 3.2.2	Courtyard dwelling designs	Chapter 3.2.4
Topography	Chapter 3.2.3	Effects of afforestation	Chapter 3.3.1
Barrier	Chapter 3.3.1	Building geometry	Chapter 3.3.2
Building geometry	Chapter 3.3.2	Internal partitioning	Chapter 3.3.3
Microclimate ventilation	Chapter 3.4.1	Opening control and slits	Chapter 3.4.2 and 3.4.4
		Roof opening and stack effect	Chapter 3.3.5
		Overhangs and projections	Chapter 3.4.3

### 4.2.2. Indoor model

The indoor model combines multi-zone energy simulation using EP shown in chapter 4.1 and microclimate energy simulation using CFD. The integrated analysis of the different zones can obtain the total energy influences of relative temperature and humidity in a building. However, the influence of the saturation pressure and the latent heat affect the multi-zone energy simulation. The saturation pressure induces the particular flow that affects the ventilations and evaporation in a zone or between zones as Fig.4.9 (a) shows. The indoor air flows should be controlled by several architectural design elements shown in Table 4.3 (b): courtyard dwelling designs, effects of afforestation, building geometry, internal partitioning, opening control and slits, roof opening and stack effect, overhangs and projections.

When the sun enters through the windows, the warm air is circulated in the building's interior space. The multi-zone energy simulation technique presents some energy-saving using thermal mass which absorbs excess heat during the day and releases the heat at night. Natural ventilation is employed for cooling of overheated air. However, a parametric ventilation model in the multi-zone model does not calculate the air movement. It solves some equations with parameters and approximates the uniform thermal conditions. For instance, FVM calculates the mean temperature of each volume. The problem is that a room with a large window allowing direct solar penetration has a partial uncomfortable condition in the room. Moreover, partially overheated air occurs by thermodynamic air circulations. A parametric model cannot analyze such a non-uniform air condition derived by thermo- and aerodynamic processes. Hence, the CFD method should be added to the multi-zone energy simulation.



**Figure 4.9.** Thermo- and aerodynamic processes, (a) thermodynamic, (b) airflow by aerodynamic microclimate [author].

**Table 4.4.** The utilization of microclimate modification [author].

Effects	Applications
Cooling	<ul style="list-style-type: none"> <li>- Maintaining the indoor temperature below that of the outdoor air</li> <li>- Decreasing cooling load and improve indoor thermal comfort condition</li> <li>- Provision radiative cooling from shade, ventilation control and evaporative cooling</li> </ul>
Heating	<ul style="list-style-type: none"> <li>- Maintaining the indoor temperature above that of the outdoor air</li> <li>- Avoidance overheating problem</li> </ul>
Dehumidification	<ul style="list-style-type: none"> <li>- Elimination the water content of the ambient air to acceptable levels</li> </ul>
Humidification	<ul style="list-style-type: none"> <li>- Provision the water content to the dry air</li> </ul>

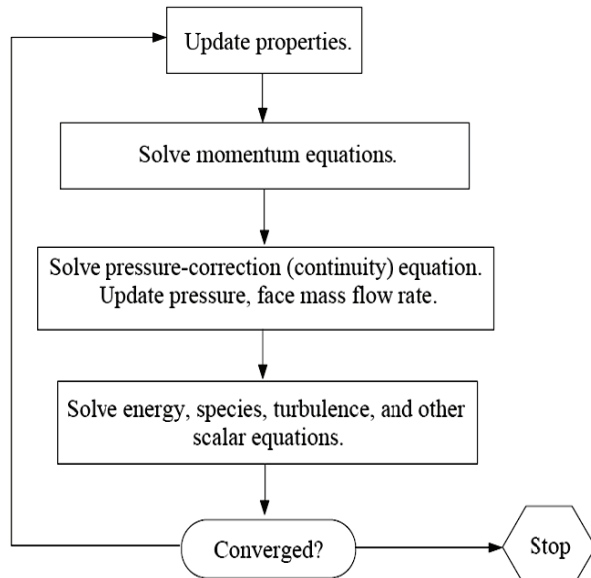
**Table 4.5.** Sub-tools of *Fluent* software [author].

Sub-tools	Purpose
Computational grid generation	<ul style="list-style-type: none"> <li>- Division of the domain into discrete control volumes</li> </ul>
Discrete dependent variables allocation	<ul style="list-style-type: none"> <li>- Integration of the governing equations on the individual control volumes</li> <li>- Construction of algebraic equations</li> <li>- Several discrete dependent variables: Velocities, pressure, temperature and conserved scalars</li> </ul>
Linear solutions	<ul style="list-style-type: none"> <li>- Linearization of the discretion equations and solution</li> <li>- Updated values of the dependent variables</li> </ul>

The thermo- and aerodynamic processes explain the exchange rates of momentum, heat sources, building zones and the atmosphere. The heat flux rates can be determined by a thermodynamic model. The heat flux can be modulated or suppressed by the aerodynamic resistance on a hard surface as Fig. 4.9 (b) illustrates. The air resistance on a surface regulates the transpiration rate, global radiation, temperature, wind speed and pressure. A wall is primarily used for house design to mark boundaries that directly modify the air-circulation patterns. This changes the energy consumption because different air patterns cause different heat gains and losses. Thus, the analysis of air movement is important to make an energy efficient design. The microclimate modification can be used to distribute the overheated air or balance the indoor thermal condition. Cooling, heating, dehumidification and humidification effects of microclimate modification can be applied to several applications shown in Table 4.4.

A simulation for complex 3D air flow with different air temperatures needs a reliable CFD tool. In this study, the *Fluent* software solving the governing integral equations for mass and momentum, energy, species transport, and other scalars such as turbulence is used. *Fluent* software package offers several sub-tools for the different purposes shown in Table 4.5. Any domain can be easily divided into discrete control volumes using a computational grid generator. The governing equations on the individual control volumes can be integrated to construct algebraic equations for discrete dependent variables such as velocities, pressure, temperature and conserved scalars. Linearization of the discretion equations and solution of the resultant linear equation system yields updated values of the dependent variables.

The governing equations should be solved sequentially (i.e., segregated from one another) because the



**Figure 4.10.** Numerical solution in the *Fluent* software [Fluent Inc. 2002].

Step	Procedure
Step 1	- Update based on the current solution and the initialized solution
Step 2	- Solve the momentum equation using current values for pressure and face mass fluxes - Update the velocity field
Step 3	- Solve <i>Poisson-type</i> equation for the pressure correction, continuity equation and linear momentum equations - Necessary corrections to the pressure and velocity fields and the face mass fluxes
Step 4	- Solve scalars equations - Turbulence, energy, species and radiation are solved - Updated values of the other variables
Step 5	- Check for equation convergence

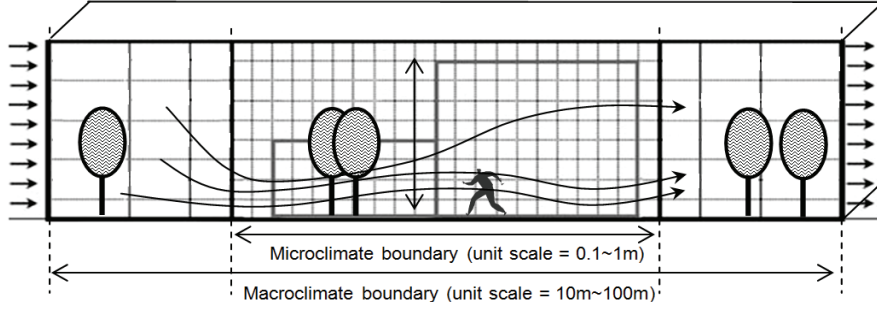
**Table 4.6.** Procedure of *Fluent* solver [author].

governing equations are non-linear (and coupled). Several iterations of the solution loop must be performed before a converged solution is obtained. The iterative procedure includes some steps shown in Fig.4.10 and Table 4.6 summarizes the process. These steps are continued until the convergence criteria are met.

### 4.3. Multi-scale EP-CFD analysis

A multi-scale method is attractive to mathematicians due to the convergence performance to the accurate solution. The multi-scale scheme can accelerate the solution by computing only corrections of a series of coarse grid levels. The use of several scales for analysis units, i.e. grids with nodes, can greatly reduce the number of iterations and the processing time, particularly when the model contains a large number of control volumes. This study employs a multi-scale method that analyzes the flows using the multi-scales between macro- and microclimates. Fig.4.11 represents the multi-scale scheme which combines the macro- and microclimate analysis.

Macroclimate data is used to calculate the average value which can combine values of small units. EP program estimates the local average value in a volume by using climate data observed at some stations in Korea. However, the results derived from climate data are not exact in some zones due to the microclimate modifications with thermo-, aerodynamics. A CFD method iteratively updates the results in small unit scales.



**Figure 4.11.** Multi-scale scheme using macroclimate and microclimate scales [author].

Since the FVM solver in EP program results in a single result per volume, the smoothness assumption for several nodes of the volume is applied. In the volume, a grid with many nodes should be set up for the CFD solution. The initial condition of CFD is that the nodes of the CFD solver for the volume have the same value to the FVM result. Only corrections of EP are calculated by the CFD method.

Let a set of linear equation as

$$A\phi_{real} + b = 0 \quad \text{Eq.29}$$

be a EP parametric linear equation.  $\phi_{real}$  is the exact solution i.e. real value. If we assume that the linear approximation is not accurate due to microclimate modifications, there may be a defect  $d$  associated with thermo-, aerodynamic components.

$$A\phi + b = d \quad \text{Eq.30}$$

A correction  $\psi$  for  $d$  should be estimated by a CFD method.

$$\phi_{real} \approx \underbrace{\phi}_{\text{EP solution}} + \underbrace{\psi}_{\text{CFD solution}} \quad \text{Eq.31}$$

Hence, the real combination of EP and CFD can seek the optimal real value as

$$A(\phi + \psi) + b = 0 \quad \text{Eq.32}$$

Instead of the real combination in Eq.32, a multi-scale analysis in this study uses EP solution  $A\phi + b = d$  and CFD update  $A\psi = -d$  as

$$(A\phi + b) + A\psi = d - d \approx 0 \quad \text{Eq.33}$$

The combination will be simulated for energy-saving house design. The simulation strategy of EP-CFD coupling is shown in Table 4.7.

**Table 4.7.** Process of EP-CFD coupling [author].

Step	Simulation strategy	Detail
Step 1	Site selection and climate data acquisition	-Choose a local area of S. Korea. -The climate data of the area is obtained from Korean Meteorological Administration. <sup>122</sup>
Step 2	Generalized climate	-Approximation of the outdoor climate by the climate data given in Step 1
Step 3	Indoor EP model	-Indoor energy efficiency is estimated by multi-zone analysis using EP in the generalized climate.
Step 4	Outdoor microclimate model	-The thermal and humidity condition are varied by the outdoor microclimate effects and topographical gradient. -The energy consumption is modified by the evapotranspiration and balance process in thermo- and aerodynamic flow. -The thermo- and aerodynamic flow is estimated by CFD.
Step 5	Indoor microclimate model	-Several microclimate factors given in chapter 4.2.2 to support insulating, heating and cooling are added and evaluated. -The energy efficiency from EP is improved by several design factors using flows which are analyzed by CFD. -The factors support the indoor multi-zone simulation to improve the indoor thermal balance which takes a role as a Passive House design.
Step 6	Evaluation of energy-saving effects	-The economical cost and total energy are evaluated by comparison between the microclimate model and EP model.

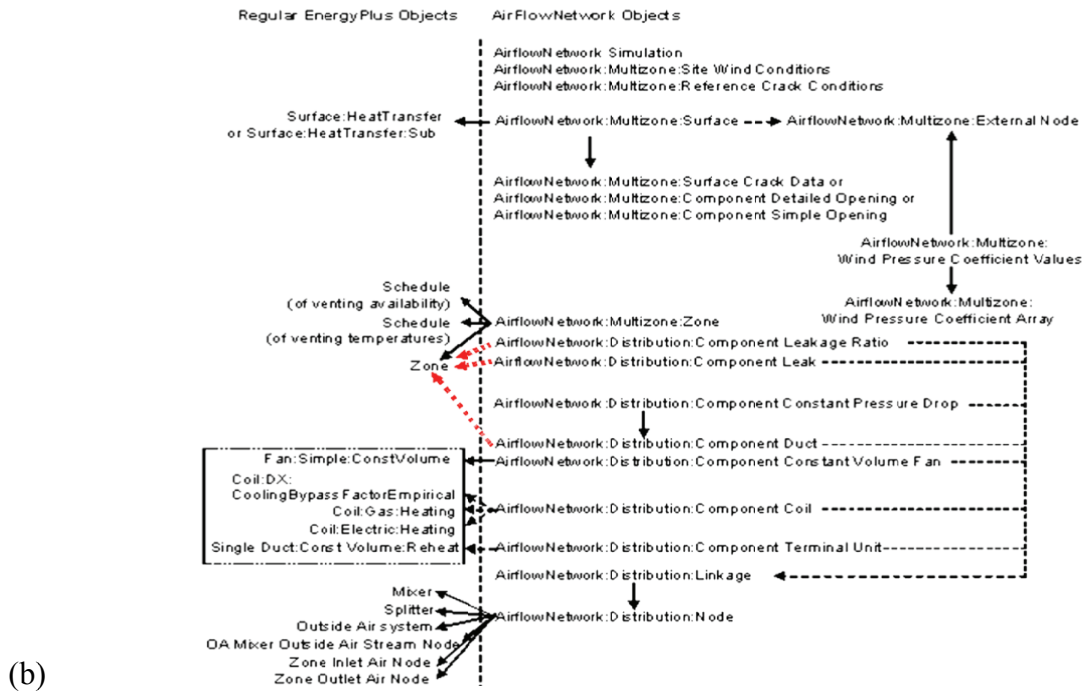
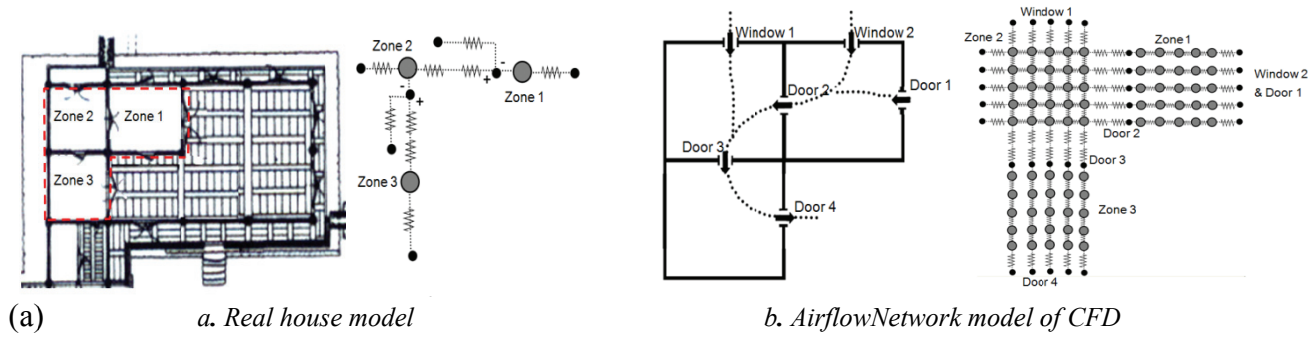
#### 4.4. Graph modeling for real house analysis

This chapter represents the graphs modeling of EP-CFD method for energy simulation shown in the previous chapters. An energy simulation with CFD is normally too complex to use for planning of a real house because a building has a lot of design elements, e.g. windows, walls, floors, doors and air leakages etc., related to airflows, and CFD uses all connections of complex design elements. A real house with several design elements shown in Fig.4.12 (a)-a needs a lot of information extracted from a building description to calculate airflows. Airflows can be modified by size, orientation and location of building surfaces which contain slits and openings. 3 zones are set up to simplify from real and complex airflows to a simple networked model such as airflow network shown in Fig.4.12 (a)-b. The airflow network model solves equations with building's physical parameters which are modified by building design elements and predicts air pressures and temperature.

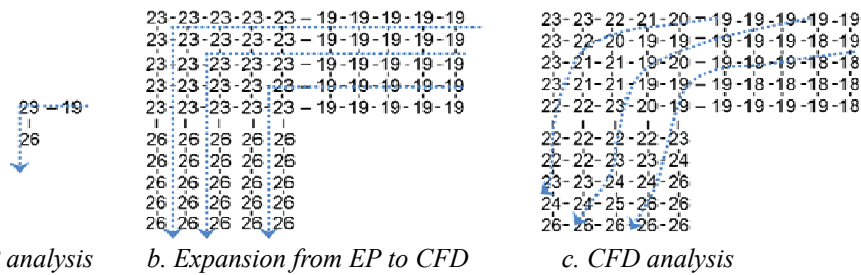
The airflow network model is defined in a set of functions in EP called *AirflowNetwork* and the functions use wind pressure coefficients to simulate multi-zone airflows driven by natural wind and air distribution system. Heat and moisture gains or losses and distribution also can be calculated by the functions. Fig.4.12 (b) represents a set of the *AirflowNetwork* functions to simulate the model shown in

<sup>122</sup> <http://www.kma.go.kr>.





**Figure 4.12.** Graph modeling, (a) graph model of EP method for the 3 zones, (b) relationship between *AirflowNetwork* and regular EP objects [author, the US department of energy 2007b].



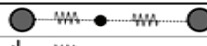

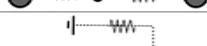
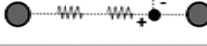
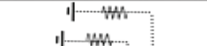
**Figure 4.13.** Allocating EP's volume average value to CFD nodes of the volume [author].

Fig.4.12 (a)-b. The *AirflowNetwork: Multizone: Zone* specifies the ventilation controls that apply to all of the openable exterior, interior windows and doors in the corresponding thermal zone. Surface-level ventilation controls<sup>123</sup> indicate whether a heat transfer surface of a wall has an opening or individual ventilation control or not. There are 3 thermal zones, Zone-1, Zone-2 and Zone-3. There are openable

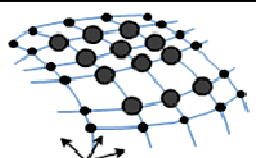
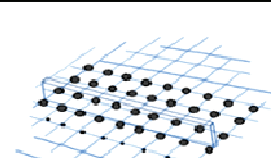
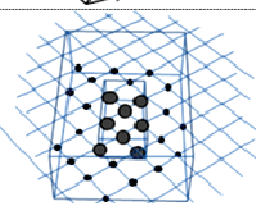
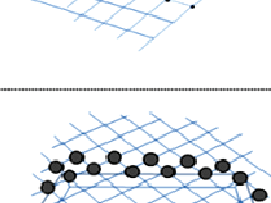
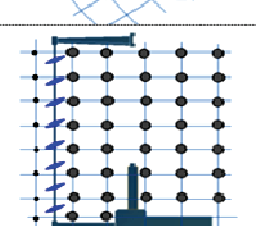
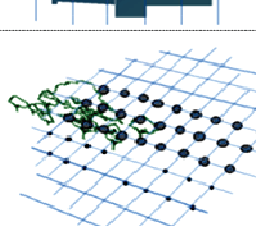
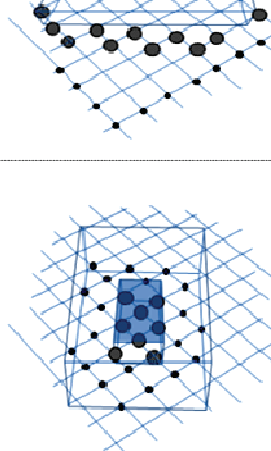
<sup>123</sup> E.g. *AirflowNetwork: Multizone: SurfaceCrackData* and *AirflowNetwork: Multizone: SurfaceObject*.

**Table 4.8.** Graph models of EP and CFD [author].

*a. Graph model of EP*

Type	Factor	Graph model	Applicable figure
Heating	Daylight Factor(DF)		Fig.2.7
	DF, Solar gain		Fig.2.8
Heating, and Cooling	DF, Solar gain, Shading		Fig.2.9
	DF, Solar gain, Natural ventilation		Fig.2.13
Insulation	U-value		Fig.2.14

*b. Graph model of CFD*

Type	Factor	Graph model	Type	Factor	Graph model
Arrange ment	Topography		Form	Barrier	
	Courtyard effect			Building geometry	
Façade element	Double façade		Courtyard roofing		
Afforestation	Opening slits				

exterior windows, Window-1, Window-2 and Window-3, and openable interior doors, Door-2 and Door-3. External Node-1 is associated with the façade that contains Window-1 and Window-2. External Node-2 is associated with the façade containing Window-3. Airflow network models can show possible airflow pattern,<sup>124</sup> and the arrows show the process among *AirflowNetwork* functions and between the

<sup>124</sup> Note that airflows of EP model show only the pattern without details.

functions and regular EP functions. The solid arrows represent a reference from object A to object B. The dashed arrows indicate the components in a linkage object. The dashed arrows pointing to the Zone object indicate the components that interact with the zone air.

Real airflow pattern is modified by wind pressure and air temperature distributions between zones and can be analyzed by CFD. A coupling of EP and CFD methods offers a combination of advantages of multi-zone flow network and airflow dynamics. However, the difference of resolutions between EP and CFD is the main problem for coupling. Fig.4.12 respectively illustrates the resolutions of EP and CFD. EP uses an analysis unit called node point which has the average value, and CFD needs more node points with the partial differentials. To combine EP and CFD, this study proposes a graph modeling which fills the copies of the EP's average values into the node points of CFD.

Volume average values of 3 zones are expanded to CFD by allocating the EP's volume average value, i.e. single node, for CFD's multiple nodes. The number of node points from EP is increased by copying the values into the expended node points of CFD as Fig.4.13-*a* and *b* show. CFD refines the average values in each zone into real and physical airflow using the differentials with the values of neighboring zones as Fig.4.13-*c* represents. The values of neighboring zones are boundary condition for the calculation for each zone. Calculating nodes and boundary conditions are respective represented by ● and ●.

In the numerical solutions, EP and CFD respectively use FVM and Finite Element Method (FEM). Table 4.8 classifies EP and CFD methods by node points which can express airflow patterns. EP can predict a single value of DF, solar gain, shading, natural ventilation and U-value etc. by all of the windows and doors in a single zone. CFD predicts airflows, speeds and directions between values of adjacent zones. A graph contains all parameters that are required for energy calculation in each zone. Graph model is simple and efficient in visualizing physical parameters in complex geometry such as a real house.

## 5. Microclimate design methods in S. Korea: Simulation results using unit EP-CFD

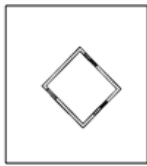
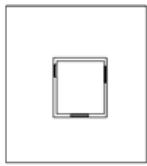
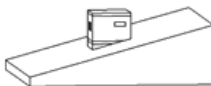
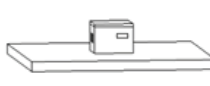
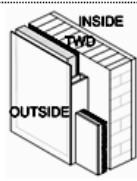
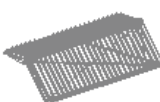
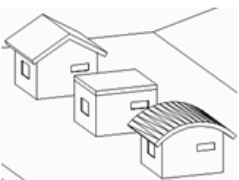


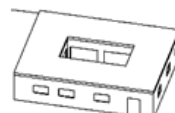
Energy simulation using EnergyPlus (EP) and Computational Fluid Dynamics (CFD) is applied to the cases shown in Table 5.1. The graph modeling described in the previous chapter is used for unit design. While EP calculates the air temperature of each zone, thermo- and aerodynamics among adjacent zones can be calculated by EP-CFD. In this study, *Fluent* software<sup>125</sup> is employed for the CFD simulation. A combination of some design elements of Korean traditional, passive and climate architecture which are expected to be efficient for heating and cooling are tested by EP-CFD simulation and classified into 4 cases. The 1st case is a combination of elements which are efficient for passive cooling, and the 2nd case includes all passive heating elements. Case 1 and 2 respectively includes design elements which are generally considered to improve the heating and cooling efficiency. Although a lot of different studies were surveyed and described in previous chapters, few studies considered the best combination since it is very difficult to counterbalance cooling and heating efficiencies. Some design elements can increase heating gain but decrease the efficiency for cooling gain and some other elements vice versa. In this study, cases of heating and cooling gains are separated firstly and the full combination of all cases is tested for the counterbalance. Case 3 is the full combination of all tested elements in case 1 and 2. Considering heating and cooling gains for heating and cooling efficient cases and full combinations, the best combination of the energy efficient design elements is chosen. The 4th case is the best combination which counterbalances heating and cooling efficiency.

For the 1st and 2nd cases, some good building elements for thermo- and aerodynamics are chosen by the Passive House standard. Thermo- and aerodynamics can be utilized to make effective ventilation ratio in passive cooling and to avoid overheating in passive heating etc.

---




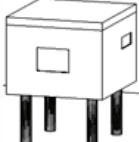
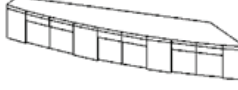
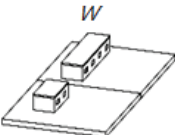
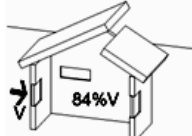
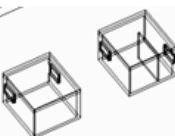
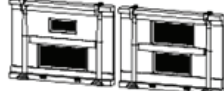

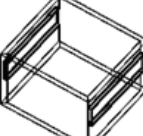
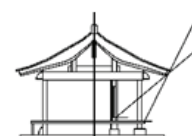
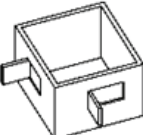
<sup>125</sup> The Fluent simulation has been carried out in cooperation with Prof. Dr.-Ing. P.U. Thamsen of the *Fluidsystemdynamik Institut* (SDI), TU-Berlin. License information: Fluent, Inc. license file for TU Berlin\_\_9482\_ren2006, License 268961540 created 11-jun-2007 by al, Windows NEW or Renewed Floating/Network License, SERVER 130.149.13.193 000102142b52 7241.

**Table 5.1.** List of Elements in classified microclimate design methods for energy-saving houses [author].

Case	A. Korean traditional houses	B. Passive House (heating)	C. Climate house design (cooling)	Case 1	Case 2	Case 3	Case 4
Orientation	To the southeast 	To the south 	To the south  Same with B		B	B	B
	Topography	0~19° slope 	flatland 				
Wall		ISO-metric detail 			B	B	B
Roof form	Gable 	Gable , flat, round 	Gable , flat, round  Same with B	A	B,C	A	A
Composition	annex buildings 	Courtyard roofing  roof window opening, cross ventilation	Courtyard effect 		A,B,C	A,B,C	A

(1) Maximum cooling efficiency can be obtained when air flows through the zone are continuous through the geometry without a discontinuity on the streamline. Only continuous streamlines of airflow through a house can bring about a strong microclimate effect because air movement through a house, which occurs through partial pressure differences, distributes indoor air temperature and humidity. Hence, it is most important to set up building geometry which has a smooth and continuous streamlines through the house. Near the windows, doors, and openings, aerodynamics occur due to differences in wind pressures and cause ventilation effects. Airflow can be mixed with thermodynamic effects such as thermal buoyancy, stack effects due to the thermal distribution in the house.

(2) Maximum heating efficiency can be obtained by a high performance Passive House design. However, overheating and imbalanced problems in the house should be avoided. The thermodynamics

Case	A. Korean traditional houses	B. Passive House (heating)	C. Climate house design (cooling)	Case 1	Case 2	Case 3	Case 4
Barrier	Barrier 	Greening, Afforestation 	Barrier 	A	B, C	A, B, C	C
Geometric	Over pilotis 	geometric form 	Building geometry 	A	B, C	A, B, C	A
Ventilation	Roof opening 		Partitioning 	A, C		A, C	C
Opening	Opening slits 	Shape, position and size 	Opening control 	A, B, C		A, B, C	A, B
Shadow	Overhang 		Projection, sash, canopy 	A, C		A, C	A, C

Case 1: For max. cooling efficiency in A, B & C

Case 2: For max. heating efficiency in A, B & C

Case 3: Full application of case 1 & 2

Case 4: The best combination of case 1 & 2

of heat transfer is sufficient to solve these problems. Heat transfer always occurs from a warmer area to a cold one and can never stop.<sup>126</sup> If thermal energy is transferred from an overheated area to a cold area, the areas reach thermal equilibrium. Thermal buoyancy, stack effects and solar chimney spreads the heat from overheated zones to cold zones and results in thermal balance. The thermal condition in thermally balanced rooms is easy to maintain and saves heating energy during cold nights. The simulation results with several design elements will be described in the following chapters.

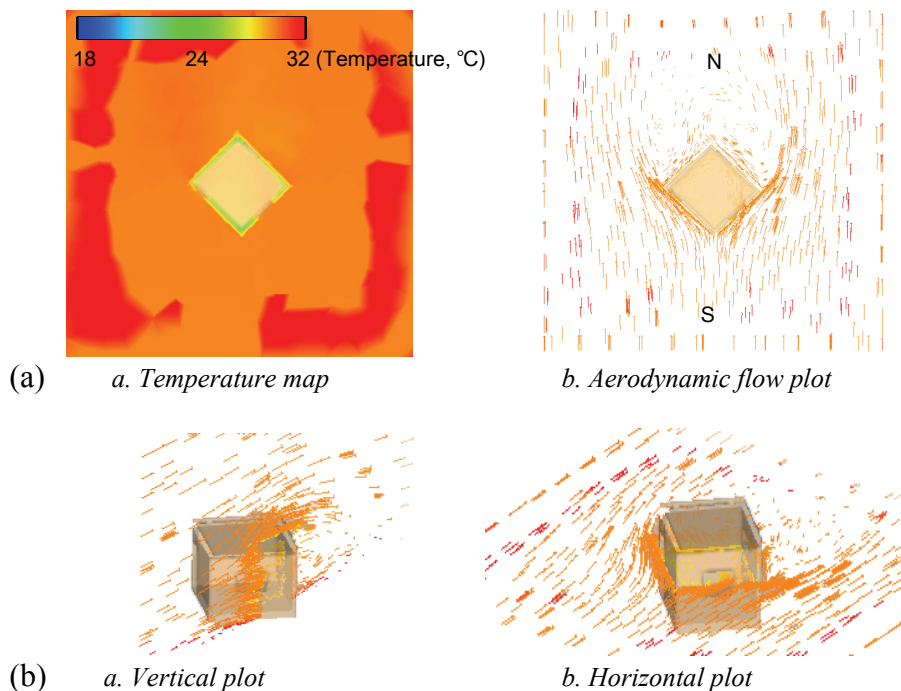
<sup>126</sup> Note that it can be slowed down.

## 5.1. Arrangement

### 5.1.1. Microclimate of building orientation: the highest heating gain and small indoor airflow

Above all, building orientation can play a significant role in determining the solar gains received. If a house is oriented to  $45^\circ$ , facing east or west will be more susceptible to receiving adverse low altitude of sunlight in the morning and evening. The building zones are heated from early on the day and the overheated air of these zones within the building is maintained during the day. Fig.5.1 (a) represents the overheated temperature in the zone using CFD simulation. The maximum temperature of the air is estimated at  $34.7822^\circ\text{C}$  and the value is much higher than for human comfort.

Hence, the strong passive cooling through airflow is needed to discharge the overheated air. The overheated air in the zone cannot be ventilated due to the small microclimate. As mentioned in Chapter 3.4.2, the opening control should be designed to drive the movement of the air more quickly and the perpendicular of the wind direction has the best efficiency to develop a large amount of air pressure. However, the amount of air through the window of a  $45^\circ$  oriented house is too small since the wall of the building set to a south easterly wind direction and flow over the exterior. Fig.5.1 (b) represents the form and the magnitude of airflow and the horizontal-vertical plots of the 3D CFD result.



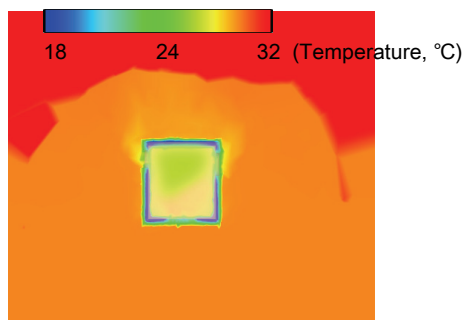
**Figure 5.1.** Result of orientation of the CFD, (a) 2D plot, (b) 3D plot [author].



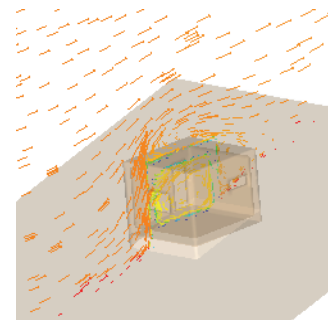
The minimum temperature  $24.5918^{\circ}\text{C}$  is found in part of the wall but the average temperature is  $29.942^{\circ}\text{C}$ . It is lower than  $30^{\circ}\text{C}$  of the single EP simulation result but a very small cooling gain from microclimate can be expected. In general practice, air temperatures in the region of  $23$  to  $25^{\circ}\text{C}$  are regarded as being acceptable as a comfort zone in summer and  $20$  to  $22^{\circ}\text{C}$  in winter. This form does not have a good microclimate cooling effect in the design but it may be utilized when the zone needs no flow and still air. One solution for the oriented building is minimizing glazing on the east-west façades or providing solar shading of the south to avoid solar penetration. Fig.5.3-a shows the comparison of temperature between the zone to the southeast and to the south.

### 5.1.2. Microclimate on topography: large microclimate cooling effect with high air pressure

Building on topography has a strong microclimate effect since by day the air above the slopes can be more easily heated than the lower area. Hence, strong anabatic airflow which was described in Chapter 3.2.3 is accompanied by strong air pressure due to the difference of air temperature. The building located higher on the hill side obtains a large amount of strong wind and the aerodynamic effect of microclimate enhances the performance of passive ventilation cooling. Fig.5.2-a illustrates the difference in thermal conditions between the higher and lower slopes. The building ventilation near the window in the thermal color map can be represented in comparison with the air temperature above the overheated ground.



*a. Thermal map*



*b. 3D flow plot of aerodynamic*

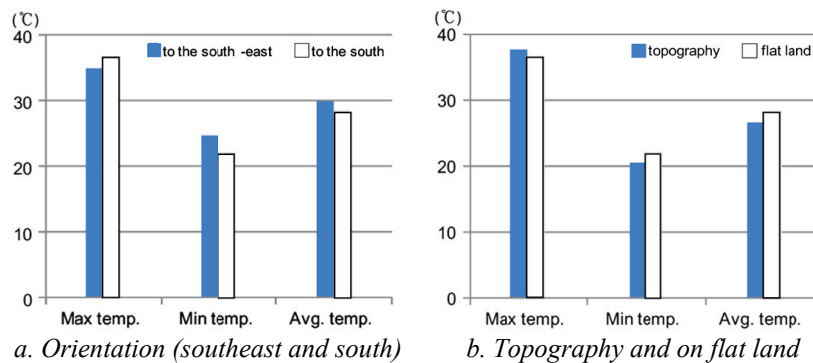
**Figure 5.2.** Result of building in topography [author].

The maximum temperature of the air is calculated by the CFD method and the quantity value in the maximum temperature is  $37.525^{\circ}\text{C}$  above the hill side. On the other side, the lowest temperature value is  $20.4619^{\circ}\text{C}$  and the difference between maximum and minimum is  $17.0631^{\circ}\text{C}$  which is much larger than the difference for flat land. The flow plot from the strong aerodynamic in Fig.5.2-b shows the small eddy current in the zone, which adapts the indoor air temperature to the outdoor quickly. The average temperature in the zone on topography is  $26.6817^{\circ}\text{C}$  and the microclimate cooling effect can be

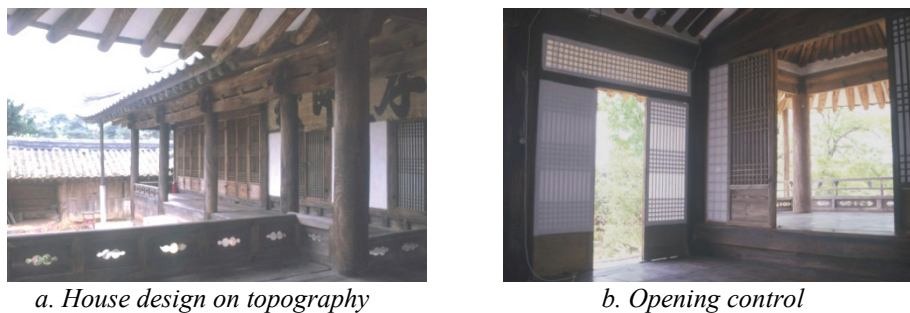


expected to reach 3°C and more than the zone on flat land. Fig.5.3-*b* represents the comparison of temperatures between the zone on topography and on flat land.

In the Korean traditional architecture scheme, a lot of microclimate design elements related to topography have been used for the summer season. The main building is normally located on the south slope of a hill side. Seasonally the window is fully opened towards the south and is used to take the cooling wind as Fig.5.4 shows. These design elements can be utilized to plan a modern house design in S. Korea.



**Figure 5.3.** Comparison of thermal condition with cooling gain [author].



**Figure 5.4.** A cooling scheme of a Korean traditional house on topography [author].

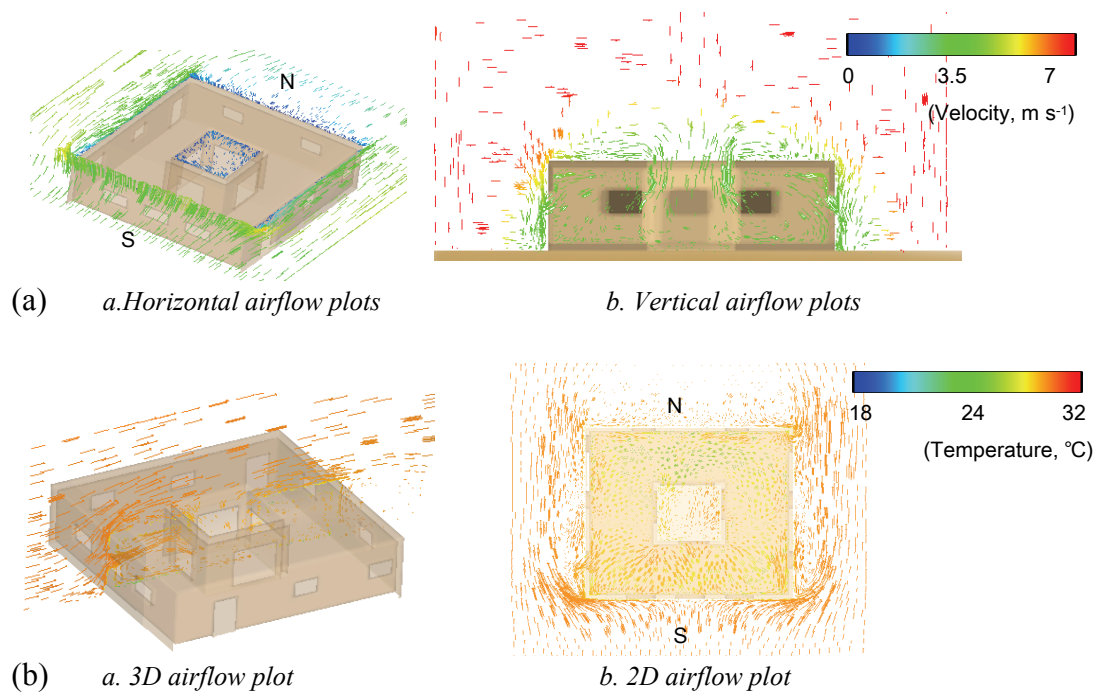
### 5.1.3. Microclimate of courtyard cooling: thermodynamic air circulation through the house

The courtyard is one of the most favorite house designs to provide easy and natural privacy, allowing for increased densities. The garden of the courtyard can also provide an indoor green space raising the quality of life. This chapter investigates the microclimate dimension of the courtyard since the real geometry of the building is more important than the insulation for the architects.

The main advantage of the courtyard house is that the courtyard easily has a partial shade and is cool while outside the building it is very hot and sunny. It is protected from the direct hot and strong winds

even when the building is orientated in any direction. Fig.5.5 (a)-a illustrates the air velocity of outdoors and courtyard. When the outdoor air velocity is over  $4\text{ m s}^{-1}$ , the aerodynamic velocity is  $0\text{ m s}^{-1}$  or very small. Hence, the microclimate gain in the courtyard is more related to the thermodynamic effect. The temperature difference between hot outdoors and cool courtyard forms a circulation vortex in the courtyard. Fig.5.5 (a)-b shows the microclimate air circulation due to the thermal difference between house and courtyard.

By day, the courtyard is cooler than the house which heats up as a result of solar radiation, and the down flow air raises the air density. The dense cool air moves through the building through the courtyard

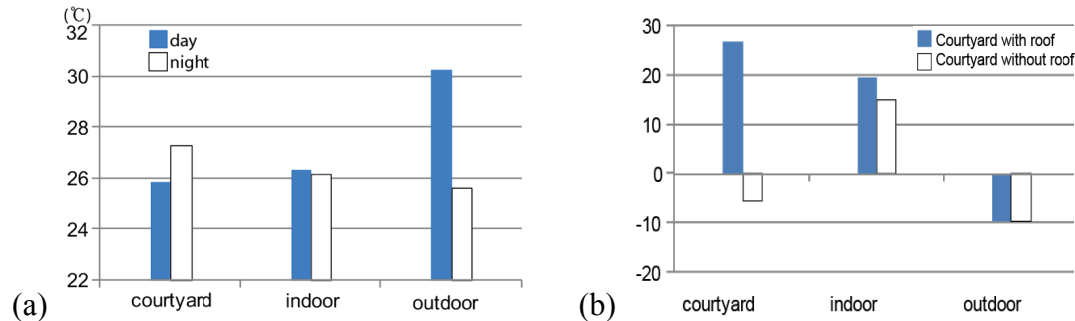


**Figure 5.5.** Result of courtyard cooling between house and courtyard, (a) air velocity and the microclimate air circulation, (b) thermodynamic air circulation [author].

openings. The wall of the house gets cool by night and the courtyard is then warmer than the house. Hence, the warm air in the courtyard rises and the pressure in the courtyard decreases. The air from outside at night comes through the house by cross-ventilation and the warmer air is evaporated in the courtyard. The night ventilation caused as a result of the courtyard is represented by the 2-D airflow plot shown in Fig.5.5 (b)-b. Fig.5.6 (a) shows the air temperatures of courtyard, indoor and outdoor by day and night.

However, in the hot and humid Korean climate, the courtyard cooling is only partially effective in the building and the total cooling efficiency is not high as Fig.5.6 (a) represents. The average indoor temperature is  $26.324^{\circ}\text{C}$  by day and  $26.147^{\circ}\text{C}$  by night. However, the microclimate airflow produced by the thermal imbalance can always make indoor airflows and this feature can be utilized for designs

which need good ventilation. For the design, the controlling of the local temperature is the most important issue so as to utilize the thermal imbalance for the microclimate. A computer simulation of 1-year shadow range of the courtyard is needed to determine the window control sequence and parameters for cooling. Fig.5.5 (b)-a shows the 3D airflow of outdoor, indoor and the courtyard.



**Figure 5.6.** Air temperature of courtyard, (a) indoor and outdoor by day and night, (b) with and without roof [author].

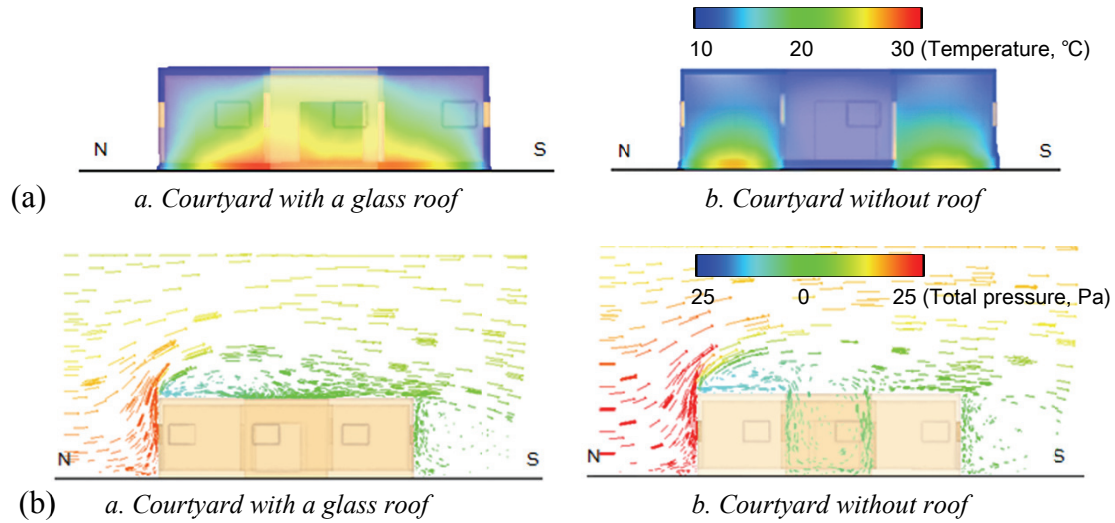
#### 5.1.4. Microclimate of courtyard roof: atrium passive heating using courtyard

The courtyard can protect against direct and strong wind but the air temperature in winter cannot be warm since the air temperature is not the same as the wind temperature. The air temperature in the courtyard is very similar to the outdoor temperature but the airflow is stable thus the effective temperature in the courtyard, which is related to the human comfort, is lower than that of the outdoor air.

To improve the heat gain of the zone, the roof glazing of the courtyard can be utilized as a passive heating method. The atrium of the courtyard can obtain radiative heat through the glass and avoid the direct heat loss by the glass. The average air temperature in the courtyard atrium is 26.814 °C. By indoor air circulation, the neighboring zone can get about 4 °C higher temperature by daytime and the average indoor temperature is 19.488 °C. The main heat loss may occur through the roof glass surfaces of the building but improved solar heat gain sufficiently recovers the amount of loss. Hence, a courtyard with a glass roof is very warm and pleasant with less wind. Fig.5.6 (b) represents the average air temperatures in the courtyard, indoor and outdoor between courtyards with a roof and a without roof. The average air temperature of the courtyard without a roof is -5.328 °C and the average indoor temperature of the building surrounding the courtyard without a roof is 14.992 °C.

Fig.5.7 (a) shows the comparison of the thermal conditions between courtyards with a glass roof and a without roof with thermodynamic air circulation. The pattern of thermal condition in the courtyard with a roof is much better. The atrium of the courtyard can block the direct cold airflow, and the cold airflow

slides on the surface of the roof and glass roof and naturally sinks down the surface of the exterior wall as Fig.5.7 (b)-a represents. On the contrary, if a roof does not exist, cold air cascades down the surface and the wall of the courtyard and the air cannot be heated well due to the shading of the courtyard as Fig.5.7 (b)-b shows.



**Figure 5.7.** Result of courtyard roof, (a) thermal condition of courtyard in winter, (b) comparison of airflows between courtyard with roof and without roof [author].

The advantage of a courtyard is the isolation of the outer wall and the glass roof maintains the thermal condition of the courtyard. Hence, the courtyard roof is necessary in the cold winter in Korea. If the courtyard is overheated by day, the cross-ventilation is also a good solution as has been described in the previous chapter. The ventilation performance of the courtyard atrium is better than in the courtyard without a roof, due to stack effects. The indoor temperature is lower than that in the courtyard and the thermodynamic microclimate can occur. If the windows of the exterior wall and courtyard wall are opened, the airflow through the zone removes the heat of the courtyard but improves the indoor climate. Fig.5.7 (a)-a exemplifies this case.

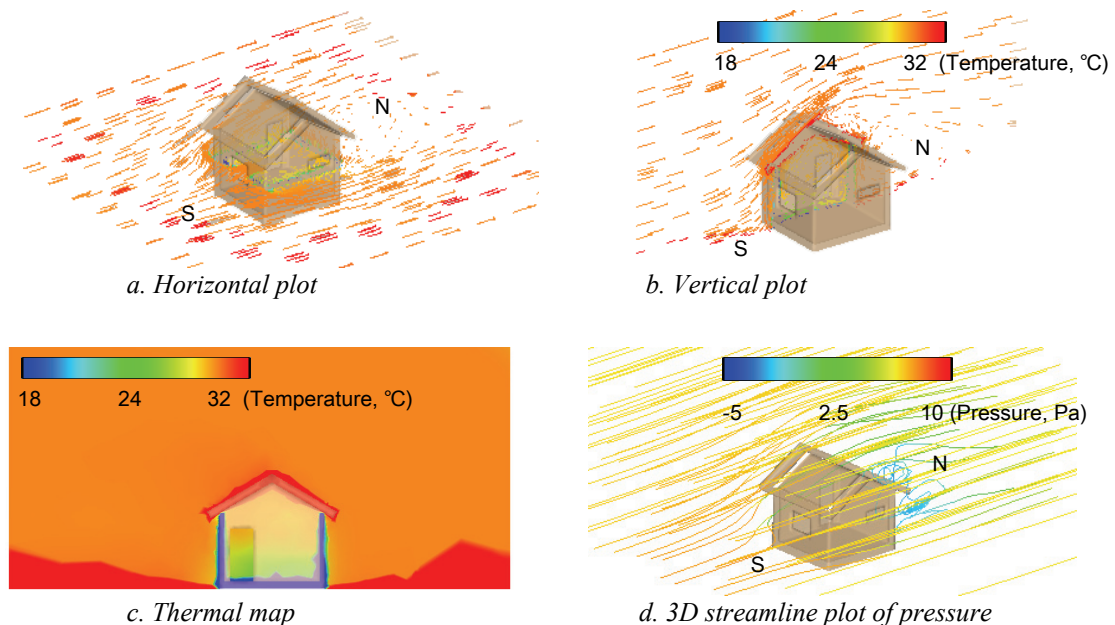
Another method is a roof opening which uses the stack effects since the overheated air is generated on the surface near the floor and tends to rise up to the roof. In this case, the direction of thermodynamic airflow is opposite to the cross-ventilation through the exterior openings. The overheated air is discharged by roof openings and the cold air comes from the windows of the zone. Thermodynamic effects by roof openings are bigger than the effects by exterior openings. Hence, the roof opening is suitable to design a large building with a courtyard. The exterior openings are an easy method and suitable for small buildings which want to store the heat by day and to use the heat for the cold night.

## 5.2. Form

### 5.2.1. Microclimate in roof shapes: strong shading and control of wind stream direction

The architect or designer typically designs the general shape of the roof in the preliminary design stage. As described in chapter 3.4.3, design of roof shapes is related to the both shading and wind streamline. The flat roof is a very common style in areas with little rain or snow to provide a platform for heating and other mechanical equipment. The flat roof can eliminate the ceiling joists. However, it is difficult to design a passive cooling system through the roof since when air is heated it becomes less dense and rises. The air movement through the zone generates local areas with high and low pressures. If a space has high air outlets in conjunction with low inlets, ventilation occurs as the air within the space is heated and the greater the vertical distance between the outlet and inlet, the greater the ventilation rate that can be obtained.

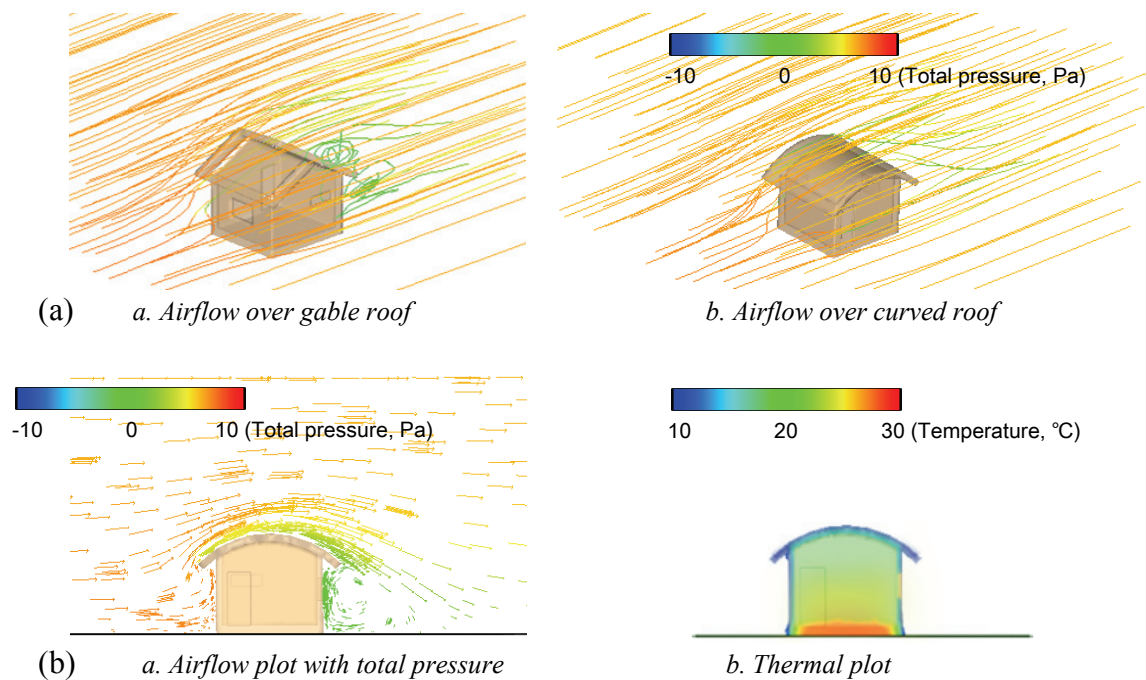
The gable roof shown in Fig.5.8 is one of the most common type of roof in residential construction and uses two slanted roofs that meet to form a ridge between the support walls. The gable roof can offer the largest ceiling space and roof outlets near the ridge are sufficient to derive a stack effect in which the wind from outdoors is heated and naturally moved into the roof outlets. The positive air pressure in the



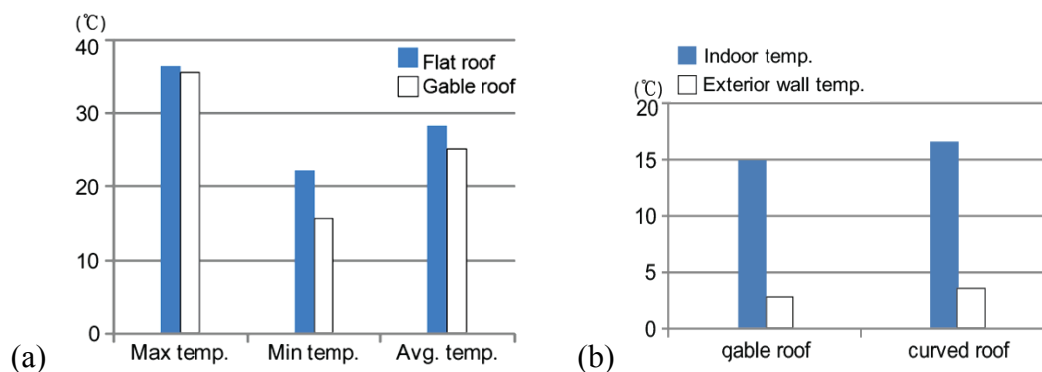
**Figure 5.8.** Result of gable roof with shading overhang and roof ventilation [author].

front side of the house is changed into negative pressure when the air is across the roof ridge. Fig.5.8-d visualizes the positive and negative pressure and the magnitude using 3D streamline plot. As a result of air pressure differentials the roof form allows for the better internal cross-ventilation and roof space ventilation allowing regular air changes. Fig.5.8-c visualizes the thermal range by pseudo coloring with rainbow colors and very clearly represents the temperature gradient between floor and roof. The maximum temperature of the air is 35.423 °C near the roof but the indoor air temperature near the roof is about 28 °C and 24 °C in the living space near the floor. The 3D airflow plot of aerodynamic is represented in Fig.5.8-b.

The edge of the roof can be used as external projections; they act as horizontal wind-catchers which raise the internal ventilation rates or the sunshade. It can efficiently reduce heat gain and improve



**Figure 5.9.** Result of curved roof, (a) air-streamline comparison between gable roof and curved roof, (b) pressure and thermal condition of curved roof [author].



**Figure 5.10.** Comparison of thermal condition (a) cooling gain between flat and gable roof, (b) indoor and exterior wall temperatures between gable and curved roofs [author].



human comfort in summer. While the roof is overheated by solar radiation, the living zone can maintain the cool air temperature in the walls, using the shading effect and the microclimate aerodynamic cooling, resulting in strong ventilation effects. The minimum temperature  $15.592^{\circ}\text{C}$  is formed in the floor and the average air temperature is  $25.168^{\circ}\text{C}$ . The 3D plot of the airflow is represented in Fig.5.8-*a* and *b*. The differences in cooling efficiency achieved by the design forms can be compared with the flat form shown in Fig.5.2. A temperature comparison between flat and gable roof is shown in Fig.5.10 (a).

### **5.2.2. Microclimate of curved roof: minimum wind resistance and small eddy current**

The roof design in cold winter is an important factor to control energy flow. The Korean winter airflow blowing from Siberia is very strong and cold. In this condition, the wind resistance of the roof affects the pattern of air currents around the zone. In the colder regions, most residential roofs have a steep slope due to the large amount of snow. However, the Korean winter is not humid but dry and the amount of snow is not great. Hence, the consideration of airflow for roof design is more important.

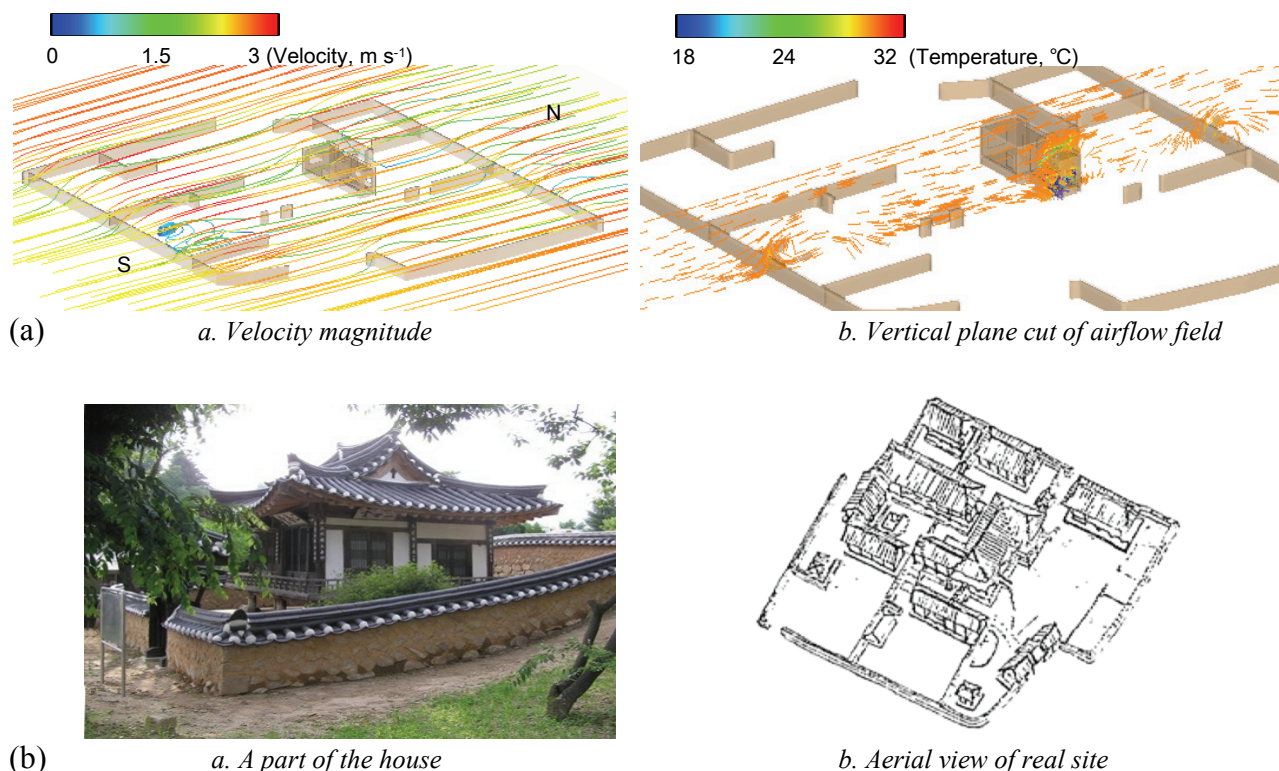
The most common design of roofs in Korea is the gable roof as Fig.5.9 (a)-*a* shows. By computer simulation, the gable roof form generates a large eddy current due to unstable pressure around the house. When a high wind blows, the positive pressure from the side and below and the negative pressure from above generate the uplift air pressure. The airflow accompanying the high wind resistance created by the roof eddies around the exterior of the house. The shape and slope of the roof deck and the edge configuration also involves similar high pressure effects. Strong local wind effects with the eddy current due to the pressure are difficult to control.

A design form is investigated in this chapter to minimize the eddy current by controlling the energy flow. A curved roof using the streamline shape shown in Fig.5.9 (a)-*b* does not disturb the flow over the model and eliminates or reduces wall effects on the house. The streamline shape allows the wind to decelerate gradually along the back part of the building. This helps prevent the boundary layer from separating, and thus produces much less pressure drag. Hence, the streamline plot of the curved roof represents the very smooth airflow lines passing the house with such a roof shape. By comparing between 5.9 (a)-*a* and *b*, the magnitude of total pressure around a house using the curved roof is much smaller than one using a gable roof. A large amount of cold wind quickly passes over the roof surface and the flow path continues naturally without producing an eddy as Fig.5.9 (b) shows. The stable airflow over the house helps to avoid a loss of heat from interior sources through the wall. In the results, the energy losses decrease and about 9% additional energy gain can be obtained. Fig.5.9 (b)-*b* shows the thermal plot of the zone and the average temperature of the zone is  $16.574^{\circ}\text{C}$ . The comparison of the average temperature of indoor and exterior between gable roof and curved roof is shown in Fig.5.10 (b).

### 5.2.3. Microclimate in fence design: deriving small wind and airflow on the site

Air movement within an environment is required to get rid of discomfort through heat and humidity and to provide fresh air to the space. In the site condition, occupants do not need strong wind for human comfort. A strong wind reduces the sensible heat and humidity due to higher evaporative cooling on the skin. However, the extremely strong airflow cannot be endured due to the wind discomfort. The general design specifications for air movement are that the air speed should not be above  $1.5 \text{ m s}^{-1}$  around the body.

For that reason, a long history of utilizing windbreaks including natural trees and artificial fences are used for preventing wind damage, increasing productivity, and improving the quality of the living environment. Fence design using walls and huge plants can be used to protect against wind and direct hot air. Layered spaces in the Korean traditional house usually use the design of low walls as a form of organic space with a cell structure divided by the walls.



**Figure 5.11.** Result of fence design in Korean house, (a) 3D streamline plot of airflow, (b) the present state of Mr. Jung's house [author].

Fig.5.11 (a)-a represents the streamline of wind control using the fence design. This simulation uses low fences which are generally constructed in Korean traditional architecture designs. The distribution

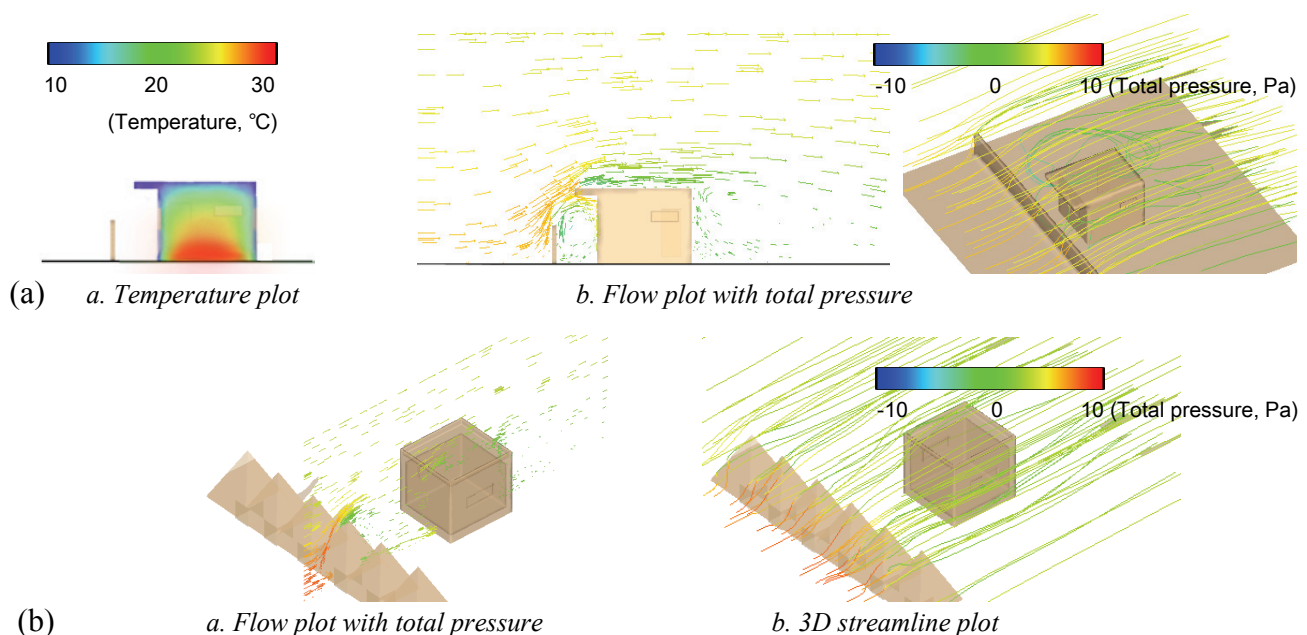


of the velocity magnitude is decreased by the walls and the small windbreaks in the fence. An effective barrier design for windbreak is perpendicular to the wind but the streamline through the site should not be blocked by the design. Hence, the continuous path of the airflow should be considered in the design stage. For the simulation purpose, the fence form is employed from “Mr. Jung’s house” which is located in *Hamyang, Kyungsangnamdo*, S. Korea. Fig.5.11 (b) shows a picture of the site and the aerial view of the real site condition. The simulation model is simplified to the single house using the real fence form. In the simulation result, the average wind speed through the site is  $2.823\text{m s}^{-1}$  but the speed on the site surrounded by the wall is decreased to the  $0.920\text{m s}^{-1}$ . The percentage of the total decrease in speed is 67.4%.

In Fig.5.12 (a)-b, the temperature and flow shape are visualized by a horizontal plane cut of the flow field. The windbreaks are placed at various distances from the buildings and walls, and different effects exerted by the building and windbreak can be shown in the flow shape. If the distance was less than 4 times of the fence’s height, the standing vortex in front of the building is dominated by the lower part of the flow field and there is no difference between porous windbreaks with afforestation and solid wall.

#### 5.2.4. Microclimate of windbreaks: cold wind protection in winter

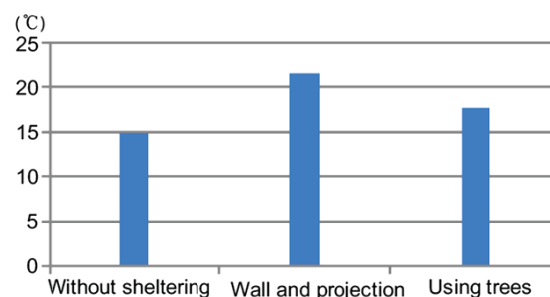
The direct wind blocking called wind shelter is the most efficient concept using microclimate in winter. Wind shelter can be provided by several design methods using other buildings, wall, natural afforestation or artificial windbreaks. However, the purpose of wind shelter is not only against wind velocity producing extra wind-chill but also driving rain and snow.



**Figure 5.12.** Cold wind protection, (a) using wall and projection, (b) using trees [author].

The main feature of winds around buildings is a circulation driven by the building geometry. The exterior surface directly meets the direct cold wind and the eddy occurred by the geometric resistance. The erection of a barrier can get rid of the direct wind but is not perfect for removing eddy currents. Hence, the geometric set-up between the building and wall that may control the microclimate air pressure is very important. The effective design feature of the set-up to remove eddy whirls generated by wind sideslip around a building is the distance between the barrier and building and the barrier height. As in the description of chapter 3.3.1, the distance is decided as 1/3 of the building size and the roof projection is included to block the airflow from the roof. By a combination of side barriers and roof overhangs, the wind-sheltering effect is exemplified as the plot wind streamlines in Fig.5.12 (a)-b. In this design, the 16% heat loss is avoided and the average temperature of the zone is 21.411°C by protecting the cold wind. The thermal condition of the zone is represented in Fig.5.12 (a)-a. The streamline very clearly illustrates the air blocking effect which the wind gets out of the house surface due to the pressure change. Sometimes the space between windbreaks and a house surface has a local climate with stable airflow.

Similar wind shelter effects can be generated by very large plants plant which can protect against the wind. Lines of trees play a role as a medium density windbreak and spread the distribution of wind speeds. The average temperature of the zone is 17.536°C. Fig.5.12 (b) respectively shows the wind blocking using trees and the streamline. The trees can weaken very strong winds but low airflows remain. If there is a gap between trees, their performance as a barrier is decreased since the flows into narrower areas may cause strong local wind effects. Hence, several rows of trees are needed to achieve the required effect. Fig.5.13 shows the comparison of average temperatures between no wind-sheltering and sheltering using a wall and projection, and using trees. Sheltering, using a wall and projection, or using trees can obtain 31% and 15% gains, respectively.



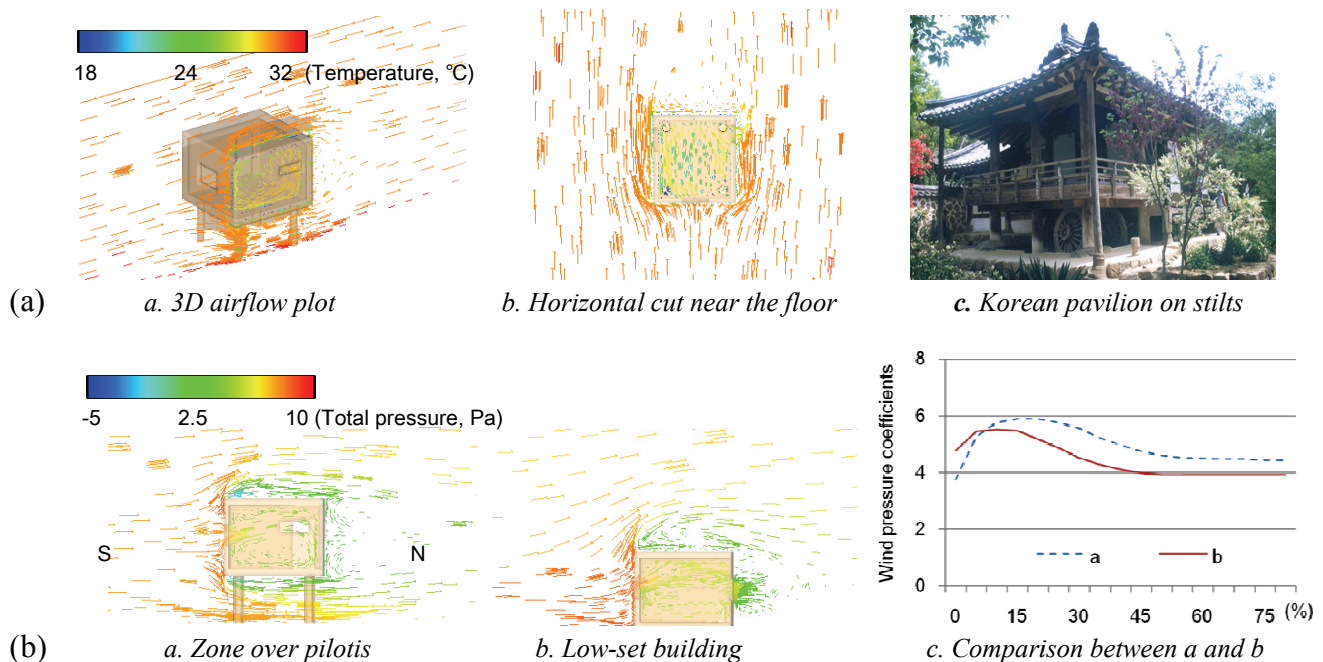
**Figure 5.13.** Average indoor temperatures of no wind shelter, shelters using wall and projection and using tree [author].

### 5.2.5. Microclimate in building over pilotis: cooling efficiency of airflow under the floor

People generally can tolerate wider ranges of humidity than of air temperature. In internal spaces, the humidity usually ranges from about the mid 30s to the upper 60s and people can tolerate humidity in that range. However, if the humidity is in the upper 60s, along with high air temperatures, and air movement is low or there is no movement, people feel uncomfortable.

A floating building using pilotis can be often observed in the subtropical climate. In the hot and humid climate, latent energy transfer with air motion is more important to get rid of humidity in the zone. The most common method is designing the largest surface for the zone for efficient evaporation. The floating architectural design offers the unit the opportunity for maximizing the volume of air currents and cross-ventilation through the space under the floor, to allow breezes to flow through the house and is efficient for cooling. Raising the building structure creates fully shaded space underneath, which helps to catch the strongest winds and to keep cool air from the shady ground space under the house. The 3D plot of airflow in Fig.5.14 (a)-a shows that raising a building on stilts is efficient for the cooling of the floor and by locating the window high up in the wall is better for ventilation.

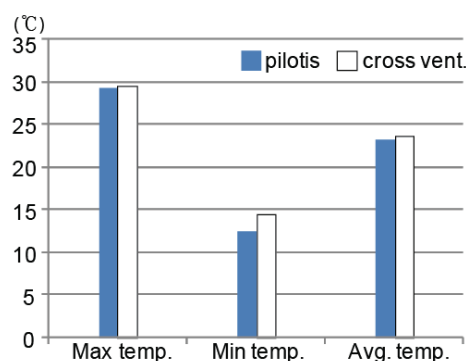
In Korean traditional architectural design, the pavilion with pilotis shown in Fig.5.14 (a)-c has been very popular as a seasonal dwelling for summer. In the simulation result, when the maximum



**Figure 5.14.** Building over pilotis, (a) result of flow field and a Korean pavilion, (b) comparison of wind pressure distribution for different porosities (%) [author].

temperature outdoors is  $29.211^{\circ}\text{C}$ , the minimum temperature  $12.426^{\circ}\text{C}$  is reached in part of the floor as Fig.5.14 (a)-b shows and the average air temperature in the zone is  $22.17^{\circ}\text{C}$ . It shows that the design is suitable for cooling in the hot and humid Korean summer. For cross-ventilation performance, Fig.5.14 (b) compares the difference of wind pressure distribution between building over pilotis and low-set building with varying degrees of porosities. At higher porosities, the flow through the building modifies the external pressures and airflow rates obtained from the pressure coefficients. A building on pilotis has a larger pressure coefficients and results in a better microclimate cooling effect since higher porosities are desirable for ventilation purposes in a warm and humid climate.

One of the most important issues for passive architectural design is the internal environmental comfort and a target for the room temperature of the building is to range between  $20^{\circ}\text{C}$  and  $23^{\circ}\text{C}$  in summer. To adopt a design for comfort would be difficult since excessive mechanical ventilation should be avoided or at least minimized in the design. Designs considering natural ventilation performance have generally been employed without airflow simulation or microclimate consideration. Wrong design achieves only small effects since the natural ventilation problem is strongly related to the microclimate pressure as Chapter 3.4.1 and 3.4.2 introduced. If the pressure difference between outdoor and indoor is zero or too small, air movement cannot occur. Hence, a single opening is not efficient for natural ventilation since air pressure differences through the window is very small even when the temperature difference exists. To obtain a better ventilation rate with cross-ventilation, window openings in opposite walls are efficient. However, only few results from researches for cross-ventilation performance of window shape and position exist. Fig.5.15 compares the thermal condition between ventilation using pilotis and cross-ventilation of low-set building. The building with pilotis can easily get a more cooling effect than cross-ventilation. However, the difference in maximum and average temperatures is not so big, i.e.  $1^{\circ}\text{C}$  to  $2^{\circ}\text{C}$ . The building with pilotis is not usual in normal house design on a flat site due to the high cost. The cross ventilation is a cost effective method although it needs more efforts for placing two opposite windows. The building with pilotis can be applied to sloping topography efficiently.

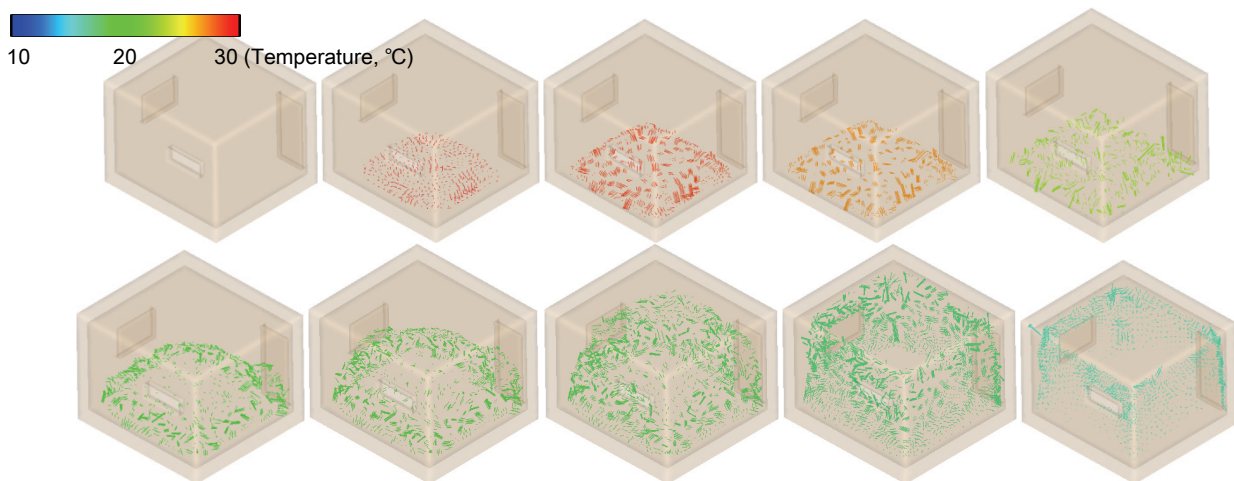


**Figure 5.15.** Comparison of thermal condition with cooling gain between ventilation using pilotis and cross-ventilation of low-set building [author].

### 5.2.6. Microclimate of heat diffusion: Indoor airflow for heat recovery

Heat diffusion is one of the microclimate effects to balance the thermal condition. If part of a mass is heated, the heat transfers to another cool part. Diffusion equilibrium is reached when the concentrations of the diffusing substance in the two compartments become equal. Heat recovery is an efficient concept to utilize heating imbalance which often occurs in passive heating and cooling design.

For example, if a room has a window which is getting the sun, the area in the sunshine is heated by solar radiation but the other area is relatively cooler than the heated area. In the afternoon, the region can be overheated. A lot of passive solar design, shading is a very important solution for the case but the heat diffusion from the overheated region which moves a part of the heat to the cold region can be a better solution.

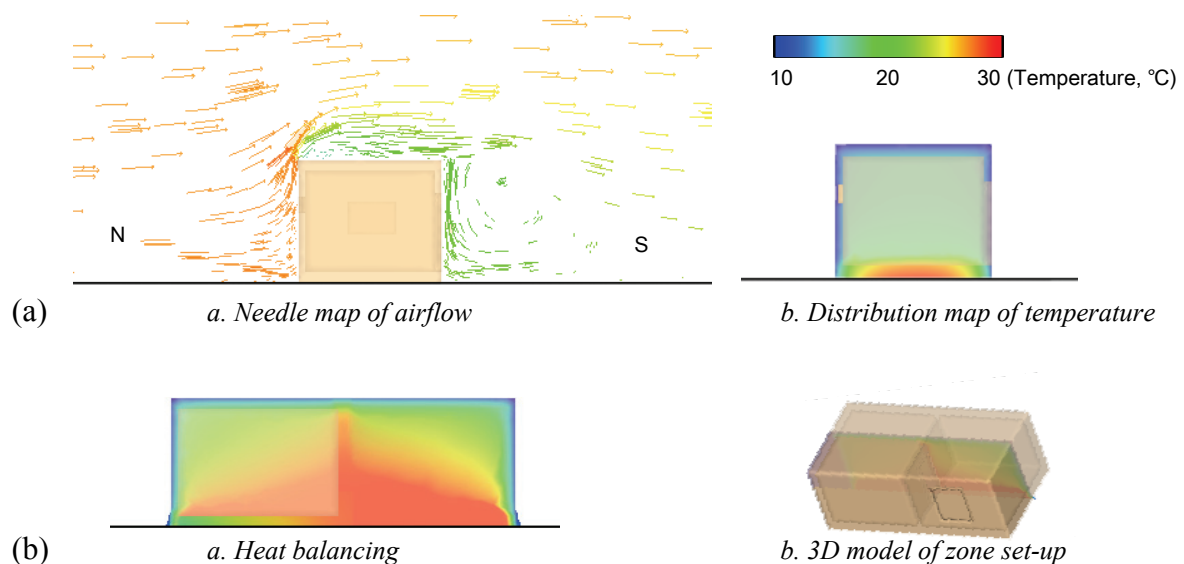


**Figure 5.16.** Thermodynamic heat diffusion process using isothermal particle tracking [author].

The heat recovery method is a process to transfer the heat energy in the air of an overheated zone to the supply air for the other zone. A combination of indoor ventilation designs can be applied to transfer heat. However, the natural ventilation concept is more complex to approximate the thermal condition of the zones. Microclimate simulations like the EP-CFD method enable the design of heat balance between the zones. Fig.5.16 shows a tracking of air particles of isothermal condition which diffuse from the air of heated source to the air of non-heated space. There are some problems in visualizing the simulation result. The thermodynamic flow in the zone cannot visualize the aerodynamic simultaneously since the magnitude of the thermodynamic is much smaller than the outdoor aerodynamic airflow. Fig.5.17 (a)-a shows the situation. Large needle flows are shown outside of the zone and no needle flows in the zone. In this case, the distribution of the temperature shown in Fig.5.17 (a)-b can be utilized in visualizing the thermodynamic.

A good application is attached to sun-space design where the outdoor air is preheated and overheated in the space and the warmer air enters into the occupied zones in a building. Another application is the aniso-thermal condition of the zones. Neighboring two zones shown in Fig.5.17 (b)-a have different passive heating zones. The left zone does not have a window and cannot directly heat, and the right zone is getting large radiative heats by a large window. Fig.5.17 (b)-b shows the 3D model of the zone set-up. To observe the thermodynamic microclimate effect, the environmental condition should not derive aerodynamic flows. By setting of no airflow, and the zones should be fully insulated by the material. The simulation result shows the heat transfer from the overheated right zone to the non-heated left zone. Although the direct heating gain of the left zone is zero, the thermodynamic heat gain can sufficiently recover the indoor temperature over 25°C.

This feature can be utilized for heat recovery. If one zone cannot have any passive heating design, the consideration of microclimate air circulation, i.e. note that similar to zone-to-zone ventilation, is useful

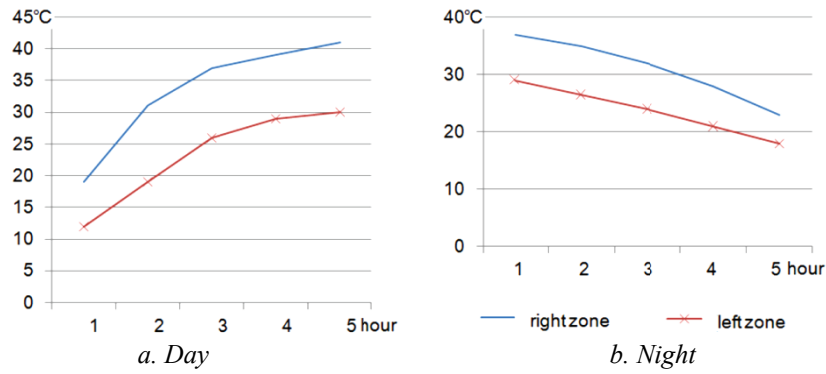


**Figure 5.17.** Difficulty in visualizing thermo- and aerodynamic simultaneously, (a) simple zone, (b) two different heating zones [author].

for passive heating design. During a cold winter night, when the temperature of the zone decreases, the circulation of the air enables the maintenance of the thermal condition by transferring heat from the neighboring zone.

Therefore, it shows that adequate indoor e.g. zone-to-zone natural ventilation designs can supply and maintain thermal comfort. Fig.5.18 represents the temperature with 5 hours passive heating by day and heat distribution by night. The temperature of the right zone quickly rises from the initial temperature 10°C to 40°C. The left zone similarly obtains the heat from the right zone and the temperature rises to 30°C. By night, the right zone loses heat by the heat balancing to the left zone. The left zone can





**Figure 5.18.** Temperature of the zone-to-zone natural ventilation [author].

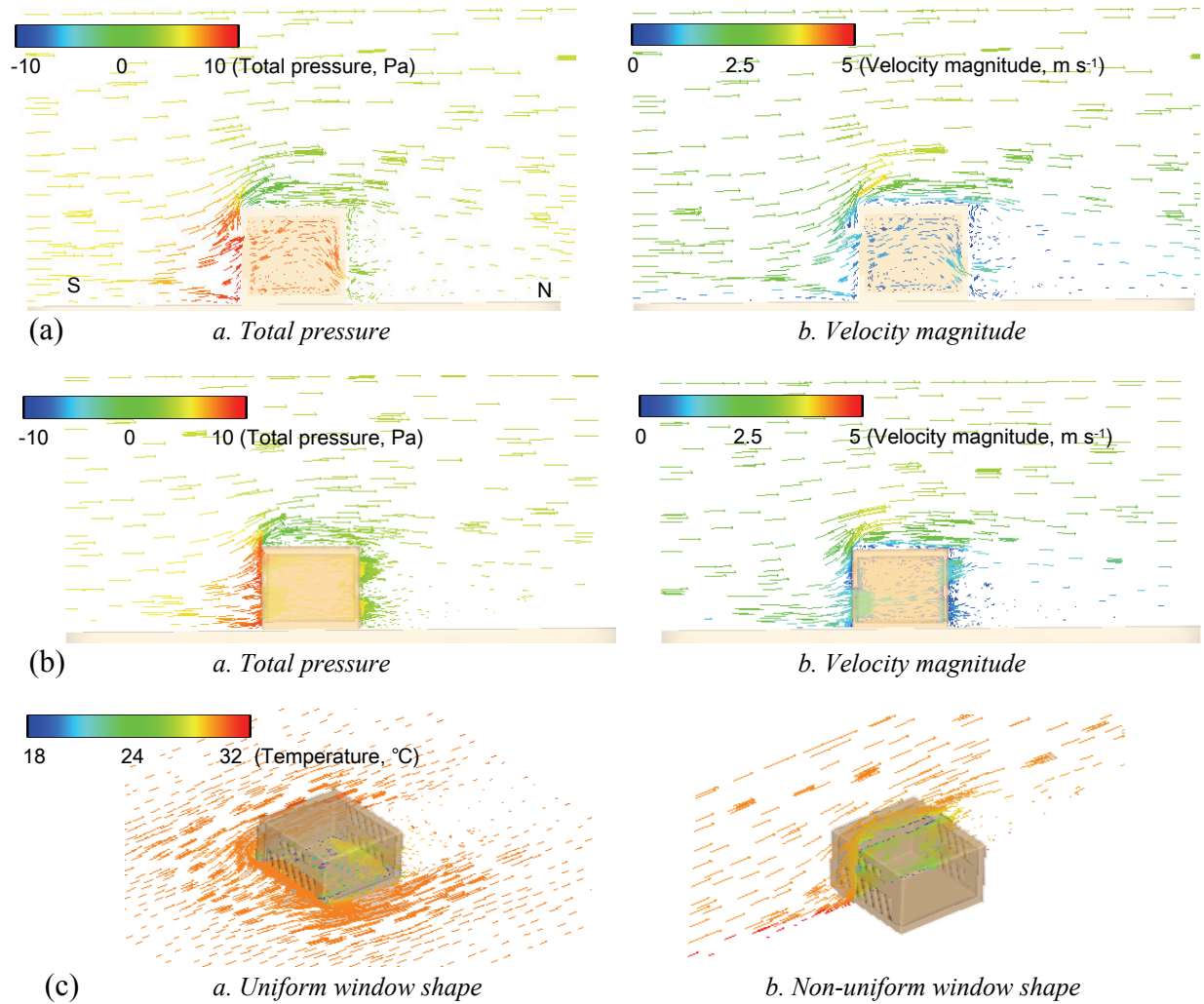
maintain the thermal comfort during the 5 hours since the heat can be recovered from the right zone when the heat of the zone losses. The design uses a door opening between left and right zones.

### 5.3. Façade elements

#### 5.3.1. Microclimate of window shape: Fast and well-distributed cross-ventilation

The uniform and non-uniform window shape is compared in this chapter. Fig.5.19 represents that the aerodynamic pressure is the driving force of the natural ventilation. Only horizontal airflows are shown since there is no difference in vertical pressure gradients. In this case uniform window shape as in Fig.5.19 (a) results in a higher indoor pressure but small flow lines near inlet and outlet. The mean input air velocity is  $1.73 \text{ m s}^{-1}$ , the indoor air velocity is  $0.04 \text{ m s}^{-1}$  to  $1.61 \text{ m s}^{-1}$  and the mean of output air velocity is  $1.37 \text{ m s}^{-1}$ . It demonstrates that aerodynamic microclimate is more important than thermodynamic microclimate for cross-ventilation. If the wind input from the inlet is not discharged through an outlet, the indoor pressure is higher but indoor air is dense and warmer. The pressure distribution is unstable as Fig.5.19 (a)-a shows and the variation of the total pressure indoors covers a wide range of 4.82 Pa to 11.26 Pa. As a result, the indoor air velocity in the zone is unstable and changes widely from  $0.04 \text{ m s}^{-1}$  to  $1.61 \text{ m s}^{-1}$ . The warmer indoor air causes the microclimate thermal pressure between indoor and outdoor and the pressure will have a rising trend. The efficiency of cross-ventilation by aerodynamic is deteriorated. Stagnant humidity in the dense air may cause a discomfort condition.

Fig.5.19 (b) shows that examples of non-uniform shapes and distributions have more aerodynamic microclimate effects in cross-ventilation. The total pressure plot has more streamlines near the inlet and outlet than the uniform window case. Although the non-uniform inlets using two large window sizes



**Figure 5.19.** Airflow pattern in cross-ventilation, (a) uniform window shape, (b) non-uniform window shape, (c) 3D streamline plot of airflow [author].

induce the large amount of wind with large pressure, indoor air has regularly distributed pressure and the magnitude is smaller than the uniform window case because the outlet quickly emits the indoor air.

Near the window, very fast airflow occurs but the density of the indoor air is low since the density of the air is proportional to the ventilation rate. The comparison of pressure and velocity between uniform window and non-uniform window is represented in Fig.5.20 (a).

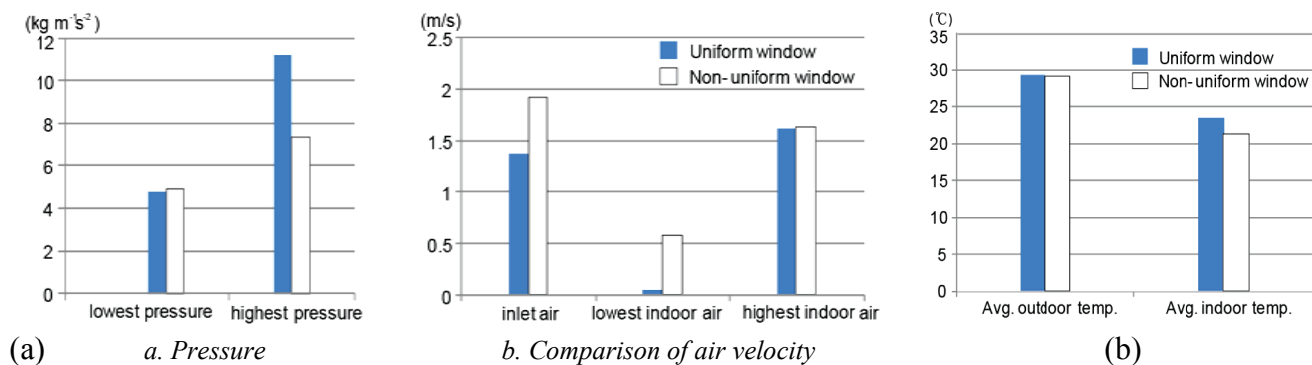
Two window openings at different heights using different window sizes form the vertical difference of pressure and the pressure difference result in indoor airflow distributed evenly. Air density is larger by inward flow through the larger window at the low level, rising air occurs. Hence, the streamline of cross-ventilation is low at the inlet and high at the outlet as Fig.5.19 (b)-b shows. The advantage is that the path of the streamlines is shorter than one for Fig.5.19 (a)-b and the indoor air can be exchanged quicker by the cross-ventilation with non-uniform window shape. As chapter 3.4.2 described, when the rooms with a wind shadow with vortex after inflow, the part of inflow is worse on distribution of air



speed or air direction than that near outlet. Another advantage of the non-uniform shape is to result in a natural path with air temperature since the hot air tends to rise up. The cool air from the inlet located in the lower side drives out the warmer air away from the outlet located in the upper side as Fig.5.19 (b)-b represents.

The larger outlet window in comparison to the inlet window produces greater airflow rates but air speed is distributed around the whole space and this situation is achieved by smaller outlets than inlets, since a partial kinetic energy is changed to static pressure around the leeward opening. However, the uniform window with inlet and outlet of the same size depends on the porosity of the zone irrespective of the angle of incidence of the wind. This design with non-uniform window can obtain the cooling gain when it is utilized to a house design of hot and humid climate to get the better ventilation performance. Fig.5.19 (c) represents the airflow patterns with temperature distribution of non-uniform window cross-ventilation.

When the average outdoor temperature is  $29.437^{\circ}\text{C}$  for the uniform window and non-uniform window shapes, the indoor temperature of uniform window shape and non-uniform window shape is respectively  $23.524$  and  $21.284^{\circ}\text{C}$ . The cross-ventilation with non-uniform window shape can obtain  $4.24^{\circ}\text{C}$  cooler than the cross-ventilation with uniform window. The comparison of average outdoor and indoor temperatures between uniform window and non-uniform window is given in Fig.5.20 (b).



**Figure 5.20.** Comparison between uniform window and non-uniform window, (a) pressure and air velocity, (b) average outdoor and indoor temperatures [author].

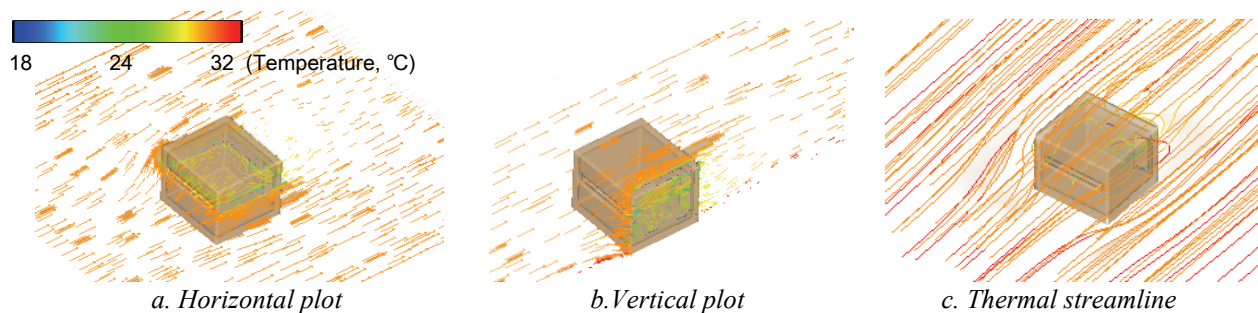
### 5.3.2. Microclimate of window shape: optimal inlet design for ventilation and passive solar design

Another important factor of natural ventilation is the pattern of indoor airflow. It is related not only to the size but also configuration of inlet window e.g. shape and position of inlet. Windows let in light and solar heat and lose heat to the outside. The larger the window, the more daylight and solar gain can enter

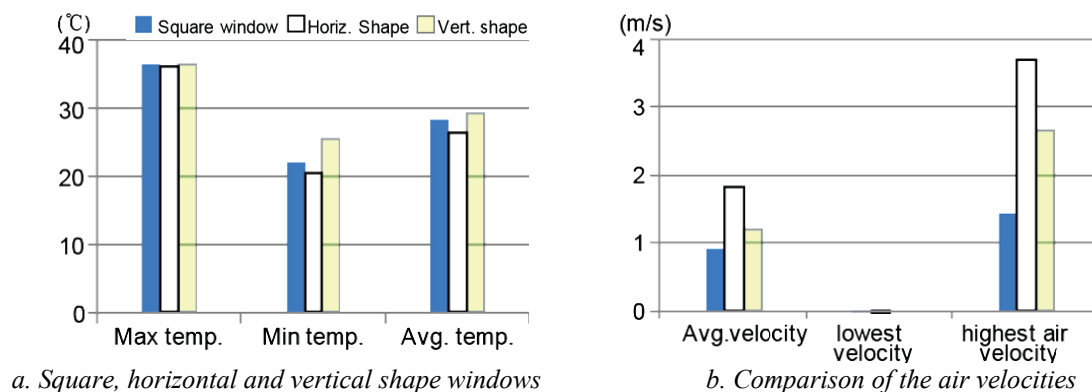
but the larger the losses are. Thus, larger windows can give better indoor ventilation in summer, however, is worse in winter due to the heat loss through the window. On the contrary, the smaller window can avoid the heat loss in winter however, the ventilation in summer or solar radiation performance in winter will be worse. Hence, this chapter investigates a good window shape to allow high efficiency of solar radiation for winter and ventilation for summer.

The aerodynamic pressure often causes horizontal ventilation and the thermodynamic pressure causes vertical upward airflows. However, hot and humid condition in Korean summer is difficult to have a difference air temperature between indoor and outdoor so the thermodynamic pressure is often very small, corresponding to only 1% to 2% of the aerodynamic pressure. Hence, the window opening should be adjusted to the aerodynamic microclimate.

The greater height of a window results in quicker air movement however, the streamline of the air is concentrated above the upper half of the room height. Window height which is larger than the room height is not efficient since air velocity decreases in the lower half and it cannot be easily blocked in winter. The optimum window shape can provide a balance between these summer and winter factors. The large width of a window is efficient to obtain solar radiation and good ventilation performance. Hence, a window opening with a medium height and a large width covering almost the width of the room has the best efficiency of natural ventilation and easiest to shield it at the same time.



**Figure 5.21.** Airflow plots of horizontal inlet with temperature [author].



**Figure 5.22.** Cooling performance for window shape and air velocities [author].

Fig.5.21 represents the wind stream of the window opening with a medium height and large width. The aerodynamic in vertical plot shown in Fig.5.21-*a* exemplifies the smaller effect than the aerodynamic in horizontal plot. The horizontal plot shows the increased air velocity but a narrowed air-streamline since the air pressure is bigger when the height of the window is smaller. The amount of air density is sufficient to obtain the indoor ventilation effect. The configuration of the window opening modifies the internal airflow speeds since the horizontally and vertically shaped inlet openings yield different shapes of air motions. Horizontally shaped inlets provide much higher internal air speeds than square or vertical inlets as Fig.5.22-*b* shows. By comparing the average air velocities, the horizontal shape has 70% to 130% larger velocity than the squared and vertical shapes and the highest air velocities are similar in the percentage gain of velocity for the horizontal shape.

The cooling gain of horizontal shape is about -3 and -1.85 °C more than the vertical and squared shapes respectively. For the indoor condition with a horizontally shape window, the maximum temperature 36.172 °C is formed in the wall near inlet due to the radiative gain and the minimum and the average indoor temperature are 20.3281 and 26.4127 °C. Fig.5.22 respectively shows the comparison of temperatures and pressures between square, horizontal and vertical shaped windows. Fig.5.21-*c* represents the thermal streamline of a horizontal shape window that exemplifies that the horizontal shape front window and door at the back can be efficiently utilized for a cross-ventilation. The optimal glazing ratio of a horizontal shape window which is the same as the width of the wall is about 35% and the window has the best cooling gain in summer and passive heating gain in winter.

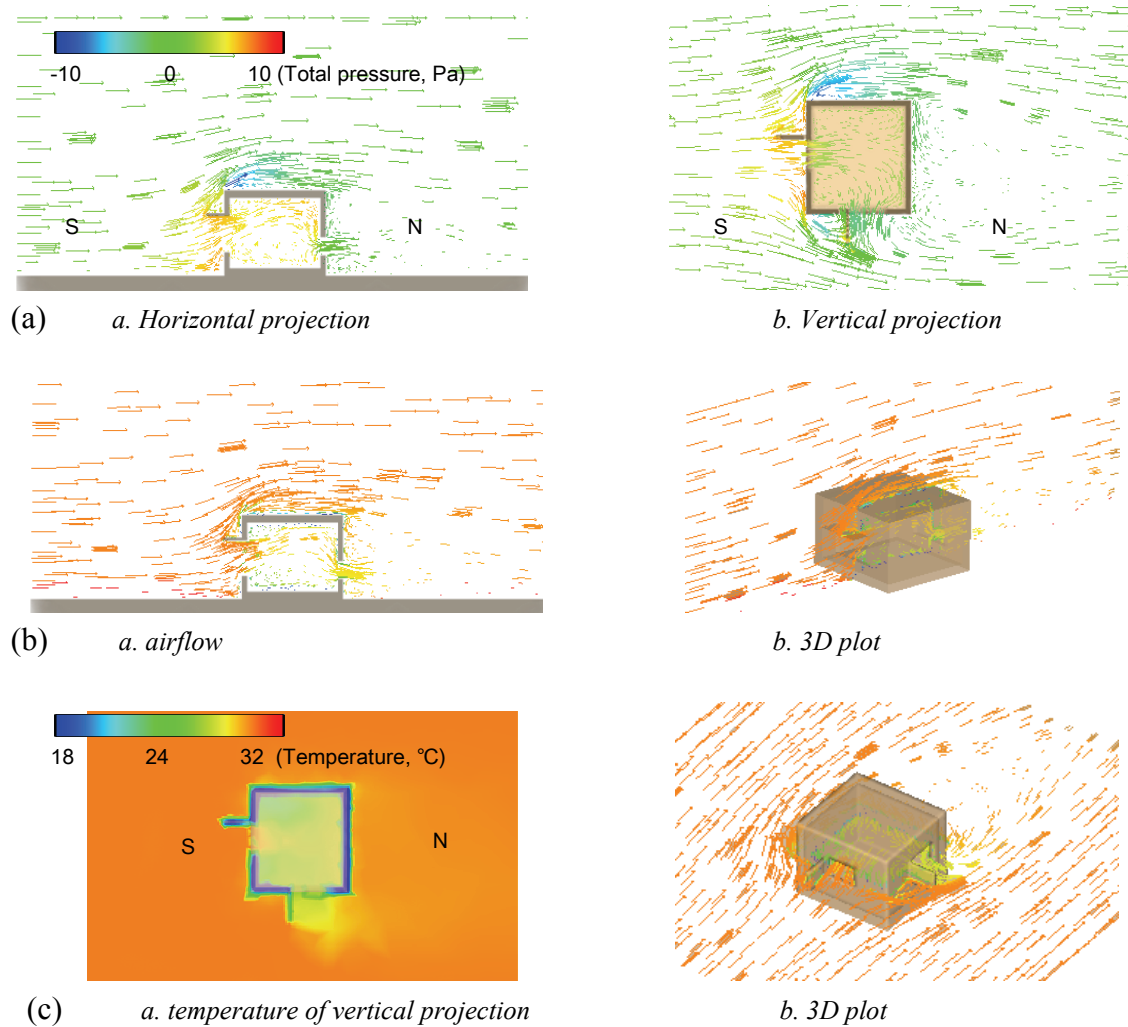
### **5.3.3. Microclimate of building projection: enhancing microclimate pressure and protecting direct solar gain**

In the previous chapter, for a building without projection, opening sizes and the shapes were important factors that determine the airflow. However, the opening design is often dependent upon the wind and solar direction and the microclimate effect is largely related to them. Hence, air density control to get more pressure difference is needed. Air pressure is produced when the difference of local density is distributed due to the amount of air input to the space. Hence, the horizontal and vertical projections e.g. external wing-walls, partitions and fins etc. affect the amount of air pressure and internal airflow rates by prevailing wind. Fig.5.23 (a) represents that external projections act as a wind-catcher which raises the internal ventilation rate for skewed and perpendicular winds due to the pressure difference near the projection.

The airflow through the window raises the velocity of indoor flow since the projection increases the amount of the wind streams entering the inside. Another advantage of the horizontal projection is efficiency to protect from direct solar radiation and hot wind from the room. The shade of inlet opening

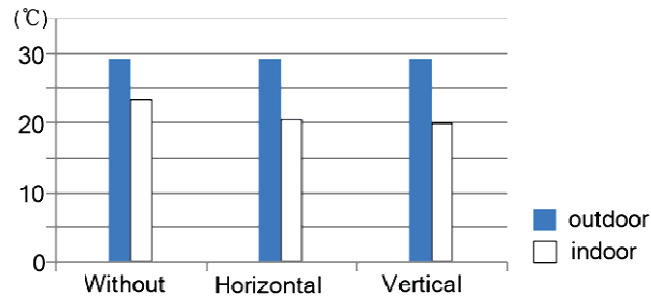
generates a cooler surface than the surface of the roof. The projection eliminates the downward hot flow at the inlet and pushes the cool air towards the ceiling. The thermal condition is represented in Fig.5.23.

Otherwise, the vertical projections shown in Fig.5.23 (a)-b are efficient to modify the pressure pattern and in result, the flow direction. When the wind is blocked by the fin of a projection, the pressure increases on the surface but a lot decreases at the back of the surface. Hence, the inlet flow is raised and significantly enhanced ventilation performance. Fig.5.23 (c)-a respectively shows the high cooling gain of the vertical projection and the airflow shape.



**Figure 5.23.** Microclimate of building projection, (a) pressure difference between of horizontal and vertical projection, (b) horizontal projection, (c) vertical projection [author].

The comparison of the thermal condition of a zone with cross-ventilation between horizontal and vertical projections and without projection is shown in Fig.5.24. If the outdoor temperature is about  $29.45^{\circ}\text{C}$  and the indoor temperatures are  $20.428^{\circ}\text{C}$  and  $19.882^{\circ}\text{C}$  by the cross-ventilation with horizontal and vertical projections and  $23.524^{\circ}\text{C}$  by the cross-ventilation without projection,



**Figure 5.24.** Comparison of thermal condition of cross-ventilation with horizontal and vertical projections and without projection [author].

respectively. The cooling gain of horizontal projection is jointly obtained by efficient shading, wind catching performances. Although the gain of vertical projection is smaller than the horizontal projection, the wind catching is still effective in the vertical projection. The result exemplifies that the ventilation performance is more important than gain of shading for the indoor temperature. Although the vertical projection sometimes cannot block the direct sun, the high ventilation performance seems to remove the indoor overheating.

# 6. Application of microclimate simulation to a real-house design

## 6.1. A real-house in a suburb of Seoul, S. Korea

Although a lot of studies for energy simulation have been done by researchers of physics, climatology and architecture, they did not try to apply their method to a real house design. Single EP simulation cannot obtain the detail of energy flow in the design and single CFD simulation is too complex to make the problem to converge into the real solution in the whole house design. In this study, the problem can be overcome by the EP-CFD method and the microclimate analysis drew several efficient design factors for energy-saving in chapter 5. The factors are applied to estimate energy gain in real designs. The application of these factors in real house models is important to prove energy performance in real house design. Note that the purpose of this chapter is not to analyze house designs, but to test the energy efficiency of the microclimate factors in these designs.

Pine Tree House which is the 6<sup>th</sup> design of *Min-Maru* series<sup>127</sup> by GAWA Design Group<sup>128</sup> is located in the highest area in the *Min-Maru* house complex. The main feature of the house is two masses with different kinds of space and the topography preservation by pilotis. Pile foundations with treated timbers are used to float the living room and the kitchen on the slope of the mountain and the room space forms a skip floor over the topography. The skip-up-floors form separated spaces for different uses as guest room, living room and bedroom by the building levels. The house has the size of 12600×14700×7600 and two stories. Fig.6.1 shows the layouts and pictures of the house.

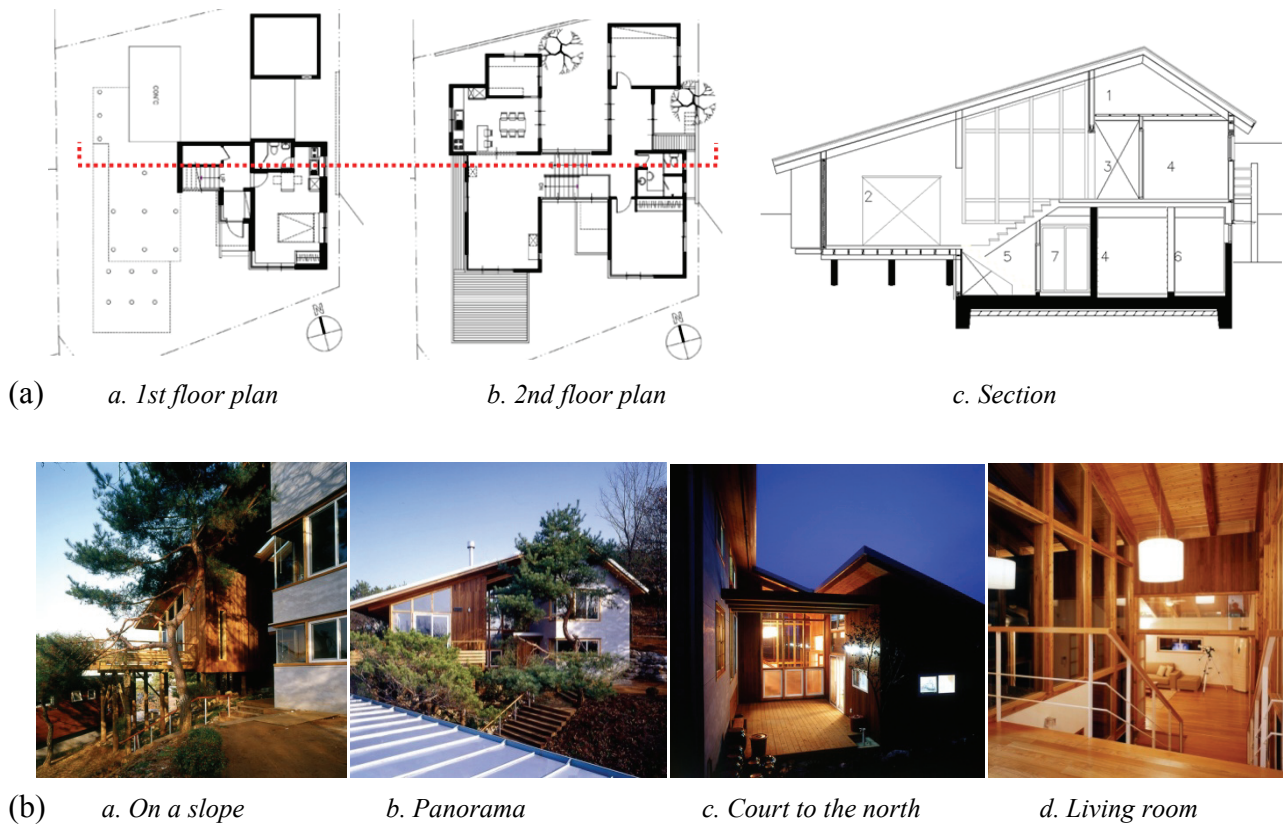
The motive of the choice of Pine Tree House is

- This house has several topographical features to be able to observe microclimate effects.
- This house has high capacity to control several microclimate effects.
- This house employs several Korean traditional designs e.g. *Maru* (Korean wooden floor), *Jungja* (Korean pavilion) and *Ondol* (a Korean floor heater) etc. which is attractive to the Korean people.

---

<sup>127</sup> A&C Publishing 2004.

<sup>128</sup> GAWA Design Group, <http://www.kawadesign.co.kr>.



**Figure 6.1.** Pine Tree House by S.Y. Choi, (a) drawings, (b) views [author].

Some limitation of this test in the real house model is that the actual measurement of microclimate was not available and the microclimate factors are estimated by computer simulation based on macro climate and the house design data. Thus, the test result may be not exactly equal to the real energy consumption however it is not exceed the allowable margin of error.

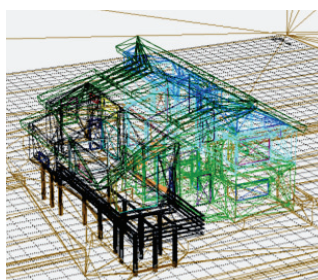
By interview with the architect and residents, this house maintains the temperature of  $18^{\circ}\text{C}$  to  $20^{\circ}\text{C}$ . The main heating of this house is floor heating using boiler and water coil and an assistance of heating of a fireplace is used. The energy consumption including hot water is approximated as a total of 1,000,000 *Won* for oil, and 300,000 *Won* for electric charges including lighting. This house is sufficiently cool in summer due to the careful design and this house does not use electrical air conditioning and cooling. The architects and occupants suppose that employing some traditional house designs in the modern house designs may be helpful to obtain such results.

The main construction using concrete with reinforcing rod and lightweight woods are represented in Table 6.1. The zones in the house are set up with microclimate design elements, geometrical features and materials. Fig.6.2-*a* and *b* represent the CAD model of the zones which are classified with layers and a plane cut of the CAD model. The sun-path diagram shown in Fig.6.2-*c* is used to estimate the solar and shadow range for EP energy simulation. The CAD model is converted to a 3D solid model since the CAD model with 2-D meshes cannot be directly used for CFD simulation. Fig.6.2-*d* shows the

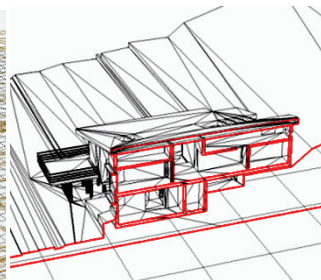


**Table 6.1.** Construction materials and outline of Pine Tree House [author].

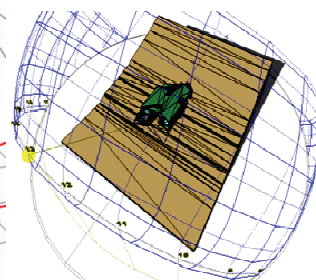
Structures	Materials	Factor	Scale
Main structure	Reinforced concrete	House style	2 stories residence
	Lightweight woods	Area of site	389.00 m <sup>2</sup>
Exterior materials	T.12CFRC boards	Area of building	126.72 m <sup>2</sup>
	T.18 APITONs (pine-tree)	Gross floor area	164.55 m <sup>2</sup>
	T.22 pair glasses	Building-to-land ratio	35.44%
Interior materials	App. wallpaper on T.9.5 plaster board	Floor area ratio	42.30%
	T.16 Pine-tree louver (for open type)	Year of completion	2003
Heating	<i>Ondol Maru</i>	Designer	<i>Gawa company</i>



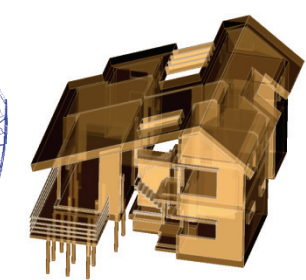
*a. Mesh drawing*



*b. Plane-cut*



*c. Sun-path diagram*



*d. 3D solid rendering*

**Figure 6.2.** CAD model of Pine Tree House [author].

3D solid model that is input model for *Fluent* software.

## 6.2. Converting Model from CAD to IFC

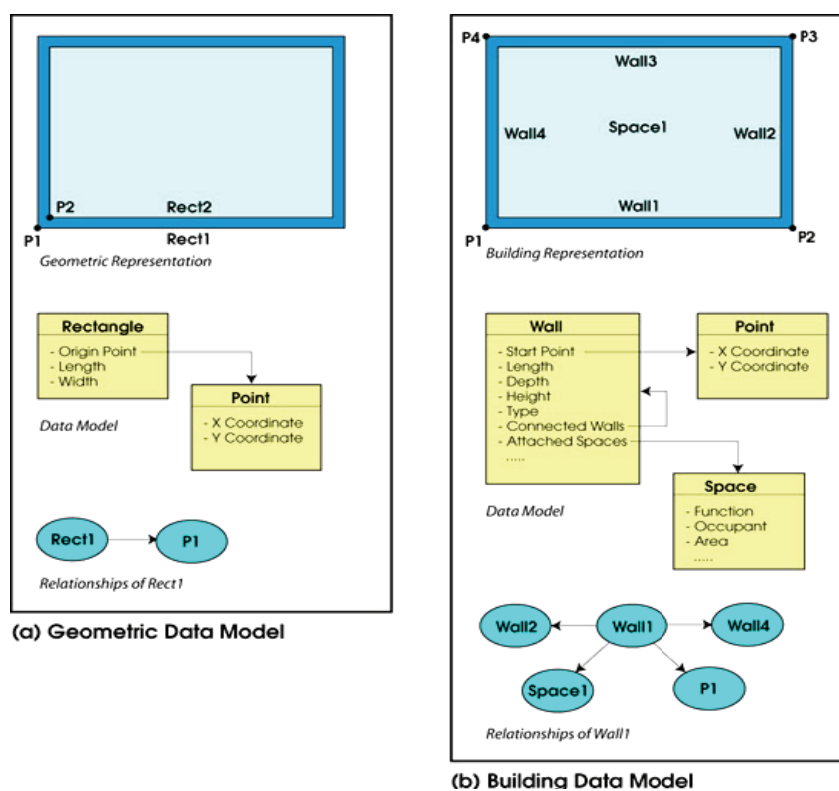
A data model in any given domain describes the attributes of the entities in that domain as well as how these entities are related to each other. Since all computer programs deal with some kinds of data, they must have some kind of underlying data model. Traditional 2D CAD and generic 3D modeling programs internally represent data using geometric entities such as points, lines, rectangles and planes etc. Thus, while these applications can accurately describe geometry in any domain, they cannot capture domain-specific information about entities. In the case of the AEC industry, technological progress has been severely constrained by the limited intelligence of such applications in representing buildings and being able to extract the relevant information from the representation that is needed for design, analysis, construction management, operation, and so on.

To overcome the limitations of general-purpose geometric representations, every design-related industry has been developing and using object-based data models that are specific to their domain. In the case of the building industry, this translates to a data model that is built around building entities and

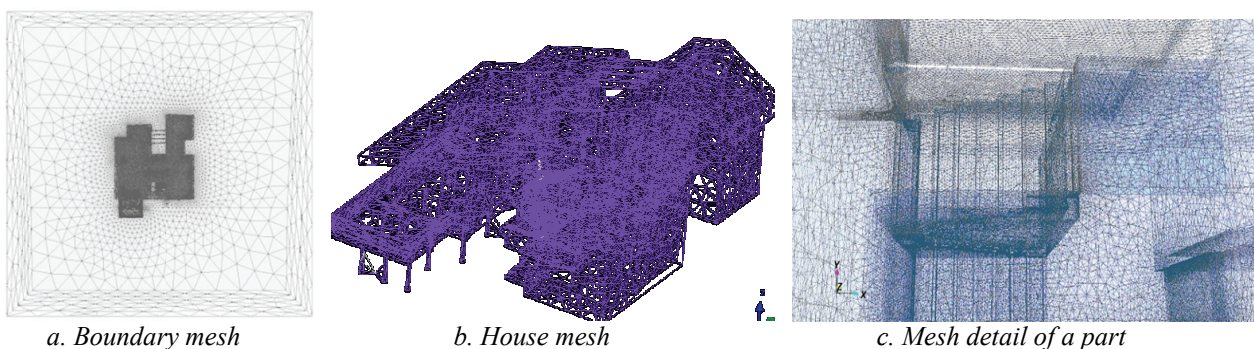


their relationships to one another (see Fig.6.3). Geometry is only one of the properties, among others, of these building entities; thus, its primacy is greatly reduced, even though the interface to creating the model is still mainly graphic. Such a data model is rich in information about the building that can be extracted and used for various purposes, e.g. documentation, visualization, or analysis.

A simple but critical example of the difference between a geometric data model and a building data model is in the representation of a space. Traditional 2D and 3D CAD programs do not represent a space because it does not exist as a distinct physical entity. However, a space entity will be an integral part of a building model, and will include the appropriate relationships to walls; ceilings, floors, and so on (for example, see the simple wall-to-space relationship shown in Fig.6.3. Industry Foundation



**Figure 6.3.** Difference between CAD and IFC [ISO/PRF PAS].



**Figure 6.4.** Adaptable mesh for better analysis resolution near model edges [author].

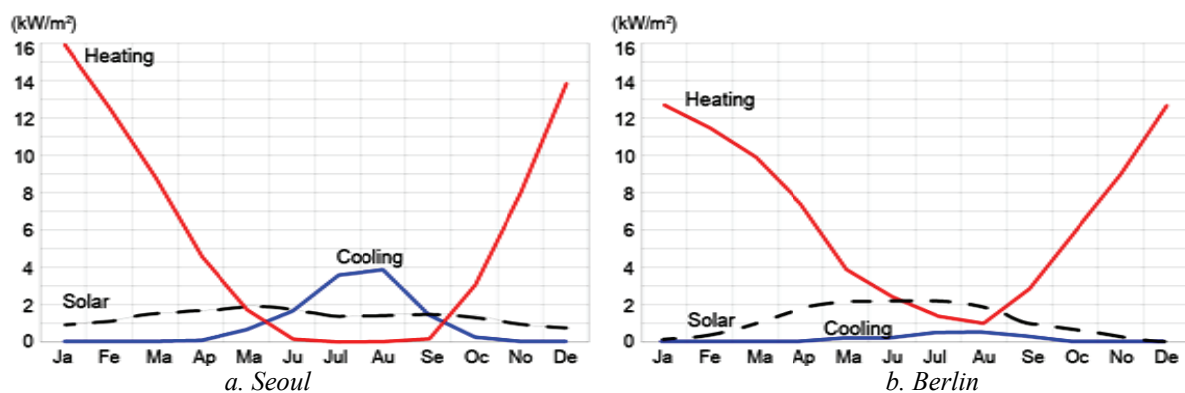
Classes (IFC) is building a data model that is the result of standardization, and it gives architects a data representation standard and file format for defining architectural and constructional CAD graphic data as 3D real-world objects, mainly so that architectural CAD users can transfer design data to and from between rival products with no compromises. Thus, information about spaces can be easily obtained from an application using a building data model, whereas several complex calculations will be required to derive the same information from an application using a geometric data model. The converting is performed by Autodesk Architectural Desktop (ADT) software. When a model finishes converting, the analysis grid can be classified to each zone. Fig.6.4 shows the examples of rough classification mesh in the house.

### 6.3. Climate data and features

For the simulation, macro climate data are prepared to use the climate features for energy simulation and microclimate analysis. The climate features which are related to building energy or microclimate effects are selected in 9 sub-data as Table 6.2 shows.

**Table 6.2.** Construction materials and outline of Pine Tree House [author].

Type of data	Unit
Diffuse solar on the horizontal	$\text{W m}^{-2}$
External dry bulb temperature	$^{\circ}\text{C}$
Direct normal solar intensity	$\text{W m}^{-2}$
Prevailing wind speed	$\text{m s}^{-1}$
Wind direction	Clockwise deg. from North
Relative humidity	0-1
Time of rainfall	0.1h
Sum of rainfall	0.1mm
Cloud covers	8 steps from 0 to 8



**Figure 6.5.** Heating and cooling loads by the difference of solar radiation between Seoul and Berlin [author].

Fig.6.5 shows the difference of heating and cooling loads between Korea and Germany. Although Korea has similar solar radiation gain, cooling load in summer is higher due to the higher air temperature and humidity and heating load in winter is due to the lower air temperature and humidity. This means that a house in Korea needs more cooling and heating energy than one in Germany.

In East Asia, interactions between the rapidly mixing atmosphere and the slowly changing oceans are largely responsible for the monsoon season, particularly as they affect Korea, China and Japan. Geographically, Korea is a transitional zone between the continental landmass of northeast Asia and the island arc rimming the western Pacific Ocean. The western coast, which is open to continental Asia, is vulnerable to the influence of the winter continental climate. The eastern coast, on the other hand, is sheltered from the winter monsoon by the *Taebaek*-range, the backbone mountain of the eastern Korean Peninsula. Although Korea has the general characteristics of a temperate monsoon climate, there is geographic diversity, particularly during the cold winter season.

The climate of Korea is characterized by four distinct seasons i.e. spring, summer, autumn and winter. The contrast between winter and summer is striking. Winter is bitterly cold and influenced primarily by the Siberian air mass while summer is hot and humid due to the maritime pacific high. The transitional seasons of spring and autumn are sunny and generally dry.

Spring begins during the middle of April in the central part of the country, and toward the end of April in the northern region. As the Siberian high pressure weakens, the temperature rises gradually. Yellow sand dust which originates in the Mongolian desert occasionally invades Korea during early spring. The sandy dust phenomena often causes low visibility and eye irritation.

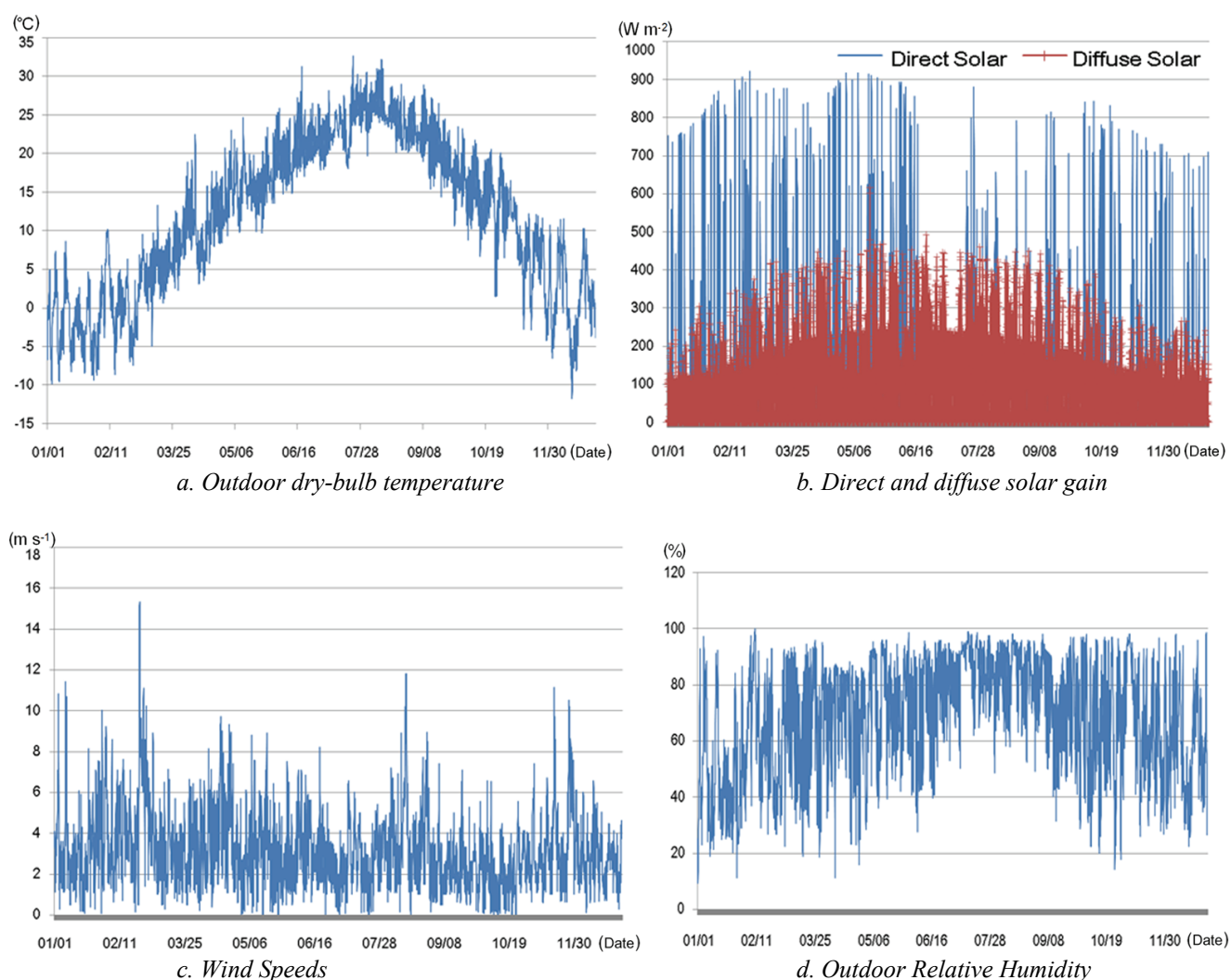
The summer can be divided into two periods; a rainy period which occurs during the early summer months, a hot and humid period which occurs during late summer. The weather during the rainy period is characterized by a marked concentration of rainfalls. More than 60% of the annual precipitation is concentrated between June and July. In particular, July sees many rainy days which are followed by short dry spells and clear skies. Much of the rainfall is due to summer monsoons which originate in the Pacific Ocean. Rainfall during the summer time is characterized by heavy showers. Daily precipitation often exceeds 200mm, with extremes topping 300mm. Occasional torrential storms caused by typhoons that pass through the peninsula from China may sometimes cause a great deal of damage, although the loss of life is rare in these instances. Annually, about 28 typhoons occur in the western Pacific. Regional temperature contrasts are not striking during the summer season although the northern interior and the littoral are cooler than temperature in the south. In August, the temperature rises abruptly as the rainy season. During this period, the weather is extremely hot and humid, particularly in the western plains and the southern basin area. The daily high temperature often rises to over 38 °C. Nights are also hot and humid.

Autumn is the season with crisp weather, much sunlight and changing autumn leaves. This is the transitional season between the hot and humid summer and the cold and dry winter months. Beginning in October, the continental air mass brings dry, clear weather. Traditionally, Koreans enjoy the season of harvest, which is one of the most important national holidays in Korea. It is celebrated as a harvest festival, and occasionally referred to as the Korean version of the American Thanksgiving. Autumn weather is nicely expressed in the simple words of the old Korean saying “The sky is high and the horses get fat”.

In winter, the monsoonal arctic air from the interior of the Asian continent brings bitter cold and dry weather and occasionally snowfall, adding warmth to the cold and dry winter weather periodically. Significant regional climate variations are caused by differences in elevation and proximity to the seas as well as by differences in latitudinal location. Regional difference in the monthly mean temperature during the month of January between the northern and the southern peninsula is about 26°C. Snow remains longer on the ground in the north. The frost-free period varies from about 130 days in the northern interior to about 180 days in the central region. In the southern coast, the frost-free period is roughly 225 days of the year.

Temperatures in Seoul are similar to those in New York City which is located 500km farther north than the latitude of Seoul. Fig.6.6-*a* shows the outdoor dry-bulb temperature over 1 year of S. Korea. The variation of annual mean temperature ranges 10°C to 16°C except for the mountainous areas. August is the hottest month with the mean temperature ranging 23°C to 33°C. January is the coldest month with the mean temperature ranging -5°C to 5°C. Annual precipitation is about 1,500mm in the central region. More than a half of the total rainfall amount is concentrated in summer, while precipitation of winter is less than 10% of the total precipitation. The prevailing winds are southeasterly in summer, and northwesterly in winter. The winds are stronger in winter, from December to February, than those of any other season as the wind speeds graph in Fig.6.6-*c* shows. The land-sea breeze becomes dominant with weakened monsoon wind in the transitional months of September and October.

The relative humidity shown in Fig.6.6-*d* is highest in July at 80% to 90% nationwide, and is lowest in January and April at 30% to 50%. It has a moderate value of about 70% in September and October. The monsoon front approaches the Korean Peninsula from the south in late June, migrating gradually to the north. Significant rainfall occurs when a stationary front lies over the Korean Peninsula. The rainy season over Korea continues for a month from late June until late July. A short period of rainfall comes in early September when the monsoon front retreats back from the north. This rain occurs over a period of 30 days to 40 days in June through July at all points of S. Korea, with only some lag in time at different stations, and accounts for more than 50% of the annual precipitation at most stations. The rainy season can be estimated by the direct and diffusion solar gain over 1 year shown in Fig.6.6-*b*. The southern coastal and its adjacent mountain regions have the largest amount of annual precipitation



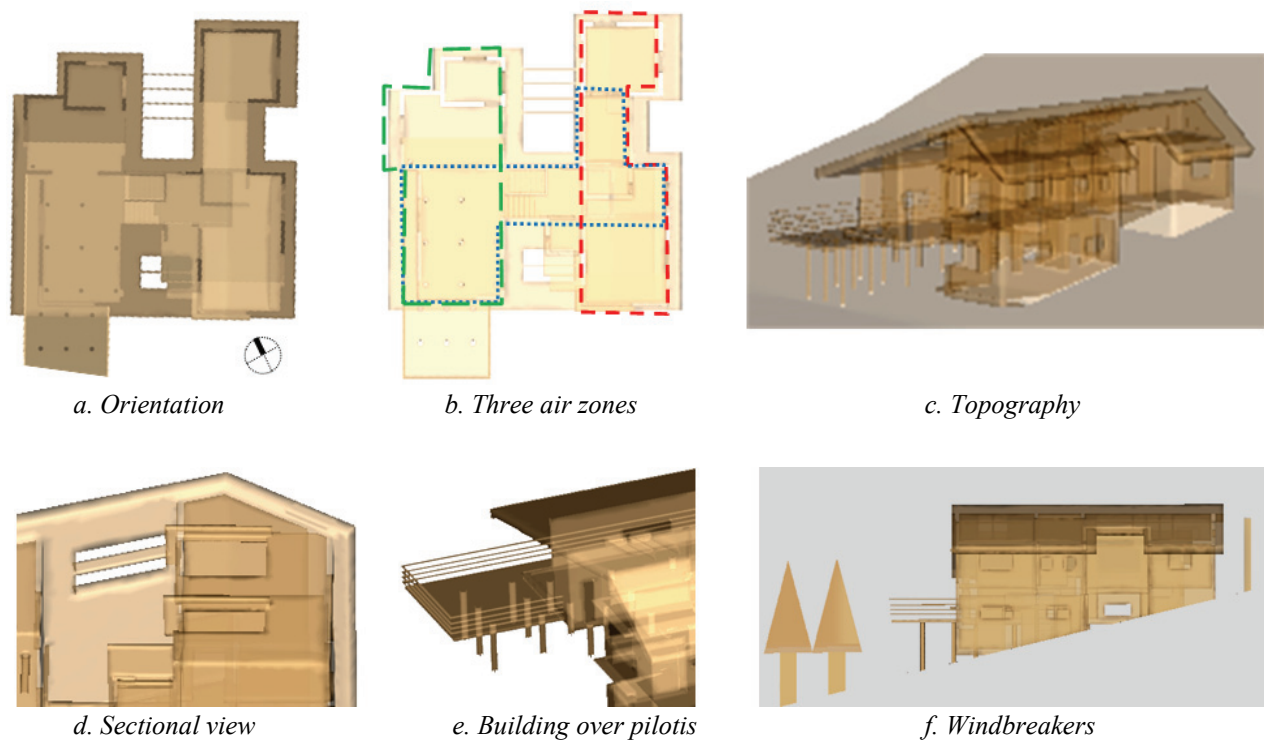
**Figure 6.6.** Korean climate analysis using EP over 1 year [author].

which is over 1,500mm. Since most of the precipitation is concentrated in the crop growing areas in the south, the water supply for agriculture is normally well met. Even though the annual mean precipitation is more than 1,200mm, however, Korea often experiences drought due to the large fluctuation and variation of precipitation, making the management of water resources difficult.

## 6.4. Microclimate design elements

Korean traditional design elements in Pine Tree House<sup>129</sup> are employed to modify microclimate effects. However, there were no scientific evidences for the designs since few studies of them have been done. Chapter 5 investigated several microclimate design elements and analyzed the efficiency of the elements using EP-CFD simulation. These studies will be applied here to the real-house design

<sup>129</sup> See Chapter 6.1.



**Figure 6.7.** Microclimate design elements of Pine Tree House [author].

elements of Pine Tree House.

First, the building orientation of Pine Tree House has a small shift to southwest as Fig.6.7-*a* shows. However, a modification is used for the simulation since most Korean traditional architecture designs prefer to choose the south or southeast direction. Although the south direction is adequate to passive solar design, the main direction of summer winds in S. Korea is southeast direction. For the best microclimate effect, the simulation model uses the modification of southeast direction for passive cooling performance with strong aerodynamic to discharge the overheated air.

The most progress of microclimate design in Pine Tree House is the usage of openings, possibly opened or closed by seasonal features. The door of the space can be opened widely to diffuse air and heat in summer. This prevents some zones with solar radiation from overheating. If a zone is overheated, indoor ventilation with openings can spread the heat to the neighboring cool zone. For the local heating, the door should be closed as well. Thus, the zones are separated into isolated zones and the geometric relationships between the zones are defined as Fig.6.7-*b* shows.

Pine Tree House is located on a low hill using architectural methods on topography. As the description in chapter 5.1.2, the topography plays roles to get strong microclimate effects with anabatic airflow. Some window designs enable large openings for the wind and partial building utilizes pilotis to avoid

heated ground and to obtain passive cooling effects. Fig.6.7-c represents the set-up of a building on the topography.

Pine Tree House uses some non-uniform window shapes to raise a ventilation performance of vertical direction of the room since two window openings at different heights using different windows sizes form the vertical difference of pressure. Fig.6.7-d shows a non-uniform window of Pine Tree House. This design generates very effective cooling gain of ventilation in summer. Some windows, especially located in the front side, use small horizontal projections shown in Fig.6.7-d which play a role as a wind-catcher that raises the internal ventilation rate. The size of the projection is not sufficiently big to protect from solar radiation however, the large gable roof sufficiently shades a direct solar penetration. The projection modifies the pressure pattern near the window and thereby derives different microclimate effects. The house does not use many vertical projections since the “H” form, i.e. perimeter rectangular court, of the house is enough to perform vertical wind-catchers since two encircled courtyards draw a high density of wind.

Instead of a roof overhang, a large gable roof is designed to block the direct solar radiation and performs a wind-catcher. A gable roof is efficient to derive a stack effect that the wind from outdoors is heated and naturally moved into the roof outlets. Some holes shown in Fig.6.7-e are accompanied with the slopes of large roof. The large roof edges act as horizontal wind-catchers like external projections that raise the internal ventilation rates or the sunshade.



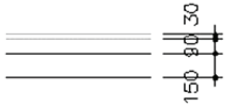

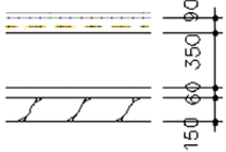



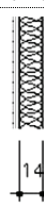

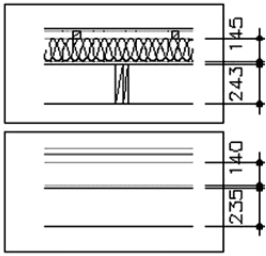

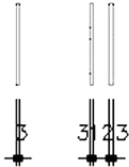

Living space in summer is very important since the hot days are much longer than cold days in Korea. Especially, the high humidity in summer is the biggest problem to design human comfort space using passive architecture designs. In traditional Korean architecture concepts, *Maru* (i.e. floor) using pilotis or pavilion using pilotis is very famous and favorite of people due to the effective cooling without artificial air conditioning. A floating architectural design using pilotis is used for a part of the living space as Fig.6.7-e shows.

The real site condition of Pine Tree House does not use the wall since the house is connected to the neighboring house. The walls of the neighboring house act as windbreaks. The geometrical influences of the neighboring house are not considered due to the complexity of simulation. However, the microclimate efficiency of solid walls and windbreaks are driven by a simple set-up shown in Fig.6.7-f. For the backside of the house, an artificial fence as a dense windbreaker is laid to prevent the Siberian cold wind from the North and the trees of medium density block only strong wind. Small wind passed through the natural trees gives a cooling effect to reduce the sensible heat of occupants and visual beauty as well.

Table 6.3 represents pictures of the design elements of Pine Tree House. The left column of the Table



**Table 6.3.** Drawing of details and snapshots for design elements of Pine Tree House [author].

Part	Drawing of detail	Picture	Elements
Partition walls			Parquetry
Intermediate floor			Kitchen court
Ground floor			
Interior wall			Yellow soil flooring
Outer wall			Lattice gate
Roof			as Maru, pavilion
Windows ( $3.72 \text{ W m}^{-2} \text{ K}^{-1}$ )			Ondol (for heating)

shows the partial details of section and the right column represents design concepts of Korean traditional houses. Parquetry is a small size of floor to generate a local cooling area and the kitchen court uses a concept of courtyard to preserve and utilize the cooking heats. The yellow soil is efficient material for floor heating since the soil includes large amount of minerals which radiates longwave ray. The *Maru* and pavilion using pilotis are an efficient structure for summer and *Ondol* is a traditional



Korean under floor heating system for indoor climate control similar in principle to a Roman hypocaust. The main components are a fireplace or stove (also used for cooking) located below floor level in outside (traditionally in separated kitchen), a heated floor underlay by horizontal smoke passages, and a vertical chimney to provide a draft. The heated floor is supported by stone piers, covered by clay and an impervious layer such as oiled paper. The *Ondol* was typically used as a sitting and sleeping area, with warmer spots reserved for honored guests. For these reasons, most modern residences in Korea utilize circulating hot water, or electrical cable.

## 6.5. Energy efficiency

Thermo- and aerodynamic microclimate design method including passive design is quantitatively evaluated by EP-CFD simulation. First, EP simulation results the average values of zones which are estimated from site and zones. The resolution of the values is one node per volume of zone, thus the EP simulation cannot estimate the streamline of real airflow. However, the method is not complex and easy to evaluate the energy performance of building zones with passive and active set-ups.

The calculation of the heating and cooling loads on a building or zone is the most important step in determining the size and type of cooling and heating equipment required to maintain comfortable indoor air conditions. Building heat and moisture transfer mechanisms are complex and as unpredictable as the weather and human behavior, both of which strongly influence load calculation results.

**Table 6.4.** Some of the factors that influence results [author].

The factors	Influenced results
Weather conditions	Temperature, moisture, wind speed, latitude, elevation and solar radiation etc.
Heating effects	Conduction/convection : walls, roofs, floors, doors and windows Radiation: wall and roof surface temperatures
Thermal properties	Insulation, glass transmittance, surface absorption
Thermal mass	The delay of indoor to outdoor temperature change
Construction quality	Air, heat, and moisture leakage
Heat added/lost	Ventilation, distribution systems
Acceptable comfort	Quality levels of occupants

If the factors as shown in Table 6.4 are once used for calculation of a complex equation, the heating and cooling loads can be obtained as the result of the equation. They are always used by active design researchers, developers of building envelop and architects etc., however, they can be useful factors to evaluate the thermal and comfort of the passive designs and the set-ups. Then, a comparison between

the passive design and active method e.g. electronic air conditioning concludes the needs of additional energy consumption of the passive designs, if the passive designs do not have sufficient condition of zero energy. The evaluation of microclimate design methods will perform such a comparison and concludes the needs of the amount of additional energy input. Although zero energy building with passive design methods is the best case, such a zero energy performance using only passive methods is too ideal and difficult to achieve.

In winter, heat loss increases the total heating load. Transmissions through the confining walls, floor, ceiling, glass and other surfaces cause heat loss. If a zone loses the heat below a comfortable temperature, occupants feel discomfort. To recover the comfort condition, energy inputs should compensate the heat loss. The infiltration through trickles and openings causes large amounts of heat loss. The wind speed also has great effect on outside surface resistance in conduction heat transfer and on high infiltration loss. Normally, the heating load is estimated for evaluation of winter design.

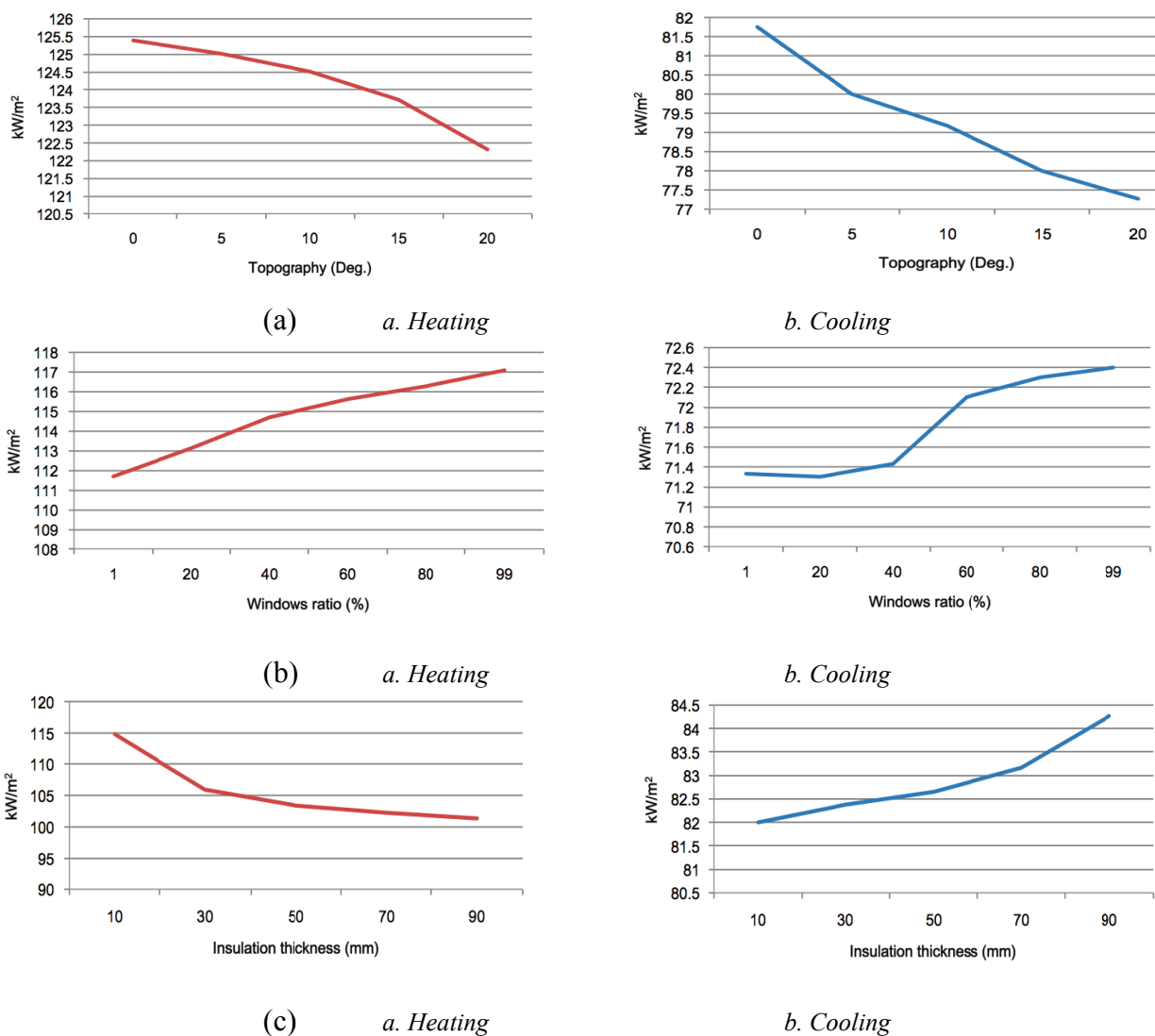
Otherwise, cooling load is related to the heating gain. If the heat is obtained in high temperature, the heat should be removed by a cooling method to make a comfort. Heat gain is the rate at which heat enters a space, or heat generated within a space during a time interval. Hence, cooling load is the rate that heat gains can be compensated to make a comfort air temperature. The difference between the space heat gain and the space cooling load is due to the storage of a portion of radiant heat in the structure. The convective component is converted to space cooling load instantaneously.

By EP simulation, changes of topographic, window ratio and insulation are evaluated. Fig.6.8 represents the heating and cooling loads which occur through the changes of different conditions. EP does not have CFD calculation, the method uses a simple parametric estimation based on analytical data related to the pressure coefficients. The differences of slope angle increases the heating load and decrease the cooling load as Fig.6.8 (a) and (b) show. The additional heating gain is caused by the solar radiation since building can be warmer and drain earlier in hillside. The cooling gain i.e. decrease of cooling load is due to the large amount of microclimate which is produced by the different thermal condition by solar radiation. Heating by day causes anabatic airflows since the heated air moves up and pressure decreases. The large amount of airflows makes a cooling gain of about  $3\text{kW m}^{-2}$  per 10 degree.

The changes of window ratio make smaller heating and cooling loads due to the large effects of the air movements. The average heating and cooling loads are respectively about  $114\text{kW m}^{-2}$  and  $72\text{kW m}^{-2}$  and the values are much smaller than the results of topography. Fig.6.8 (b) represents the graphs heating and cooling loads. EP simulation shows that the larger window is not helpful for cooling since the increase of radiation through the window causes overheating and the cooling load is increased in summer. Although the windows are a cause of the heat loss in winter, the increase of heating gain through the window increases the heating gain.

The modification of insulation thickness in Fig.6.8 (c) yields very interesting results. The insulation is a very important method for passive solar, ventilation and cooling methods. For the passive solar, the increase of insulation thickness results in the heating gain, since the radiation heat can be preserved. However, the thick insulation is not efficient for cooling since the thick material disturbs the passing air through the wall. The zone with a thick insulation needs about  $2\text{kW m}^{-2}$  additional cooling loads.

Although the EP simulation could calculate the energy performances of different designs, it cannot calculate the real flow streamline with partial changes of physical conditions. Hence, CFD simulation method is coupled to the EP simulation. A great advantage by coupling is to obtain the better convergence to the solution since the initial values can be given by EP simulation results. After calculating EP method, the results' values and the state of parameters are put in *Fluent* software. CFD calculation updates the average node with a single value from EP simulation into large amount of nodes

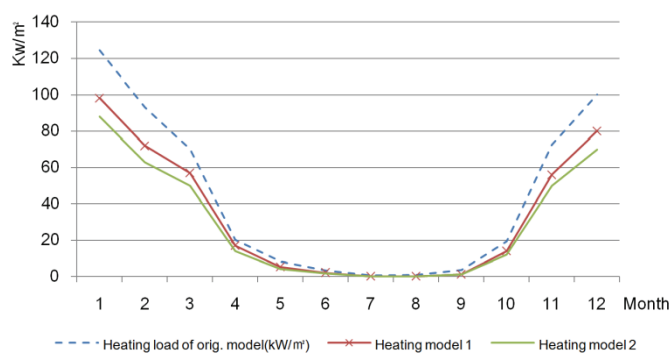


**Figure 6.8.** Heating and cooling loads, (a) by change of slope angle, (b) by change of window ratios, (c) by change of insulation thickness [author].

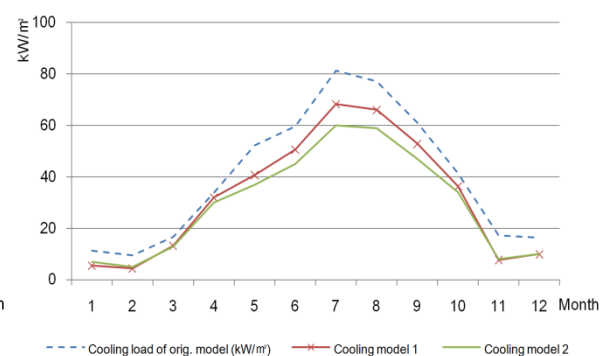
with the values. The geometrical features which derive the thermo- and aerodynamic states can be analyzed by CFD method.

**Table 6.5.** Heating and cooling models based on the simulation results of microclimate design elements [author].

Category	Original model	Heating model 1	Heating model 2	Cooling model 1	Cooling model 2
Orientation	Southwest	South	South	South	South
Site condition	Topography	Topography	Topography	Topography	Topography
Wind-sheltering	-	Medium density wind-sheltering using trees	Artificial wall and large horizontal projection	-	-
Roof design	Normal shape gable roof	Normal shape gable roof with insulation	Gable roof with insulation with projection	Normal shape gable roof with insulation	Very large size gable roof with insulation
Window	Double glazed window HTC <sup>130</sup> : 3.3W m <sup>-2</sup> K <sup>-1</sup>	Double glazed window with wooden frame	Insulation HTC: 1.8W m <sup>-2</sup> K <sup>-1</sup>	Double glazed with insulation	Double glazed with insulation
Geometry	Building using pilotis	-	-	Horizontal projection	Building using pilotis
Insulation	-	Normal insulation HTC: 0.40W m <sup>-2</sup> K <sup>-1</sup>	Super-insulation HTC: 0.059W m <sup>-2</sup> K <sup>-1</sup>	-	-
Airflow	Natural ventilation & air-conditioner	Inter-zone thermodynamic air balancing	Inter-zone thermodynamic air balancing	Cross-ventilation	Cross-ventilation
Window shape	Mixture of uniform and non-uniform shapes	-	-	Uniform shape	Non-uniform shape



*a. Heating load*



*b. Cooling load*

**Figure 6.9.** Comparison of heating and cooling loads EP-CFD method using microclimate design models [author].

<sup>130</sup> HTC: Heat Transmission Coefficient.

4 energy-saving test models, i.e. 2 for heating and 2 for cooling are derived from the simulation results of microclimate design elements shown in Chapter 5, and compared to the energy performance of the original model. Table 6.5 shows the 4 test models. The original model has a virtual house condition based on the Pine-tree house. The house is located on a slope to the southwest with a gable roof and double glazed window. For the heating model, wind-sheltering and insulation are added. For the cooling model, geometry and window shape are changed. The heating and cooling gains using modifications of Pine Tree House using the 4 models are compared to the results of the full application in the original model, i.e. blue dashed lines. The heating and cooling models can be jointly used for thermal condition for both winter and summer. Fig.6.9-*a* shows the comparison of heating loads between original model and 2 heating models and Fig.6.9-*b* represents the cooling load comparison between original model and 2 cooling models.

The original model of Pine Tree House has a lot of Korean traditional design elements that enables to derive microclimate effects. However, the model does not consider passive solar design with strong insulation. Hence, the heating model 1 slightly modifies the original house for a better passive heating performance. Energy performance using design elements of Pine Tree House is analyzed by streamline of thermo- and aerodynamics showing physical distribution of temperature, pressure and kinetic energy etc. Fig.6.9 shows the heating and cooling load from CFD method. Only 12 times of the simulations are performed due to the complexity of calculation.<sup>131</sup> The dashed lines indicate the results of the full application by using all design elements. Some design elements are efficient only for one between heating and cooling. For example, design elements for a high ventilation performance are good for summer but not efficient for winter. Hence, the main aim of EP-CFD simulation is to find some good combinations which accomplish positive microclimate effects.

The orientation is shifted to the south and the wind-sheltering using medium density trees. The insulation is added and inter zone thermodynamic is utilized for air balancing between zones. The main changes in the “heating model 1” are the consideration of passive solar designs. The simulation results in Fig.6.9-*a* shows the improvement of peak heating load of more than  $30\text{kW}\cdot\text{m}^{-2}$  in winter due to the passive heating gain. For the heating model, wind-sheltering and insulation are added. For cooling model, geometry and window shape are changed.

Designs using pilotis, non-uniform shape window which enhances the aerodynamic is not employed since aerodynamic microclimate makes better effects for cooling but worse effects for heating. The 2nd heating model is a trial to improve the 1st model. The enforcement of density in wind-sheltering shows a better performance to block the direct and small cold wind. The insulation of the roof and the window is used. The modification reduces  $8.3\text{kW m}^{-2}$  in maximum heating load in cold winter as Fig.6.9-*a*

---

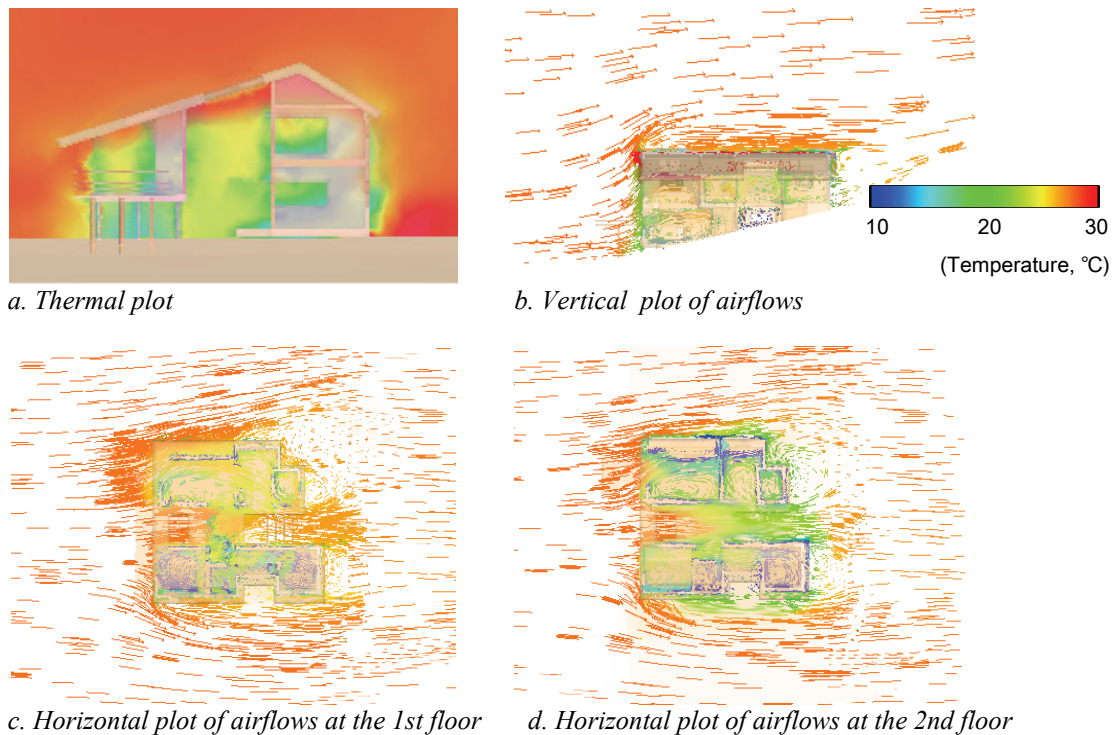
<sup>131</sup> Note that CFD simulation generally needs about 1000~1000000 times more computation costs than EP method.

shows.

A lot of progress of heating gain has been due to the studies of Passive House. However, passive cooling in hot and humid climate, such as S. Korea's increases is getting attention from a lot of researchers since few studies have been done. So far, microclimate design methods are methods that efficiently obtain the cooling gain by considering streamline by thermo- and aerodynamic pressures in the designs. The 2 modifications of the original model for cooling are proposed to obtain the better cooling gain and to decrease the cooling load in the hot and humid summer. The first model changes the orientation to south.

The glass insulation is employed since the intrusion of hot winds was often observed in the microclimate simulations of Chapter 5. The thick wall insulation is not considered due to the result of Fig.6.8 (c), however roof insulation is very important to block the overheated air in the roof.

To improve the blocking performance of the heated downwind from roof, cooling model 1 and 2 use a horizontal projection and a large gable roof respectively. The 1st cooling model uses uniform shape window for cross-ventilation. In addition, the cooling performance of the 1st cooling model is improved by employing the building using pilotis and strong ventilation using non-uniform shape windows. The 1st cooling model reduces the  $14\text{kW m}^{-2}$  of peak cooling loads and the 2nd model obtains additional cooling gain of  $10\text{kW m}^{-2}$ . The 2nd model totally reduces more than  $20\text{kW m}^{-2}$  in peak cooling loads in summer and shows the lowest cooling load in summer as Fig.6.9-*b* shows.



**Figure 6.10.** EP-CFD simulation results of Pine Tree House [author].

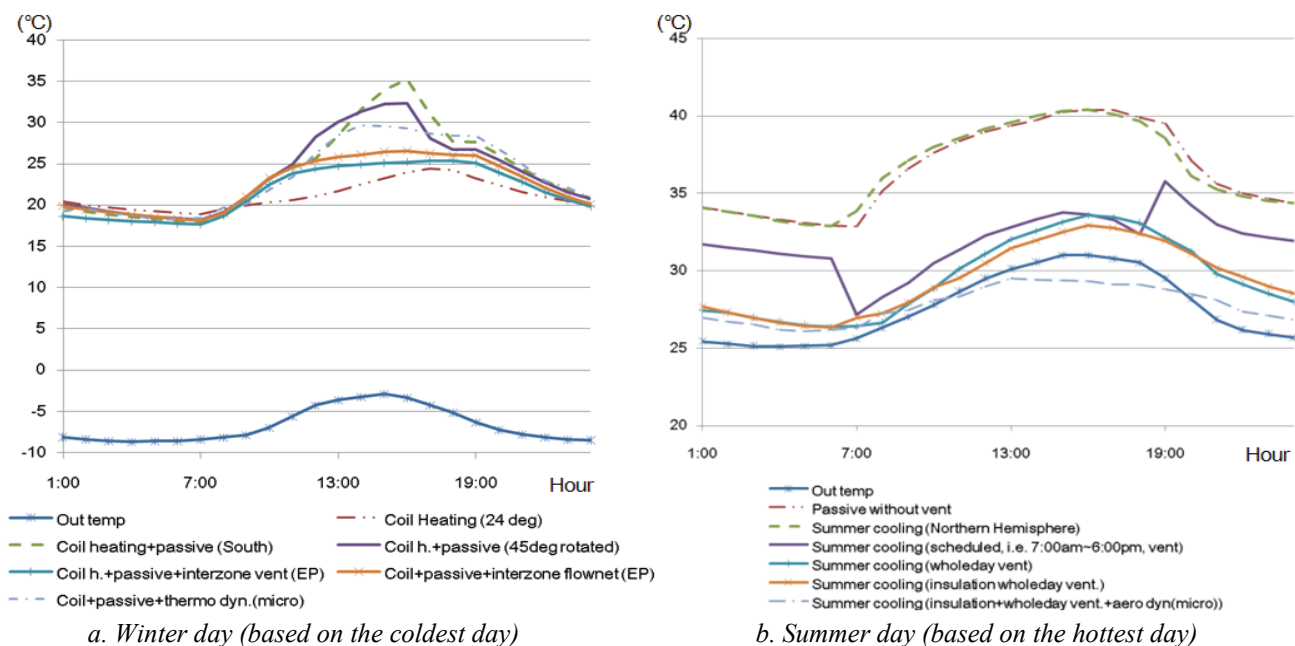
The large gable roof and the non-uniform windows are a very efficient method to enable to improve the streamline of microclimate flow and the performance of solar control. Fig.6.10 shows the EP-CFD simulation results using needle flow plots and Table 6.6 shows the part of a building and the percentage of heat loss. The results show the decisive point for heating and cooling design since the heat loss has great effects related to the human comfort.

The efficiency of passive designs can be compared to active methods since active methods can show us the amount of envelopes and operation time. A simple HVAC model in EP is used to calculate zone temperature. Fig.6.11 represents the temperature comparison between passive and active methods.

In a cold winter day, the zone temperature using coil heating with a target temperature of 24°C can offer 20°C to 23°C. The passive method using improved insulation raises the indoor temperature without energy input but causes an overheating problem at 12:00pm to 2:00pm. To solve the problem, the active

**Table 6.6.** Part of a building and percentage of heat loss (i.e. based on the Fine Tree house models) [author].

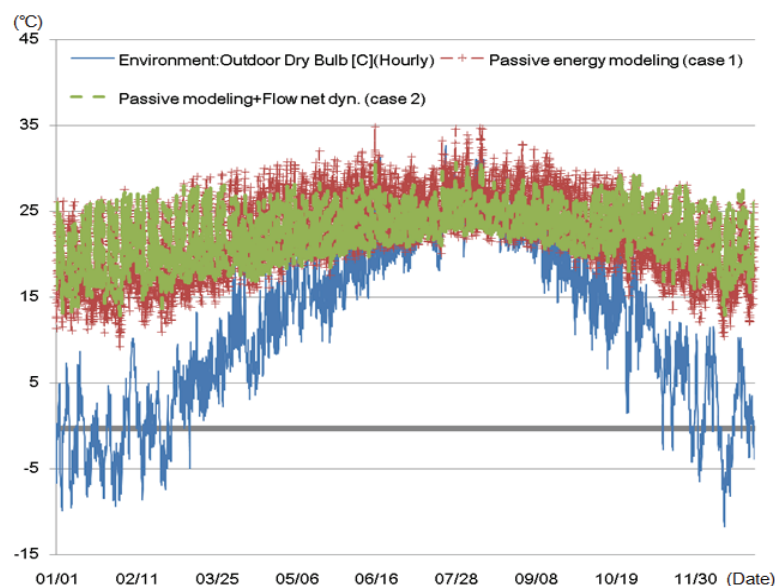
Part of a building	Heat loss (%)
Walls	15~20
Roofs	10~20
Floors	10~15
Windows	20~40
Air filtration	20~40



**Figure 6.11.** Zone temperature comparison between passive method and HVAC model [author].

method uses inter-zone ventilation by using thermal sensors and controller. EP has the computer simulation module for inter-zone ventilation and the result shows the good passive heating performance with comfort thermal condition of 18°C to 26°C. The inter-zone flow net method in EP enables to estimate the inter-zone ventilation by the virtual air-circulation network. It is not a real air circulation method<sup>132</sup> and parametric approximation method. The method shows a similar thermal performance of 19°C to 27°C. The microclimate thermodynamic using inter-zone opening and small inlet opening with passive solar design can offer a thermal condition of 19°C to 29°C which overcomes the overheating problem. The peak temperature is uncomfortable 29°C but the duration of the temperature is only 1 hour. The passive methods can save about 20% heating and electronic cost of the active methods.

In a hot summer day with an average maximum temperature, the zone without ventilation is overheated by passive solar design and the thermal range is 32°C to 41°C. The large cooling load is needed to reduce the heat of the zone. The objective is to compare the passive cooling methods with a performance of an active cooling and to find the best. A scheduled active cooler which starts operation at 7:00am and ends at 6:00pm can reduce 20% of the daytime temperatures. If the active cooler is turned off, the zone temperature is raised. Whole day ventilation in an insulated zone can offer a better thermal condition which has a smoothly varying curve in the range of 23°C to 33°C. A mixed-ventilation shows similar a performance with the whole day ventilation but the input energy of whole day ventilation needs 48% additional energy. A summer cooling method using passive cooling and microclimate aerodynamic simultaneously improves the cooling performance and the thermal condition is laid on the



**Figure 6.12.** 1 year temperature comparison between a passive method and a combination of passive method and flow net of microclimate design [author].

<sup>132</sup> Note only CFD is a real airflow calculation based on partial differential method.



range of 23 °C to 29 °C. The HVAC is very efficient in winter to make isothermal conditions but does not have a big advantage in summer. A large amount of air passing through the zone can quickly reduce the heat from a hot and humid zone, and the best method is to utilize cross-ventilation.

The 1-year performance between simple passive modeling and a passive modeling combined with microclimate design method shows that microclimate method reduces the thermal variance. Fig.6.12 represents the 1 year temperature by EP simulation. CFD cannot be utilized for 1 year calculation due to the complexity hence; the calculation utilizes the flow net method in EP after setting of the microclimate design elements. In the result, thermal variances in simple passive method are larger than 10 °C but the combination with microclimate has smaller variances of 5 °C to 10 °C. The main advantage of microclimate design elements improve the airflow between outdoor and indoor in summer and enable to utilize inter-zone air current in winter. Consequently, higher indoor temperatures in winter and lower temperatures in summer are obtained. The features make it possible to save building energy costs by reducing heating and cooling loads.

## 7. Conclusions

Energy-saving is recently getting more attraction due to the increases of energy security in many countries. Increase of living standards has caused huge energy consumption for heating, cooling and air conditioning in many parts of the world. Nowadays, energy simulation, which analyzes climate, the physical features of architectural material and designs simultaneously, has become more popular. Energy loads of architecture are virtually predicted by energy simulation and then a controller adopts the HVAC system based on the prediction. Several methods provide quantities of predictions, of the performance of HVAC: experiment measurement, analytical model and multi-zone model.<sup>133</sup> However, these methods are not suitable to be applied to passive heating and cooling without a controlling system. Passive heating and cooling can significantly reduce energy costs required for mechanically aided HVAC methods. However, the shortcoming is that it is difficult to control. Geometric analysis with heat and airflows is additionally needed to make passive heating and cooling designs controllable.

Microclimate can modify heating and cooling loads, thereby overall energy consumption. The observation of microclimate for energy simulation is essential since the energy consumption is largely related to the local climate. Decisions taken by architects can have a significant impact on energy consumption, indoor climate performance, thermal comfort and productivity. Architects need to be able to predict air movement, temperature distribution and concentrations. Using well proven computational techniques such as dynamic thermal energy modeling and CFD, effects of microclimate modifications in architectural designs can be simulated without physical modeling tests. Dynamic thermal energy modeling measures thermodynamic effects e.g. inter-zone thermal balance and buoyancy force and CFD simulation is undertaken to examine the aerodynamic operation of the natural ventilation concepts.

At the design stage, architects can predict annual energy and microclimate performance using these methods. The contributions of this study include four main parts:

- Study of energy simulation, dynamic thermal energy modeling and CFD simulation tools.
- Development of a dynamic energy simulation method suitable for microclimate analysis
- Study of microclimate modification for energy-saving by architecture design elements.
- Design recommendation for passive, microclimate and energy-saving house design.

---

<sup>133</sup> See chapter 3.3.2.

## (1) Study of energy simulation, dynamic thermal energy modeling and CFD simulation tools

Energy simulation in a complex building geometry calculates very complex equations with several physical parameters. However, multi-volume, or multi-zone method reduces the complexity of the calculation by single node per zone. This method needs an algebraic equation representing partial differential equations of a zone and the solution is an average value. Most commercial software uses a multi-zone model and EnergyPlus (EP) is the most famous program to estimate the heating and cooling gain and energy consumption. However, single node per zone is too rough to consider airflow e.g. buoyancy and ventilation effects etc.

CFD method numerically solves a set of partial differential equations with a grid array of many nodes per zone. The method can calculate the dynamics of distributed air temperatures, velocity throughout an entire building and hence it is more suitable for microclimate analysis than the multi-zone method. An advantage is that CFD can use realistic 3D geometry definition which is corresponding to CAD design. However, the method requires large computational power since it is complex to apply the method to building geometry. The most famous software for CFD is *Fluent*. The study presents comparisons between the multi-zone and CFD method shown in Table 7.1.

## (2) Development of a dynamic energy simulation method suitable for microclimate analysis

Microclimate can be measured by a very complex combination of several factors e.g. heating location, solar radiation, inter-zone ventilation, size of opening, wind force and buoyancy force etc. For the simplicity, this study proposes a novel method to analyze microclimate of energy imbalance which is estimated by the multi-zones energy simulation. In this study, the term microclimate refers to energy distribution and its variations e.g. thermo- and aerodynamics in space and time.

**Table 7.1.** Comparisons between multi-zone and CFD method [author].

	Multi-zone (EP)	CFD (Fluent)
Number of nodes	1 per a zone	More than 1000 per a zone
Heating analysis	Average temperature	Interzone balance, buoyancy force
Cooling analysis	Average temperature	Natural ventilation, wind force
Advantage	Simplicity	Accuracy

**Table 7.2.** Accuracy of thermal prediction [author].

	Cooling (°C)	Heating (°C)
EP	28	22
EP-CFD	22.8~32.4	17.2~24.7
Differences	-5.2~4.4	-4.8~2.7

At the early design stage, architects cannot detail fix the planning. Therefore, the multi-zone model rather than CFD can fit the prediction task and provide a whole building analysis to improve the design. CFD method always needs a careful preparation for the early stage of simulation. Instead of requiring the initial condition for CFD, EP-CFD method, i.e. the coupling method of multi-zone and CFD, calculates the average temperature of each zone by multi-zone method and puts in differences of the calculated temperatures to CFD for microclimate analysis. This method was validated for the buoyancy and inter-zone balance by comparing it with the single EP simulation. Table 7.2 shows that the EP-CFD can obtain more accurate results for microclimate effects with variances about  $\pm 18.57\% \sim 21.82\%$  for a heating and cooling calculation than single EP. Although results from EP are the homogeneous average temperature in a zone, results from EP-CFD show thermal distribution. Simulation results in Chapter 5 and 6 also show similar variances within the range between maximum and minimum temperatures.

### (3) Study of microclimate modification for energy-saving by architectural design elements

This study investigated microclimate modification using design elements of Korean traditional and passive house for energy-saving. Microclimate modification involves the best use of architectural design elements to maximize or limit sunlight, shade and air movement. The modifications involve the design of the house and associated construction e.g. wall, fences and courtyard etc. Landscape modifications involve the use of plants to further increase or decrease the impact of the sun and wind upon the local environment. Several design elements strongly influence the degree to which interior comfort requires energy inputs for heating or air conditioning.

**Table 7.3.** Strength of thermo- and aerodynamic microclimate for architectural design elements [author].

	Microclimate in a building	Thermodynamic	Aerodynamic
Arrangement	A. Building orientation	*****	*****
	B. Topography	*****	****
	C. Courtyard	*	-
	D. Courtyard roof	***	*
Form	E. Gable roof	****	**
	F. Curved roof	-	*
	G. Fence design	-	****
	H. Windbreak	-	*****
	I. Huge plant	-	***
	J. Building over pilotis	***	*****
Façade	K. Uniform window shape	-	**
	L. Non-uniform window shape	*	*****
	M. Horizontal window shape	**	***
	N. Vertical projection	*	***
	O. Horizontal projection	*	***

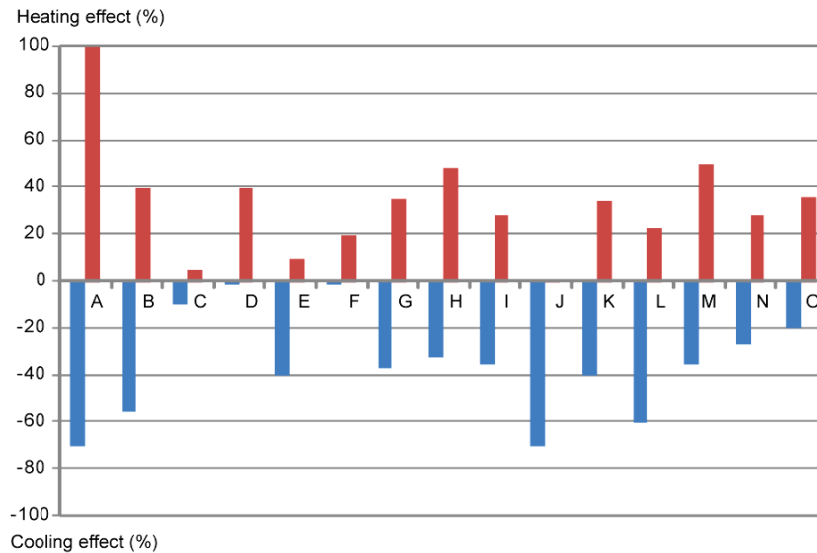
(\*\*\*\*\*: very strong, \*\*\*\*: strong, \*\*\*: efficient, \*\*: effective, \*: expectable)

The elements are orientation, topography, roof shape, fence design, piloties, window shape and courtyard etc.,<sup>134</sup> which are potentially efficient for energy-saving on various site conditions in S. Korea, and they can be classified into cooling or heating elements. These elements are applied to EP-CFD energy simulation to estimate heating and cooling loads and flow directions. Microclimate analysis, which is combined within the energy simulation, enables to predict and choose the elements for energy-saving. Microclimate effects can be observed by distribution of air temperature in building sectors and the distribution can be represented by thermo- and aerodynamic flows. The strength of thermo- and aerodynamic microclimate effects for design elements are compared in Table 7.3. The elements, i.e. courtyard, curved roof, fence design, windbreak, huge plant, uniform window shape, with few or no effects are marked using “-”.

Building orientation has the strongest effects for both thermo- and aerodynamic microclimate since a concentration of solar access makes rising trend of the air and the difference of air pressure. Topography has also strong thermodynamic effects since by day the air above the slopes can be more easily heated than the lower area. The orientation is important to determine the directions of solar and wind access for heating and cooling respectively. Although microclimate of a courtyard is slight due to less daylight and natural ventilation, roof glazing of a courtyard provides better heating gain and more thermodynamic effect such as stack effect. Gable roof form is one of the most efficient designs which can utilize the stack effect for roof ventilation. However, thermodynamic of gable ventilation is stronger than the courtyard’s stack effect because fresh air coming from eaves of gable roof causes an effective aerodynamic effect pushing warm air in the room out. Curved roof is the method which minimizes aerodynamic effect in winter since it has very small air resistance. Wind-sheltering using fence design, windbreak and huge plants are efficient aerodynamic method to reduce strong winds in winter and save heating energy. The performances of wind-sheltering depend on the density of the elements and the order of aerodynamic strength is fence design, huge plants and windbreak. Windows act as solar and air inlets, which are very important for both heating and cooling. The shapes of windows modify the amount of inflows and streamline of the flows. Different size windows i.e. non-uniform windows shape induces a higher ventilation performance due to the pressure difference than the uniform window shape. Although aerodynamic effects of the horizontal window shape is smaller than one of the non-uniform window, the horizontal window is more efficient for heating because it can get more solar energy. Vertical and horizontal projections, e.g. external wing-walls, partitions and fins etc., can be combined with window designs and play a role as a wind blocker or a wind-catcher and they can be utilized as shading devices. The aerodynamic microclimates for vertical and horizontal projections have similar strengths although they generate different airflow shapes. Fig.7.1 classifies the thermo- and aerodynamic microclimate into heating and cooling elements and represents energy performances. If the elements in Table 7.3 are corresponded to heating and cooling

---

<sup>134</sup> see Chapter 5.



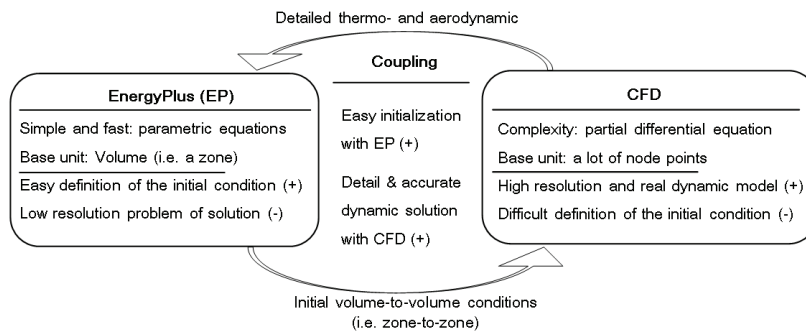
**Figure 7. 1** Classification by heating and cooling effects of elements in Table 7.3 [author].

effects in Fig.7.1, we can know that all thermo-dynamic effects are not directly related to the heating gain, and aero-dynamic effect does not mean directly better cooling. However, the effects of microclimate modification are worthy of a close attention.

#### **(4) Energy simulation method for microclimate modification: EP-CFD coupling**

There are two computer simulation methods to analyze building energy performance: parametric method and Computational Fluid Dynamics (CFD) method. The parametric method uses a simplified geometry, e.g. graph or connection model, for multi-zone. The advantage of this method is simplicity since it can divide a complex energy balance problem into several sub-components with parametric equations. However, the resolution of solution is not sufficient to observe the microclimate modifications with building designs.

A naturally ventilated and thermally inhomogeneous building includes microclimate modifications due to the evolution of outside airflow and inside buoyancy, stack effects and thermal flows with a fluctuating direction, magnitude, turbulence, temperature, humidity and radiations fluxes. CFD is a modeling technique that analyzes the airflow using fluid dynamic. CFD can predict the air speed and direction, temperature, humidity, turbulence levels and concentrations of contaminants at thousands of node points in a zone including the microclimate modifications. However, a lack of the initial condition is the main problem since CFD methods always need a detailed initial condition as much as increased node points.



**Figure 7.2.** Energy simulation method using EP-CFD coupling [author].

In this dissertation, a hybrid method of parametric equation and CFD is proposed. While the initial energy condition is calculated by a parametric equation in the EnergyPlus (EP) software, a CFD method considers the result of EP method as the initial condition of CFD solver and estimates the difference between the parametric estimates and the real building condition with microclimate modifications. This method can automatically initialize without any complex manual definitions and obtain much detailed, accurate and dynamic energy condition as Fig.7.2 depicts.

## (5) Design recommendation for arrangement

Microclimate modification for heating gain is closely related to the common knowledge of Passive House, green building and sustainable architecture. A low-energy house reduces the energy resource and minimizes environmental impacts, i.e.

- Maximizing the opportunities to use solar energy
- Compact plan forms reduce infiltration losses
- Optimized glazing ratios for heat gains and lighting
- Using thermal mass to reduce fluctuations in room temperatures
- Sheltering the building from strong cold wind.<sup>135</sup>

However, the demand for cooling can be reduced by careful consideration of the site, building geometry, design elements for

- Maximizing the potential use of natural wind for natural ventilation
- Using thermo- and aerodynamic flow to avoid overheating
- Controlling the streamline of airflow using design elements
- Reducing the internal loads by distributing and balancing
- Shield windows from unwanted solar gain in the hot season.

<sup>135</sup> This reduces the unwanted cold air infiltration.

**Table 7.4.** The thermal effects of glazing directions in S.Korea [author].

Clockwise orientation from North	Thermal effect
150°~190°	Best
83°~150° and 190°~260°	Fair
0°~83° and 260°~360°	worst

Design recommendation based on EP-CFD energy simulations may be helpful for architects to assess energy conservation early and throughout the design process. A house is carefully sited and arranged to reduce energy-use for heating and cooling. Standard design elements e.g. site, form, windows, walls, and roofs etc., are selected to control/collect/store solar heat or to ventilate/ discharge/ exchange the heat. Typically, reductions of heating and cooling loads allow smaller HVAC equipment, resulting in little or no increase in construction cost.

South-facing building orientation: Installing south-facing glazing enables the collection of solar energy, which is partially stored in walls, floors, and/or ceiling of the space, and later released. Glazing must face within 15° of true south, and the affected areas must be compatible with daily temperature swings. The savings of heating energy are augmented by productivity-enhancing benefits of lighting. The functioning of the space should not be compromised by direct glare from glazed openings or by local overheating. The optimum building orientation can be simulated by using average daily incident radiation on a vertical surface. The thermal effects for some building orientations are compared in Table 7.4, The best building orientation in Seoul, Korea is South to South-Southeast i.e. clockwise 157.5° to 180° from North as Fig.3.3 depicts.

Topography: Differences in slopes make remarkably large modifications of microclimate, since the solar radiation and wind velocity are much large. A house on the slope is more suitable to use summer breezes. Air movements such as anabatic and katabatic winds occur generally due to the difference of radiation supply in a hilly area. If the opening control utilizes the upward and downward winds, the winds exchange the indoor air temperature to the outdoor quickly. An open floor plan and openings are located to catch prevailing breezes are efficient for summer cooling. Topography moderates the room temperature, saves energy and preserves open space.

Local wind environment: For hot and humid summer, ventilation is beneficial for convective or evaporative cooling. The movement of air through a building geometry is generated by differences in air pressure as well as temperature. The layout of the surrounding buildings acts as barriers, diverting the flows into narrower. The resulting patterns of airflow are affected more by building geometry and orientation than by air speed.

Building arrangement: It is important to make the largest passive heating effect with good solar access.



Solar access is possible by keeping the south elevation free from obstructions. Arrangement of buildings creates a wind shadow which is a low-pressure area at the back of each house. The best arrangement is to stagger the houses according to the prevailing wind direction.

## **(6) Design recommendation for form**

**Sun space:** Avoid configurations that produce heat losses or gains with no compensatory benefits. The sun space should bring daylight to the interior while providing a solar chimney for natural ventilation during mild weather. In some cases, atriums can collect useful solar heat in cold climates—serving as a kind of transition zone, with larger temperature swings than would otherwise be appropriate in the rest of the building. The atrium's configuration should be defined at the earliest possible stages of the design process, before an undesirable or arbitrary configuration is locked in.

**Courtyard dwelling:** A courtyard does not perform well due to less daylight and natural ventilation. Sunspace performs in a similar way to a courtyard, although the ventilation is better than a courtyard due to stack effects. There may be a need to consider ventilation to the upper floors due to the low stack pressures at higher levels. Roof glazing can be applied to a courtyard to provide lighting and to improve the heating gain with the passive heating method. Atrium of courtyard easily obtains solar heat through the glass and avoids the direct heat loss. Solar heat gain can be controlled through use of fritted glass or louvers.

**Roof opening and stack-effect ventilation:** Heated air rises within a mid- or high rise building to the top, where it exits through roof openings. This process induces ventilation of the adjoining spaces below. Spaces that are not adversely affected by increased air motion are appropriate targets for natural ventilation, which effectively conditions the space during fair weather without using air conditioning. In the very hot seasons, night cooling with cross-ventilation is more effective than stack-effect ventilation. An atrium often serves as an ideal solar chimney to exhaust hot air.

**Building shape:** The shape of a building determines how much area is exposed to the outdoors through exterior walls and ceilings. Exposed area should be minimized to save energy. When a house has a complex shape, exposed surface area increases both construction and energy costs. Narrow form uses less energy in total, and this leads to a reduction in electrical load. This outweighs any slight increase in infiltration losses due to a large façade area.

**Differentiated Façades:** Differentiated façade is really an approach to determinate designs and styles and is known as one of the most effective low-energy house strategies. The appearance of various façades makes differ in the environmental loads. The architects create variations in the façade design,

the use of space behind the façade, and the low-energy house strategies being employed.

**Windbreak:** For winter, a house should be buffered against chilling winds to reduce infiltration into interior spaces and lower heat loss. A windbreak may be in the form of a narrow path, a garden wall, or a dense stand of trees. Windbreaks reduce wind velocity and produce an area of relative calm on their leeward side. The extent of this wind shadow depends on the height, depth, and density of the windbreak, its orientation to the wind, and the wind velocity. Windbreaks work either by deflecting the wind up and over a building thereby forming a protective wind shadow, or by catching it in the twigs and branches of a double or triple row of trees which breaks up its speed. A well designed windbreak can reduce wind velocity by 85%, and reduce winter heating costs by 10% to 25%.

### **(7) Design recommendation for façade elements**

**Window:** The architect applies functional criteria to the size, proportion, and location of windows. When a windows size becomes larger, much more solar could enter the indoor, and the indoor temperature would rise. It is a disadvantage to reduce temperature in the hot and humid summer of Korea. Suitable window sizes should be optimized by glazing ratio. A window with a large width is better to obtain both solar radiation and good ventilation than one with a large height. For summer cooling, location of windows should be carefully chosen to serve as air inlets to face prevailing winds. Windows can be controlled by projection. The projection located ahead (or afterward) of a window respectively blocks (or catches) the wind. When cross-ventilation is planned for window shape, different sizes between inlets and outlets induce higher ventilation rate wind with large pressures. For the cold season, trickles around windows should be blocked since they usually are the major source of air leakage which affects significantly the building energy. With double glazing windows, the indoor temperature rises about 2 °C in winter while 0.1 °C in summer. Double glazing windows are a benefit for thermal comfort.

**Glazing ratio:** Buildings with a very small glazing ratio consume more energy than ones with larger glazing ratios. However, increasing glazing ratios much above about 50% produces little extra benefit. The optimum glazing ratio is in the region of 35% for building surfaces. The optimum glazing ratio for roof-light is no more than 20%. Before finalizing, glazing ratios should be checked for overheating possibilities in summer.

**Thermal mass:** For an optimum effect of passive house, floor and wall finish materials with high heat storage capacity must be exposed to direct illumination by the low winter sun. Thermal mass is ideally placed within the building and situated where it still can be exposed to winter sunlight but insulated from heat loss. However, for hot humid summer season, it needs to be strategically located to prevent

overheating. It should be placed in an area that is not directly exposed to solar gain and allowed adequate ventilation at night to carry away stored energy without increasing internal temperatures any further. The best solution is a proper shading design considering sun's altitude because the sun's altitude is higher than summer.

**Shading:** Shading should be used to provide cost-effective, aesthetically acceptable, functionally effective solar control. Particularly in summer, shading is very important to decrease indoor temperature and to avoid an overheating problem. It works well on south façades where overhangs provide effective shading for the space and the angle of shading device should be optimized for moderate solar penetration. Shading west façades is critical in reducing peak cooling loads. A wide range of shading devices are available, including overhangs on south façades, fins on east and west façades, interior blinds and shades, louvers, and special glazing such as fritted glass. Reflective shading devices can further control solar heat gain and glare. Devices without moving parts are generally preferable. Movable devices on the exterior are typically difficult to maintain in corrosive environments or in climates with freezing temperatures. Other design elements, such as overhanging roofs, can also serve as shading devices.

## **(8) Future work**

In this study, microclimate modification and energy simulation for a lot of design elements are studied for achieving comfortable indoor environment and minimizing energy consumption in low storey and high density. However, almost in all major cities in Asian countries, development of residential buildings is characterized by high rise apartments. Environmental influence in most apartments is much greater than single family houses. While increasing insulation levels and sealing air leaks in the building and ductwork are applied to newly developed houses, energy efficiency for similar thermal conditions is difficult in the low storey and high density housing. The studies of microclimate modification for low-energy house should be adapted and developed for energy-saving in low storey and high density houses. This means the spatial expansion from a small house to a low housing and high rise building.

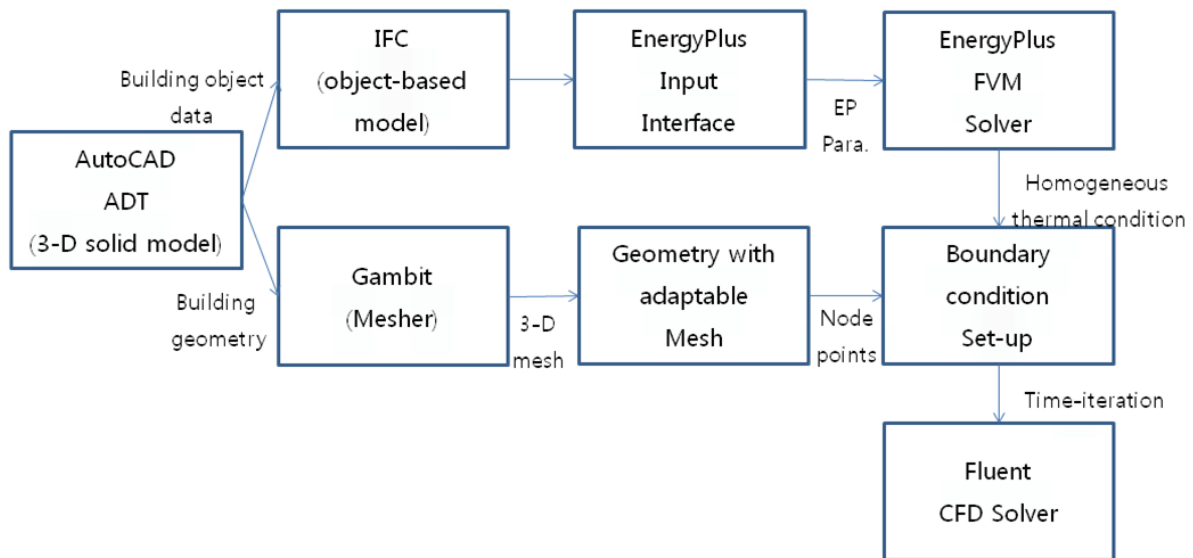
Architects and building planers want to maintain or increase the accuracy and quality of estimates. The microclimate is an extremely complex system consisting of a lot of feedback loops and nonlinear relationships between the different natural and artificial elements. Building microclimate is also influenced by neighboring buildings and urban geometry. Studies in this thesis do not consider the effects of neighboring buildings. For high accuracy result, combining method with other climate analysis tools which can handle larger scale, e.g. urban, than a building is needed. The topics arises a lot of ideas for future works: flow around and between buildings, thermal exchange processes at the ground surface,

at walls and vegetations etc. turbulence around building canyon, etc.

Other interesting issue is to measure the accuracy of the computer simulation by using the physical simulation e.g. wind tunnel test, sensor measurement, etc. Although the computer simulation methods are quick, economic and efficient solution using virtual design analysis, they may result in some inaccuracy and non-practical solutions when unconsidered elements sometimes causes remarkable effects. Real measurements using physical sensors monitoring the temperature, humidity, air velocity etc. or wind tunnel test analyzes these inaccurate situations and helps to establish the more accurate and practical measures for the microclimate effects. The future works will include material tests, physical unit analysis, microclimate sensor measurements, wind tunnel tests for building geometries, etc.

# Appendix

## A-1. Data flow in EP-CFD simulation



## A-2. EnergyPlus (EP) building parameters

```

BUILDING,
\unique-object
\required-object
\min-fields 7
A1 , \field Building Name
\required-field
\default NONE
N1 , \field North Axis
\note degrees from true North
\units deg
\type real
\default 0.0
A2 , \field Terrain
\note Country=FlatOpenCountry | Suburbs=CountryTownsSuburbs | City=CityCenter |
Ocean=body of
water (5km) | Urban=Urban-Industrial-Forest
\type choice
  
```

```

\key Country
\key Suburbs
\key City
\key Ocean
\key Urban
\default Suburbs
N2 , \field Loads Convergence Tolerance Value
\units W
\type real
\minimum> 0.0
\default .04
N3 , \field Temperature Convergence Tolerance Value
\units deltaC
\type real
\minimum> 0.0
\default .4
A3 , \field Solar Distribution
\note MinimalShadowing | FullExterior | FullInteriorAndExterior
\type choice
\key MinimalShadowing
\key FullExterior
\key FullInteriorAndExterior
\key FullExteriorWithReflections
\key FullInteriorAndExteriorWithReflections
\default FullExterior
N4 , \field Maximum Number of Warmup Days
\type integer
\minimum> 0
\default 25
A4 ; \field Calculate Solar Reflection From Exterior Surfaces
\note deprecated field. Use SolarDistribution Value
\type choice
\key No
\key Yes
\note The choice Yes requires that Solar Distribution = FullExterior or FullInteriorAndExterior
\default No

```

The IDF form is

```

BUILDING,
PSI HOUSE DORM AND OFFICES, ! Building Name
36.87000, ! Building Azimuth
Suburbs, ! Building Terrain
4.0E-02, ! Loads Convergence Tolerance
0.4, ! Temperature Convergence Tolerance
FullInteriorAndExterior, ! Solar Distribution
25; ! Maximum Number of Warmup Days

```

## A-2. Energyplus climate weather data file access

```
DesignDay,  
\min-fields 15  
A1 , \field DesignDayName  
\type alpha  
\required-field  
\reference DesignDays  
N1 , \field Maximum Dry-Bulb Temperature  
\required-field  
\units C  
\minimum> -70  
\maximum< 70  
\note  
\type real  
N2 , \field Daily Temperature Range  
\note Must still produce appropriate maximum dry bulb (within range)  
\note This field is not needed if Dry-Bulb Temperature Range Modifier Type  
\note is "delta".  
\units deltaC  
\minimum 0  
\default 0  
\type real  
N3 , \field Humidity Indicating Temperature at Max Temp  
\note this will be a wet-bulb or dew-point temperature coincident with the  
\note maximum temperature depending on the value of the field  
\note Humidity Indicating Temperature Type  
\note required-field if Relative Humidity schedule is not used  
\units C  
\minimum> -70  
\maximum< 70  
\type real  
N4 , \field Barometric Pressure  
\required-field  
\units Pa  
\minimum> 70000  
\maximum< 120000  
\type real  
\ip-units inHg  
N5 , \field Wind Speed  
\required-field  
\units m/s  
\minimum 0  
\maximum 40  
\ip-units miles/hr  
\type real  
N6 , \field Wind Direction  
\required-field  
\units deg
```

```

\minimum 0
\maximum 359.9
\note North=0.0 East=90.0
\type real
N7 , \field Sky Clearness
\required-field
\minimum 0.0
\maximum 1.2
\default 0.0
\note 0.0 is totally unclear, 1.0 is totally clear
\type real
N8 , \field Rain Indicator
\minimum 0
\maximum 1
\default 0
\note 1 is raining, 0 is not
\type integer
N9 , \field Snow Indicator
\minimum 0
\maximum 1
\default 0
\note 1 is Snow on Ground, 0 is no Snow on Ground
\type integer
N10, \field Day Of Month
\required-field
\minimum 1
\maximum 31
\type integer
\note must be valid for Month field
N11, \field Month
\required-field
\minimum 1
\maximum 12
\type integer
A2 , \field Day Type
\required-field
\note Day Type selects the schedules appropriate for this design day
\type choice
\key Sunday
\key Monday
\key Tuesday
\key Wednesday
\key Thursday
\key Friday
\key Saturday
\key Holiday
\key SummerDesignDay
\key WinterDesignDay
\key CustomDay1

```



```

\key CustomDay2
N12, \field Daylight Saving Time Indicator
\minimum 0
\maximum 1
\default 0
\note 1=Yes, 0=No
\type integer
A3 , \field Humidity Indicating Temperature Type
\note Type of humidity indicating temperature (Wet-Bulb or Dew-Point)
\type choice
\key Wet-Bulb
\key Dew-Point
\key Schedule
\default Wet-Bulb
A4 , \field Relative Humidity Day Schedule
\object-list DayScheduleNames
\note only used when previous field is "schedule"
\note the hour/time interval values should specify relative humidity (percent) from 0.0 to 100.0
A5 , \field Dry-Bulb Temperature Range Modifier Type
\note Type of modifier to the dry-bulb temperature calculated for the time step
\type choice
\key Multiplier
\key Delta
\default Default Multipliers
A6 ; \field Dry-Bulb Temperature Range Modifier Schedule
\object-list DayScheduleNames
\note the hour/time interval values should specify range from 0.0 to 1.0 of the
\note maximum temperature

```

### A-3. EnergyPlus input data file for solar penetration calculation

```

ZONE,
Zone2, !- Zone Name
...;
LIGHTS,
Zone2, !- Zone Name
BLDG Sch 3, !- SCHEDULE Name
1464.375, !- Design Level {W}
...;
SURFACE:HeatTransfer,
Zone2-WallExt-South, !- User Supplied Surface Name
WALL, !- Surface Type
Vabs0.50, !- Construction Name of the Surface
Zone2, !- InsideFaceEnvironment
...;
SURFACE:HeatTransfer:Sub,
Zone2-WallExt-South-Wndo0, !- User Supplied Surface Name
WINDOW, !- Surface Type

```

DOUBLE PANE WINDOW, !- Construction Name of the Surface  
 Zone2-WallExt-South,!- Base Surface Name

...;

**DAYLIGHTING:DELIGHT,**

DElight Zone2, !- User Supplied DELight Zone Name

Zone2, !- Host Zone Name

1, !- Lighting control type

0.0, !- Min input power fraction for continuous dimming

0.0, !- Min light output fraction for continuous dimming

0, !- Number of steps for stepped control

1.0, !- Probability lighting will be reset when needed

0.5; !- Gridding Resolution {m2}

**DAYLIGHTING:DELIGHT:Reference Point,**

RefPt 4, !- User Supplied Reference Point Name

DElight Zone2, !- DELight Zone Name

2.25, !- X-coordinate of reference point {m}

4.0, !- Y-coordinate of reference point {m}

0.9, !- Z-coordinate of reference point {m}

1.0, !- Fraction of zone controlled by reference point

1000.; !- Illuminance setpoint at reference point {lux}

**DAYLIGHTING:DELIGHT:Complex Fenestration,**

CFS-REDIRECT, !- User Supplied Complex Fenestration Name

BTDF^GEN^LIGHTSHELF^0.25^20.0^1.00^0.5, !- Complex Fenestration Type

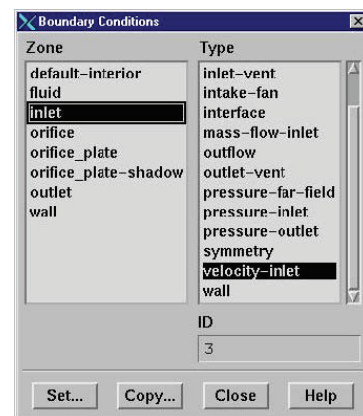
Zone2-WallExt-South, !- Base Surface Name

Zone2-WallExt-South-Wndo0, !- Doppelganger Surface Name

0.0; !- Fenestration Rotation {deg}

#### A-4. Boundary condition setup in Fluent

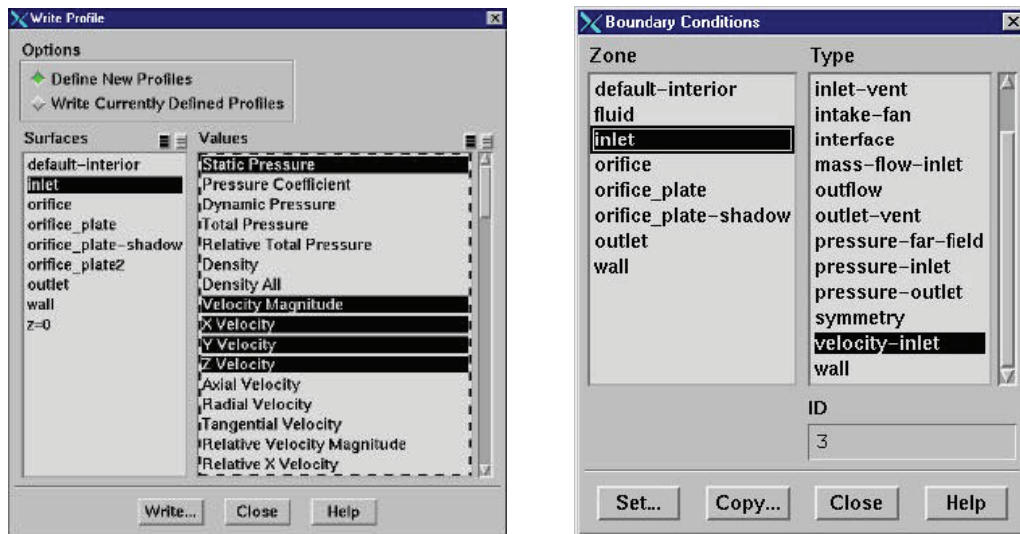
1. Zones and zone types are initially defined in pre-processor.
2. To change zone type for a particular zone:
3. Define Boundary Conditions...
4. Choose the zone in Zone list.
5. Can also select boundary zone using right mouse button in Display Grid window.
7. Select new zone type in Type list.



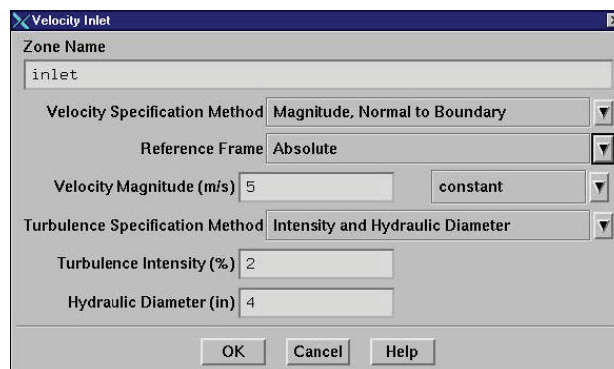
8. Explicitly assign data in BC panels.

- To set boundary conditions for particular zone:
- Boundary condition data can be copied from one zone to another.
- Boundary condition data can be stored and retrieved from file.

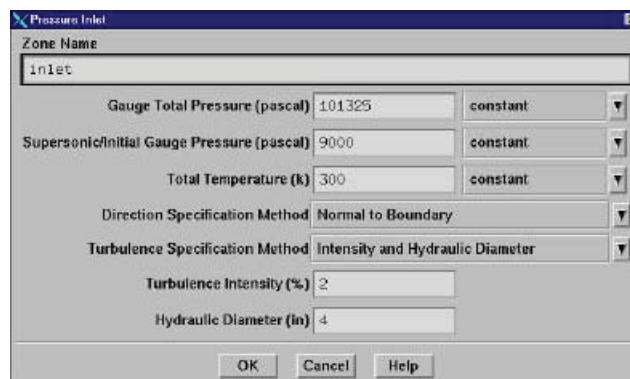
- Boundary conditions can also be defined by UDFs and Profiles.



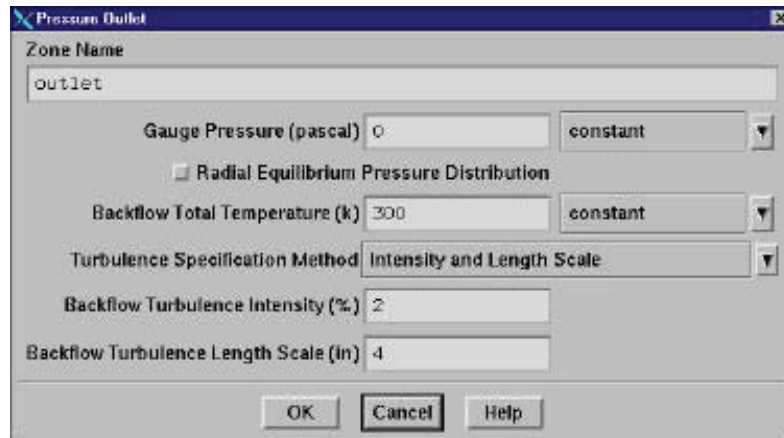
9. Setup of velocity Inlet by specify Velocity by Magnitude, Normal to Boundary, Components and Magnitude and Direction



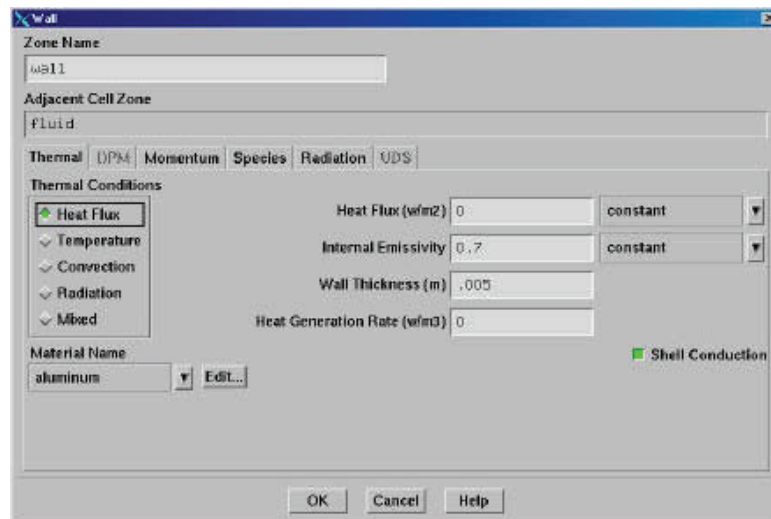
10. Setup of pressure inlet by specifying total *Gauge* pressure, total temperature and inlet flow direction



11. Setup of pressure outlet by specifying static *gauge* pressure



12. Setup of Wall Boundaries by specifying solid regions, thermal boundary conditions, wall roughness and translational or rotational velocity



13. Setup of Internal Face Boundaries by specifying Fans, Radiators, Porous jump, preferable over porous media and interior walls.

# Bibliography

- A&C Publishing, "Details: Architecture + Interior", Min-Maru 6 houses by S.Y. Choi, Nr.9, 2004.
- Ahn, H.K., "Analysis of indoor climate of Jang-Kyung-Gak in Hae-In Temple", *Kyeong Hee University*, 1993.
- Akbari, H., Rosenfeld, A.H., Taha, H., "Cool construction materials offer energy saving and help reduce smog", *ASTM standardization news* 23, 1995.
- Alvarez, S., Sanchez, F., "Guidelines on Microclimate around Buildings", Final Report, *POLIS project*, 1998.
- Albrecht, R., Paker, L., Rehberg, S., Reiner, Y., "Umweltlastung durch ökologische Bau- und Siedlungsweisen", Band 1, Band2, *Bauverlag GMBH, Wiesbaden und Berlin*, 1084.
- Alonso, D.V., Dominguez, S.A., "Use of Vegetation and Water to Promote Passive Cooling", The 1st International Conference on Ecology and the City 2001, *Universidad de Barcelona*, 2001.
- Anderson, J., Shiers, D., "The green guide to specification", an environmental profiling system for building materials and components, 3rd edition, *Blackwell Science*, 2002.
- Antolini, H.L., "Solar heating & cooling", Active & passive systems, hot water heaters, pools, spas & tubs, 4th edition, *Lan publishing Co.*, 1980.
- Arnfield, J., "Canyon geometry, the urban fabric and nocturnal cooling: a simulation Approach", *Phys. Geogr.*, 1990.
- Arnfield, J., Herbert, J.M., Johnson, G.T., "A numerical simulation investigation of urban canyon energy budget variations", Proc. 13th Int. Conf. on Biometeorol. And Aerobiol., Albuquerque, New Mexico, 1998.
- Aronin, J.E., "Climate & Architecture", Progressive Architecture Book, *Reinhold Publishing Corporation*, 1953.
- Avissar, R., "Potential effects of vegetation on urban thermal environment", *Atmos. Envir.*, 1996.
- Aynsley, R.M., Melbourne, W., Vickery, B.J., "Architectural Aerodynamics", *Applied Sciences Publishers Ltd., London*, 1977.
- Baik, J.J., Park, R.S., Chun, H.J., Kim, J.J., "A laboratory model of urban street canyon flows", *J. Appl. Meteorol.*, 2000.
- Baker, N., Steemers, K., "Energy and Environment in Architecture", *E & FN Spoon*, 1999.
- Barry, G.R., Chorley, R.J., "Atmosphere, weather and climate", 5th edition, *Methuen & Co Ltd. London*, 1987.
- Beausoleil-Morrison, I., "The Adaptive Coupling of Heat and Airflow Modeling Within Dynamic Whole-Building Simulation", Ph.D. Thesis, Energy Systems Research Unit, Department of Mechanical Engineering, *University of Strathclyde, Glasgow, UK*, 2000.

- Bensalem, R., "Wind-driven Natural Ventilation in Courtyard and Atrium-type Buildings", Ph.D. Thesis, *University of Sheffield, Great Britain*, 1991.
- Bensalem, R., "Climate-responsive", Lund Institute of Technology, *Lund University*, 1995.
- Bittencourt, L.S., "Ventilation as a Cooling Resource for Warm-humid Climates: An Investigation on Perforated Block Wall Geometry to Improve Ventilation inside Low-rise Buildings", Ph.D. Thesis, *Universidade Federal de Alagoas*, 1993.
- Bohe, W.M., "Energiesparhäuser: eine neue Generation von Gebäuden", *Deutsche Verlags Anhalt Stuttgart*, 1996.
- Bourbia, F., Awbi, H.B., "Building cluster and shading in urban canyon for hot-dry Climate", *Renewable Energy*, 2004.
- Boutet, T.S., "Controlling Air Movement: A Manual for Architects and Builders", *Mac Graw- Hill, NY*, 1987.
- Britannica Encyclopaedia / 브리태니커 백과사전, 2004.
- Brown, D.E., Fox, M., Pelletier, M.R., Hoffman, L., "Sustainable Architecture White Papers", Earth Pledge Foundation Series on Sustainable Development, *Earth Pledge Foundation*, 2001.
- Busato, L., "Passive cooling and energy efficient strategies for the design of a hotel on the Southern coast of Pernambuco, Brazil", LEARN, *London Metropolitan University*, 2003.
- Calder, K.E., "Koreas Energy Insecurities Comparative and Regional Perspectives", *the Korea Economic Institute of America (KEI)*, 2005.
- Casey, F.J.M., "Comfort in heat without AC", *AEI*, 2002.
- Chan, A.T., So, E.S.P., Samad, S.C., "Strategic guidelines for street canyon geometry to achieve sustainable street air quality", *Atmos. Envir.*, 2001.
- Chen, Q., Xu, W., "A zero-equation turbulence model for indoor airflow simulation", *Energy and Buildings*, 1998.
- Chiras, D.D., "The Solar House: Passive Heating and Cooling", *Mother Earth News*, 2002.
- Clark, M., "Designing for climate - Buildings and Urban Design in the Tropics", *James Cook University*, 2003.
- Clarke, J.A. "Environmental systems performance", Ph.D. Thesis, Department of Architecture and Building Science, *University of Strathclyde, Glasgow, UK*, 1977.
- Clarke, J.A., "Energy Simulation in Building Design", 2nd edition, *Butterworth-Heinemann*, 2001.
- Cofaigh, E.O., Fitzgerald, E., "A Green Vitruvius", Principles and Practice of Sustainable Architectural Design, *James & James Press*, 1999.
- Cofaigh, E.O., Olley, J.A., Lewis, J.O., "The climatic dwelling", an introduction to climate-responsive residential architecture, *James & James Ltd.*, 1996.
- Comfortable low energy architecture (CLEAR), "Climatic design", *London Metropolitan University*, 2004.
- Crawley, D.B., Lawrie, L.K., Winkelmann, F.C., Buhl, W. F., Pedersen, C.O., Strand, R.K., Liesen, R.J., Fisher, D.E., Witte, M.J., Henninger, R.H., Glazer, J., Shirey, D., "EnergyPlus: New, Capable, and Linked", *In Proceedings of the Performance of Exterior Envelopes of Whole Buildings VIII*, December 2001.
- Crosbie, M.J., "The Passive Solar Design and Construction Handbook", 2nd edition, *Wiley Press*, 1997.
- Dabberdt, W.F., Ludwig, F.L., Johnsson, W.B., "Validation and applications of an urban diffusion model for vehicle

emissions”, *Atmos. Envir.*, 1973.

Daoudi, N.S., “Comfort and discomfort in a study space”, *AEE*, 2002.

Dăng, P.N., “Architektonisch-technische Lösungen zur Verbesserungen des Mikroklimas in Gebäuden unter Bedingungen des heißen feuchten Klimas/ Architectural engineering devices for improve indoor microclimate under the hot and humid conditions”, *Hanoi college of Civil Construction*, 1985.

Degiovanni, A., “Conduction dans un “mur” multicouche avec sources: extension de la notion de quadripole”, *International Journal of Heat and Mass Transfer*, Volume 31, 1988.

De Paul, F.T., Shieh, C.M., “Measurements of wind velocity in a street canyon”, *Atmos. Envir.*, 1986.

Dingman, S.L., “Physical Hydrology,” 2nd edition, *Englewood Cliffs, Prentice Hall, NJ*, 2002.

Djunaedy, E., “External coupling between building energy simulation and computational fluid dynamics”, *Technische Universiteit Eindhoven*, 2005.

Drexel, T., “Die neuen Öko-Häuser”, *DVA, München*, 2004.

Dzioubinski, O., Chipman, R., “Trends in Consumption and reduction: Household Energy Consumption”, *economic & social Affairs*, 1999.

Economic Commission for Europe, “Guideline on Sustainable Human Settlement Planning & Management”, *United Nations*, 1996.

Edward, B., Turrent, D., “Sustainable housing”, *Principles & Practice, Taylor & Fransis*, 2005.

Escourrou, G., “Le climat et la ville”, *Géographie d'aujourd'hui. Nathan. Paris*, 1991.

Fairey, P.W., “Passive Cooling and Human Comfort”, *Florida solar energy center*, 1994.

Fanger, P.O., “Thermal Comfort-analysis and Applications in Environmental Engineering”, *New York: McGraw-Hill*, 1970.

Feist, W., Peper, S., Görg, M., “CEPHEUS-Project information No. 36”, Final Technical Report Efficient Passive Houses as European Standards (CEPHEUS), July 2001.

Fleury, B., “Ventilative Cooling, Paper presented at Workshop on Passive Cooling”, Application of CFD to naturally ventilated Buildings, A guide for practitioners, [www.flovent.com](http://www.flovent.com), *Ispira. CEC, Joint Research Centre Flomerics Ltd.* 1990.

Flourentzou, F., Van der Maas, J., Roulet, C.A., “Natural ventilation for passive cooling: measurement of discharge coefficients”, *Energy and Buildings*, 1998.

Fluent Inc., “Airpak 2.1 Tutorial Guide”, April 2002.

Foster, N., “Solar Architektur für Europa”, *Birkhäuser*, 1996.

Foster, N., Scheer, H., “Solar Energy in Architecture and Urban Planning: Third European Conference on Architecture”, *James & James Science Publishers Ltd*, 1993.

Franke, E., “Stadtklima, Ergebnisse und Aspekte für die Stadtplanung”, Beiträge zur Umweltplanung, *Karl KrämerVerlag, Stuttgart*, 1977.

Gandemer, J., Barnaud, G., Sacré, C., Millet, J.R., “Guide sur la Climatisation Naturelle de l’Habitat en Climat Tropical Humide. Tome 1: Methodologie de Prise en Compte des Parametres Climatiques dans l’Habitat et Conseils Pratiques”, *CSTB, Nantes*, 1992.

- Gao, Y., Chen, Q., "Coupling of A multi-zone airflow analysis program with a computational fluid dynamics program for indoor air quality studies", *Proceedings of the 4th International Symposium on Heating Ventilating and Air Conditioning, Beijing, China*, 2003.
- Geiger, R., Aron, R.H., Todhunter, P., "The climate near the ground", 5th edition, *Vieweg*, 1995.
- Gissen, D., "Big and Green: Toward Sustainable Architecture in the 21st Century", *Princeton Architectural Press*, 2002.
- Givoni, B., "Man, Climate and Architecture", *Elsevier publishing company limited*, 1969.
- Givoni, B., "Passive and Low energy cooling of buildings", *Van Nostrand Reinhold, New York*, 1994.
- Gonzalo, R., "Bewusst Bauen", Wege zum solaren und energiesparenden Planen, Bauen und Wohnen, *Edition Erasmus*, 1994.
- Goulding, J.R., Lewis, J.O., Steemers, T.C., "Energy conscious design", a primer for architects, *Batsford for the commission of the European Communities*, 1992.
- Gunßer, C., "Wohnen am Hang", *Deutsche Verlags-Anstalt, Stuttgart, Muenchen*, 2001.
- Güttler, P., "Berlin und seine Bauten", *Ernst & Sohn Verlag für Architektur und technische Wissenschaften Berlin*, 2002.
- Guyot, G., "Physics of the environment and climate", *John Wiley & Sons*, 1998.
- Haglund, B., Rathmann, K., "Vital signs", Thermal mass in passive solar and energy conserving buildings, *University of Idaho*, 1996.
- Han, P.W., "The environmental ecological interpretation of a traditional Korean settlement", *Architectural institute of Korea*, 1996.
- Hawkes, D., Forster, W., "Energy Efficient Buildings: Architecture, Engineering, and Environment", *W. W. Norton & Company*, 2002.
- Heckmann, O., "Grundrißatlas, Wohnungsbau", *Birkhäuser*, 1994.
- Hens, H., "Building Physics-Heat, Air and Moisture", Fundamentals and Engineering Methods with Examples and Experiences, *Ernst & Sohn*, 2007.
- Hensen, J., "A comparison of coupled and de-coupled solutions for temperature and air flow in a building", *ASHRAE Transactions*, 1999.
- Herzog, T., Kaiser, N., Volz, M., "Solar Energy in Architecture and Urban Planning", European conference on Solar Energy in Architecture and Urban planning, *Prestel Publishing*, April, 1996.
- Höppe, P.R., "Heat balance modeling", *Experientia* 49, 1993.
- Hollmuller, P., Lachal, B., "TRNSYS compatible moist air hypocaust model", Final report, *Centre universitaire d'études des problèmes de l'énergie, CH - 1205 Genève*, 1998.
- Honjo, T., Takakura, T., "Simulation of thermal effects of urban green areas on their surrounding areas", *Energy and Buildings*, 1990.
- Hosker, R.P.J., "Flow around isolated structures and building clusters: a review", *ASHRAE Transactions*, 1985.
- Hottel, H.C., Sarofim, A.F., "Radiative Transfer", Chapter 3, *McGraw-Hill*, 1967.



- Hussein, M., Lee, B.E., "An investigation of wind forces on the 3D roughness elements in a simulated atmospheric boundary layer flow", *University of Sheffield, UK*, 1980.
- ISO/PRF PAS 16739 IFC 2. x Platform specification.
- Jendritzky, G., Menz, G., Schirmer, H., Schmidt, K.W., "Methodik zur räumlichen Bewertung der thermischen Komponente im Bioklima des Menschen", Beiträge der Akademie für Raumforschung und Landesplanung, *Hannover Universität*, 1990.
- Jittawikul, A., "Climatic maps for passive cooling methods utilization in Thailand", *Journal of Asian architecture and building engineering*, 2004.
- Jones, A.R., "Sustainable Architecture: The Green Buildings of Nikken Sekkei", *Academy Press*, 2000.
- Joo, C.S., "A study on the architectural planning of the hill housing", *Hanyang University*, 1989.
- Jozwiak, R., Kacprzyk, J., Zuranski, J.A., "Wind tunnel investigations of interference effects on pressure distribution on a building", *Journal of wind engineering and industrial aerodynamics*, 1995.
- Kang, B.S., "도시집합주택의 계획/Plan of city residence", 공동주택연구회/Korea research council for multi-family housing, 도서출판 발언/Bal Eon, 1996.
- Katayama, T., Tsutsumi, J., Ishii, A., "Full-scale measurements and wind tunnel tests on cross-ventilation", *Journal of Wind Engineering and Industrial Aerodynamics*, 1992.
- Katayama T., Tsutsumi, J., "Investigation and numerical simulation of the wind effects on thermal comfort in a house", *Journal of wind engineering and industrial aerodynamics*, 1996.
- Kendrick, J.F., "An overview of combined modeling of heat transport and air movement", *Technical Note 40, Air Infiltration and Ventilation Centre, Coventry, UK*, 1993.
- Kim, B.S., Kim, K.H., "A Study on Thermal Environment and the Design Methods to Save Energy in Small Glass-Skin Commercial Buildings", *Journal of Asian architecture and building engineering*, 2004.
- Kim, J.J., Baik, J.J., "A Numerical Study of Flow and Pollutant Dispersion Characteristics in Urban Street Canyons", *Journal of Applied Meteorology*, 1999.
- Kim, H.J., "A study on the design characteristics of hillside apartment housing based on a gradient", *Architectural institute of Korea*, 2001.
- Kim, H.T., Kim, S.I., Park, B.J., "A study on the State of air motion and it's velocity distribution in the room by the models testing", *Architectural institute of Korea*, 1988.
- Kim, M.K., "A Study on the Ecological Expressive Characteristics of Traditional Residence in Korea", *Architectural institute of Korea*, 2000.
- Kim, M.K., "A Study on the Characteristics of the Ecological Expression in Traditional Korean Residence", *Gyeongsang National University*, 2001.
- Kiraly, J., "Architektur mit der Sonne," 7nd edition, *C.F. Müller Verlag Heidelberg*, 1996.
- Klingele, M., "Architektur und Energie," Planungsgrundlagen für Büro- und Verwaltungsbauten, *Verlag C.F. Müller*, 1994.
- Knowles, R.L., "Sun, Rhythm and Form", *MIT press, London*, 1981.
- Koenigsberger, O.H., Ingersoll, T.G., Mayhew, A., Szokolay, S.V., "Manual of Tropical Housing and Building", *Longman, London*, 1974.

- Köhler, M., “Ökologische Untersuchungen an Extensiven Dachbegrünung/ Ecological Analysis of Extensive Green Roofs”, *Poster zu Verhandlung der Gesellschaft für Ökologie*, 1989.
- Korea Electric Power Corporation /한국전력통계, <http://www.kepco.co.kr>, 2007.
- Korea National Statistical Office, Republic of Korea, <http://www.nso.go.kr/>, 2003.
- Köster, H., “Tageslichtdynamische Architektur”, Grundlagen, Systeme, Projekte, *Birkhäuser*, 2004.
- Krusche, P.M., Althaus, D., Gabriel, I., “Ökologisches Bauen”, Herausgegeben vom Umweltbundesamt, *Bauverlag GMBH Wiesbaden und Berlin*, 1982.
- Kuttler, W., “Stadtklima”, *Umweltchem Ökotox*, 2004.
- Landsberg, H.E., “The urban climate”, International geophysics series, *Academy press, New York*, 1981.
- Lechner, N., “Heating, Cooling, Lighting: Design Methods for Architects”, *John Wiley & sons*, 1991
- Lee, E.J., Kim, G., Kim, J.T., “Optimization of slope and orientation of building integrated photovoltaic systems based on local climatic aspect in Korea”, *Kyung Hee university, Republic of Korea*, 2004.
- Lee, K.H., “The environmental characteristic of Korean traditional house from the view in passive environmental control”, *The Architectural Institute of Korea*, 1986.
- Lee, K.I., “World collective theme houses”, *도서출판 발언/Bal Eon*, 1993.
- Lee, S.H., Heo, I.H., Lee, K.M., Kwon, W.T., “Classification of Local Climatic Regions in Korea”, *Korean Meteorological Society*, 2005.
- Lee, S.J., “Investigation for planning adaptable house to regional characteristic in the south seaside province of Korea”, *Korea University*, 1988.
- Lee, S.M., “Architectural environment of Jangkyunggak at Haein Temple”, *Dongguk University*, 1999.
- Lee, Y.W., “A study on the location of Hae-in temple”, *Han yang University*, 1986.
- Lefèvre, P., “Architectures durables”, 50 réalisations environnementales en France et. en Europe : Allemagne, Angleterre, Italie, Hollande, *Edisud, Paris, Systèmes solaires*, 2002.
- Liddament, M., “Air Infiltration Calculation Techniques: An Applications Guide”, *Air Infiltration and Ventilation Centre, Bracknell*, 1986.
- Liu, Y., “Climatic Design in Beijing, China, a Study of a Residential Multi-storey Building”, *AEE*, 2002.
- Lomas, K.J., Eppel, H., Martin, C.J., “Bloomfield, D. P. Empirical validation of thermal building simulation programs using test room data”, International Energy Agency ECBCS Annex 21 Report, *Building Research Establishment, Watford, UK*, 1994.
- Loxson, F.M., Clarke, G., “A National Assessment of Passive Nocturnal Cooling from Horizontal Surface”, *San Antonio: Solar Data Center, Trinity University*, 1980.
- Ludwig, J.W., “Solar 4.Architektur und Energie”, *America Haus*, 1981.
- Markus, T.A., Morris, E.N., “Buildings, Climate and Energy”, *Pitman Publishing, London*, 1980.
- Matsumoto, T., “Lifestyles and Energy Consumption in Households”, *The University of Kitakyushu*, 2003.

- Mayer, H., Höppe, P., "Thermal comfort of man in different urban environments", *Theor. Appl. Climatol.*, 1987.
- Mayer, H., "Human-biometeorological assessment of urban microclimates according to the German VDI-guideline 3787 part II", Prepr. *2nd Urban Envir. Symp. Albuquerque, New Mexico*, 1998.
- Mayer, H., Matzarakis, A., "Methoden zur human-biometeorologischen Bewertung von Klima- und Lufthygiene für die Stadt- und Regionalplanung", Die Richtlinie VDI 3787 Blatt 2, Teil I: Klima, *Kommission Reinhaltung der Luft im VDI und DIN Normenausschuss, Schriftenreihe Band 31*, 1999.
- Mayer, M., "Urban bioclimatology", *Experientia*, 1993.
- Mazria, E., "The passive solar energy book, a complete guide to passive solar home, greenhouse and building design", *Rodale Press*, 1979.
- McPherson, E.G., Nowak, D.J., Rowntree, R.A., "Chicago's urban forest ecosystem: Results of the Chicago urban forest climate project", General Technical report, *USDA forest service*, 1994.
- McPherson, E.G., Nowak, D.J., "Quantifying the impact of trees: The Chicago Urban Forest Climate Project", *Unasylva No.173*, 1993.
- McPherson, E.G., Simpson, J.R., "Shade trees as a demand-side resource", *Home energy 2*, 1995.
- Meir, L.A., Pearlmutter, D., Etzion, Y., "On the microclimatic behavior of two semi enclosed attached courtyards in hot and dry region", *Building and Environment*, 1995.
- Mendler, S.F., Odell, W., Lazarus, M.A., "The HOK Guidebook to Sustainable Design", *Wiley Press*, 2000.
- Mills, G., "An Urban Canopy-Layer Climate Model", *Theor. Appl. Climatol.*, 1997.
- Moffat, A.S., Schiler, M., "Landscape design that saves energy", *William Morrow and Co., New York*, 1981.
- Möllring, F., Schempp, D., Krampen, M., "Solares Bauen", 2nd edition, *Rudolf Müller Verlag, Köln*, 1994.
- Monteith, J.L., "Principles of environmental physics", *Edward Arnold, London*, 1973.
- Moore, S., Trulsson, N.B., McGregor, S.M., "Living Homes: Sustainable Architecture and Design", *Chronicle Books*, 2001.
- Mostaedi, A., "Sustainable Architecture: Hi-Tech Housing", *Ginkgo Press*, 2003.
- Nakamura, Y., Oke, T., "Wind, temperature and stability conditions in an eastwest oriented urban canyon", *Atmos. Envir*, 1988.
- Negrao, C. O. R., "Conflation of Computational Fluid Dynamics and Building Thermal Simulation", Ph.D. Thesis, Energy Systems Research Unit, Department of Mechanical Engineering, *University of Strathclyde, Glasgow, UK*, 1995.
- Novoselac, A., "Combined airflow and energy simulation program for building mechanical system design", *The Pennsylvania State University*, 2005.
- Oke, T.R., "The distinction between canopy and boundary - layer urban heat island", *Atmosphere*, 1976.
- Oke, T.R., "Boundary Layer Climates", 2nd edition, *Methuen. London, New York*, 1987.
- Oke, T., Johnson, G.T., Steyn, D.G., Watson, I.D., "Simulation of surface urban heat islands under "ideal" conditions at night", *Boundary-Layer Meteorol.*, 1991.
- Olgyay, V., "Design with climate", Bioclimatic approach to architectural regionalism, 4th edition, *Princeton University*, 1973.

- Owens, S., "Energy, environmental sustainability and land-use planning", *Sustainable Development and Urban Form*, Pion, London, 1982.
- Porteous, C., "The New Eco-Architecture: Alternatives from the Modern Movement", *E & FN Spon*, 2001.
- Pople, N., "Gebäude Visionen: Architektur der Zukunft", *Kohlhammer*, 2001.
- Ridky, R., "Siedlungsökologische Eckwerte zum Bebauungsplan, Mit Gestaltungshilfen zur Topographieanpassung für umweltschonende Wohnbaumaßnahmen", Dortmund *Vertrieb für Bau- und Planungsliteratur*, 1991.
- Roaf, S., "Ecohouse 2", a design guide, *Architectural press*, 2003.
- Rosenlund, H., "Climatic Design of Buildings using Passive Techniques", *Luvit Education Centre, Sweden*, 2000.
- Saini, B.S., "Architecture in Tropical Australia", *Lund Humphries for the Architectural Association London*, No.6, 1970.
- Santamouris, M., Daskalaki, E., "Case Studies: In Natural Ventilation", *James and James Science Publishers*, 1998.
- Santamouris, M., Papanikolaou, N., Koronakis, I., Livada, I., Asimakopoulos, D., "Thermal and airflow characteristics in a deep pedestrian canyon under hot weather conditions", *Atmos. Envir.*, 1999.
- Santamouris, M. Asimakopoulos, D., "Passive cooling of buildings", European Commission directorate general XVII for Energy, *James and James Science Publishers, London*, 1996.
- Scherer, D., "Infrared image database of Kreisel in Berlin", Fachgebiet Klimatologie, Institut für Ökologie, *Technische Universität Berlin*, 2006.
- Schittich, C., "In Detail Solar Architecture", strategies, visions, concepts, *Birkhäuser*, 2004.
- Seoul Statistical Yearbook, *Seoul Metropolitan Government*, 2007.
- Sharma, A., Dhote, K.K., Tiwari, R., "Climatic Responsive Energy Efficient Passive Techniques in Buildings", *IE(I)Journal-AR*, 2003.
- Shashua-Bar, L., Hoffman, M.E., "Vegetation as a climatic component in the design of an urban street", *Energy and Buildings*, 2000.
- Shin, S.C., "에너지기술개발 동향 및 우리나라 전략/ Energy technical development trend and the strategy", *Science & Technology policy institute*, 2005.
- Simpson, B.J., Purdy, M.T., "Housing on sloping sites", *Construction Press, London and New York*, 1984.
- Smagorinsky, J., "Global atmospheric modeling and the numerical simulation of climate weather and climate modification", *Wiley, New York*, 1974.
- Smith, P., Pitts, A.C., "Concepts in practice Energy", *B.T. Batsford*, 1998.
- Smith, P.F., "Sustainability of the cutting edge", Emerging technologies for low energy buildings, *Architectural Press*, 2003.
- Smith, P.F., "Architecture in a Climate of Change", 2nd edition, *Architectural Press*, 2005.
- Stimmann, H., Kieren, M., "Die Architektur des neuen Berlin", *nicolai*, 2005.
- Taha, H., "Urban climates and heat islands: albedo, evapotranspiration and anthropogenic heat", *Energy and Buildings*, 1997.

- Talyor, P.A., Lee, R.J., “Simple guidelines for estimating wind speed variations due to small scale topographic features”, *Climatol. Bull.*, 1984.
- Tan, G., “Study of natural ventilation design by integrating the multi zone model with CFD simulation”, *Massachusetts Institute of Technology*, 2005.
- Tanimoto, J., Hagishima, A., Chimklai, P., “An approach for coupled simulation of building thermal effects and urban climatology”, *Energy and Buildings*, 2004.
- The Chartered Institute of Building Service Engineers (CIBSE), “The Chartered Institute of Building Services Engineers Handbook”, 1997.
- The Intergovernmental Panel on Climate Change (IPCC), “IPCC Fourth Assessment Report (AR4): Climate Change 2007”, 2007.
- The Kentucky Division of Energy (KDOE), “Energy Efficient Home Plans for Kentucky”, A Plan Booklet of Energy Efficient Homes with Performance Analysis, *Commonwealth of Kentucky*, 2003.
- The Korea Institute of Construction Technology (KICT), “친환경건축물 비용편익분석연구용역결과/ The cost-benefit analysis research result of environmental construction”, 2005.
- The US department of energy, “Getting Started with EnergyPlus”, *University of Illinois*, 2007a.
- The US department of energy, “Input Output Reference: The Encyclopedic Reference to EnergyPlus Input and Output”, *University of Illinois*, 2007b.
- The US department of energy, “EnergyPlus Engineering Reference: The Reference to EnergyPlus Calculations”, *University of Illinois*, 2007.
- The 2005 World Sustainable Building Conference (WSBC), “Sustainable design book”, *SB 05, Building a sustainable future, Tokyo*, 2005.
- Toudert, F.A., “Dependence of Outdoor Thermal Comfort on Street Design in Hot and Dry Climate”, *Freiburg, Albert-Ludwigs-Universität Freiburg*, November 2005.
- Treberspurg, M., “Neues Bauen mit der Sonne”, Ansaetze zu einer klimagerechten Architektur, *Springer-Verlag, Wien, New York*, 1994.
- Tuomaala, P., “The Implementation and evaluation of airflow and heat transfer routines for building simulation tools”, VTT publication 471, Ph.D. Thesis, *Helsinki University of Technology*, 2002.
- Ulseth, R., Stang, J., Hoel, T.I., Noeres, P., Klose, P., Hölder, D., Althaus, W., Ahonen, M., Koo, K.D., “District Heating and Cooling in Future Buildings”, *IEA-District heating and cooling project*, 1999.
- Vandaele, L., Wouters, P., “The PASSYS services summary report”, Commission of the European Communities, *Research and Development, Brussels, Belgium*, 1994.
- Van Treeck, C., Rank, E., “Geometrical and topological issues for coupling dimensionally reduced multizone models with high-resolution CFD techniques”, Lehrstuhl für Bauinformatik, *Technische Universität München*, 2004.
- Vickery, B.J., Karakatsanis C., “External wind pressure distributions and induced internal ventilation flow in low-rise industrial and domestic structures”, *ASHRAE Transactions, BRE*, 1978.
- Walker, R.R., Shao, L., Woolliscroft, M., “Natural ventilation via courtyards: the application of CFD”, *In Proceedings 14th AIVC Conference, Copenhagen*, 1993.

Walton, G.N., "The Thermal Analysis Research Program Reference Manual Program (TARP)", *National Bureau of Standards (now National Institute of Standards and Technology)*, 1983.

Ward, I.C., "Energy and environmental issues", for the practicing architect, *Thomas Telford*, 2004.

Wedding, J.B., Lombardi, D.J., Cermak, J.E., "A wind tunnel study of gaseous pollutants in city street canyons", *J. Air Pollut. Contr.*, 1977.

Wiren, B.G., "Effect of surrounding buildings on wind pressure distribution and ventilation heat losses for single family houses", *Int. Swedish inst. for building Research.*, 1985.

Wiren, B.G., "Effect of surrounding buildings on wind pressure distribution and ventilation heat losses for single family houses", *the international Swedish institute for building Research, Gavle. Sweden*, 1987.

Woodruff, N.P., Zingg, A.W., "Wind tunnel studies of fundamental problems related to windbreaks, *U.S. Department of Agriculture, Washington, D.C.*, 1952.

Yannas, S., "Adaptive Skins and Microclimates", the 21st Conference on Passive and Low Energy Architecture, *Eindhoven, the Netherlands, PLEA*, 2004.

Yeang, K., "Tropical Urban Regionalism", building in a Southeast Asian city, *Singapore Concept Media*, 1987.

Yoshida, A., Tominaga, K., Watani, S., "Field measurements on energy balance of an urban canyon in the summer season", *Energy and Buildings*, 1990/91.

Zhai, Z., Chen, Q., "Strategies for coupling energy simulation and computational fluid dynamics programs", *Seventh International IBPSA Conference Rio de Janeiro, Brazil*, 2001.

Zhai, Z., "Developing an integrated design tool by coupling building energy simulation and computational fluid dynamics", Ph.D. Thesis, Department of Architecture, *Massachusetts Institute of Technology*, 2003.

<http://www.building envelopes.org>

<http://www.kawadesign.co.kr>

<http://www.stadtentwicklung-berlin.de>

<http://www.trnsys.com>

<http://www.fluent.com>

<http://www.kma.go.kr>

<http://www.lohmeyer.de/air-eia/casestudies/>